THE UNIVERSITY OF HULL

Nanoparticles at Liquid Interfaces

being a Thesis submitted for the degree of
Doctor of Philosophy in the University of Hull

by

Timothy J. G. Lees, M.Chem.

June 2008

Science is built up of facts, as a house is built of stones; but an accumulation of facts is no more a science than a heap of stones is a house.

Henri Poincaré (1905)

Acknowledgements

I would like to thank my supervisors, Prof. B.P. Binks, Dr. J.H. Clint, Prof. P.D.I. Fletcher and Dr. P. Taylor, for their high standard of supervision and support throughout the duration of this project.

I thank the E.P.S.R.C. and Syngenta (Bracknell) for the provision of a studentship.

I show gratitude to all members of the Surfactant and Colloid Group, past and present for support and friendship. I would like to particularly thank Dr. T.S. Horozov and Dr. C.P. Whitby.

I would like to thank Tony Sinclair for the SEM images and Jan Helder for the TEM images.

I thank the members of the glass and mechanical workshops for their help.

I thank Gaz, Marc, GP and all the other member of the UCH Sharks American Football Team for the good times away from the lab and the excellent distraction.

I own a great debt to the staff of CEBE for their support while writing this work.

Finally, I thank my family and Stacey for their support, encouragement and love without which this undertaking would not have been completed.

Publications and presentations

The work contained in this thesis has given rise to the following publications and presentations:

1. *Growth of gold nanoparticle films driven by the coalescence of particle-stabilized emulsion drops*, B.P. Binks, J.H. Clint, P.D.I. Fletcher, T.J.G. Lees, P. Taylor, *Langmuir*, **22**, 4100 (2006).

2. *Growth of nanoparticle films driven by the coalescence of particle-stabilized Foam Bubbles*, B.P. Binks, J.H. Clint, P.D.I. Fletcher, T.J.G. Lees, P. Taylor, *Chem. Commun*, **33**, 3531 (2006).

3. Oral presentation "*Oil-in-water solid-stabilised emulsions: effect of addition of non-aqueous co-solvent*", at the Student Conference 2005, Biezenmortel, 12th – 15th July 2005.

4. Poster entitled "*Growth of gold nanoparticle films at the oil-water interface"*, at New Developments in Emulsions and Foams, Manchester, 12th – 14th December 2005.

5. Oral presentation "Delayed spreading of particle-stabilised emulsions on solids", at the University of Hull, Department of Chemistry, 19th June 2006.

6. Poster entitled "*Growth of nanoparticle films driven by the coalescence of emulsion drops / foam bubbles*", at EUFoams 2006, Potsdam, 2nd – 6th July 2006.

List of Symbols

Some of the symbols and abbreviations used in this thesis are given here; other are defined locally in the text.

DCDMS	Dichlorodimethylsilane
DSA 10	Krűss Drop Shape Analysis System DSA 10
Γ^*	Critical threshold concentration of emulsifier
Γ_M	Emulsifier adsorption in a complete monolayer
HIPE	High internal phase emulsions
HLB	Hydrophile-lipophile balance
IFT	Interfacial tension
IPM	Isopropyl myristate
d_{32}	Mean volume-surface diameter
ODA	Octadecylamine
OTS	Octadecyltrichlorosilane
o/w	Oil-in-water
Φ	Volume fraction of dispersed phase
PDMS	Polydimethlysilane
PTFE	Polytetrafluorethylene
SEM	Scanning electron microscopy
SPR	Surface plasmon resonance
γ	Surface tension
T	Absolute temperature
TEM	Transmission electron microscopy
θ	Three-phase contact angle measured through the water phase
w/o	Water-in-oil

Abstract

This thesis is concerned with the study of two phase systems stabilised by nanometre sized solid particles. The understanding of how modifying these particles at the oil(air)-water interface can change the properties of the bulk systems they stabilise is important for a number of industrial applications including agrochemicals, pharmaceuticals, cosmetics, food technology, paints, paper processing and oil recovery**.**

Each section of this work investigates a different solid-stabilised system. For each of these systems a novel way to change the properties of the system through modification of the particle behaviour at the fluid interface is identified, or a behaviour which is unique to solid-stabilised systems is investigated.

For aqueous suspensions of gold colloid it was found that modification by a long chained amine at the oil-water interface led to the rapid growth of particle films at the fluid interface on shaking. The particle film grew from the planar oil-water interface and up the walls of the hydrophilic vessel the system was contained in. A mechanism for this film growth is proposed in which coalescence of particle-laden emulsions droplets with the planar oil-water interface leads to an increase in the interfacial concentration of the particles. When at a suitable concentration, the surface pressure of the particles at the oil-water interface drives the rapid growth of the particle films. This film growth was not limited to emulsion systems and the spontaneous growth of hydrophobic silica and Teflon particle films was observed, driven by the collapse of a particle-stabilised foam system.

Addition of small amounts of low dielectric co-solvents to the continuous phase of an oil-in-water emulsion, stabilised by hydrophilic silica particles, was found to greatly enhance the stability of the system to coalescence. This was attributed to a combination of aggregation of the silica particles, reduction in surface charge density of the particles and influence on the concentration of particle adsorbed at the oil-water interface.

Finally, both transitional and catastrophic phase inversion was induced *in situ* in solid-stabilised systems. Evaporation of the continuous phase of a solid-stabilised oil-in-water emulsion was used to alter the oil:water ratio of system and induce an interesting spreading behaviour on solid substrates. The removal of the hydrophobic coating on modified silica particles at the oil-water interface, by addition of base to the aqueous phase, was shown to produce more stable water-in-oil emulsions. If sufficient base was present the emulsion system could be inverted from water-in-oil to oil-in-water.

NANOPARTICLES AT LIQUID INTERFACES

Contents **Page**

Chapter 1 Introduction 1

Chapter 4 Film Spreading by foam bubble coalescence 107

Chapter 5 Emulsions stabilised by hydrophilic silica 138

CHAPTER 1

INTRODUCTION

1.1 Industrial relevance of solid particles at liquid interfaces

Solid particles are used widely across many different industries. They find applications in agrochemicals, pharmaceuticals, cosmetics, food technology, paints, paper processing and oil recovery. In many of these applications particles are used as antifoams to prevent the uncontrolled formation of foam during automated processing. More recently particles have been used to stabilise both oil-water and air-water interfaces as an alternative to low molecular weight molecules and polymers. One advantage of using particles to stabilise emulsions is apparent in agrochemicals where formulations are often sprayed onto fields. Particles, unlike low molecular weight molecules, do not lower the oil-water interfacial tension (IFT). This means that a large amount of work needs to be done in order to create new interfaces so when a solid stabilised system is sprayed large drops of formulation are formed and quickly fall to the ground. The same system stabilised by low molecular weight molecules would have low interfacial and surface tensions. Due to the reduced tensions if the system was sprayed the action of forcing the system through the nozzle would produce very fine drops as little energy is required to form new interfaces. These would take longer to fall to the ground increasing the risk of the product drifting away from the targeted area.

1.2 Emulsions

1.2.1 Introduction to emulsions

An emulsion is a thermodynamically unstable mixture of two immiscible liquids typically water and oil. In the absence of any other material the two immiscible liquids, or phases, would rapidly come back together and the bulk oil and water phases would be recovered. In order to prevent this emulsion systems contain a third material which is called the emulsifier. Emulsifiers can act in a number of different ways but all impart stability to the emulsion system. Traditionally, emulsifiers are low molecular weight surfactants (size typically 0.4 – 1 nm) or surface active polymers (size typically 1 – 5 nm).[1] Surfactant molecules are comprised of a water liking, or hydrophilic, head which is usually charged and a non-polar or, hydrophobic, tail. Due to their small size, surfactants are capable of adsorbing very rapidly to oil-water interfaces. Once adsorbed, the repulsion between the head groups reduces the free energy cost of creating new interface and therefore lowers the IFT. As well as lowering the IFT, surfactants provide electrostatic stabilisation to the interfaces they adsorb to. Proteins adsorb at the oil-water interface and provide stability either through electrostatic or steric repulsion between approaching interfaces.[2,3] The extent of this can be dependent on the configuration of the protein at the oil-water interface. Proteins can be globular in configuration but are also able to unfold. There has been interest in the literature into responsive or ‘smart’ polymers which are able to respond to changes in their environment, such as pH or salt concentration, with a change in their configuration and therefore a change in their properties.[4,5]

It is possible to produce an emulsion system in which water droplets are dispersed in bulk oil which is described as a water-in-oil (w/o) emulsion. In the same manner it is possible to produce a system where oil droplets are dispersed in bulk water described as an oil-in-water (o/w) emulsion. Figure 1.1(a) shows both a w/o and o/w system. The phases are often referred to as the dispersed and continuous phases. In the case of an o/w emulsion the oil is the dispersed phase and the water the continuous phase. It is worth noting, as shown in Figure 1.1(a), that the curvature of the oil-water interface is different in an o/w than in a w/o system. In an o/w system the curvature is away from the water phase whereas in a w/o system the curvature is towards the water phase.

1.1.2 Emulsification

There are a number of ways of forming an emulsion but the simplest, and the one adopted in this work, is to provide mechanical agitation to the system, also called homogenisation. All forms of emulsification provide energy to the system in order to do the work required to form new interfaces. Droplet size is dependent on system properties as well as homogenisation time and intensity.

Figure 1.1. Schematic representation of (a) an o/w and w/o emulsion system and (b) the respective oil-water interfacial curvatures in each system.

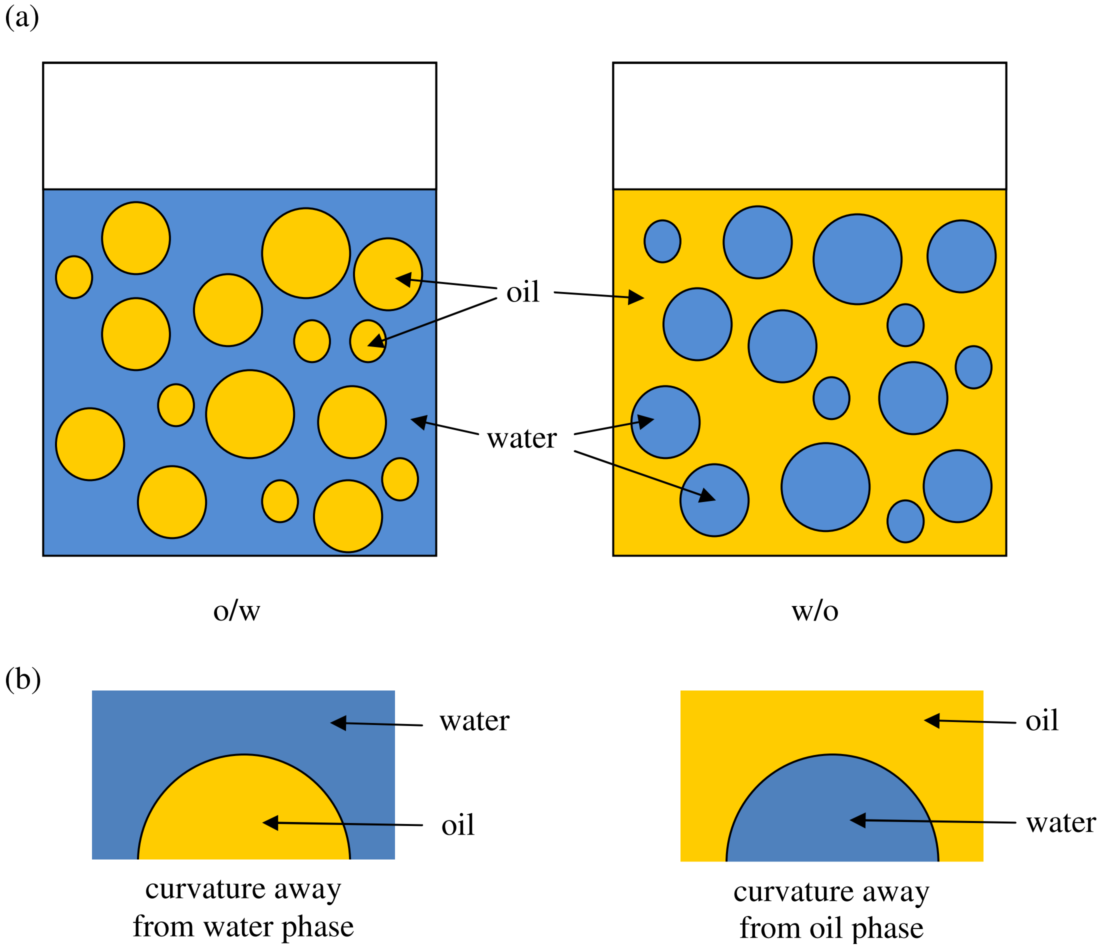

Typically, droplet sizes are usually between 0.1 to 20 μm. Emulsification is a complex process which until recently has been poorly understood. Work summarised by Denkov *et al.* has described the process of emulsification, particularly with respect to the theoretical models which describe the processes involved.[6] The drop size recovered after emulsification is the result of two competing processes, drop-to-drop coalescence and drop breakage. The contributions of these two processes are governed by dispersed phase volume fraction, hydrodynamic conditions and the concentration and type of emulsifier.[5-7]

The dependence of emulsion droplet size on emulsifier concentration falls into one of two regions; one region in which the system is emulsifier poor and one region in which the system is emulsifier rich. In the emulsifier poor region the drop size produced is strongly dependent on the emulsifier concentration. As the concentration of emulsifier is increased the recovered emulsion droplets size is decreased. Since in this region there is not enough emulsifier to stabilise the interface formed, it is sensible that an increase in the concentration of emulsifier would result in stabilisation of more interface and thus smaller droplets. In the emulsifier rich region there is sufficient emulsifier to stabilise all interfaces created during emulsification. In this region, emulsion droplet size is independent of emulsifier concentration and is more dependent on droplet break up.

Since interfaces have a charge, there is an electrostatic barrier to emulsifier adsorption. If this barrier is reduced by using an emulsifier with a low charge, or a high concentration of salt to shield the charges, then there is a very close similarity between the various types of emulsifiers.[8,9,10] When the barrier to adsorption is removed and the system is in the emulsifier poor regime droplets are formed and the emulsifier rapidly adsorbs at the interface. Initially the droplets have an insufficient concentration of emulsifier to provide stability and when they come into contact with each other they coalesce. As coalescence events occur the available droplet interface is reduced and the emulsifier interfacial concentration increased to a point at which a complete monolayer of emulsifier is formed. At this point coalescence is prevented. This process is termed “partial coalescence”.[11,12]

A simple mass balance model has been suggested to explain the size of droplets recovered in the region where partial coalescence is observed i.e. in the emulsifier poor region. This model is based on the principle that in this regime emulsion droplets coalesce until the point at which a critical threshold concentration of emulsifier, Γ^*, is achieved. It makes the assumption that all the emulsifier is adsorbed at the interface. The value of Γ^* is independent of both oil volume fraction and stirring intensity. Under these assumptions the mean volume-surface diameter of the droplets, d_{32}, is derived for emulsions where the emulsifier is initially dispersed/dissolved in the continuous phase using the following mass balance equation[7]

$$d_{32} = \frac{6\Phi}{(1-\Phi)}\frac{\Gamma^*}{C_{INI}} = \frac{6\Phi}{(1-\Phi)}\frac{\theta^*\Gamma_M}{C_{INI}} \tag{1.1}$$

where C_{INI} is the initial emulsifier concentration in the continuous phase, Φ is the volume fraction of the dispersed phase. Γ_M is the emulsifier adsorption in a complete monolayer and $\theta^* = \Gamma^* / \Gamma_M$ is the dimensionless threshold surface coverage. This equation only holds for systems in which there is no barrier to emulsifier adsorption.

Equation 1.1 shows how droplet size is inversely proportional to the initial emulsifier concentration, C_{INI} for the reasons described above. It also highlights the strong dependence of the drop size, d_{32}, on dispersed phase volume fraction Φ. The drop surface area is proportional to Φ, whereas the amount of available emulsifier is proportional to $(1-\Phi)$. As volume fraction of dispersed phase is increased, the amount of interface formed during emulsification will also increase. This will require a larger amount of emulsifier to stabilise and at the same time the amount of continuous phase, in which the emulsifier is dispersed, is being reduced. The same mass balance equation can be modified to consider what happens when the emulsifier is dissolved/ dispersed into the droplets

$$d_{32} = \frac{6\Gamma^*}{C_{INI}} = \frac{6\theta^* \Gamma_M}{C_{INI}} \tag{1.2}$$

Equation 1.2 shows the dependence of droplet size on oil volume fraction is now not present when the emulsifier is dispersed into the droplets. It is possible to have values of θ^* greater than unity which is the case in systems stabilised by multilayers of emulsifiers. In this case a larger amount of emulsifier is required to create a stable system compared with a system that only requires a monolayer.

In the emulsifier rich region if the barrier to emulsifier adsorption is removed then the size of the droplets produced is independent of emulsifier concentration and solely dependent on drop break up. In this region the difference between low molecular weight surfactants, which reduce IFT, and solid particles, which do not, is marked. Another important difference between the emulsifiers is the kinetics of adsorption. Low molecular weight surfactants are capable of very rapid adsorption and in most cases equilibrium concentrations and tensions sufficiently describe their effect on tensions. With particles and proteins the kinetics of adsorption are much slower and dynamic tensions have to be used. Since low molecular weight surfactants rapidly adsorb to the interface, and reduce the IFT, they are effective at stabilising small droplets in this region. Particles adsorb slowly and do not reduce IFT therefore they stabilise large droplets. This explains the experimental need to have large concentrations of particles to effectively stabilise systems, often as high as 2 weight (wt.) %. The concentration of low molecular weight surfactant required to stabilise the same system is orders of magnitude lower.

As described above the difference in emulsifiers is described by Denkov *et al.* using the difference in adsorption kinetics.[6] The process of emulsification is described as a combination of drop deformation, drop breakage, drop collision and drop coalescence which is illustrated in Figure 1.2 (redrawn from reference 6). The process of emulsification can be described in terms of the time taken for the emulsifier to adsorb (t_A), the time for drop deformation (t_D) and the time taken for drop collision to occur (t_C). If t_A is shorter than t_C and t_D then collision will occur between drops with complete, or almost complete, emulsifier layers and coalescence will be prevented, or limited. In contrast if the t_A is longer than t_C and t_D then coalescence will occur. t_A can be estimated for

Figure 1.2. Schematic representation of the processes of drop deformation (a) followed by drop breakage (b) followed by drop collision (c) and, finally followed by (d) drop coalescence. For the cycle shown the time taken for emulsifier to adsorb (t_A) is longer than the time taken for the drops to deform and collide ($t_D + t_C$).[6]

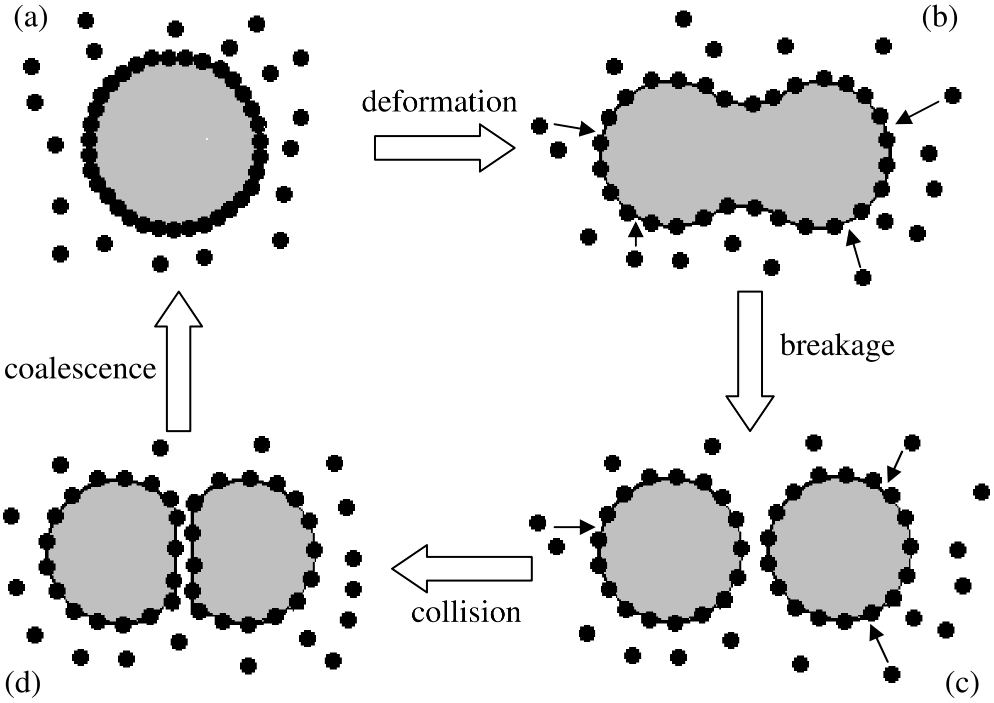

barrier-less adsorption there is expected to be little difference between proteins and surfactants. For particles, particularly those with a large mass, the adsorption is expected to be slower.

In systems that do not contain high concentrations of salt or those stabilised by emulsifiers with a relatively high surface charge then a barrier to emulsifier adsorption is present with the charged oil-water interface.[8,13] This barrier can significantly reduce the probability that a particle will approach the interface and therefore significantly reduce the ability of the particles to stabilise the system, even at high particle concentrations. Under these conditions the geometry of the particles becomes more important. For instance it is easier for a needle shaped particle, or one that is fractal in nature, to approach the interface than a spherical particle.[14] When considering fractal particles, such as fumed silica, it is the size of the primary aggregate which governs the particles ability to adsorb.

1.1.3 Emulsion stability

Even with the presence of an emulsifying agent emulsions can exhibit signs of instability. There are four mechanisms which can contribute to emulsion breakdown.[15] The process by which two emulsion droplets come together forming a single larger droplet is called coalescence. Coalescence results in a reduction in oil-water interfacial area. If unchecked, coalescence eventually results in full phase separation of the oil and water phases and complete destruction of the emulsion system. Coalescence is irreversible and in order to recreate an emulsion energy would have to be supplied to the system.

Due to the difference in density between the dispersed and continuous phase it is possible for emulsion droplets either to rise to the top, creaming, or sink to the bottom, sedimentation, of the continuous phase.[16] This happens without changing the droplet size distribution and produces a region which is rich in dispersed phase, referred to as the cream or sediment, and a depleted serum phase. Creaming/sedimentation is reversible, gentle shaking of the emulsion system will redisperse the creamed phase and the dispersed state will be recovered. Although creaming/sedimentation does not lead to phase separation it can increase the rate of coalescence because it brings the dispersed phase droplets into closer proximity.

It is possible that after emulsion formation the discreet emulsion droplets can come together and adhere to each other to form loose aggregates, this process is call flocculation and aggregates are called flocs. Flocculation is governed by the balance between van der Waals attractions and electrostatic repulsion of the emulsion droplets. This process does not lead to phase separation but can increase the rate of creaming/sedimentation and coalescence.

The final way in which emulsions can exhibit instability is called Ostwald ripening. This occurs when large emulsion droplets grow larger at the expense of smaller droplets. This is due to the difference in solubility of the dispersed phase in the continuous phase. The driving force is a higher La Place pressure in the smaller drops than in the larger as described by Lifshitz and Slezov[17] and Wagner.[18] Ostwald ripening is irreversible and one of most effective ways to suppress this mechanism is to create a system with droplets of the same size, or a monodisperse emulsion. It is the polydispersity in droplet size which creates the difference in solubility leading to this type of instability. Figure 1.3 illustrates each of the processes which can cause emulsion instability.

1.3 Solid particles at liquid interfaces

1.3.1 Particles in dispersions and films

1.3.1.1 DLVO Theory

The DLVO (Derjaguin, Landau, Verwey and Overbeek) theory can be used to describe the qualitative features of the interactions between dispersed colloids in suspension.[19] It is equally applicable to both colloidal particle suspensions and emulsion droplet interactions and can be used to describe emulsion stability towards flocculation. DLVO theory assumes that the main contributors to colloidal stability are long range interactions. These long range forces are attractive van der Walls forces (V_A) and repulsive electrostatic forces due to charged surface groups or ion adsorption from solution. The total interaction potential (V) can be expressed as

$$V = V_A + V_R \tag{1.3}$$

Figure 1.3. Schematic representation of the different mechanisms of emulsion breakdown (a) coalescence, (b) aggregation, (c) creaming and (d) Ostwald ripening.

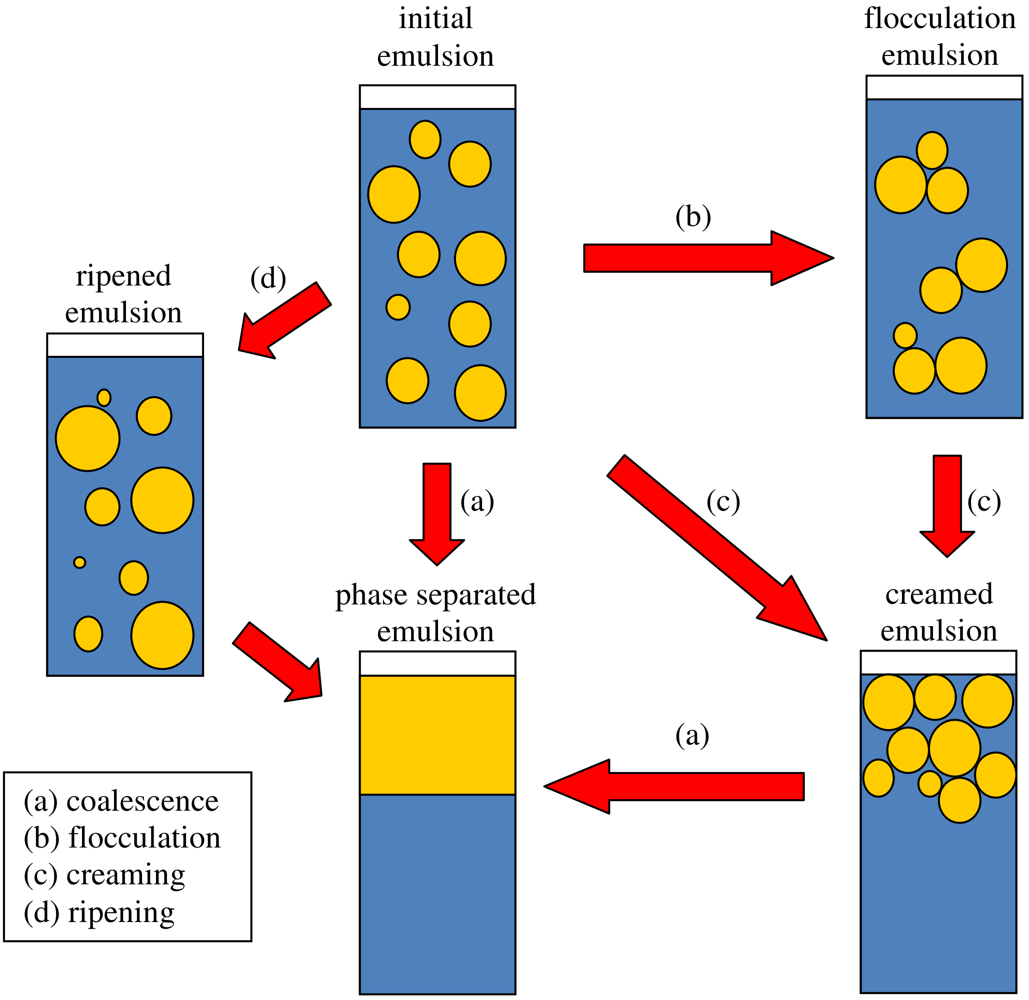

where both V_A and V_R are a function of the distance (d) between the interacting colloids. Depending on the relative strengths and ranges of the two opposing interactions, the interaction versus distance curve can be generated as shown in Figure 1.4. At large or small distances the attractive force may dominate the repulsive force, whereas at intermediate separations the double-layer repulsion gives rise to drop in the potential energy barrier to aggregation as long as this repulsion is not shielded by the presence of electrolyte ions. Normally if a colloidal particle passes into the primary minimum it so deep that the aggregation is effectively irreversible. If the mean distance between the colloidal particles is larger than the secondary minimum then the system gains energy by bringing the particles together. If emulsions droplets are brought together in this manner then they can coagulate into the primary minimum whilst retaining their identity as individual droplets. If the thin liquid film of continuous phase between the droplets is stable then the droplets will remain intact. If this film ruptures then coalescence occurs.

1.3.1.2 Capillary Pressures

Although it is true that solid particles stabilise emulsions through two main mechanisms[24] (described below in Section 1.3.2) it is worth taking some time to understand capillary pressure and what role it plays in the stability of solid-stabilised emulsions. The ultimate stability of solid-stabilised emulsions towards coalescence is dependent on the stability of the thin film created when two droplet come together.

Figure 1.4. Plot of total interaction potential ($V = V_A + V_R$) as a function of the distance between the colloidal particles. Both primary and secondary minima are shown.

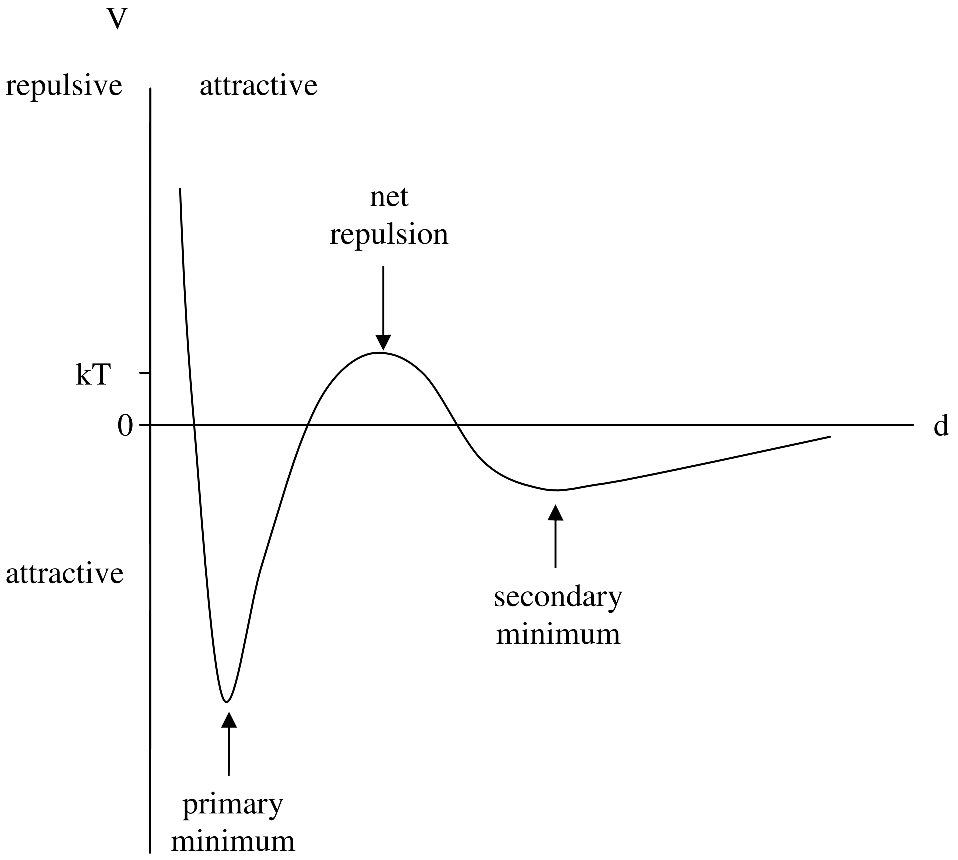

The theoretical approach for understanding the stabilisation of thin liquid films considers the shape of the meniscus surrounding the particles at the liquid interface.[20,21] Figure 1.5 shows the shape of the meniscus surrounding a particle which is bridging two liquid interfaces i.e. a particle within a monolayer. For regular arrays of particles the meniscus shape depends on the capillary pressure across the interface, P_C; particle radius, a; three-phase contact line angle, α; oil-water interfacial tension, σ; interparticle distance, b; and if the particles form a monolayer or bilayer. Figure 1.6 shows a thin liquid film stabilised by (a) a monolayer and (b) a bilayer. The theoretical treatments consider the effect on meniscus shape, and the resulting effect on the minimum distance between the two interfaces, h_{MIN}, of only P_C since all other parameters are considered to be fixed. The full theoretical treatment is described adequately elsewhere[20,21] and predicts that for the case where the emulsion film is stabilised by a monolayer, see Figure 1.5, then the maximum capillary pressure that a film can resist, P_C^{CR}, is proportional to $1/a$ i.e. smaller particles stabilise films more effectively. P_C^{CR} is also shown to rapidly decrease with an increase in b, the interparticle distance in the film. In addition to the dependencies on particle size and interparticle distance, particle wettability is also an important factor. The lower the contact angle the more stable the film i.e. films are not stable for values of α near 90°. The theoretically calculated values of the critical capillary pressures that emulsion films can withstand before film rupture is always orders of magnitude higher than the experimentally measured values. This is because the models presume that the particles are uniformly spread across the fluid interfaces. In real systems particle can be found in concentrated regions with particle free “pores” in the layer.

Figure 1.5. The shape of the fluid interface surrounding a bridging particle at the fluid interface.

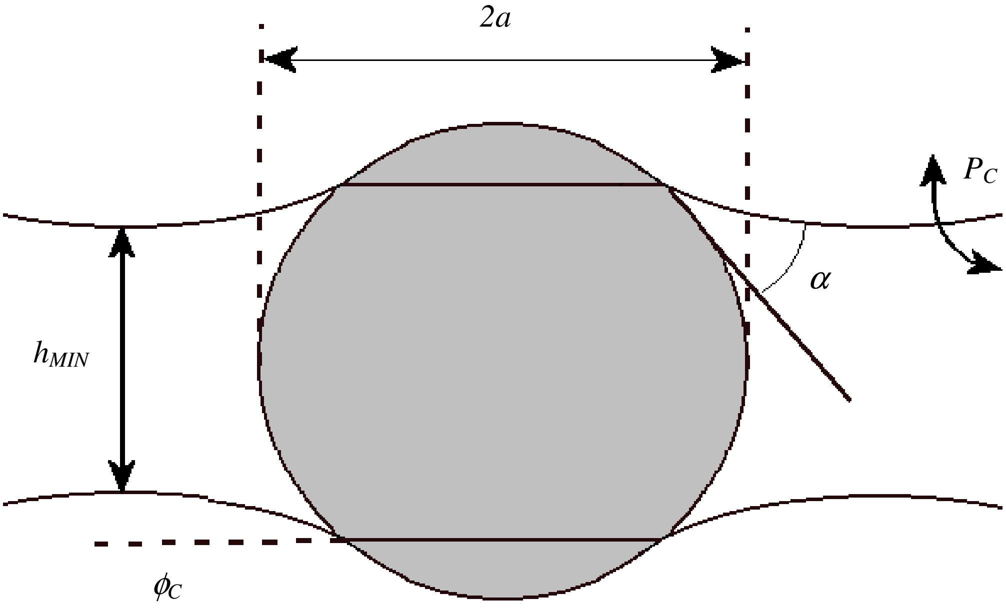

Figure 1.6. Schematic representation of two possible configurations of particle-stabilised thin liquid films between two particle-laden emulsion droplets. *h* is the interfilm distance, *b* is the interparticle distance and *a* is the particle diameter.

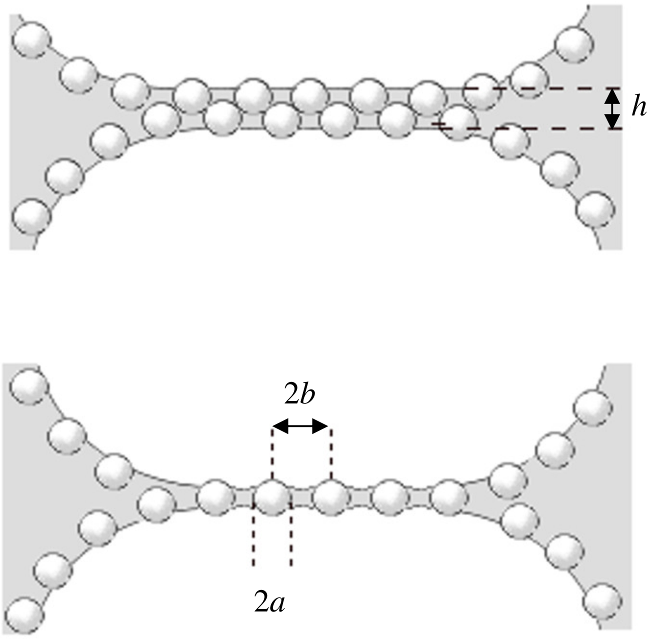

1.3.2 Solid-stabilised emulsions

Since the early work of Pickering, which built upon earlier observations by Ramsden, it has been shown that surfactant free emulsions can be made and stabilised by solid particles alone (size typically 10 nm – 5 μm).[22,23] There are many similarities and differences between the way in which low molar mass surfactants and solid particles (micro- or nano-) stabilise emulsions.[24]

Particles absorb strongly to liquid-liquid interfaces by removing some of the high energy oil-water interface. The energy of adsorption is dependent on the three-phase contact angle (θ). The surface hydrophobicity, and hence the three-phase contact angle, play a large role in determining which type of emulsion is observed. Hydrophilic surfaces exhibit low θ_{ow} (measured through the aqueous phase) and stabilise oil-in-water (o/w) emulsions, whereas hydrophobic surfaces have a large θ_{ow} and stabilise water-in-oil (w/o) emulsions. The forces acting on a particle at an oil-water interface and the three phase contact angle it forms are shown in Figure 1.7. It has been shown that the energy of attachment of a single particle to an oil-water interface passes through a maximum at $\theta_{ow} = 90^o$, i.e. at intermediate hydrophobicities the most stable emulsions are formed. At extremes of wettability, i.e. θ_{ow} approaching 0^o or 180^o, particles do not adsorb strongly to oil-water interfaces and therefore are poor emulsion stabilisers.[25]

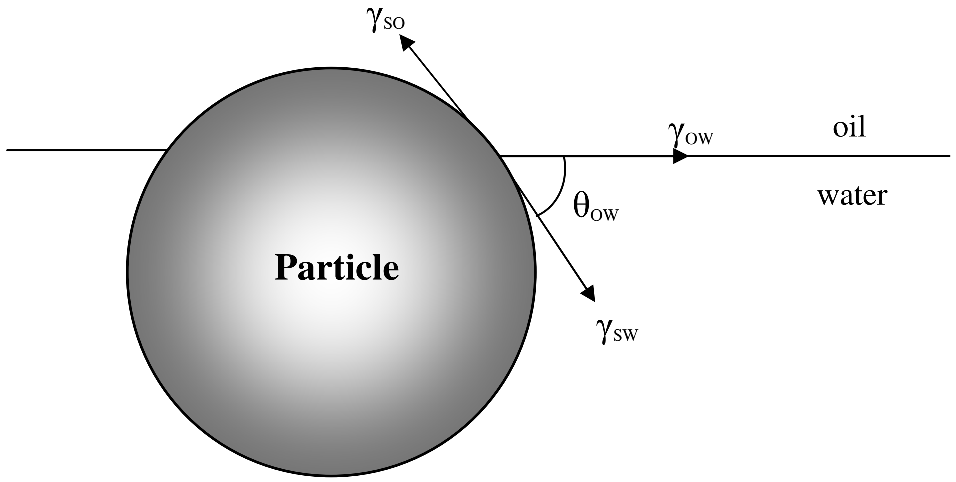

Figure 1.7. Schematic diagram of a solid particle at an oil water interface showing the surface forces γ_{so}, γ_{ow} and γ_{sw} which are the three interfacial tensions between the solid and oil, the oil and the water and the solid and the water respectively, and the contact angle θ_{ow} measured through the aqueous phase.[26]

Presuming that a solid particle is small (less than a few microns in diameter) so that the effects of gravity are negligible, the energy required to remove the particle from the interface E is given by the following

$$E = \pi r^2 \gamma_{OW} (1 \pm \cos\theta_{OW})^2 \tag{1.4}$$

where r is the radius of the particle, γ_{OW} is the oil-water interfacial tension and θ_{ow} is the three phase contact angle measured through the water phase.[27] The sign within the brackets is negative when considering particles coming from the water phase, and positive for those coming from the oil phase. This means that the strength of attachment of a particle to the interface, and hence its ability to stabilise emulsions, is linked to particle size, particle wettability and the interfacial tension of the base oil-water interface. Particles do not adsorb strongly to the oil-water interface at extremes of hydrophobicity i.e. very hydrophilic or very hydrophobic. For a typical system E will be many times that of the thermal energy kT meaning that once at the interface, particles are considered to be irreversibly adsorbed. Other properties which can effect emulsion stabilisation are particle shape, particle concentration and the tendency of the particle to interact with each other. This had led to a wide range of particles being used as emulsion stabilisers including silica, clays, carbon, oxides and fat crystals.

The extent to which a solid is wetted by either phase is one factor in determining the type of emulsion that is formed. The work of Finkle *et al.* was the first to identify the relationship between the type of solid and emulsion type.[28] If a solid is preferentially wetted by either of the phases, this phase which wets the particle most is likely to be the continuous phase. The second factor in determining emulsion type is oil:water ratio. The phase with the largest volume is likely to be the continuous phase. It is possible that for one hydrophobicity of particle both types of emulsion can be observed. This change is induced by altering the oil:water ratios and can be done *in situ* to invert the emulsion from one type to the other. Phase inversion induced by altering the oil:water volume fraction is called catastrophic phase inversion. It is possible that for a given oil:water ratio, both types of emulsion can be observed by altering the wettability of the particles stabilising the system, either *in situ* or by preparing a series of systems stabilised by particles of different wettabilities. This is the equivalent of altering the HLB (hydrophile-lipophile balance) in surfactant stabilised systems.[29] This type of inversion is called transitional phase inversion.[30]

The stabilisation of emulsions by solid particles alone can be explained by the combination of two mechanisms.[31] Firstly, the absorption of the particles to the liquid-liquid interface forms a mono- or multi-layer which creates a physical barrier to coalescence. The more strongly a particle is held, the greater this barrier meaning the most stable emulsions are formed by particles of contact angle 90° where the energy of absorption is at its highest. The second mechanism is present if the particles within the continuous phase are capable of interacting with one another, forming a three dimensional network, which can increase the viscosity of the continuous phase.[32] This increase in viscosity leads to a decrease in the ability of the emulsion droplets to move and therefore a decrease in the rate of creaming/sedimentation and a decrease in the rate of coalescence. The extent to which a solid can stabilise an emulsion depends on particle size, particle shape, particle concentration, particle wettability and the microstructures formed by the particles themselves. The flocculation state of the particles is often identified as an important property, several studies have concluded that without some form of weak flocculation particles cannot stabilise emulsions.[33,34]

1.3.3 Solid-stabilised foams

There are many similarities between the behaviour of foams and emulsions.[35] Figure 1.8 shows a schematic representation of a particle-stabilised

Figure 1.8. Schematic representation of a particle-stabilised foam showing the direction of films drainage and the location and possible particle configuration of the solid particles.

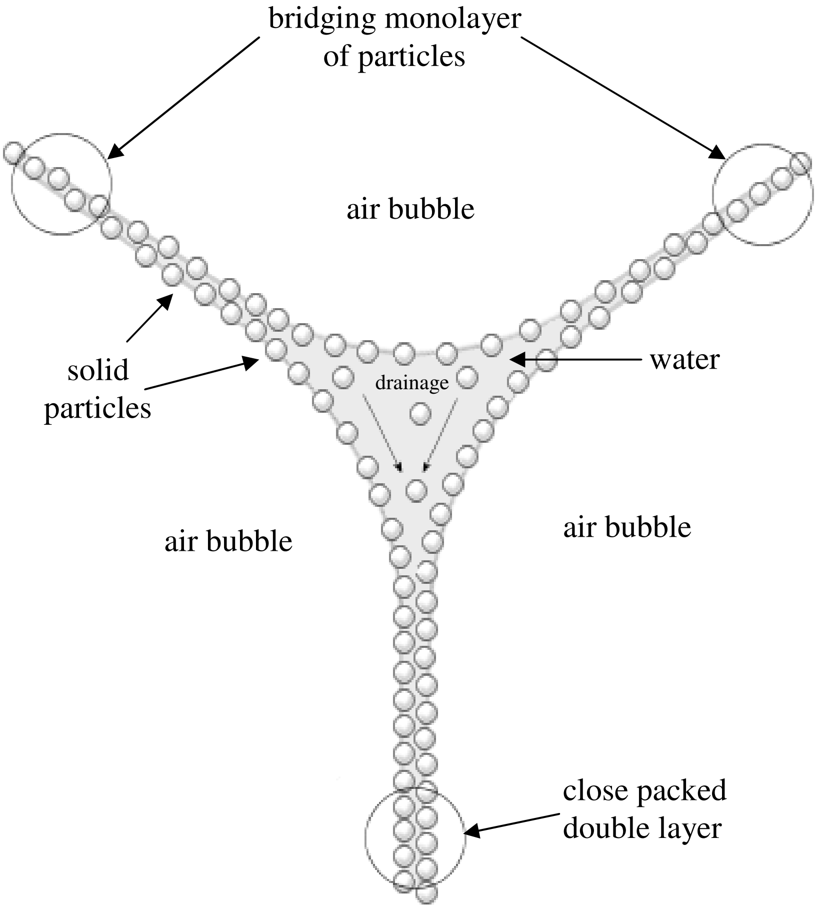

foam. Foams are a dispersion of air-in-water and can be considered analogous to an emulsion of air-in-water (a/w). Given this similarity in structure, it is not surprising that there are many similarities in the underlying mechanisms and principles of stability in both emulsion and foam systems. There are however, many notable differences. The dispersed volume phase is far larger in foams than in emulsions.[16] Foam bubbles are generally 10^3 times as large as emulsion droplets and these bubbles are much more compressible than emulsion droplets resulting in a typical polyhedral shaped structure for foams.[36] Analogous structure in emulsions do exist, however these are only observed in systems with very high dispersed phase volume fractions, such system are called high internal phase emulsions (HIPEs).[11] These system can be stabilised by solid particles alone.[37]

As with emulsion stabilisation, solid particles have been used for some time in conjunction with surfactants to stabilise aqueous foams. How they behave depends strongly on the surfactant type, particle size and concentration.[38,39] In these mixed systems, hydrophilic particles can act to slow drainage from the foam films and increase the stability of the system without adsorbing to the air-water surface. Hydrophobic particles can have the opposite effect, entering the air-water surfaces of the system and causing destabilisation. Recent work has begun to explore the use of solely solid particles to stabilise foam systems.[40,41,42]

Foams exhibit the same type of instabilities as described in Section 1.1.3 for emulsions. Film drainage which is the flow of continuous phase downwards through the foam due to gravity is the equivalent of creaming/sedimentation in emulsions. Film drainage can be very pronounced given the density difference between air and water. Film drainage results in film thinning and is the primary driving factor in producing the “dry” polyhedral structures present in some foams.[43] As in creaming/sedimentation in emulsions, film drainage produces a system where the chances of coalescence taking place is increased. Bubble coalescence is very similar to emulsion droplet coalescence and occurs when the thin film separating air bubbles ruptures. Coalescence of air bubbles is irreversible and if unchecked will lead to the collapse of the foam. Disproportionation is the analogous process of Ostwald ripening in emulsions. Disproportionation results in the growth of larger bubbles at the expense of smaller ones. Flocculation is less obvious in foams given the high dispersed phase volume fraction. However, flocculation can still occur between bubbles in the aqueous phase that have yet to join the main body of the foam. Figure 1.9 illustrates the structure of foam in three separate regions; (a) the top of the foam where the system is “dry”, (b) the bottom of the foam where the system is “wet”, and finally (c) where discreet bubbles are dispersed in the aqueous phase.

The mechanism of stabilisation of the thin films present in foams is similar to that for emulsions described above and relies on the energy of detachment of the solid particle from the air-water surface. The energy of detachment is calculated using Equation 1.4 when the oil-water interfacial tension is replaced by the air-water surface tension. It is worth noting that the literature regarding the stability of foams describes this stability in two different systems. One system in which the foam is being created and destroyed at the

Figure 1.9. Schematic representation of the structure of foam in three separate regions; (a) the top of the foam where the system is "dry", (b) the bottom of the foam where the system is "wet", and finally (c) where discreet bubbles are dispersed in the aqueous phase.

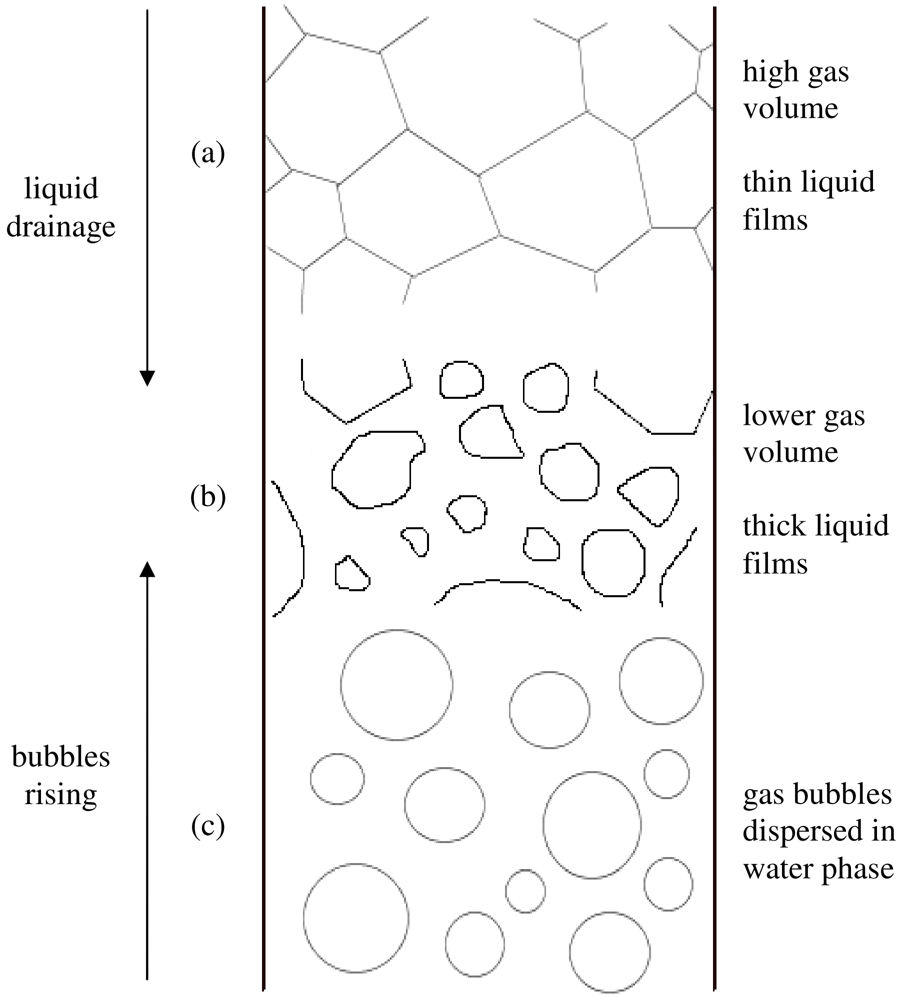

same time; the second in which equilibrium stability is described. For dynamic processes such as ore flotation, where foam is created and destroyed at the same time, the first stability is more relevant. In applications such as food technologies the equilibrium stability, analogous to the stability described in the literature for emulsions, is far more relevant. One interesting example of the use of solid particles to stabilise foams is in the formation and stabilisation of aluminium foams to create novel, lightweight material with high strength to weight ratios.[44]

1.3.4 Evaporation of emulsion systems

Previous work from our group[45,46] and elsewhere[47,48] has shown that there is a difference in evaporation rates between structured and non-structured liquids. When considering the evaporation of a two phase system the evaporation rate of the dispersed phase is retarded with respect to the pure liquid. This effect is increased in solid-stabilised systems where the thin film between the air-water (oil) surface of the bulk continuous phase and the oil-water interface of the dispersed phase droplet is thicker than in surfactant-stabilised systems.[49]

1.4 Aims of the study and structure of the thesis

The main aim of this study is to further the understanding of the effect of particle behaviour on the properties of the systems they stabilise. In particular the effect of modifying the particle in some way *in situ* at the oil-water interface.

Moreover, we are interested in identifying methods of producing more stable systems while identifying properties unique to particle-stabilised systems. Chapter 2 will introduce both the materials used in this work and the experimental procedures adopted.

Chapter 3 investigates the formation and modification of gold particles at the oil-water interface and describes an unusual spreading phenomenon induced by coalescence of particle-laden emulsion droplets. Chapter 4 is concerned with extending the investigation of the unusual spreading phenomenon to include particle film growth driven by the collapse of particle-laden foam bubbles. An explanation for the spreading phenomenon is given.

Chapter 5 investigates how the addition of a small amount of ethanol to particle-stabilised o/w emulsions can greatly enhance the stability of the system. The possible mechanisms for the increased stability are described and explored.

By altering the oil-water ratio of a solid stabilised system *in situ* through evaporation of the continuous phase Chapter 6 investigates the novel spreading of a drop of o/w emulsion after it has catastrophically inverted. Chapter 7 looks at altering the hydrophobicity of the particles stabilising an emulsion system by exposing hydrophobically modified silica particles to base to remove the hydrophobic coating. Particles were rendered sufficiently hydrophilic to induce *in situ* transitional phase inversion. Finally, Chapter 8 will provide a summary of the main conclusions.

1.5 References

---

[1] D.J. Shaw, *Introduction to Colloid and Surface Chemistry*, **3rd Edition**, Butterwort/hs, London (1980).

[2] T.D. Dimitrova, F. Leal-Calderon, T.D. Gurkov and B. Campbell, *Adv. Colloid Interface Sci.*, **108**, 73 (2004).

[3] S.C. Russev, T.V. Arguirov and T.D. Gurkov, *Colloids Surf. B*, **19**, 89 (2000).

[4] C. Alava and B.R. Saunders, *Colloids Surf., A*, **270-271**, 18 (2005).

[5] S. Shahalom, T. Tong, S. Emmett and B.R. Saunders, *Langmuir*, **22**, 8311 (2006).

[6] S. Tcholakova, N.D. Denkov and A. Lips, *Phys. Chem. Chem. Phys.*, **10**, 1608 (2008).

[7] S. Tcholakova, N.D. Denkov, D. Sidzhakova, I.B. Ivanov and B. Campbell, *Langmuir*, **19**, 5640 (2003).

[8] S. Tcholakova, N.D. Denkov and T. Danner, *Langmuir*, **20**, 7444 (2004).

[9] N. Vankova, S. Tcholakova, N.D. Denkov, I.B. Ivanov, V. Vulchev and T. Danner, *J. Interface Colloid Sci.*, **312**, 363 (2007).

[10] K. Golemanov, S. Tckolakova, P. Kralchevsky, K.P. Ananthapadmanabhan and A. Lips, *Langmuir*, **22**, 4968, (2006).

[11] S. Arditty, C. Whitby, B.P. Binks, V. Schmitt and F. Leal-Calderon, *Eur. Phys. J. E*, **11**, 273 (2003).

[12] S. Arditty, V. Schmitt, J. Giermanska-Kahn and F. Leal-Calderon, *J. Colloid Interface Sci.*, **275**, 659 (2004).

[13] T.D. Gurkov, S.C. Russev, K.D. Danov, I.B. Ivanov and B. Campbell, *Langmuir*, **19**, 7362 (2003).

---

[14] N.D. Denkov and K.G. Marinova, in *Colloidal Particles at Liquid Interfaces*, ed. B.P. Binks and T.S. Horozov, Cambridge University Press, Cambridge, 383-444 (2006).

[15] J.H. Clint, *Surfactant Aggregation*, Chapman and Hall, New York, (1991).

[16] E. Dickerson, *An Introduction to Food Colloids*, Oxford University Press, Oxford, 83, (1992).

[17] I.M. Lifshitz and V.V. Slezov, *Zh. Eksp. Teor. Fiz.*, **35**, 479 (1958).

[18] C.Z. Wagner, *Electorchemistry*, **35**, 581, (1961).

[19] R.J. Hunter, *Foundations of Colloid Science*, **Vol. 2**, Clarendon Press, Oxford (1995).

[20] N.D. Denkov, I.B. Ivanov, P.A. Kralchevsky and D.T. Wasan, *J. Colloid Interface Sci.*, **150**, 589 (1992).

[21] P.M. Kruglyakov and A.V. Nushtayeva, *Adv. Colloid Interface Sci.*, **108**, 151 (2004).

[22] S. U. Pickering, *J. Chem Soc.*, **91**, 2001 (1907).

[23] W. Ramsden, *Proc. Royal Soc.*, **72**, 156 (1903).

[24] B.P. Binks, *Curr. Opin. Colloid Interface Sci.*, **7**, 21 (2002).

[25] B.P. Binks and S.O. Lumsdon, *Langmuir*, **16**, 8622 (2000).

[26] B.P. Binks and J.H. Clint, *Langmuir*, **18**, 1270 (2002).

[27] S. Levine, B.D. Bowen and S.J. Partridge, *Colloid Surf*, **38**, 325 (1989).

[28] P. Finkle, H.D. Draper and J.H. Hildebrand, *J. Am. Chem. Soc.*, **45**, 2780 (1923).

[29] W.C. Griffin, *J. Soc. Cos. Chem.*, **1**, 311 (1946).

[30] B.P. Binks and S.O. Lumsdon, *Langmuir*, **16**, 2539 (2000).

---

[31] B.P. Binks and S.O. Lumsdon, *Langmuir*, **16**, 3748 (2000).

[32] S. Abend, N. Bonnke, U. Gutschner and G. Lagaly, *Colloid Polym Sci.*, **276**, 730 (1998).

[33] B.P. Binks and S.O. Lumsdon, *Phys. Chem. Chem. Phys.*, **1**, 3007 (1999).

[34] E.H. Lucassen-Reynders and M. van den Tempel, *J. Phys. Chem.*, **67**, 731 (1963).

[35] T.N. Hunter, R.J. Pugh, G.V. Franks and G.J. Jameson, *Adv. Colloid Interface Sci*, **137**, 57 (2008).

[36] R.J. Pugh, *Adv. Colloid Interface Sci.*, **114-115**, 239 (2005).

[37] A. Bismark, V. Ikem, A.Menner, M.Salgueiro and M.S.P. Shaffer, *Chem. Commun.*, 4274 (2007).

[38] P.M. Kruglyakov and P.R. Taube, *Colloid J.*, **34**, 194 (1972).

[39] R.J. Pugh, *Adv.Colloid Interface Sci.*, **64**, 67 (1996).

[40] S.K. Bindal, A.D. Nikolov, D.T. Wasan, D.P. Lambert and D.C. Koopman, *Environ. Sci. Technol.*, **35**, 3941 (2001).

[41] S.P. Armes, B.P. Binks, S. Fujii, R. Murakami and A. Schmid, *Langmuir*, **23**, 8691 (2007).

[42] B.P. Binks, B. Duncumb and R. Murakami, *Langmuir*, **18**, 9143 (2007).

[43] R.J. Pugh, *Adv. Interface and Colloid Sci.*, **64**, 67 (1996).

[44] S.W. IP, J.M. Toguri and Y.Wang, *Can. Metall. Q.*, **38**, 81 (1999).

[45] K.J. Beverley, J.H. Clint and P.D.I. Fletcher, *Phys. Chem. Chem. Phys.*, **1**, 149 (1999).

[46] K.J. Beverly, J.H. Clint and P.D.I. Fletcher, *Phys. Chem. Chem. Phys.*, **2**, 4173 (2000).

---

[47] S.E. Friberg and Q. Yin, *J. Disp. Sci. Technol.*, **20**, 395 (1999).

[48] S.E. Friberg and B. Langlois, *J. Disp. Sci. Techol.*, **13**, 223 (1992).

[49] I.A. Askargorta, Ph.D. Thesis, University of Hull, (2003).

CHAPTER 2

EXPERIMENTAL

2.1 Materials

2.1.1 Water

All water used was first de-ionised using reverse osmosis (Elgostat) then treated by a Milli-Q reagent water system. Surface tension measurements showed a typical value of 71.9 mN m^{-1} at 25 ^{o}C and a resistivity always above 18 MΩ cm.

2.1.2 Organic liquids

2.1.2.1 Oils

The oils used in this study are summarised in Table 2.1, together with their purity and source. All oils were passed through neutral aluminium oxide 3 times to further purify them further before use.

Oil	Source	Purity (%)
Cyclohexane	Aldrich	99
Dodecane	Aldrich	> 99.5
Isopropyl myristate (IPM)	Aldrich	99
Toluene	Fischer	99.9

Table 2.1. Summary of organic oils used.

2.1.2.2 Solvents

The non-aqueous solvents used in this study are summarised in Table 2.2, together with their purity and source. All solvents were used as received without further purification.

Solvent	Source	Purity
Acetonitrile	Fischer Scientific	> 99 %
Butan-1-ol	Fischer Scientific	AR
Ethanol	Fischer Scientific	AR
Propan-1-ol	Fischer Scientific	AR

Table 2.2. Summary of non-aqueous solvents used.

2.1.3 Particles

2.1.3.1 Fumed silica

Fumed silica powder was supplied by Wacker-Chemie and was prepared using a flame hydrolysis process. The standard techniques for the formation of silica particles date back to the 1960's.[1] Volatile silicon tetrachloride was introduced into a hydrogen/oxygen flame at approximately 1,200 °C. Hydrolysis produces dense silica particles with diameters of approximately 10 nm and hydrogen chloride according to the following chemical reaction

$$SiCl_4 + 2H_2 + O_2 \rightarrow SiO_{2\,(\mathrm{particle})} + 4HCl$$

Within the flame, the primary nanoparticles of silica irreversibly fuse to form branched primary aggregates with diameters in the range 100 – 500 nm. A primary aggregate is defined as a collection of primary particles that have fused to form a face-to-face sintered structure. These primary aggregates can flocculate reversibly to form agglomerates. An agglomerate is defined as a network of aggregates loosely held together at discrete points.[2] This process is represented schematically in Figure 2.1.

Fumed silica is formed from a tetrahedral structure. Individual Si atoms are linked by siloxane bridges (Si-O-Si). On the surface of the silica particles roughly

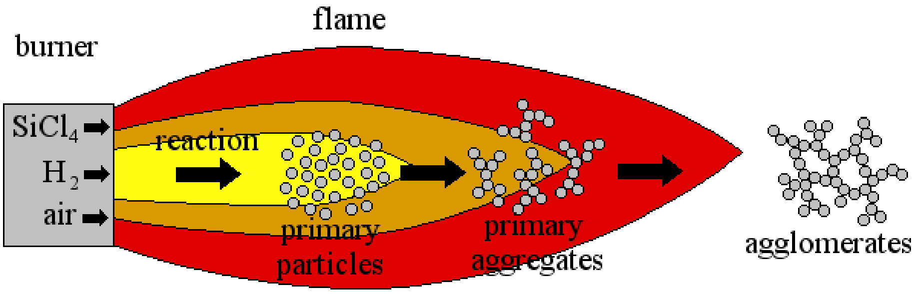

Figure 2.1. Schematic representation of the production of fumed silica via flame hydrolysis.

one in every two Si atoms has an OH group, i.e. silanol group (SiOH). These silanol groups are the origin of the hydrophilic nature of untreated silica particles. Silica particles can be chemically modified to cap the hydrophilic SiOH groups with hydrophobic species such as methyl groups. In this study two different coatings are used. The hydrophilic silica is treated with either dichlorodimethylsilane (DCDMS) or polydimethylsilicone (PDMS) according to the following reaction

$$\text{-Si-OH} + SiCl_2R_2 \rightarrow \text{-Si-O-}(SiClR_2) + HCl$$

where R is a methyl group for DCDMS and a longer chain for PDMS. It is possible that the remaining chlorine can now continue and react with another surface silanol group

$$\text{-Si-}(OSiClR_2) + \text{-Si-OH} \rightarrow \text{-Si-O-}(SiR_2)\text{-O-Si-}$$

The extent of coating is expressed by the amount of free silanol groups on the surface, i.e. a silica surface coated 20 % with DCDMS would be designated 80 % SiOH. Figure 2.2 shows a schematic representation of both a modified (hydrophobic) and unmodified (hydrophilic) silica particle. Table 2.3 lists the different silica particles used in this study, from very hydrophilic to very hydrophobic, for the two different types of surface treatment, DCDMS and PDMS. Since for both cases, DCDMS and PDMS coated, the particle being treated is the same then HDK N20 is 100 SiOH % for both the DCDMS and PDMS series.

All silica samples were prepared, characterised and supplied by Wäcker-Chemie, Germany.

2.1.3.2 Gold particles

Colloidal gold was formed by the citrate reduction of the gold salt hydrogen tetrachloroaurate(III).trihydrate using a modification of the method described by Chow and Zukoski.[3] Hydrogen tetrachloroaurate(III).trihydrate (99.9 %) and sodium citrate tribasic dihydrate (>99.0 %) were supplied by Aldrich and used without further purification. Aqueous citrate solution (20 cm^3) was added to aqueous gold salt solution (180 cm^3, concentration given later) at 70°C and the mixture held at this temperature with rapid stirring for 10 minutes. The gold salt solution was initially straw yellow in colour and then ~ 30 s after the addition of the citrate the solution became clear, then rapidly black. The colour of the solution

Figure 2.2. Schematic representation of (a) modified and (b) unmodified silica particles. For simplicity the particle is shown as spherical and hydrophilic groups are coloured blue and hydrophobic groups orange.

(a)

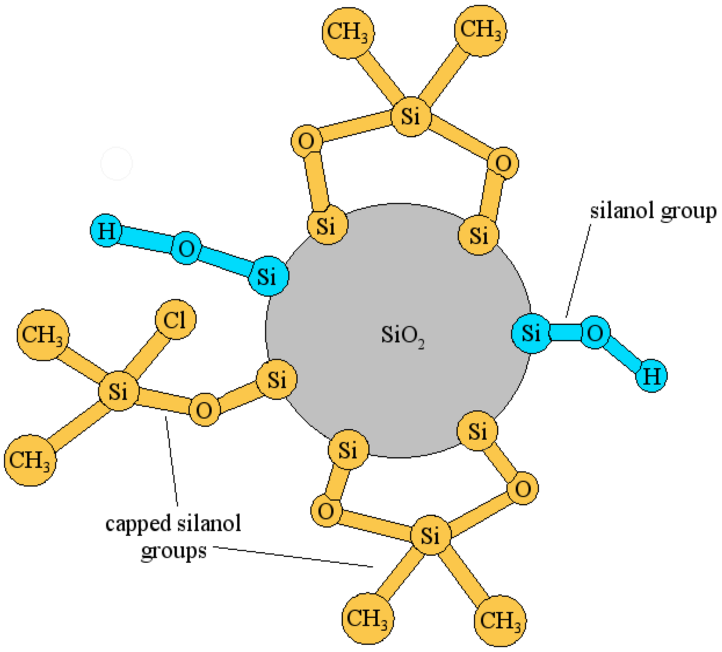

(b)

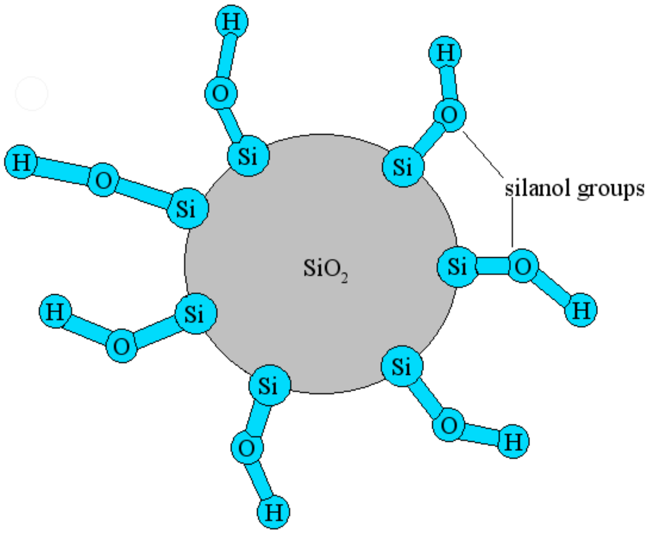

Table 2.3. Summary of the silica particles used with their free surface silanol content.

Silica particle code	**Mole % SiOH groups remaining on the particle surface**
HDK N20	100
SLM 4330002/68-18	88[a]
SLM 4330002/83-2648	78[a]
SLM 433002/135	71[a]
SLM 433002/150	67[a]
SLM 4330002/68-10	51[a]
SLM 4330002/68-20	42[a]
SLM 4330002/68-12	32[a]
H18	18[a]
SLM 4330002/01-1	92[b]
SLM 4330002/01-9	79[b]
SLM 4330002/01-2	58[b]
SLM 4330002/01/7	50[b]
SLM 4330002/01-10	43[b]
SLM 4330002/01-8	30[b]

[a] refers to DCDMS-coated

[b] refers to PDMS-coated

turned from black to purple, purple to blue and finally blue to wine red. At this point the reaction was stopped because the colour of the solution is an indication that the particles are in the desired size range.

The colour of gold colloid suspensions originates from the surface plasmon resonance (SPR) of the individual gold particles within the suspension. As the number of atoms in a metal cluster falls, and hence the size of the particle decreases, quantum size effects on the optical properties of that cluster become more important. SPR is the coherent excitation of all free electrons within a conduction band, leading to an all in-phase oscillation. For particles whose diameter is still small compared with the wavelength of light this oscillation occurs in the visible spectrum. The surface plays a large role in this feature as it places the constraints on the polarisibility of the metal. In this sense this type of behavior is intermediate between bulk optical properties and quantum effect; the effect could be described as a small particle or thin layer effect. The position and intensity of the SPR band gives an indication of the size and concentration of the particles. Large particles have a SPR at higher wavelengths.[4] This band is also sensitive to chemisorption and aggregation, although the exact changes in the spectra are dependent on the system being studied. A comprehensive introduction to this topic can be found in the textbook by Kreibig and Vollmer[5] and in the reviews by El-Sayed and Link[6] and Mulvaney[7].

The concentrations of hydrogen tetrachloroaurate(III).trihydrate and citrate after mixing but prior to reaction were 2.68 and 5.36 mM respectively. These concentrations were used in order to obtain the maximum gold content in a non-flocculated colloidal dispersion. It was found that higher reagent concentrations produced a flocculated gold colloid, presumably because the final ionic strength exceeded the critical flocculation concentration. Higher gold concentrations can be achieved only by additional treatment to remove the unwanted reaction by-products. The particle diameter distribution, determined using transmission electron microscopy, showed a single peak centered at 30 nm with a half width at half maximum of 9 nm.

2.1.3.3 Polytetrafluorethylene particles

Polytetrafluorethylene (PTFE) particles (Zonyl®MP1400 made by DuPont and supplied by E&E Ltd., UK) with a primary aggregate diameter of 7 – 12 μm and a specific surface area of 3 $m^2 g^{-1}$ were also used.

2.1.4 Other reagents

Throughout the course of this work some other materials have been used which are summarised in Table 2.4. In addition to these materials, planar silicon wafers with a thickness of 525 +/- 50 μm were supplied by Compart Technologies.

Reagent	Supplier	Purity (%)
Nitrogen gas	Energas	>99.9
Octadecylamine (ODA)	Fluka	> 99
Octadecyltrichlorosilane (OTS)	Aldrich	> 90
Sodium chloride	BDH	> 99

Table 2.4. Summary of the other materials used.

2.2 Methods

2.2.1 Contact angle measurements

The three-phase contact angle, measured through the aqueous phase, of an aqueous drop on a surface under either air or oil was measured using a Krűss Drop Shape Analysis (DSA) 10 instrument. All measurements were made at 25 ± 1 ^{o}C. To measure the static advancing three-phase contact angle a drop of the aqueous phase being studied would be formed on the surface using a 100 μl syringe fitted with a flat tipped steel needle. The volume of the drop would then be increased until the three phase contact line began to advance. At this point the needle is carefully removed and the image of the drop captured and processed using the DSA 10 instrument. In order to measure the receding three phase contact angle, the drop is formed in the same way as above but part of the drop is removed until the three phase contact line began to recede. Again at this point the needle is carefully removed and the image of the drop captured and processed. Another method to recover the static receding contact angle, when measuring under oil, is first to place the aqueous drop onto the surface under air and then carefully introduce the oil phase.

Depending on the system being studied it was necessary to pre-equilibrate the aqueous and oil phases first before taking the measurements. In studying the contact angle of the meniscus between the bulk phases in the gold film climbing experiment it was crucial that the oil and aqueous phases were pre-equilibrated. The measurements were made on a series of hydrophobically modified slides, which had been exposed to a 1 wt. % per volume solution of OTS in toluene for different lengths of time at room temperature under an N_2 atmosphere. Before exposure to the OTS solution the slides were cleaned by sonicating in ethanol for 30 minutes. After exposure to the OTS solution the slides were washed thoroughly with fresh toluene, then with fresh ethanol and finally placed in an oven at 80 ^{o}C overnight to drive off any moisture trapped in the hydrophobic layer. The four different protocols for investigating the direction of the meniscus in the gold climbing experiments are listed below.

(a) Non-pre-equilibrated: oil first

The modified slide was taken and placed in a glass cell which held ~ 9 ml of dodecane containing 8 x 10 $^{-5}$ M ODA and allowed to thermally equilibrate for 5 minutes. A drop of the standard aqueous gold colloid was formed under the oil and contacted the slide surface. The drop was left to equilibrate for 5 minutes and the contact angle measured.

(b) Non-pre-equilibrated: aqueous first

A drop of the standard aqueous gold colloid was formed under air and contacted the slide surface within a DSA cell. ~ 9 ml of dodecane containing 8 x 10 $^{-5}$ M ODA was added to the cell and the system was left to equilibrate for 5 minutes. The contact angle was then measured.

(c) Pre-equilibrated: oil first

Before the contact angle measurements were made the two phases were pre-equilibrated in the following way. The standard aqueous gold colloid and the dodecane containing 8 x 10 $^{-5}$ M ODA were added together in a 5:1 volume ratio in a stoppered hydrophilic glass test tube. The system was then shaken vigorously by hand for 20 seconds and the gold film allowed to grow. Once film growth had ceased, the two phases were transferred to a different vessel and separated. A drop of the pre-equilibrated standard aqueous gold colloid was formed under air and contacted the slide surface within a DSA cell. ~ 9 ml of the pre-equilibrated ODA in dodecane solution was added to the cell and the system was left to equilibrate for 5 minutes. The modified slide was taken and placed in a glass cell which held ~ 9 ml of the pre-equilibrated ODA in dodecane solution and allowed to thermally equilibrate for 5 minutes. A drop of the pre-equilibrated standard aqueous gold colloid was formed under the oil and contacted the slide surface. The drop was left to equilibrate for 5 minutes and the contact angle measured.

(d) Pre-equilibrated: aqueous first

The two phases were pre-equilibrated as described above. A drop of the aqueous phase was placed on the modified glass slide under air and then ~ 9 ml of the oil phase added. The drop was allowed to equilibrate for 5 minutes and the contact angle measured.

2.2.2 Particle dispersions

Homogeneous dispersions of silica in either pure water or oil were prepared by dispersing a known mass of the dry powder in the liquid using a high intensity ultrasonic vibracell (Sonics & Materials) with a tip diameter of 3 mm operating at 20 kHz and up to 10 W for 2 minute time periods. In order to prevent heat build up it was necessary to cool the dispersion using an ice bath. When hydrophilic silica was dispersed into water the resulting dispersion was usually bluish and fluid. When hydrophobic silica was dispersed into oil the resulting dispersion was usually clear and, depending on the concentration of particles, the system could be gelled.

In order to disperse hydrophobic particles into water it was necessary first to wet them with an aqueous alcoholic phase (~ 25 % ethanol by volume), then to sonicate. The ethanol was removed by repeated centrifugation / wash cycles. No fewer than 7 cycles were used. Initially the hydrophobic particles dispersed well into the aqueous alcoholic phase. However, as the ethanol concentration is lowered by the centrifugation / wash cycles, the dispersion becomes more and more flocculated. The resulting dispersion is heavily flocculated but all the hydrophobic particles are wet by the aqueous phase.

2.2.3 Emulsion preparation and characterisation

The standard protocol for the preparation of emulsions is as follows. The required amount of aqueous and oil phase are added together into a 20 ml glass sample tube. The system is then homogenised for 2 minutes at 11,000 rpm using an Ultra Turrax T25 homogeniser fitted with an 18 mm head. The term ‘preferred’ is used to describe a system which has equal volumes of oil and water. The type of emulsion is then characterised by either measuring its conductivity using a Jenway 4510 conductivity meter calibrated or by the qualitative method called the drop test. If a drop of water continuous emulsion is added to a bulk water phase then the drop of emulsion should disperse. If it is added to a bulk oil phase the drop of emulsion should remain discrete and sediment. If a drop of oil continuous emulsion is added to bulk oil then it should disperse and if it is added to bulk water then it should remain discrete and cream. This is illustrated in Figure 2.3.

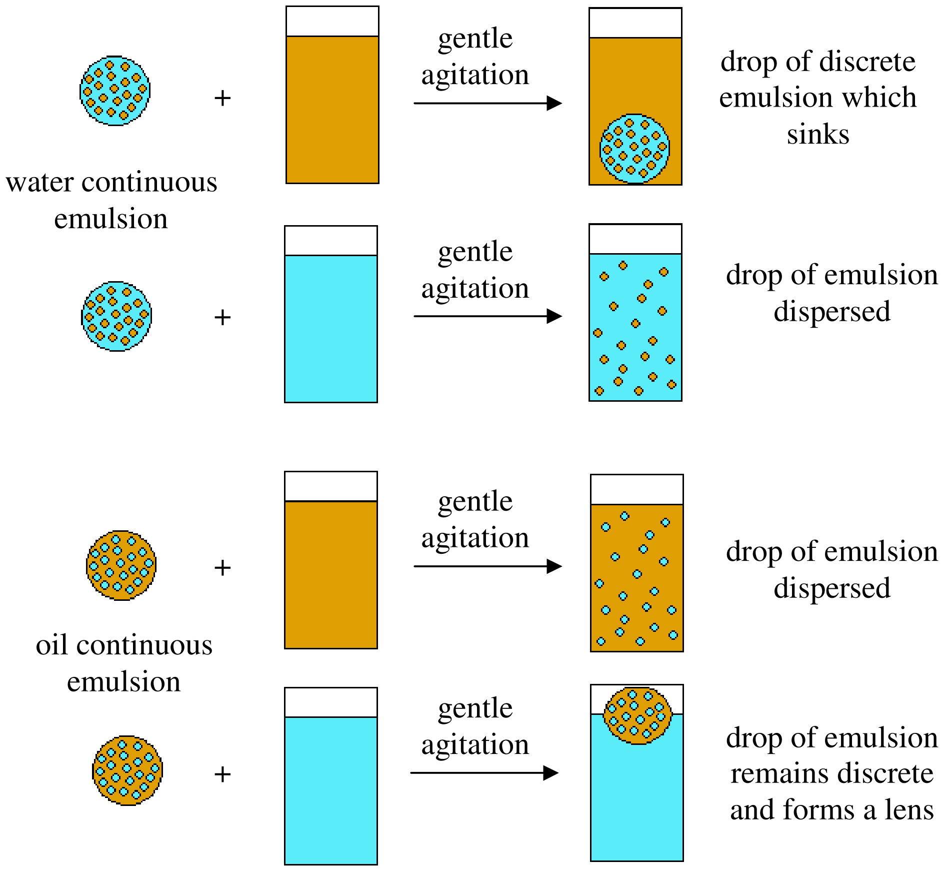

Figure 2.3. Schematic representation of the drop test indicating the continuous phase of an emulsion.

The stability of an emulsion was studied by following the appearance of the emulsion with time and noting the positions of any boundaries. Using equations 2.1 and 2.2 the volume fraction of oil (ϕ_{OR}) and water (ϕ_{WR}) resolved at a certain time can be calculated

$$\phi_{OR} = \frac{V_{OR}}{V_{TOT}\phi_O} \tag{2.1}$$

$$\phi_{WR} = \frac{V_{WR}}{V_{TOT}(1-\phi_O)} \tag{2.2}$$

where $V_{OR,\mathrm{WR}}$ is the volume of oil (water) resolved after a certain amount of time, V_{TOT} is the total volume of the system and ϕ_O is the volume fraction of oil in the emulsion. ϕ_{WR} and ϕ_{OR} are expressed relative to the volume fraction of water and oil added originally. Using equation 2.3 the amount of emulsion cream resolved with time (ϕ_{CR}), relative to the total volume of the system, can be calculated

$$\phi_{CR} = \frac{V_{CR}}{V_{TOT}} \tag{2.3}$$

where V_{CR} is the volume of the cream resolved after a certain time.

It was necessary to prepare emulsions stabilised by hydrophilic silica containing different amounts of ethanol in the aqueous phase. This was done according to 2 different protocols.

(a) Protocol 1

10 ml of emulsion was prepared in the following way. Hydrophilic silica powder was initially dispersed into the required amount of pure water by sonication for 2 minutes at 10 W using the ultrasonic probe. During sonication the solution was

cooled using an ice bath. To this silica dispersion, the necessary amount of co-solvent was added and the system shaken. The combined volume of the aqueous phase was maintained at 5 ml. After the addition of 5 ml of dodecane, the system was homogenised for 2 minutes using an Ultra Turrax T25 homogeniser operating at 11,000 rpm with a 18 mm head.

(b) Protocol 2

10 ml of emulsion was prepared in the following way. Hydrophilic silica powder was dispersed into a pre-prepared aqueous/co-solvent solution by sonication for 2 minutes at 10 W using the ultrasonic probe. During sonication the solution was cooled using an ice bath. The combined volume of the aqueous phase was maintained at 5 ml. After the addition of 5 ml of dodecane, the system was homogenised for 2 minutes using an Ultra Turrax T 25 homogeniser operating at 11,000 rpm with a 18 mm head.

In the case of both protocols 1 and 2, the addition of co-solvent led to an increase in the turbidity of the system. The increase in turbidity became apparent to the eye at different concentrations of co-solvent depending on the nature of the co-solvent used. For example, for the addition of ethanol an increase in turbidity became apparent at a volume fraction of 0.15. The increase in turbidity became more pronounced at higher ethanol concentrations until at an ethanol volume fraction of 0.4 visible aggregates could be seen.

2.2.4 Films grown through emulsion drop coalescence

Except where otherwise stated, the standard gold film spreading conditions were as follows. 5 cm^3 of the gold dispersion containing 2.68 mM Au at a pH of ~ 4 and 1 cm^3 of dodecane containing 0.08 mM ODA were contained within a stoppered glass test tube of internal diameter 13 mm. The aqueous phase was wine red in colour and the oil phase was transparent. Hand shaking for 20 s caused a visible, gold metallic colored film to rise up the walls to the top of the test tube (approx. 70 mm above the oil-air surface) within a few seconds. When required, the pH of the aqueous phase was altered by the addition of small volumes of 1 M NaOH. For some experiments the inner walls of the test tubes were hydrophobically modified using a 1 wt. % solution of octadecyltrichlorosilane (OTS) in toluene under a nitrogen atmosphere for different set times.

The film growth, due to the coalescence of 1 emulsion drop with the planar oil-water interface was studied in the experimental apparatus shown in Figure 2.4. (a) is the setup used to study a drop of dodecane containing ODA rising through a continuous phase of aqueous gold colloid and (b) is the setup used to study the sedimentation of a drop of aqueous gold colloid falling through a continuous phase of dodecane containing ODA.

In both cases the drop was formed using a 1 ml syringe. In (a) the drop was formed on the tip of a steel syringe which was pushed through a rubber seal on the

Figure 2.4. Experimental setup used to study (a) a drop of dodecane containing ODA rising through a continuous phase of aqueous gold colloid and (b) a drop of aqueous gold colloid falling through a continuous phase of dodecane containing ODA. The diameter of the glass tube is 9 mm.

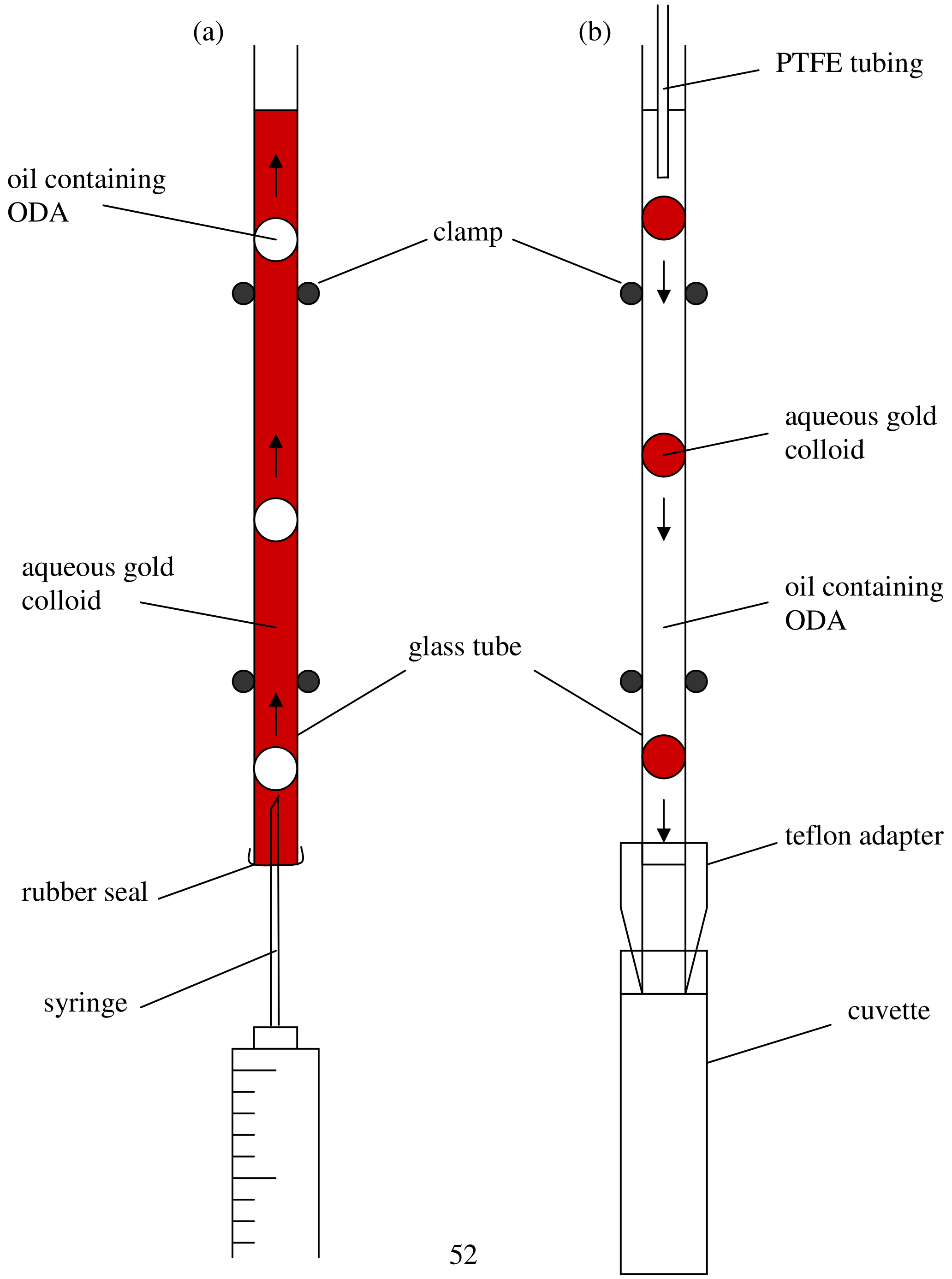

bottom of the glass tubing and in (b) the drop was formed at the end of a length of PTFE tubing suspended at the top of the tubing. In order to form a drop which took a sufficient length of time to rise / fall through the continuous phase the diameter of the drop had to be only slightly less than that of the glass tubing (9 mm). In both cases, when the drop diameter was only slightly less than that of the glass tubing, the drop took ~ 25 seconds to rise / fall the length of the aqueous phase (90 cm). Digital images of the rising / falling drops were captured using a Kodak Easyshare CX7530 5.0 megapixel camera set at the highest resolution.

2.2.5 Films grown through foam bubble coalescence

Two types of particle were used. The first was fumed silica particles and the second was PTFE particles. The film growth experiments can be summarised as follows. A small mass, typically 0.01 g, of hydrophobic particles was placed on the surface of 10 ml of water in a measuring cylinder (28 mm inner diameter, 200 mm height). Vigorous hand shaking for 20 s produces a few ml of unstable foam bubbles. When shaking is stopped, coalescence of the foam bubbles with the planar air-water surface causes a water film stabilised by the silica particles to climb rapidly up the inner glass walls of the measuring cylinder, typically within a second or so. If the system is re-shaken, the film is lost and foam bubbles are re-formed which, when shaking stops, again coalesce causing the film to re-climb the walls.

Films for microscopy were produced in a home-built cell which had a well of dimensions 13 x 63 x 3 mm. Following addition of water and particles, a standard microscope slide was placed on top of the well to seal it. Shaking of the cell produced a particle film on the lower surface of the slide which could then be removed, dried and imaged. The cell is shown in Figure 2.5

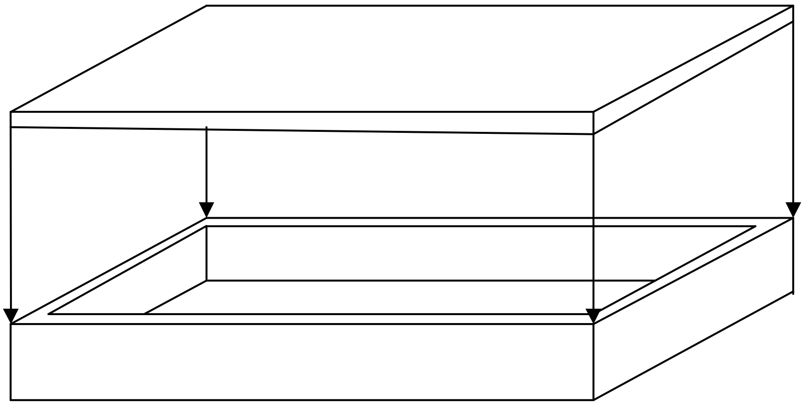

Figure 2.5. Schematic representation of the homebuilt film growth cell dimensions of 13 x 63 x 3 mm.

2.2.6 Interfacial tension measurements

The pendant drop mode of the Krűss Drop Shape Analysis System DSA 10 was used to measure the oil-water interfacial tension (IFT) of various systems as a function of the drop size for different aqueous phases. An aqueous drop was suspended from the tip (diameter 3.034 mm) of a flat, steel syringe needle. The IFT is measured as a function of the drop volume at 25 ^{o}C. The software fits a profile to the outside of the drop and then using Laplace fitting calculates the IFT. The tip of the needle is submerged into dodecane and then the drop is formed. Once formed, the drop is allowed to reach thermal equilibrium (5 minutes). The volume of the drop and the IFT are recorded using the DSA 10. Once the initial volume and IFT have been established, the drop volume is reduced sequentially and the IFT recorded at each volume until the smallest practical volume is reached (limited by the shape of the drop). Once this volume has been achieved the drop is re-expanded sequentially until the original volume has been reached to measure any hysteresis. The theoretical and experimental parameters of measuring IFTs by the pendant drop method are investigated in two papers by Song and Springer who, as well as suggesting optimum conditions for performing the experiment, identify the common sources of error.[8,9]

2.2.7 Particle dispersion sedimentation rate

Aqueous dispersion of hydrophilic silica were prepared and studied using the automated dispersion stability analyser (DiStA 24) designed and operating in our laboratory. The analyser operates by taking consecutive images of the samples and analysing them using a personal computer (PC). The analyser can make many measurements over a long time and is effective at studying both rates of sedimentation and the aging of an emulsion system, i.e. creaming, sedimentation and coalescence.[10] Once formed the silica dispersions were shaken and then immediately transferred into the sample holders. The software was set to take a measurement every 2 minutes for 5 measurements, then a measurement every 5 minutes for 10 measurements, then a measurement every 12 minutes for 100 measurements, followed finally by a measurement every 30 minutes for 72 measurements. In total the samples were studied for 57 hours.

2.2.8 Scanning electron and transmission electron microscopy

Scanning electron micrographs were taken using a Zeiss EVO 60 SEM instrument with a voltage of 22 kV and a probe current of 20 pA. Samples for SEM were coated with an Au/Pd (mass ratio 82:18) film of 1.5 nm thickness and attached to the sample mount using a conductive silver solution. SEM images were recorded with the samples tilted up to 40^{o} from horizontal.

Transmission electron micrographs of gold colloid were taken in the following way. A drop of the colloidal suspension to be studied was placed on a carbon coated, 300 mesh copper grid. The grids were left for 15 min. to allow the particles to settle onto the carbon film and to dry the sample, after which time they were ready to view. The grids were viewed in a Jeol 100C transmission electron microscope at 100 kV.

2.2.9 Evaporation of solid-stabilised oil-in-water emulsions

Hydrophobic glass slides (25 x 25 mm) were prepared by exposure to a 1 wt. % per volume solution of OTS in toluene under N_2 for different lengths of time, washed with fresh toluene and fresh ethanol and placed in an oven at 80 °C overnight to drive off any moisture trapped in the hydrophobic layer. The wettability of the slide depends on the length of time exposed to the OTS solution. A typical slide would be exposed to the solution for 30 minutes giving a contact angle of a water drop on the surface under air of 100 +/- 5 degrees.

Standard emulsification was performed, i.e. 2 minutes at 11,000 rpm and a drop of the emulsion (~ 50 μl) placed on the hydrophobically modified slide and allowed to evaporate. The appearance of the drop was followed with time using the DSA 10 instrument and the tracker man feature which allows the capture of a digital image at regular intervals. The drop was open to the atmosphere. Typically 1 picture would be taken every second for 3 hours. The still images were then converted to video files (.avi) using VideoMach 3.5.2 software. After formation of the video file it was necessary to keep only every 10th frame and delete the rest due to the large number of image files generated on each run and the demand on physical storage this creates.

During the experiment no attempt was made to control either the flow of gas over the system or the temperature. This is because the kinetics of the phenomena observed were not being studied and these parameters would simply change the rate of evaporation.

In order to study the effect of volume fraction of dispersed phase on the stability of the drop of emulsion it was necessary to calculate the volume of each drop from its image. As the drop of emulsion evaporates the fine focus of the image captured on the DSA 10 is often lost. This means that the DSA software is unable to extract the profile of the drop and because of this is unable to calculate the volume of the drop. The visual basic code found in Appendix I was constructed to calculate the volume of a drop from its image.

The drop profile is recorded using the DSA 10 and the image is then processed using Image Pro Plus 5.0 software. Image Pro Plus returns a 'bit map analysis' of the image which can be opened in Excel. Each pixel is represented by a cell in Excel with an intensity value. When the above code is run on the bitmap analysis it returns the volume of the drop in $(\text{pixel})^3$ as a function of the cut-off intensity. The cut-off intensity is simply the value below which a cell is included in the volume calculation. The macro was tested using an ideal drop so that the volume could be measured using the DSA as well. Figure 2.6 (a) is a section of the bit map analysis of the ideal drop with a cut off intensity of 60. All the cells which are included in the volume calculation are shaded grey. Figure 2.6 (b) is the plot of drop volume versus cut-off intensity returned by the macro for this drop. The horizontal line marked on (b) is the volume measured by the DSA instrument.

Figure 2.6. (a) Section of the bit map analysis of the calibration drop and, (b) plot of drop volume versus threshold intensity returned by the macro. The horizontal line marked on (b) is the volume measured by the DSA instrument.

(a)

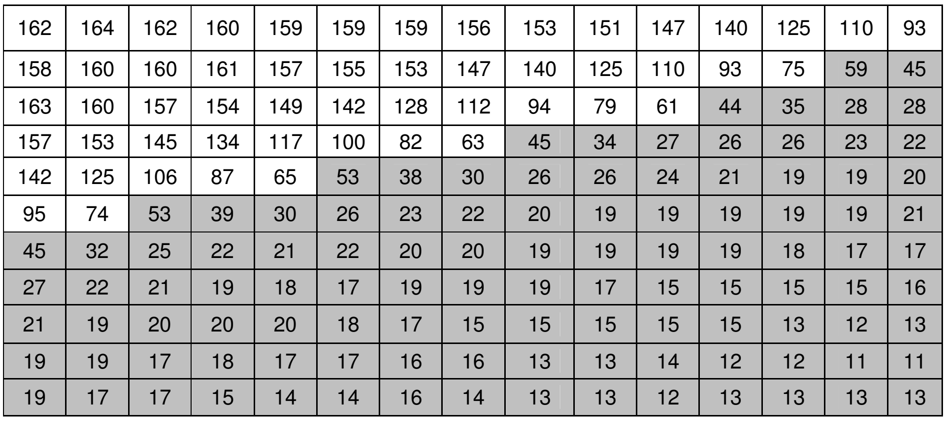

162	164	162	160	159	159	159	156	153	151	147	140	125	110	93
158	160	160	161	157	155	153	147	140	125	110	93	75	59	45
163	160	157	154	149	142	128	112	94	79	61	44	35	28	28
157	153	145	134	117	100	82	63	45	34	27	26	26	23	22
142	125	106	87	65	53	38	30	26	26	24	21	19	19	20
95	74	53	39	30	26	23	22	20	19	19	19	19	19	21
45	32	25	22	21	22	20	20	19	19	19	19	18	17	17
27	22	21	19	18	17	19	19	19	17	15	15	15	15	16
21	19	20	20	20	18	17	15	15	15	15	15	13	12	13
19	19	17	18	17	17	16	16	13	13	14	12	12	11	11
19	17	17	15	14	14	16	14	13	13	12	13	13	13	13

(b)

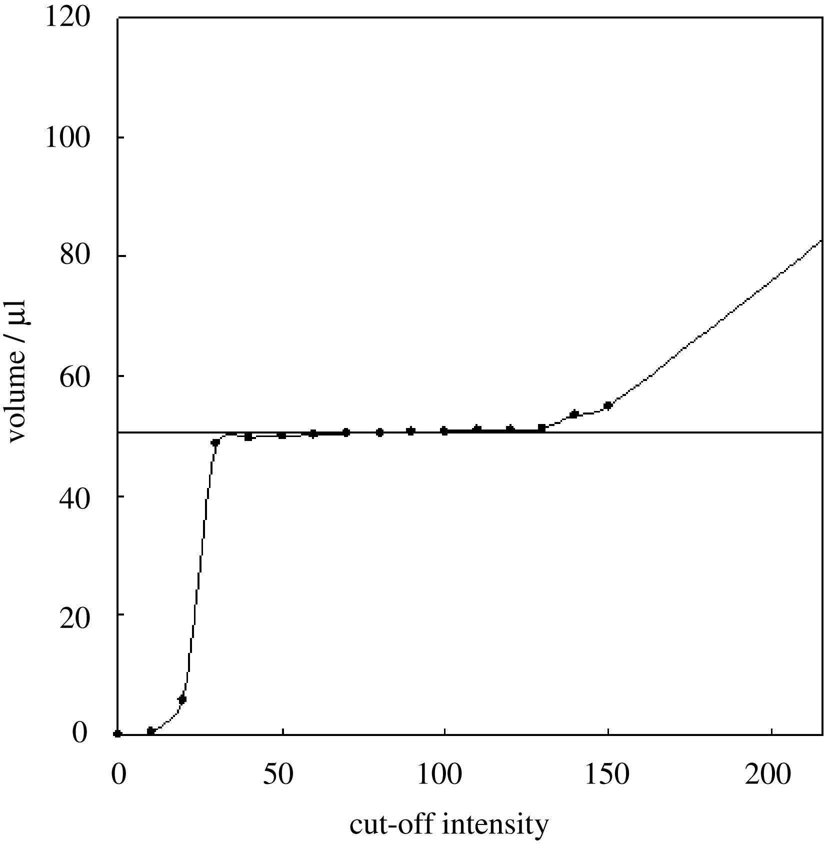

2.2.10 In-situ modification of hydrophobic silica by base

Hydrophobic silica particles (H18, 20 % SiOH) were modified in the following way. 2 wt. % (per volume of the total emulsion) silica particles were initially dispersed into the aqueous phase (7.5 ml water) by wetting with ethanol. 25 wt. % ethanol was added in order to sufficiently wet the particles and allow them to enter the aqueous phase. The system was then sonicated for 2 minutes at 10 W using the ultrasonic probe as described previously. The ethanol was removed by 7 washing and centrifugation cycles. Figure 2.7 shows that after this number of cycles the ethanol concentration can be calculated to be approximately 5 x 10^{-4} wt. %. Each wash/centrifugation cycle comprised of 5 minutes centrifugation at 3,500 rpm after which the clear supernatant was removed from above the sedimented silica. (Some of the silica particles, presumably those that were not wet completely by the ethanol and still contained some air, rose to the air/water surface). After each centrifugation the supernatant was removed and the sample was returned to the same weight by the addition of fresh water and then dispersed by sonication for 2 minutes at 10 W. After the final centrifugation fresh water was added so that the sample was the same weight as before the addition of the ethanol.

After the first sonication, when the concentration of the ethanol was high, the particles appeared well dispersed, i.e. homogeneous with no visible flocs. After each wash/centrifugation cycle, as the ethanol concentration decreased, the system became less homogeneous and mm sizes flocs were visible.

Figure 2.7. Concentration of ethanol remaining in the aqueous dispersion as a function of the number of centrifugation / wash cycles.

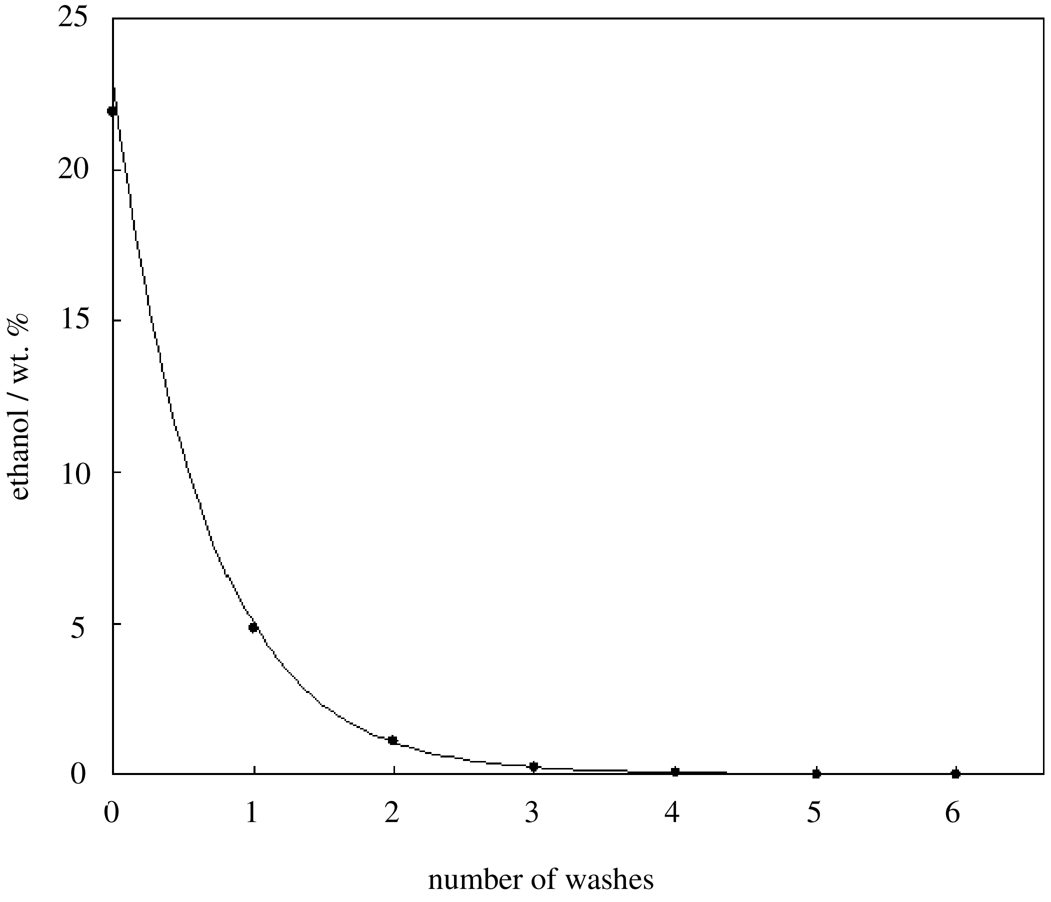

15 ml of emulsion was then prepared using the aqueous particle dispersion of hydrophobic particles. The w/o emulsion was stabilised by 2 wt. % hydrophobic particles initially dispersed into the aqueous phase. The oil used was dodecane and the oil volume fraction was 0.5. In order for the coating on the particle to have sufficient opportunity to be hydrolysed the system was emulsified for 2 hours. The system was homogenised at 11,000 rpm using the Ultra Turrax for 3 minutes followed by 30 seconds rest then another 3 minutes homogenisation etc. until the total homogenisation time was 2 hours. During homogenisation the system was thermostatted at 40 ^{o}C using a Grant LTD6G thermostat and the temperature of the system was checked at regular intervals to ensure that it did not deviate from this value. At 21 minute intervals the system was removed from the bath and the identity of the continuous phase identified by both conductivity measurements and by drop test. The appearance of the system was also noted. After homogenisation the system was stored in a water bath at 25 ^{o}C and the appearance of any phases with time noted.

2.2.11 UV/Visible absorbance spectroscopy

UV/Visible absorbance spectroscopy was performed on a Unicam UV3 spectrophotometer at 25 ^{o}C. Samples of aqueous gold colloid suspension were prepared by dilution with pure water and analysed in suprasil quartz cells with a path length of 10 mm and a volume of ~ 7 ml supplied by Hellma. Each sample was measured versus air against a baseline of pure water versus air in the same cell. The data from the spectrophotometer was collected and analysed using Vision32 software.

2.2.12 Hydrophobic modification of glass surfaces

If the surface being modified was the inside of a curved glass vessel then a flat glass substrate was modified at the same time to allow the contact angle of the inside of the glass vessel to be measured by the standard contact angle technique. Before the modification, the glass surface was dried in an oven at 180 ^{o}C. The modification was performed under an N_2 atmosphere with the traces of H_2O removed by scavenging with P_2O_5. A 1 wt. % by volume solution of OTS in toluene was prepared and the glass surface exposed to the solution. The OTS solution was allowed to react for the required amount of time at room temperature and then the glass surface was washed with fresh toluene twice, then ethanol twice then placed in an oven at 180 ^{o}C overnight to drive off any water trapped in the hydrophobic layer. After modification, using a sessile drop technique on the DSA 10 instrument, the contact angle of a water drop on a flat glass substrate under air was determined.

2.2.13 Optical microscopy

Optical microscopy of emulsions was performed using a Nikon Labophot optical microscope fitted with DIC-U camera (World Precision Instruments) at both 10x and 40x magnification. Images of the drops were edited using Adobe Photoshop

5 software. The sample was prepared by dilution with aqueous phase in a ratio of ~ 1:15. The diluted sample was then placed on a microscope slide containing a dimple and covered with a glass cover slip.

2.3 References

---

[1] A. Fink and W. Stober, *J. Colloid Int. Sci.*, **26**, 62 (1968).

[2] Wäcker-Chemie manufactures literature, *There's more to it than you think. HDK – Pyrogenic Silica*, www.wacker.com (accessed June 2008).

[3] M.K. Chow and C.F. Zukoski, *J. Colloid Interface Sci.*, **165**, 97 (1994).

[4] S. Link and M.A. El-Sayed, *J. Phys. Chem. B*, **103**, 8410 (1999).

[5] U. Kreibeg and K. Vollmer, *'Optical properties of Metal Clusters'*, Springer, Berlin, (1995).

[6] S. Link and M.A. El-Sayed, *Int. Rev. Phys. Chem.*, **19**, 409 (2000).

[7] P. Mulvaney, *Langmuir*, **12**, 7888 (1996)

[8] B. Song and J. Springer, *J. Colloid Interface Sci.,* **184**, 64 (1996).

[9] B. Song and J. Springer, *J. Colloid Interface Sci.*, **184**, 77 (1996).

[10] B.P. Binks and T.S. Horozov, *Langmuir*, **21**, 9007 (2004).

CHAPTER 3

GOLD PARTICLES MODIFIED AT THE OIL-WATER INTERFACE BY A LONG CHAINED AMINE

3.1 Introduction

There is a lot of interest within the literature regarding the optical properties of dilute dispersions of nano-sized colloidal metal particles.[1,2,3] Connected with this, much effort has been put into the phase transfer of metallic nanoparticles from the aqueous phase into an organic phase and vice-versa.[4,5,6] However, little work has been done to investigate the behaviour of electrostatically stabilised particles as they pass through the oil-water interface while transferring from the aqueous into the organic phase. This represents a relatively complex system compared to uncharged particles. Examples of this type of system are aqueous dispersions of gold[7], palladium[8] or silver particles[9,10] in the nano-size range stabilised by citrate, which can be transferred into an organic phase, typically toluene or heptane, by interaction with a long chained amine or thiol.[11,12] Since the long chain thiol and amine are effectively insoluble in the aqueous phase, the modification of the particles must occur at the interface. It is possible to imagine a system where the concentrations of particles and surface modification agents are such that it is possible to bring a particle to the interface and coat enough of the surface to retain the particle at the interface, but not enough for phase transfer from the aqueous to the organic phase to occur.[13]

This behaviour has been noted by Mayya and Sastry[14] who were investigating the transfer of carboxylate modified gold particles from the aqueous phase into an organic phase by interacting them with long chained amines. They noted that for particular concentrations of long chain amine and gold colloid, and at certain pH values, it was possible to trap the particles as a gold film at the oil-water interface. Not only were the particles immobilized at the oil-water interface but also they spread rapidly up the side of the glass vessel. They proposed that the particles were spreading on a thin film of liquid at the vessel-air interface driven by the Marangoni effect.

This chapter focuses on extending the understanding of this interesting phenomena and providing a more satisfactory mechanism for the spreading. Solid-stabilised systems typically contain a relatively high wt. % of particle and this chapter initially explores the synthesis of concentrated suspensions of gold colloids. Using the concentrated gold colloid suspensions the film climbing is explored as a function of pH and vessel hydrophobicity. A new mechanism is presented and confirmed using a series of single drop experiments.

3.2 Preparation of aqueous gold colloids

Colloidal gold was formed by the citrate reduction of aqueous Au^{3+} ion, present in the form $AuCl_4^-$. During the synthesis, after the addition of citrate to the boiling salt solution, there is a series of colour changes. Initially there is a 5 – 10 second period where no change occurs, then the solution rapidly turns black (< 1 second). After this sharp colour change, the solution gradually turns through purple, then blue, before turning the characteristic deep wine red colour of nanometre gold colloidal particles. The time taken for these colour changes to occur depends both on the concentration of the reactants and the temperature of the reaction. This series of colour changes is reported and explained by Zukoski et al.[15] who show that the formation of small gold particles is through intermediate large, diffuse, fluffy aggregates which are responsible for the black colour. These act as reservoirs for Au^{3+} and citrate ions, finally reducing in size as the reaction takes place to lead to smaller more dense particles. As the particles reduce in size this changes the wavelength of the surface plasmon resonance (SPR) absorption band resulting in the colour change. The colloidal material formed in this process is electrostatically stabilised by adsorption of citrate molecules onto the surface of the particles resulting in a net negative charge. Because of this the citrate had to be present in excess in the system in order to reduce both the Au^{3+} ions and stabilise the resulting colloidal material. The vast majority of literature on the synthesis of gold colloids is for the study of the optical properties of the system; this requires only low concentrations of particles in solution due to the high optical density of this type of material.[16,17,18] The study of particles at interfaces, and particularly the stabilisation of emulsions by particles, requires significantly more particles to be present in the system.[19] Even though the citrate stabilises the gold particles, it is desirable to have as low a concentration of free citrate as possible in the final gold colloid dispersion. Due to the polyionic nature of the citrate ions they effectively shield the electrical double layer around the colloidal particles reducing the repulsion, and inducing flocculation if the concentration is above a critical level. To have as high a concentration of gold in the final dispersion as possible, the excess citrate had to be kept to a minimum. Colloidal dispersions of gold could be formed and stabilised with a molar ratio of 2:1 citrate to gold.

A range of initial $HAuCl_4$ salt concentrations has been used to synthesise the gold colloid with the citrate to gold ratio fixed at 2:1. The maximum concentration of $HAuCl_4$ salt that can be used, and still produce stable gold colloids, is 2.6×10^{-3} mol dm^{-3}. This corresponds to ~ 0.2 g in 200 ml or 0.10 weight percent per volume. Higher concentrations of $HAuCl_4$ can be used to form gold colloids; however these colloids are not stable and over a period of 48 hours turn black and sediment. For example, concentrations as high as 3.0×10^{-3} mol dm^{-3} could be used. The system produced was initially stable and deep wine red in colour but rapidly darkened to black and sedimented. Figure 3.1 shows the UV-Vis absorbance spectra for the standard synthesis of the gold colloid. This was formed using an initial gold

Figure 3.1. UV-Vis absorbance spectra for several aqueous gold colloidal dispersions formed from different initial concentrations of $HAuCl_4$. Path length was 10 mm and the sample was diluted with water in a 1:5 ratio.

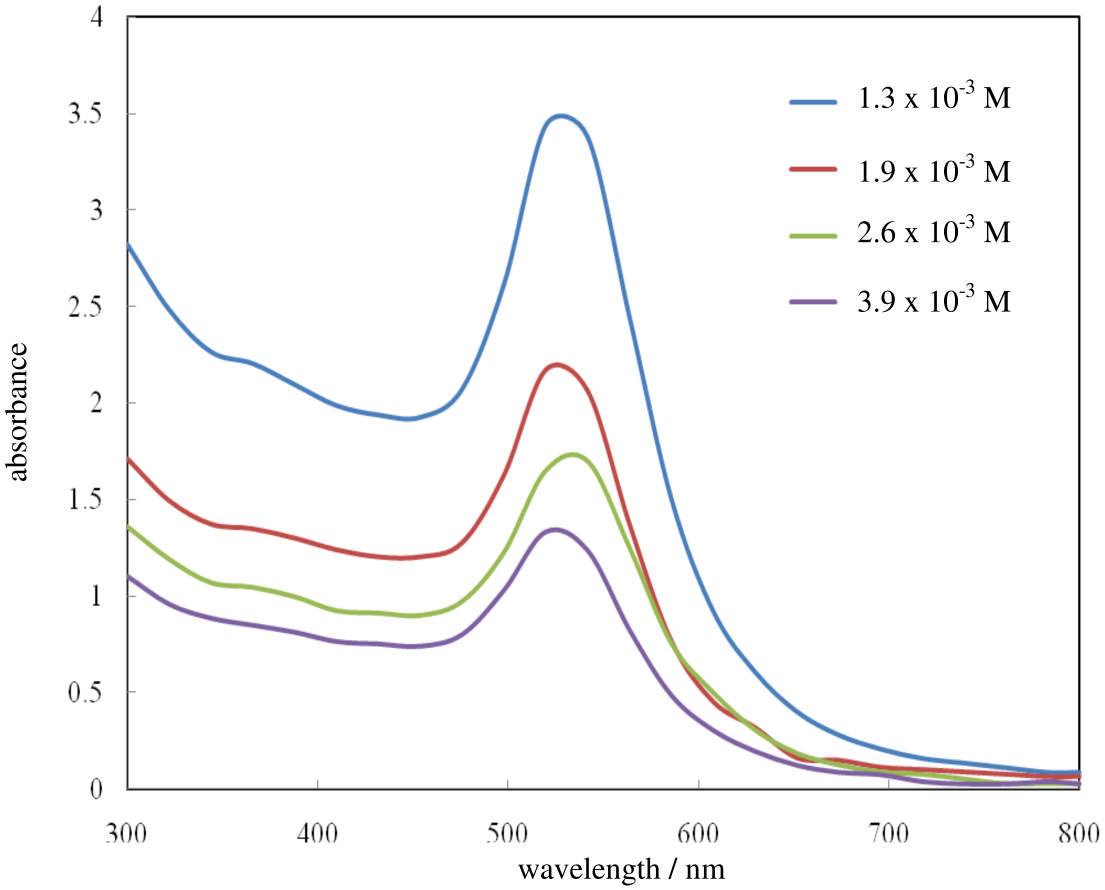

salt concentration of 2.6 x 10^{-3} mol dm^{-3}, a citrate to gold molar ratio of 2:1 and heating for 10 minutes at 70 °C. The UV-Vis spectra of some other gold colloidal dispersions formed under different conditions are also shown in Figure 3.1. As can be seen from the spectra the SPR bands all lie in the same position indicating that the particle size range is relatively small. By comparing these positions of the surface plasmon resonances to others published in the literature, it can be predicted that the particles have diameters in the size range 25 – 35 nm.[20]

As shown in Figure 3.2 this estimation can be confirmed by the TEM analysis. The majority of the particles are spherical, or spherical with facets. However a small number are not spherical in shape, being elongated or triangular but have similar sizes to the spherical particles. These small numbers of non-spherical shaped particles are judged not to affect the behaviour of the system as a whole so have been discounted while performing the size distribution analysis. From all the synthesis the average particle size was typically 29 nm and did not vary by more than ± 5 nm.

Systems formed at initial $HAuCl_4$ concentrations lower or equal to 2.6 x 10^{-3} mol dm^{-3} were visually stable, i.e. they did not change appearance to the naked eye for in excess of 3 months (all colloid formed was used well within this time limit). There is also no significant change in the spectra of these samples with time. The UV-Vis spectra would indicate the formation of aggregates by a decrease

Figure 3.2. (a) Transmission electron micrograph image of the gold colloid formed by using an initial $HAuCl_4$ concentration of 2.6 x 10^{-3} mol dm^{-3}. The majority of particles are spherical and of a similar size. Scale bar represents 50 nm.

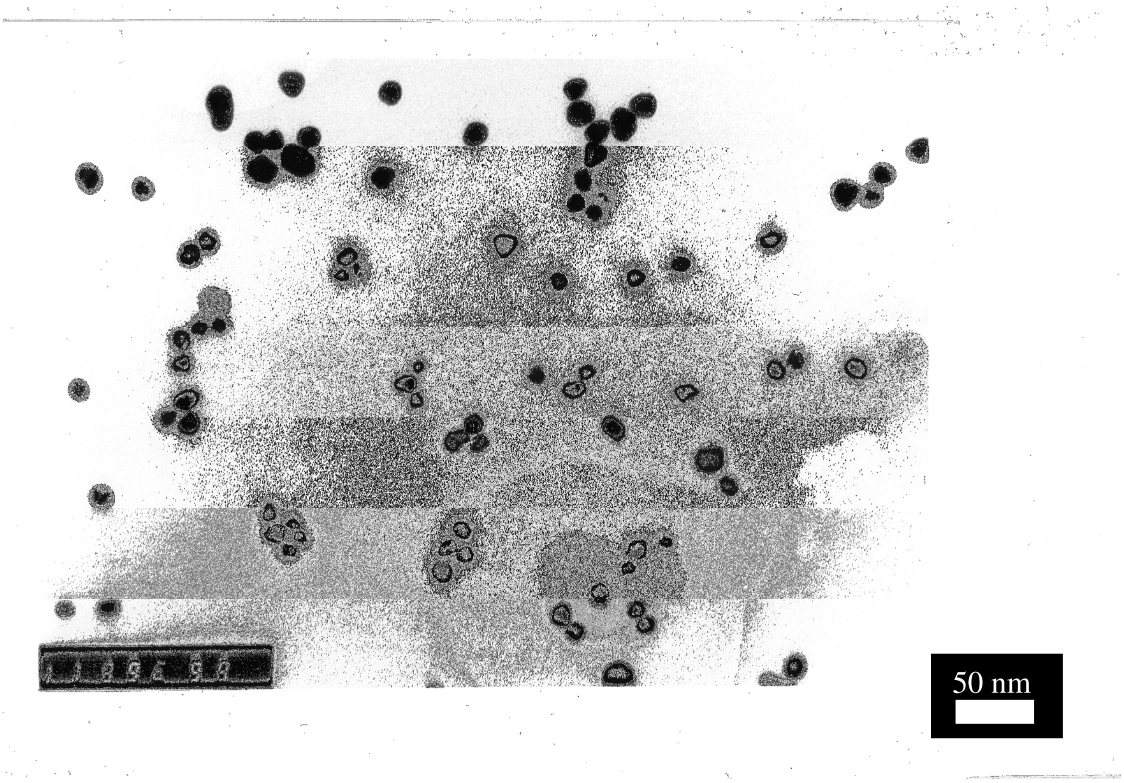

(b) Typical gold particle size distribution after a standard synthesis. The mean particle diameter is 29 nm with a standard deviation of 6 nm and a co-efficient of variation of 0.2. (The co-efficient of variation is the ratio of standard deviation to mean).

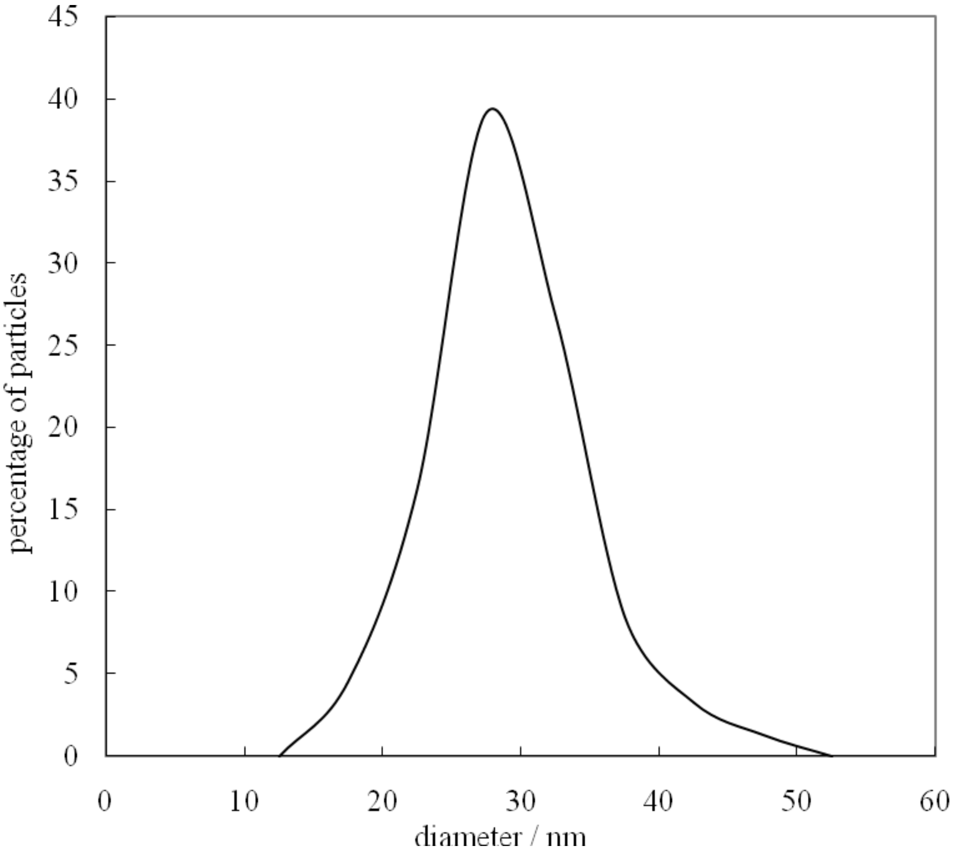

in intensity of the SPR band and an increase in the intensity of the tail after this band. Neither of these changes are seen.

The systems were not stable to the addition of salt and the aggregation induced was irreversible to the simple addition of more solvent, i.e. water. 1 mol dm^{-3} NaCl solution was titrated into a sample of gold colloid formed using an initial concentration of 2.6×10^{-3} mol dm^{-3} $HAuCl_4$**.** The point at which the colloid aggregated was not immediately obvious since there was a gradual colour change from red to blue to purple to black followed by sedimentation as the salt concentration was increased. The point of aggregation was taken to be when enough salt had been added so that the sedimentation became obvious to the naked eye. This value was found to be 24.2 mmol dm^{-3}, which agrees closely with the value given in the literature of 24.0 mmol dm^{-3}.[21]

In order to study the stability of the system with respect to salt addition, separate samples were made at various salt concentrations, shaken well for ~ 5 seconds, diluted with water in a ratio of 1:5 to arrest further aggregation and their UV-Vis absorbance spectra measured. These spectra can be seen in Figure 3.3. As salt concentration in the system increases the SPR (strong absorbance at ~ 525 nm) decreases. This is an indication that the amount of gold present as discrete nano-sized particles decreases with salt addition. Along with this decrease, is an increase in absorption in the 'tail' section of the spectra (> 600 nm). This is

Figure 3.3. UV-Vis absorbance spectra for a sample of gold colloid formed using an initial concentration of 2.6 x 10^{-3} mol dm^{-3} $HAuCl_4$ at different concentrations of NaCl. Path length was 10 mm and the sample was diluted with water in a 1:5 ratio.

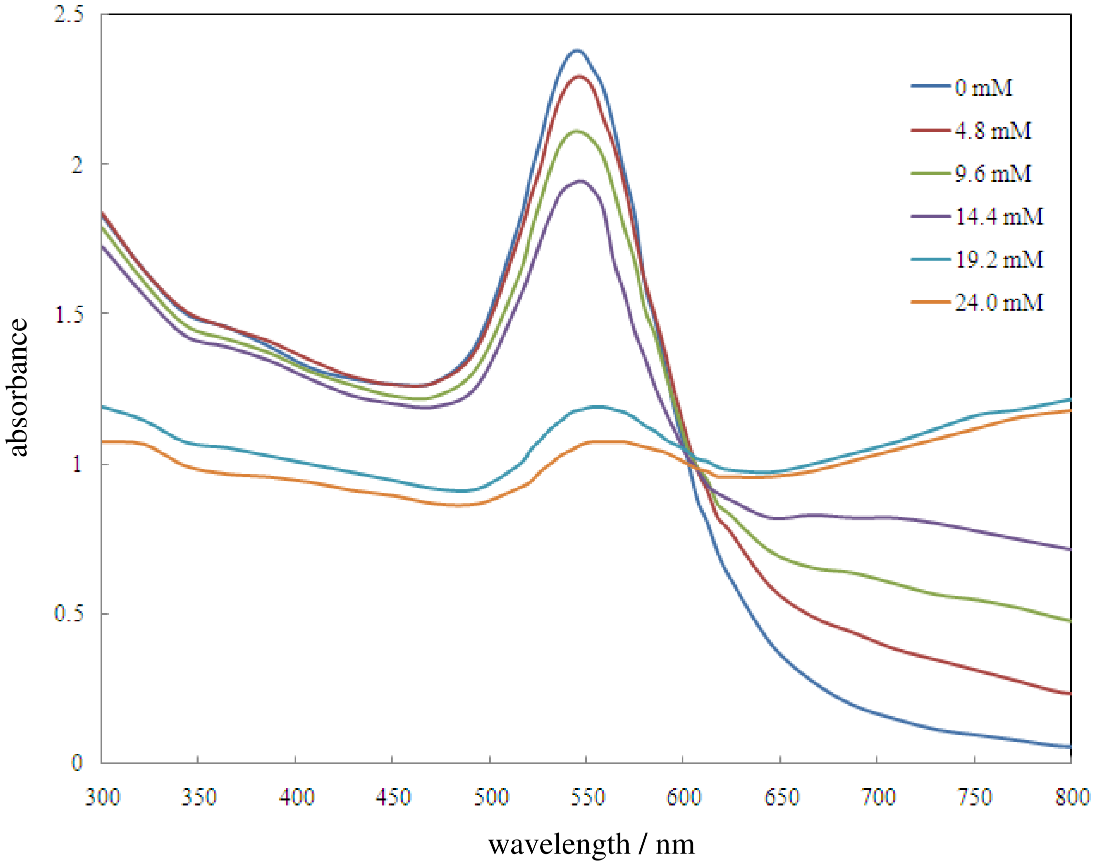

likely to be an indication of the formation of aggregates of particles. This type of behaviour is expected from electrostatically stabilised colloids.

3.3 Film Climbing

When an aqueous colloidal gold dispersion and oil phase containing a low concentration of gold are shaken together, the result is an unstable emulsion system which rapidly breaks to give a highly coloured film that rapidly spreads from the planar oil-water interface. The direction and rate of this film climbing can be controlled by altering the pH of the aqueous phase and the wettability of the vessel the system is contained in. Figure 3.4 shows the interactions between the positively charged ODA molecules and the negatively charged aqueous gold colloid at the oil-water interface. This modification of the gold, and adjustment of the particles wettability, is responsible foe the particles increased surface activity. It is worth noting that ODA is soluble in the oil phase only so the interactions with the gold particles must take place at the oil-water interface.

The standard conditions for the following work are defined as the gold colloid formed from an initial gold salt concentration of 2.6 x 10^{-6} M $HAuCl_4$, dodecane containing 8 x 10^{-4} M ODA, aqueous to oil volume ratio fixed at 5:2 and shaking by hand for 20 seconds.

Figure 3.4. Schematic representation of the interactions between the positively charged ODA molecules and the negatively charged aqueous gold colloid at the oil-water interface. The interface is shown on the right before and after shaking.

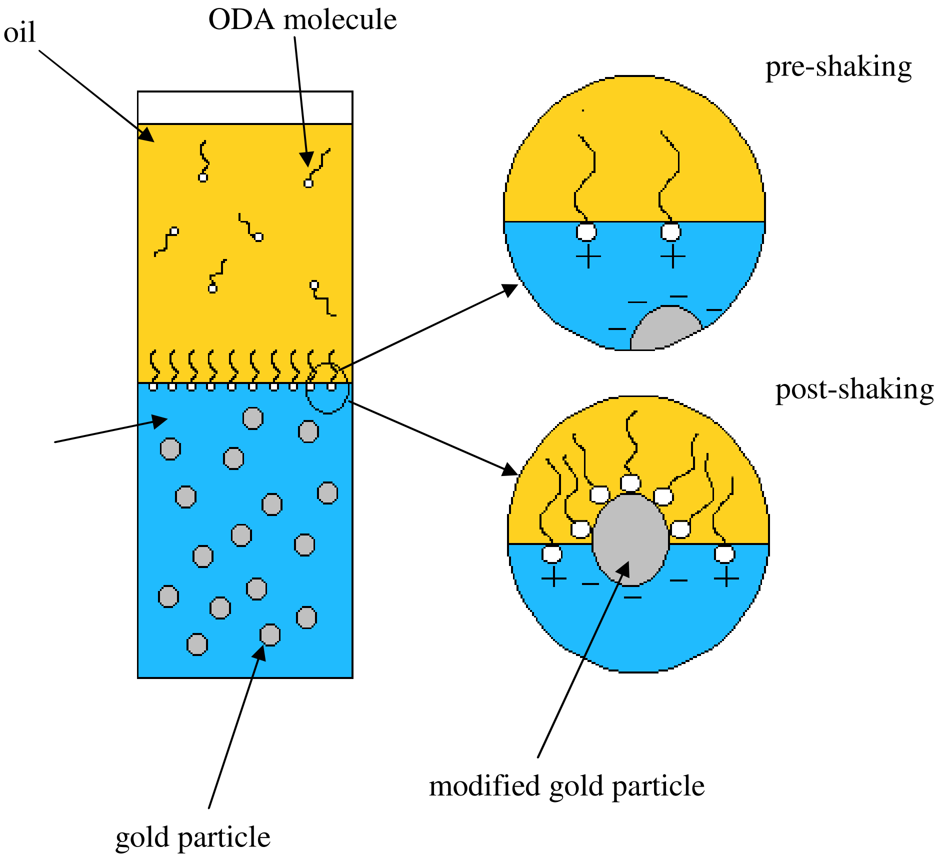

3.3.1 Effect of pH

Surface modification of the gold colloid by ODA in dodecane, at the standard concentrations, was studied as a function of the aqueous phase (hydrosol) pH. It was expected that altering the charge on the ODA molecule would change the interaction between the colloidal gold particles and the ODA molecules; this in turn should affect the climbing rate. The pH was altered by the addition of 1 M NaOH. The system comprised of 5 ml of aqueous colloid and 1 ml of 8 x 10^{-5} M ODA in dodecane which had been hand shaken vigorously for 20 sec. Table 3.1 shows the pH range studied.

Sample	pH
1	3.85
2	5.57
3	7.70
4	11.35
5	12.23

Table 3.1. pH of gold hydrosol adjusted by adding 1 M NaOH to the standard gold colloid. Sample 1 is the pH of the unaltered hydrosol.

Adjusting the pH of the gold hydrosol had several effects on the gold climbing rate and oil droplet formation. Increasing the pH led to slower climbing rates for the gold films. Gold films were present at low and intermediate pH (samples 1, 2 and 3); in contrast there was no film present in samples 4 and 5. An increase in the stability of the droplets formed at the oil-water interface was seen as the pH was increased from sample 1 through to sample 3. In each case, the droplets formed in samples 1, 2 and 3 were coated with gold films. A rim of droplets was formed in samples 4 and 5 (at oil-water interface); they were not visible coated with gold particles and were stable for only a short period. As the pH is increased the colour of the hydrosol changed from deep red to deep purple, an indication of particle aggregation. Samples 4 and 5 were not stable with respect to sedimentation over time (both in the modification experiment and in the pure colloid). Sample 5 turned black overnight and sedimented within 24 hours whereas sample 4 remained purple and sedimented over a period of about a week. Samples 1, 2 and 3 were stable to sedimentation. These trends are summarised in Figure 3.5.

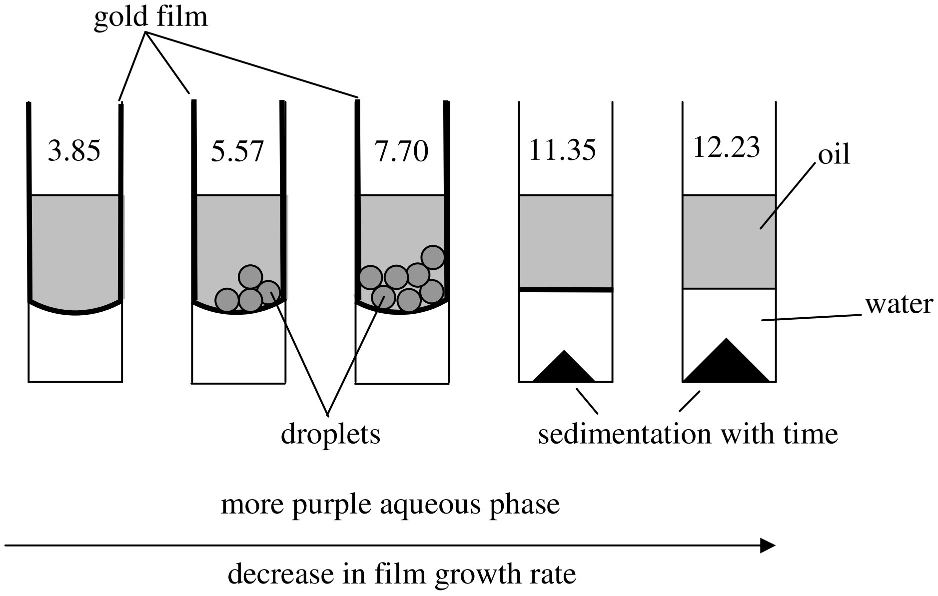

Figure 3.5. Representation of the behaviour of the system described above with increasing pH (given). Note upper phase is oil and is clear in each system. The lower phase is hydrosol.

It was observed that the growth rate of the film decreased from sample 1 to sample 3 and that samples 4 and 5 had no film growth. At high pH there will be less charge on the ODA molecules and less electrostatic attraction to the negatively charged gold particles. As the pH of the aqueous phase approaches the pH at which ODA is neutral then the film growth slows and beyond this stops. The pK_a of ODA is 10.60.[22] pK_a is the negative log of the acid dissociation constant and when the pH is equal to the pK_a the molecule is not dissociated and therefore carries no charge. As the value of the pH moves away from that of the pK_a the molecule becomes more dissociated and carries a greater charge. Table 3.2 gives the growth rates and observations made on the same system but using a different synthesis of the same gold colloid and Figure 3.6 plots the growth rate of the film as a function of aqueous phase pH. Film growth rates were calculated by measuring the time taken for the film to reach the top of the vessel (~70 mm). As the pH is increased the growth rate of the gold particle film decreases.

The growth rate of the films of colloidal gold particles modified by ODA *in situ* at the oil-water interface can be controlled by altering the pH of the aqueous phase and adjusting the electrostatic interactions between the gold particles and the ODA molecules.

Table 3.2. Observations and climbing rates (CR) of the gold film formed when 5 ml of aqueous gold colloid and 1 ml of ODA in dodecane, at the standard concentrations, were hand shaken for 20 seconds in a stoppered glass vessel at different values of the aqueous phase pH.

pH	CR / mm s^{-1}	Observations
4.1	35	On shaking, gold coated drops form in aqueous phase but then rapidly coalesce with each other and the vessel walls. Growth of a strongly coloured film up the walls of the container from the oil-water interface. Film is gold in reflectance and blue in transmission and climbs to the top of the vessel (~ 70 mm).
6.1	23	As above but coalescence and film growth are less rapid.
7.7	12	As above but coalescence and film growth are less rapid and the intensity of the gold film is reduced.
9.4	6	Film growth is slower and initially the film is transparent. Film continues to increase in blue colour for 30 sec. after film has reached the top of the vessel.
9.7	5	Some gold coated drops are formed but the concentration of gold in the film is less than above. Film growth is slower and the film is transparent. Some gold colour at oil-water interface.
10.4	4	Clear drops formed which coalesce. Some gold colouring at the oil-water interface (less than above). Very slow growth of a transparent film.
10.9	3	Clear drops formed which coalesce. Some gold colouring at oil-water interface (less than above). Very slow growth of a transparent film.
11.5	3	No gold colouring at oil-water interface. Very slow growth of a transparent film.

Figure 3.6. Climbing rate of the gold film formed when 5 ml of aqueous gold colloid and 1 ml of ODA in dodecane, at the standard concentrations, were hand shaken for 20 seconds in a stoppered glass vessel at different values of the aqueous phase pH.

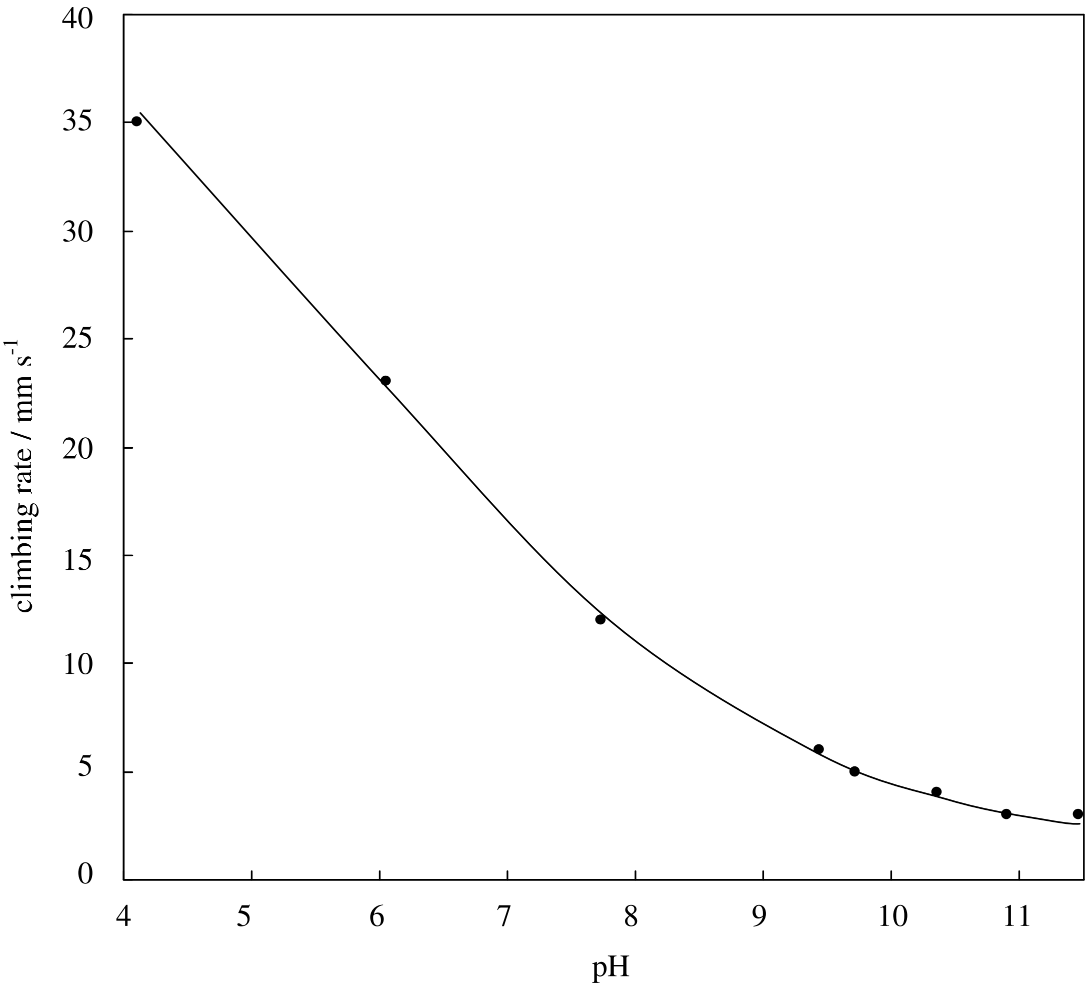

3.3.2 Effect of hydrophobicity of vessel

The hydrophobicity of the vessel that the system is held in plays a crucial role as to the type of film growth observed. When the system is contained within a hydrophilic vessel (as above) the growth of the film is upward from the oil-water interface, through the oil-air surface. When the system is held in a hydrophobic container then the film growth is downward surrounding the aqueous phase on the water-hydrophobic vessel interface. In each system, the gold particles can be found at the interface that has the highest energy. For the hydrophilic glassware this is the oil-water interface between the bulk oil and bulk water, the oil-water interface between the bulk oil and the film of water on the glass vessel and the air-water interface between the water film on the vessel and air. For the hydrophobic glassware this is the oil-water interface between the bulk oil and bulk water and the oil-water interface between the bulk aqueous phase and the oil film on the hydrophobic glassware. This is illustrated in Figure 3.7.

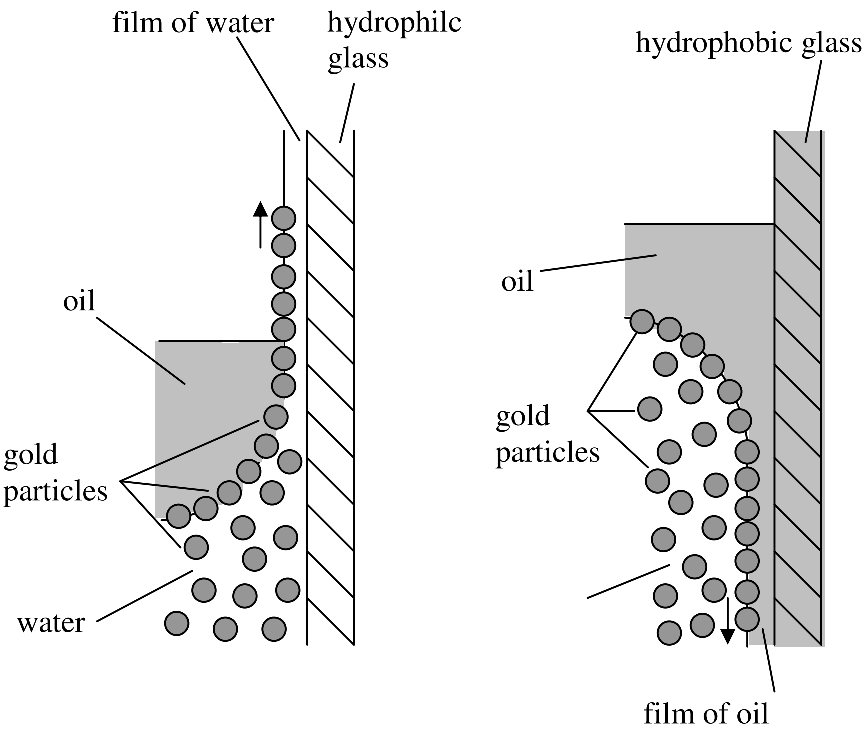

Figure 3.7. Diagram illustrating the spreading of gold particles on liquid films for both hydrophilic, unmodified glass (left), and hydrophobic, modified glass (right), surfaces.

Figure 3.8 shows the appearance of the vessels immediately after shaking, but after completion of the gold film spreading. As can be seen in the un-modified, hydrophilic vessel (left) the gold film climbs up from the oil-water interface to cover the internal wall of the vessel with a gold film which is strongly coloured gold in reflectance and blue in transmission. As the vessel wall becomes sequentially more hydrophobic $5^{\circ} \rightarrow 30^{\circ} \rightarrow 50^{\circ}$ in the second and third vessels, the gold film still climbs up from the oil-water interface but each time the intensity of the gold film decreases. In the vessel with contact angle of 50° (middle) it can be seen that some of the gold is located between the lower aqueous phase and the glass wall. As the vessel is modified further 50° → 70° → 80° an increasing amount of gold is located between the lower aqueous phase and the modified glass wall, until at a contact angle of 80° (right) almost all the gold is here.

This shows that the direction of film growth can be controlled by the modification of the vessel containing the system. Below a contact angle of 50° the film growth is upward, above this value it is downward. Initially as the hydrophobicity of the vessel is increased the intensity of the colour of the film is decreased.

3.4 Single drop experiments

In order to remove the effect of shaking on the system, the behaviour of a single drop of aqueous (oil) phase falling (rising) through a bulk oil (aqueous) phase was studied using the experimental apparatus described in section 2.2.4 and Figure 2.4. Briefly, a drop of the phase to be studied was formed on the tip of a needle and allowed to pass through the corresponding bulk phase. When this drop coalesces with the planar oil-water interface observations of the film growth were made.

Figure 3.8. Hydrophobically modified vessels immediately after shaking and the completion of film growth. From left to right the contact angle of a drop of water under air on the vessel surface is 5 (un-modified), 30, 50, 70 and 80°.

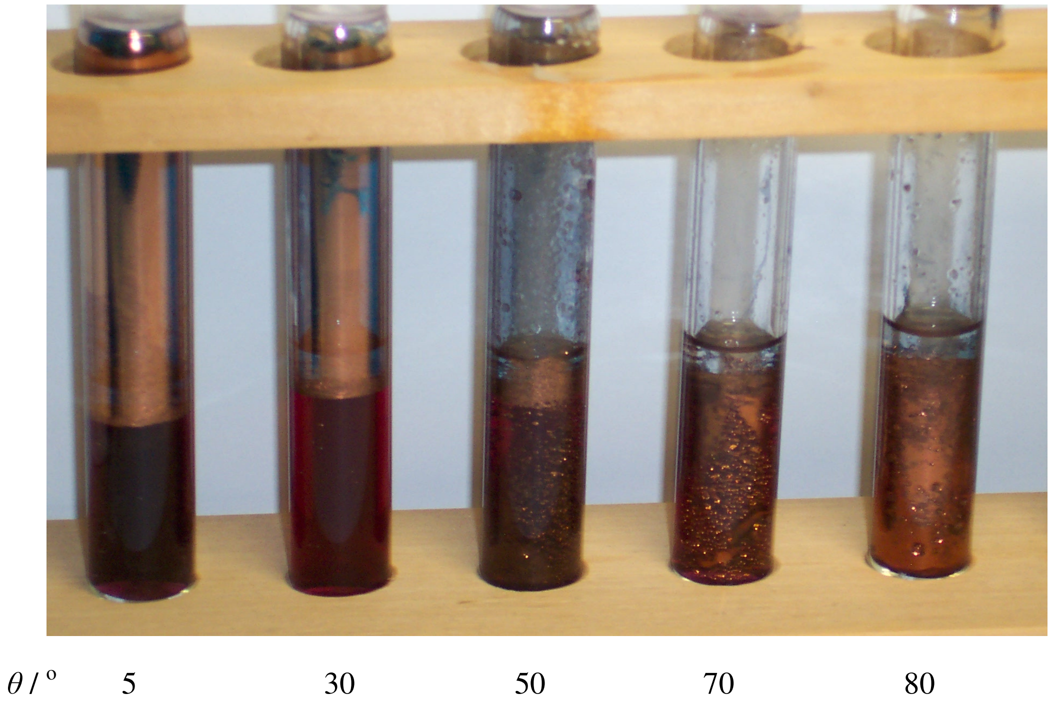

3.4.1 Oil drop rising through aqueous phase

The rising of a drop (~ 0.5 ml) of dodecane, containing 8 x 10^{-5} M ODA, through a continuous phase of the standard aqueous gold colloid (~ 60 ml) was studied and the following observations made.

- As each oil drop travelled up through the aqueous phase, the oil-water interface around the drop became progressively more metallic gold in appearance.

- The first coalescence event occurred between an oil drop and the air-water interface. When this event occurred, although faint, there was a clear film of material rising up the vessel walls. The film was transparent and was only noticeable whilst moving.

- The subsequent coalescence events occurred between the rising oil drops and the planar oil-water interface. As each coalescence event occurred, the film which had risen from the oil-water interface became more highly coloured.

- It was clear by observation that the growth / darkening of the film was linked to the coalescence of the oil drops with the planar oil-water interface.

- Figure 3.9 shows the appearance of one of the rising gold-coated oil drops when it was trapped momentarily in the glass tube.

This experiment allows the direct observation of the link between an emulsion droplet coalescing with the planar oil-water interface and the growth of the gold particle film. It also allows the direct observation of the development of the gold film around the oil drop as it rises through the aqueous phase.

3.4.2 Aqueous drop falling through oil phase

The following observations were made on a drop (~ 0.5 ml) of aqueous gold colloid falling through a continuous phase of dodecane (~ 60 ml), containing 8×10^{-5} M ODA.

- There was no change in the visual appearance of the drop as it travelled down through the aqueous phase.

- The first drop contacted the glass / aqueous phase interface at the bottom of the cuvette. It remained spherical for ~ 5 seconds then spread on the bottom of the cuvette.

Figure 3.9. Image of a drop of dodecane, containing 8 x 10^{-5} M ODA, coated with a film of gold colloid rising through a continuous phase of aqueous gold colloid. The internal diameter of the glass tube is 9 mm.

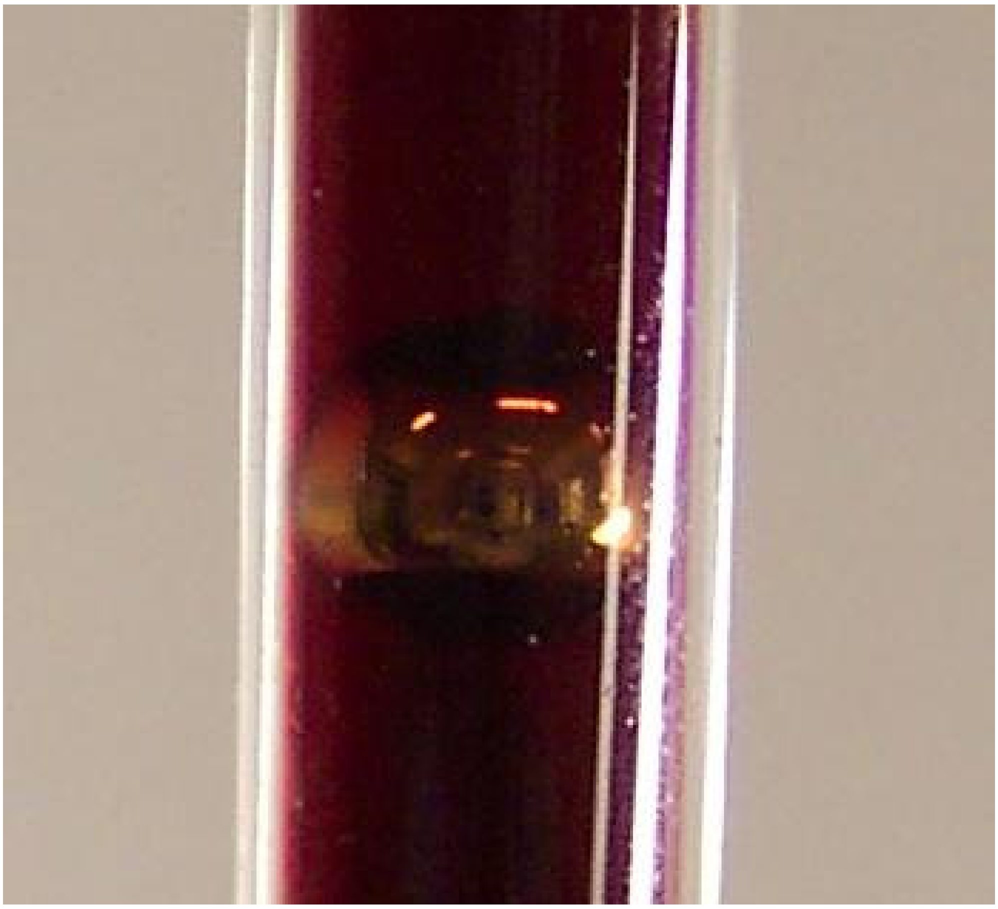

- The next drop, which contacted the oil-water interface, remained discrete and spherical for ~ 5 seconds before coalescing with the aqueous phase.

- Each subsequent drop behaved the same. There was no change in its appearance as it travelled through the oil phase and when in contact with the oil-water interface at the bottom of the tube it remained stable for ~ 5 seconds before coalescing with the aqueous phase.

- No film formation was observed.

It is possible that in this system there are not enough gold nanoparticles present within the sedimenting drop to adsorb at the oil-water interface. This, combined with the difference in the hydrodynamic flow with respect to the two phases, when compared to the experiment in Section 3.4.1 results in very little or no gold particle adsorption at the oil-water interface and therefore no film growth.

3.4.3 Aqueous drop falling through oil phase (high ODA concentration)

The following observations were made on a drop (~ 0.5 ml) of aqueous phase falling through a continuous phase of dodecane (~ 60 ml) containing 8×10^{-4} M ODA .

- There was no change in the visual appearance of the drop as it travelled through the aqueous phase.

- Each drop was stable to coalescence for at least 2 hours. The drops sat on top of one another in the glass tube as illustrated in Figure 3.10.

- Figure 3.10 also demonstrates that with time the aqueous drops of gold colloid turned from red to purple (an indication of particle aggregation) and the particles began to sediment within the drops.

- At the bottom of Figure 3.10, a region where a drop has coalesced can be seen. The film, which was located around the drop, remains largely intact.

It is likely that at this concentration, the ODA is behaving like a surfactant and stabilising the oil-water-interface. In order to confirm this, the experiment would have to be repeated at high concentration of ODA, but with no particles in the aqueous phase.

Figure 3.10. Appearance of aqueous colloid drops resting on top of one another after passing through a continuous phase of oil containing 8 x 10^{-4} mol dm^{-3} ODA. The image was taken 1 hour after the drops were formed. The internal diameter of the glass tube is 9 mm.

3.5 Mechanism of spreading

Here we describe the mechanism of the formation and spreading of the film of gold nanoparticles which is represented schematically in Figure 3.11. On shaking, the mixture of aqueous gold colloid and dodecane containing ODA forms an emulsion with a low surface coverage of particles. Even though the surface coverage is low the amount of oil-water interface is greatly increased and therefore the number of particles adsorbed at this interface is also increased. Once at the oil-water interface the hydrophilic gold particles are modified by the ODA. This is likely to render the particles more hydrophobic and therefore more surface-active. When the emulsion drop coalesces with the planar oil-water interface then the particles are transferred to the planar interface between the two bulk phases. The additional surface pressure of the adsorbed particles causes the particle-laden water film to spread. This process can be thought of as being similar to that of partial or limited coalescence, where emulsion drops will continue to coalesce until they have a sufficient surface coverage of particles to remain stable.[23] Depending on the direction of the meniscus, which is governed by the contact angle of the aqueous phase on the vessel wall under oil, the film will spread either upwards for contact angles < 90° or downwards for contact angles > 90°.

At the point that the oil-water interface contacts the vessel surface the meniscus can either be orientated upwards or downwards. In order for the mechanism presented to be correct, the value of this contact angle (measured

Figure 3.11. Schematic illustration of how coalescence of particle-stabilised emulsion drops with the flat oil-water interface causes spontaneous spreading of a particle-stabilised thin water film up the container walls. For simplicity, we have shown emulsion drops formed only in the water phase. Although not shown, it is also possible that the particle film takes oil with it as it climbs.

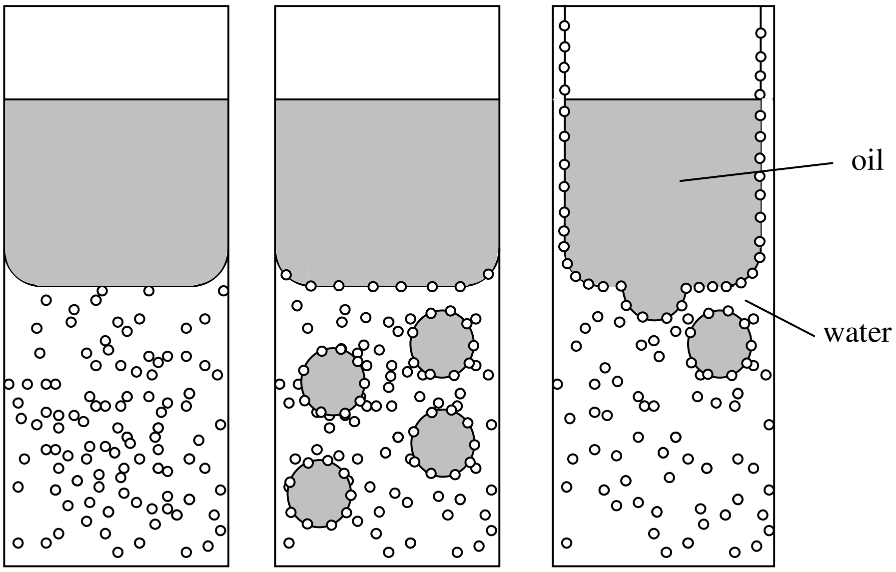

An aqueous particle dispersion (white) beneath an oil phase (grey) within a hydrophilic container

Shaking the mixture produces emulsion drops with a low surface concentration of particles adsorbed at the oil-water interfaces

Coalescence of the emulsion drops with the flat oil-water interface transfers particles to the interface between the bulk phases. The additional surface pressure of the adsorbed particles causes the particle-laden water film to spread up the hydrophilic walls through the water phase) must correlate with the direction of the film growth, i.e. for contact angles < 90^o the film should travel upwards and > 90^o downwards. During the shaking process the ODA will partition between the aqueous phase (very little), oil phase and the oil-water interface. The following series of experiments measures the contact angles for both pre-equilibrated and non-pre-equilibrated systems on a series of hydrophobically modified slides of different wettability. In Section 3.3.2 the gold spreading experiment was performed in a series of vessels of different wettabilities. The vessels were hydrophobically modified by exposure to 1 wt. % OTS in toluene for a known length of time. Using this information the contact angle measured on the hydrophobically modified slides can be correlated with the direction of the film growth. The contact angles quoted in section 3.3.2 are of a water drop on the modified glass surface under air.

The particle film growth which occurs after shaking does so in a system where the ODA has had chance to fully equilibrate both with the oil-water interface and adsorb onto the gold particle surfaces. In considering the macroscopic contact angle that the aqueous gold suspension makes with hydrophobically modified glass under the dodecane phase (containing ODA) it could be important to account for the difference in ODA levels between an oil phase which has been pre-equilibrated with the gold suspension and one that had not. It could also be important to establish the difference in advancing and receding contact angles for both the pre-equilibrated and non-pre-equilibrated systems. The investigation into these systems is described below.

3.5.1 Contact angles for both pre-equilibrated and non-pre-equilibrated systems: oil phase contacting the slide first

Here a modified glass slide was placed into either pre-equilibrated or non-pre-equilibrated dodecane containing ODA and a drop of either pre-equilibrated or non-pre-equilibrated gold colloid was formed under the oil and contacted on the slide surface, i.e. the slide is first contacted with the oil phase. This was done for the range of modified glass slides from hydrophilic to hydrophobic. Figure 3.12 shows the appearance of a drop of the aqueous gold colloid on the glass slide under dodecane containing ODA for the different times (t) the glass slide was exposed to 1 wt. % OTS solution in toluene. Figure 3.13 plots the contact angle of the drop of gold colloid on the modified slide under oil containing ODA as a function of time.

The contact angle measured is the advancing three-phase contact angle. The slide is first contacted with oil and an aqueous drop is added. The three-phase contact line then advances along the slide until the drop reaches equilibrium. It can be seen that for non-pre-equilibrated systems the contact angles are all substantially above 90 ^{o} for the whole range of substrate hydrophobicities. For the pre-equilibrated system the contact angle rapidly increases with increasing hydrophobicity meaning that it cannot be the advancing three-phase contact angle that governs the direction of the film growth if the proposed mechanism is correct, since the point at which the contact angle passes through 90^{o} does not agree with the direction the film is observed to travel in Figure 3.8.

Figure 3.12. Aqueous gold colloid (~ 20 μl) under dodecane containing ODA on a modified slide (oil contacted the slide first) as a function of the time (t) that the slide was exposed to a 1 wt. % solution of OTS in toluene, for (a) non-pre-equilibrated and (b) pre-equilibrated systems.

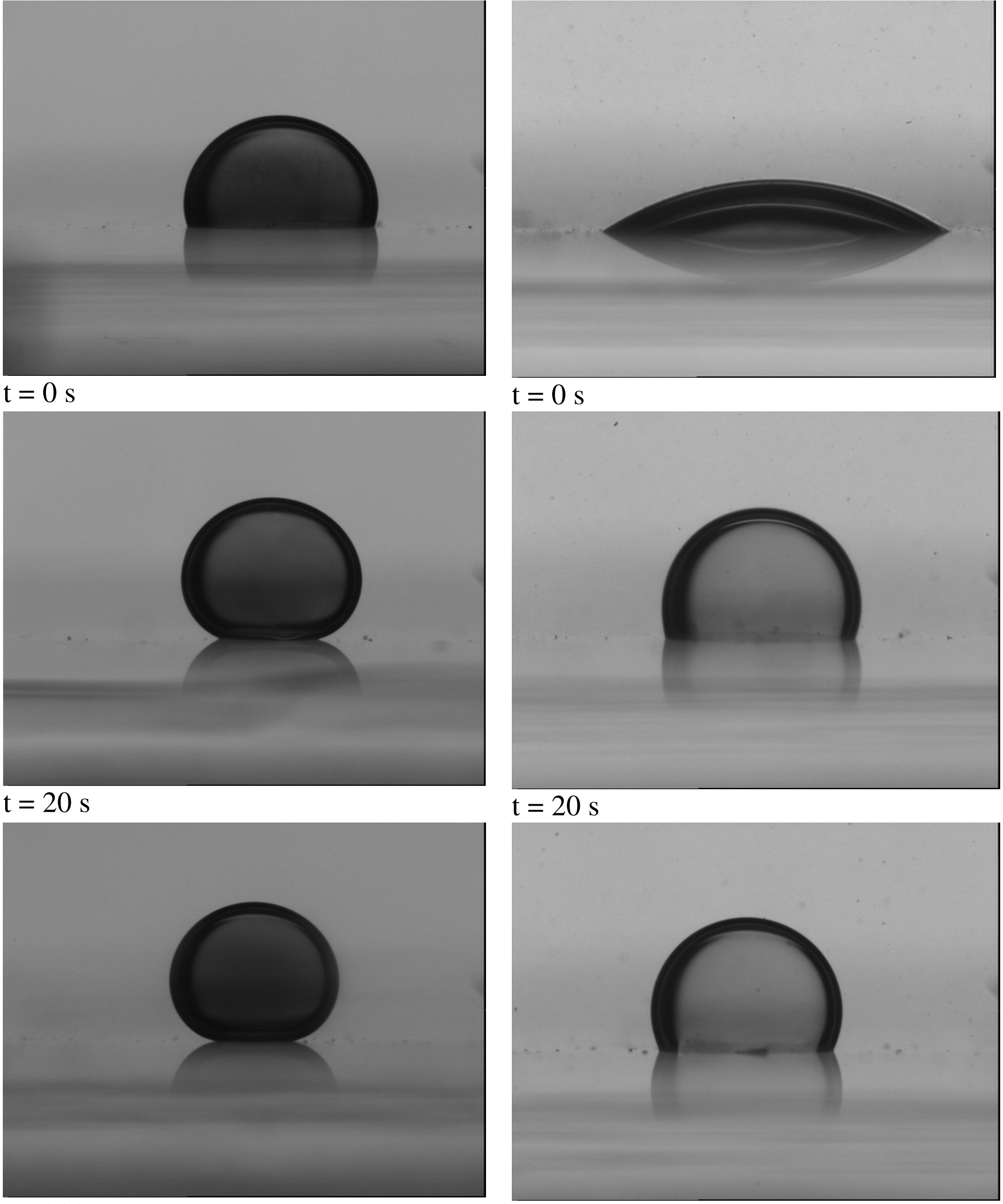

Figure 3.13. Contact angle of a drop of gold colloid on modified glass under dodecane containing ODA, where the slide is initially contacted by the oil, as a function of (a) time (t) the glass slide was exposed to a 1 wt. % solution of OTS in toluene and (b) log (t). Filled circles are non-pre-equilibrated and open ones are pre-equilibrated systems.

(a)

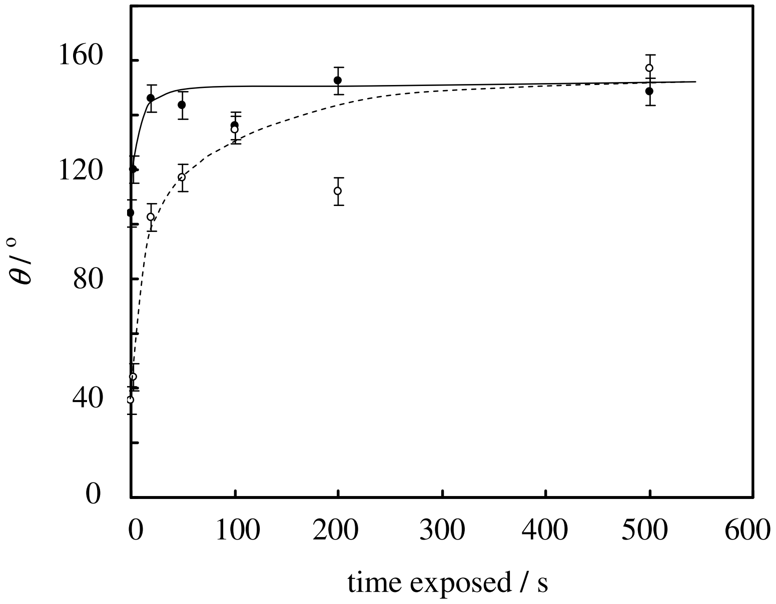

(b)

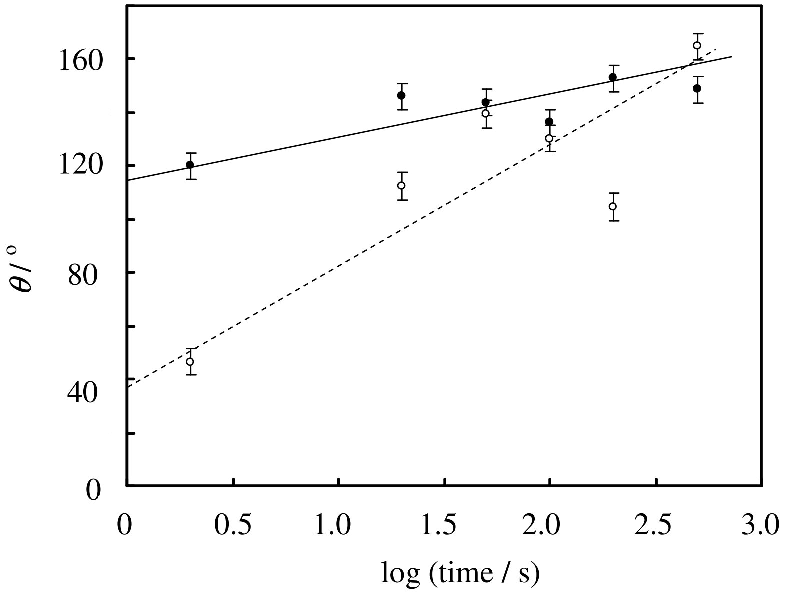

Although the comparison between the pre-equilibrated and non-pre-equilibrated systems is interesting, a direct comparison is not simple. Both phases are equilibrating during the pre-equilibration. The dodecane phase is losing a large amount of the ODA by adsorption onto the gold particles and the aqueous phase is losing some of the gold particles by adsorption onto the oil-water interface and subsequent modification by the ODA. This could explain the large differences, particularly on the hydrophilic surfaces, between the contact angles on the pre-equilibrated and non-pre-equilibrated systems. In the non-pre-equilibrated systems there is still a relatively high concentration of ODA in the oil phase. This ODA will adsorb onto the surface of the glass slide and render it more hydrophobic. The more hydrophobic the slide, the smaller this effect is and the closer the values of the contact angle for the pre-equilibrated and non-pre-equilibrated systems.

3.5.2 Contact angles for both pre-equilibrated and non-pre-equilibrated systems: aqueous phase contacting the slide first

Here, a modified glass slide was placed into a DSA cell, which allows measurements to be performed under oil, and a drop of pre-equilibrated or non-pre-equilibrated aqueous gold colloid was formed on the slide under air and then the pre-equilibrated or non-pre-equilibrated oil phase was added, i.e. the slide is first contacted with aqueous phase. This was done for the range of modified glass slides from hydrophilic to hydrophobic. Figure 3.14 shows the appearance of the drop of aqueous gold colloid on the glass slide under dodecane containing ODA for different

Figure 3.14. Drop of aqueous gold colloid under dodecane containing ODA on a glass slide (aqueous phase contacting first) as a function of time (t) the slide was exposed to 1 wt. % OTS in toluene (a) non-pre-equilibrated and (b) pre-equilibrated systems. The volume of each the drop is 50 μl.

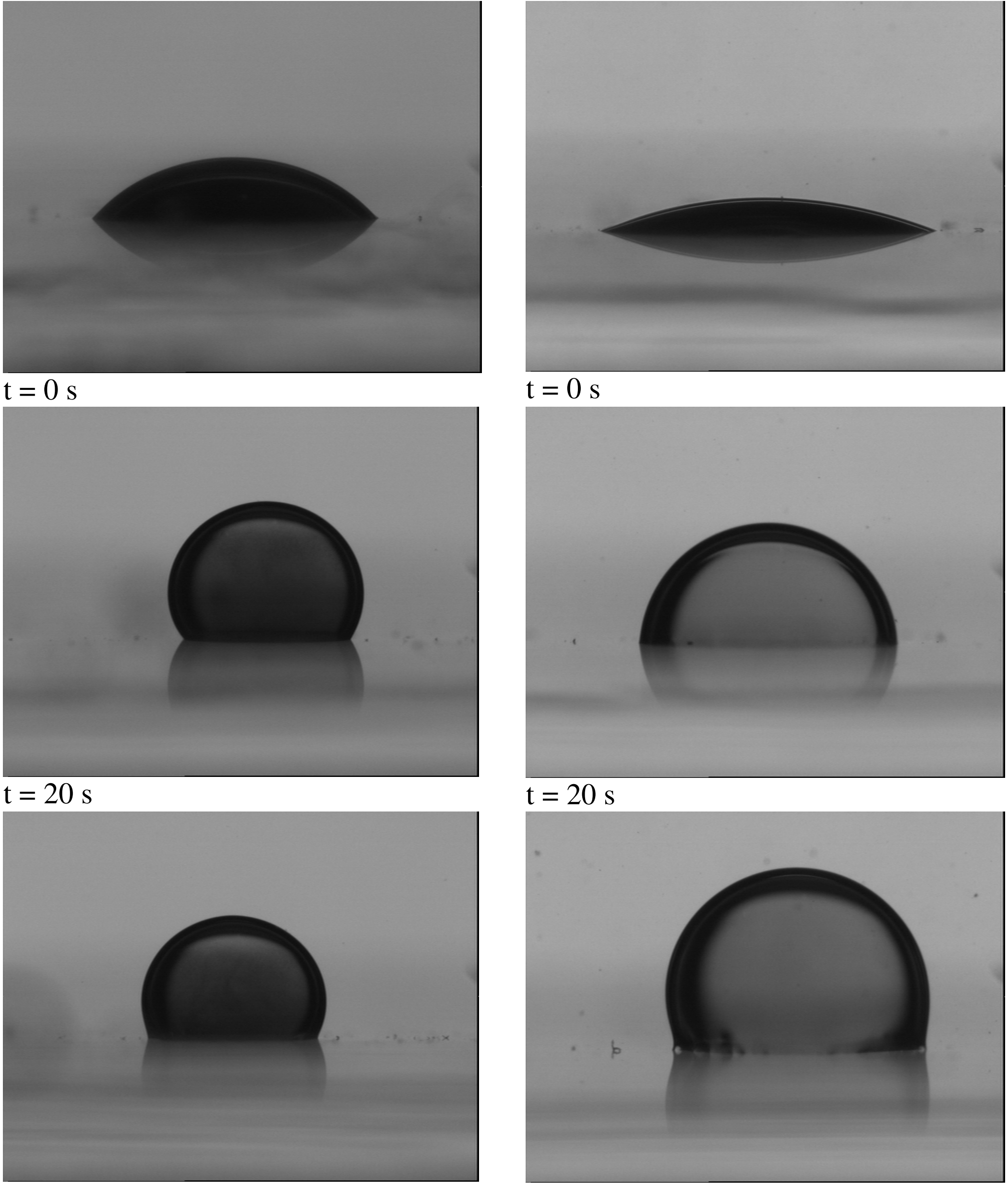
(a) non-pre-equilibrated

(b) pre-equilibrated

times (t) exposed to the 1 wt. % OTS solution in toluene for both pre-equilibrated and non-pre-equilibrated systems. Figure 3.15 plots the contact angle of the drop of gold colloid on the modified slide under oil containing ODA (aqueous contacting first) as a function of time for both pre-equilibrated and non-pre-equilibrated systems.

Here the contact angle that is measured is the receding contact angle, i.e. the slide is contacted first by the aqueous phase. The aqueous drop initially spreads while under air but once in contact with the oil phase it recedes and the oil wets a region of the slide that was originally wet by the aqueous phase. As is expected, the contact angles here are lower than the advancing values, and importantly those for the pre-equilibrated system are consistent with the proposed mechanism.

This experiment was repeated to give a larger number of data points and Figure 3.16 shows the average contact angle versus time (t). The left-hand vertical dashed line shows the time below which a gold film will climb upwards from the oil-water interface and the right-hand dashed vertical line is the point above which the film spreads downwards around the aqueous phase. The point at which the receding contact angle for the pre-equilibrated system is equal to 90 ^{o}, (the point at which the film should change from spreading upwards to spreading downwards) is between these two lines. If the proposed mechanism is correct it is this contact angle that governs the direction of film growth in the system.

Figure 3.15. Contact angle of a drop of gold colloid on modified glass under dodecane containing ODA (slide is initially contacted by the aqueous phase) as a function of (a) the time (t) the glass slide was exposed to a 1 wt. % solution of OTS in toluene and (b) log (t). Filled circles are non-pre-equilibrated and open circles are pre-equilibrated systems.

(a)

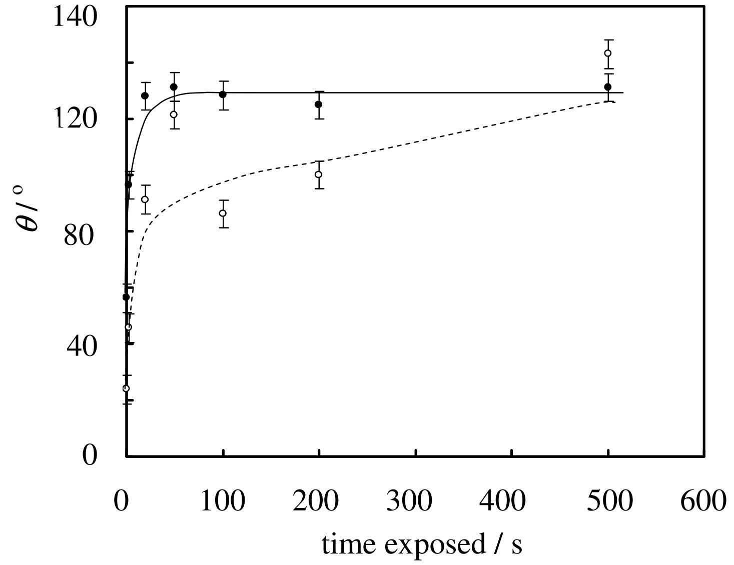

(b)

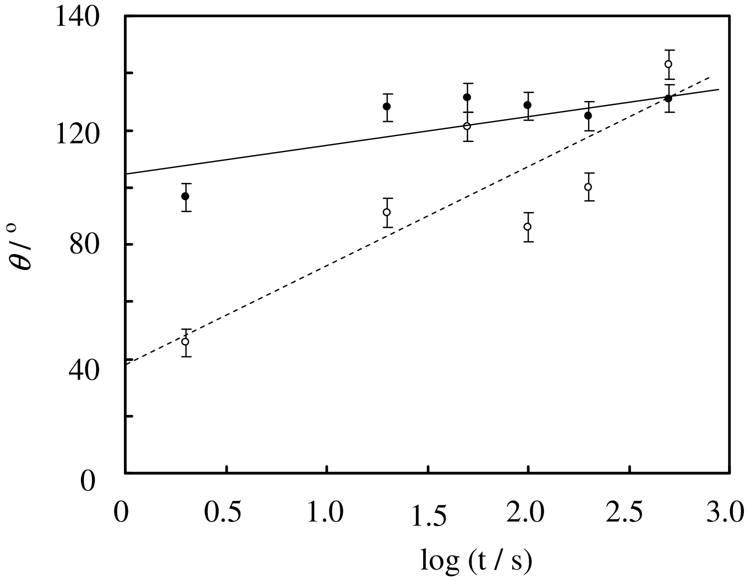

Figure 3.16. Contact angle of a pre-equilibrated drop of gold colloid on hydrophobically modified glass under pre-equilibrated dodecane containing ODA, where the slide is initially contacted by the aqueous phase, as a function of log (t). The left-hand vertical dashed line shows the value of t where it is known below which a gold film will climb upwards from the oil-water interface and the right-hand dashed vertical line is the value of t above which the film spreads downwards.

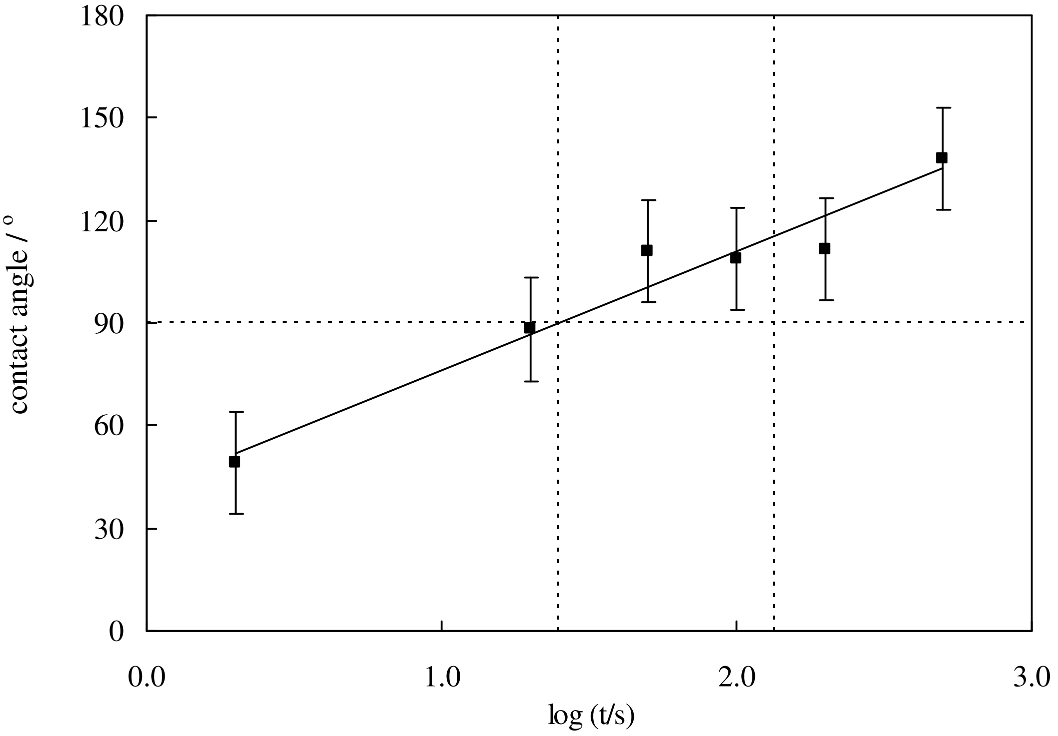

3.6 Conclusions

A mechanism which explains the phenomenon of the formation of a rapid climbing film of gold nanoparticles, from the planar oil-water interface, when a mixture of aqueous phase containing citrate-stabilised gold particles and a dodecane phase containing ODA are shaken together is presented. This mechanism is shown to be consistent with the study of a single drop of the oil phase rising through a bulk aqueous phase and coalescing with a planar oil-water interface. In addition, the receding contact angle of a pre-equilibrated system changes from below 90^o to above 90^o for substrate hydrophobicity that agrees with the observations of the direction of film growth in a series of hydrophobically modified vessels. The mechanism proposed in this chapter has been confirmed in recent work by Cheng and Velankar.[24]

3.7 References

---

[1] W. Wang, S. Efrima and O. Regev, *Langmuir*, **14**, 602 (1998).

[2] A.B. Panda, S. Acharya, S. Efrima and Y. Golan, *Langmuir*, **23**, 765 (2007).

[3] J.F. Wang, M.S. Gudiksen, X.F. Duan, Y. Cui, and C.M. Lieber, *Science*, **293**, 1455 (2001).

[4] P. Mulvaney and S. Underwood, *Langmuir*, **10**, 3427 (1994).

[5] F. Caruso and K.S. Mayya, *Langmuir*, **19**, 6987 (2003).

[6] F.Caruso and D.I. Gittins, *Ang. Chem. Int. Ed.*, **40**, 3001 (2001).

[7] M. Sastry, A. Kumar and P. Mukherjee, *Colloids Surf. A*, **181**, 255 (2001).

[8] D.I Gittins and F. Caruso, *Ang. Chem. Int. Ed.*, **40**, 3001 (2001).

[9] W. Wang, X. Chein and S. Efrima, *J. Phys. Chem. B*, **103**, 7238 (1999).

[10] H. Duan, D. Wang, D.G. Kirth and H. Mohwald, *Angew. Chem. Int. Ed.*, **43**, 5639 (2004).

[11] L. Brandt, J.R. Heath and D.V. Leff, *Langmuir*, **12**, 4723 (1996).

[12] A. Kumar, M. Sastry and A. Swami, *Langmuir*, **19**, 1168 (2003).

[13] H. Schwartz, Y. Harel and S. Efrima, *Langmuir*, **17**, 3884 (2001).

[14] K.S. Mayya and M. Sastry, *Lamgmuir*, **15**, 1902 (1999).

[15] M.K. Chow and C.F. Zukoski, *J. Colloid Interface Sci.*, **165**, 97 (1994).

[16] S. Link and M.A. El-Sayed, *J. Phys. Chem. B*, **103**, 4212 (1999).

[17] S. Link and M.A. El-Sayed, *J. Phys. Chem. B*, **103**, 8410 (1999).

[18] P. Mulvaney, *Langmuir*, **12**, 788 (1996).

[19] B.P. Binks and S.O. Lumsdon, *Phys. Chem. Chem. Phys.*, **12**, 3007 (1999).

[20] S. Link and M.A. El-Sayed, *J. Phys. Chem. B*, **103**, 4212 (1999).

---

[21] Jirgensons B and Straumanis M.E., *A Short Textbook of Colloid Chemistry*, 2nd Edition, Pergamon Press, p. 326, (1962).

[22] *CRC Handbook of Chemistry and Physics*, 75th edition, ed. by David R. Lide, CRC Press, Cleveland, OH (1994/5).

[23] S. Arditty, B.P. Binks, C.P. Whitby, F. Leal-Calderon and V. Schmitt, *Eur.Phy. J. E*, **11**, 273 (2003).

[24] H-L. Cheng and S.S. Velankar, *Colloids Surf. A*, **315**, 275 (2008).

CHAPTER 4

FILM SPREADING BY FOAM BUBBLE COALESCENCE

4.1 Introduction

Mayya and Sastry[1] reported a technique for the spontaneous growth of colloidal nanoparticle superlattice films onto a glass surface from an aqueous dispersion. They took an aqueous dispersion of 13 nm diameter gold particles capped with 4-carboxythiophenol and added an immiscible layer of toluene containing a low concentration of octadecylamine. After vigorous shaking for 30 s and "once the biphasic solution settled down after the shaking process", a violet coloured film of gold particles rapidly climbed the inner wall of the container starting from the oil-water interface. They were able to immerse a prewetted glass slide in the oil-water interface causing the films to grow up the slide so that they could then remove and characterise the gold nanoparticle films. Further work on the mechanism of this process by Binks *et al.*[2] (also reported Chapter 3) showed that the growth of the particle stabilised film was driven by coalescence of particle-stabilised emulsion drops with the oil-water interface between the bulk oil and water phases.

The particles are irreversibly adsorbed so the reduction in emulsion drop interfacial area has to be offset by a corresponding expansion in the film area by growth up the inner walls of the vessel. Similar film growth has also been observed in systems containing silver nanoparticles stabilised by sodium oleate in water-toluene mixtures.[3] All of the systems showing this type of film growth have involved oil-water systems and have included a surface active agent which is thought to adsorb at both the oil-water and particle surfaces. This study shows that rapid film growth can occur in much simpler systems consisting of water and particles alone in the absence of both oil and surfactant.[4]

Water films stabilised by hydrophobic particles are found to spread rapidly up the inner walls of a glass vessel containing water and hydrophobic particles when it is shaken. Shaking produces unstable particle-stabilised foam bubbles whose coalescence with the air-water interface drives film growth up the inner walls of the container. This mechanism is analogous to that proposed in Chapter 3 to explain the growth of gold metallic films at the oil-water interface driven by emulsion drop coalescence except here the film is driven by the coalescence of particle laden foam bubbles. Fumed silica particles, some modified to be more hydrophobic, along with polytetrafluorethylene (PTFE) particles are used in this work showing that the phenomena of rapid film growth driven by coalescence is not specific to gold-stabilised emulsions and that the phenomena is more general. The effect of changing the particle concentration, the hydrophobicity of the particles, the amount of shaking and vessel diameter, on both the rate and extent of film climbing, are investigated.

4.2 Silica particle film climbing

4.2.1 Effect of particle concentration

The effect of altering the number of particles present in the system was studied. Briefly, the experiment can be summarised as follows, different masses of hydrophobic particles, 20 % SiOH, were placed on the surface of 10 ml of water in a measuring cylinder (28 mm inner diameter by 200 mm height) and shaken by hand for 20 s. The resulting film height was then recorded along with the time taken for the climbing to stop.

Figure 4.1 shows the relationship between particle concentration and film height and Figure 4.2 shows the relationship between particle concentration and growth rate. In all cases the errors were estimated from three repeat experiments. Figure 4.1 shows that initially when particle concentration is increased the maximum film height also increases, very rapidly a plateaux is reached and the addition of more particles does not lead to an increase in the film height observed. The opposite is seen in Figure 4.2, as the concentration of particles is increased the film growth rate slows. Both trends are attributed to the fact that as more particles are added on

Figure 4.1. Film height reached when different amounts of 20% DCDMS coated fumed silica particles are shaken for 20 s by hand with 10 ml of water in a glass vessel 200 mm high and 28 mm in internal diameter.

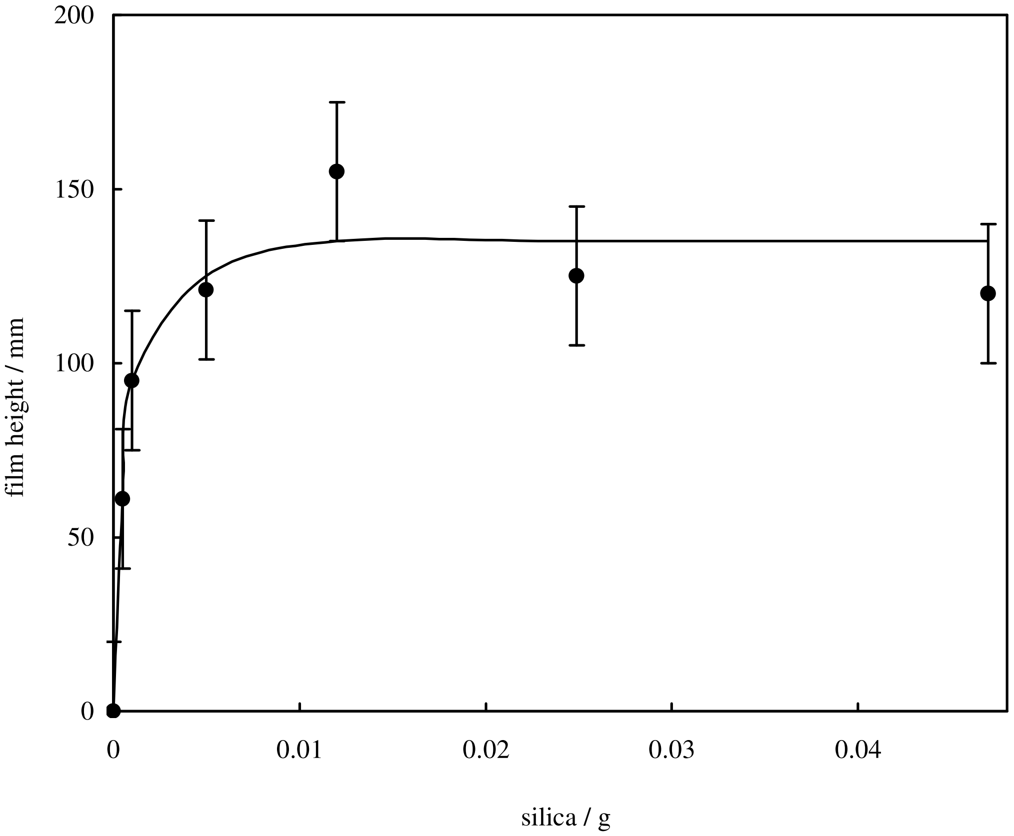

Figure 4.2. Film growth rate when different amounts of 20% DCDMS coated fumed silica particles are shaken for 20 s by hand with 10 ml of water in a glass vessel 200 mm high and 28 mm in internal diameter.

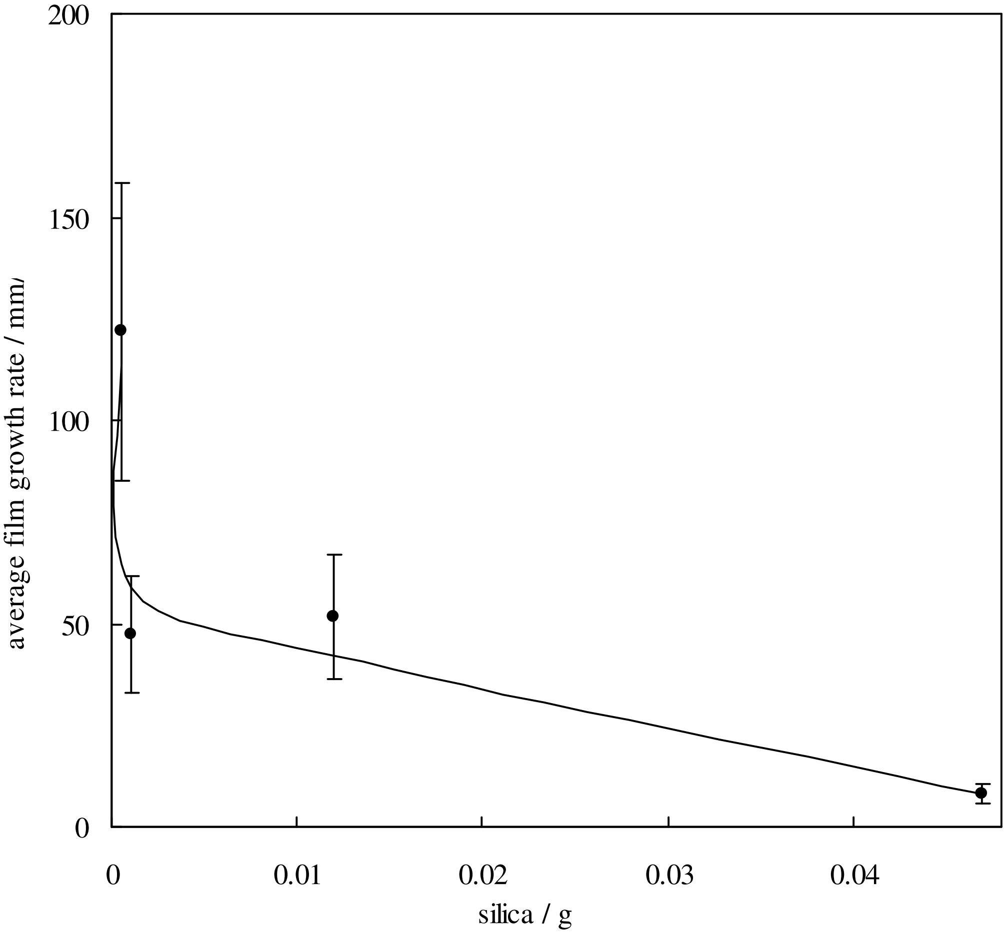

top of the water there are more free particles not attached to the air-water surface. These particles are carried by the growing film even though they are not attached to the water surface, increasing the weight of the film, and reducing both the rate that the film grows and the height that it reaches. Figure 4.3 shows the contrast in appearance of vessels contains systems with low and high particle concentrations.

Interestingly, at high particle loadings (above 0.05 g for this system), when particles growth had ceased, particle coated drops of water could be seen resting on the air-water surface in the meniscus. These water 'marbles' were large and ranged in size from below 1 mm up to 1 cm in diameter. They were stable to coalescence and when bumped into each other by tilting the vessel gentle they did not rupture or coalesce. When covered they were stable for at least 2 weeks but if left exposed to the atmosphere then evaporation eventually led to just the silica skin remaining. This system could be thought of as the inverse of a solid-stabilised foam i.e. water-in-air (w/a). Solid-stabilised w/a systems are described in the literature by Binks *et al.*[5]

A film growth experiment was performed with a high particle loading (0.250 g of 20 % DCDMS coated silica shaken for 20 s with 10 ml water) and after film growth was complete the contents of the measuring cylinder were carefully poured into a Petri dish. The sub-phase of water was dyed blue to a concentration where the two water phases, the bulk sub-phase and the super-phase in the particle laden water drops, were distinct from each other. Figure 4.4 clearly shows the

Figure 4.3. Appearance of vessels containing (a) 0.0005 g, (b) 0.0010 g and (c) 0.0249 g of 20 % SiOH DCDMS coated silica particles and 1 ml of water shaken by hand for 20 s in a glass vessel 200 mm high and 28 mm in internal diameter.

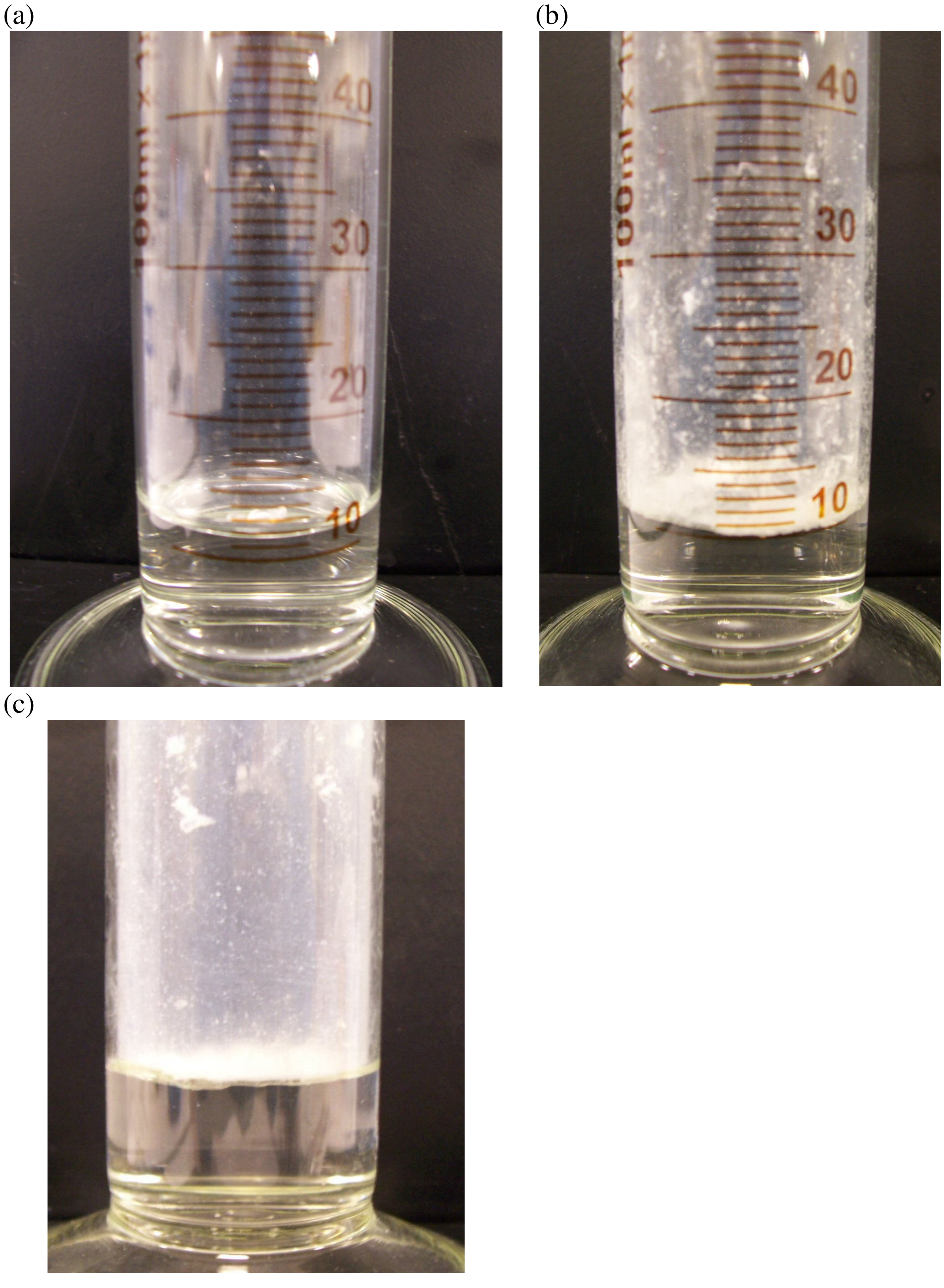

Figure 4.4. Appearance of a Petri dish containing the system formed when 0.250 g of 20 % DCDMS coated silica was shaken for 20 s with 10 ml water in a glass vessel 200 mm high and 28 mm in internal diameter. The sub phase has been dyed blue to provide a contrast. The large water marble is 9 mm across at the longest point.

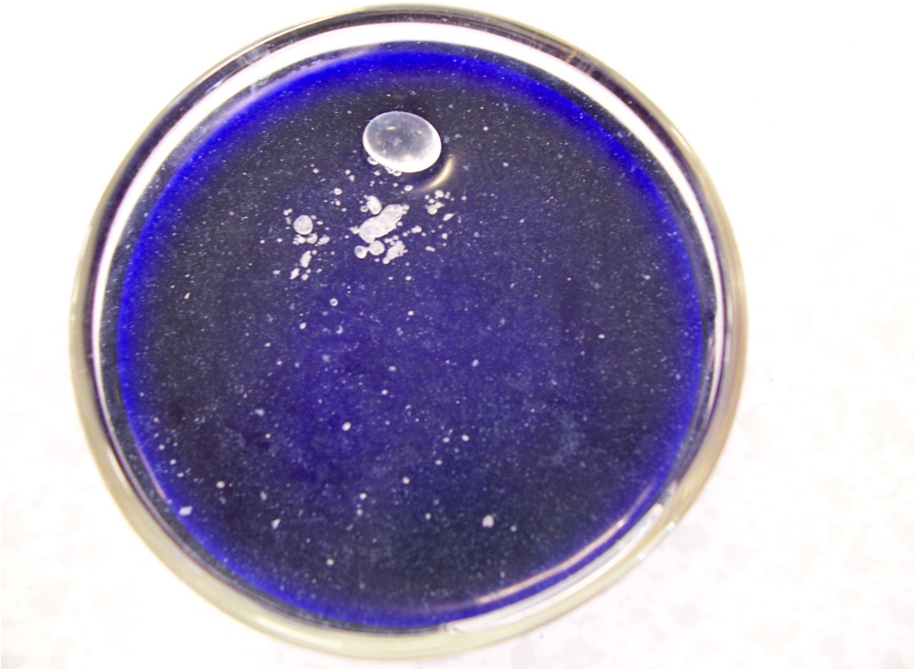

particle stabilised water marbles resting on the planar particle laden air-water surface. The water marbles are large enough to cause deformation on the air-water surface. Even after two weeks there was no transfer of dye from the bulk phase into the drops and no visible change in appearance of the system.

During shaking additional air-water surface is generated by bubbles formed in the water phase. Silica particles attach to the surface of these bubbles and are transported to the planar air-water surface when the bubbles rise. If the bubbles coalesce with the planar air-water surface the particles are transferred onto the planar interface, increasing the surface pressure and driving the film growth. This mechanism is akin to the one described in Chapter 3 to explain the rapid film growth driven by emulsion drop coalescence. However, at the same time that bubbles of air are forced into the bulk water phase during shaking, drops of water will be projected from the bulk water phase into the bulk air phase. If there is a sufficient amount of excess dry particles not attached to the planar interface between the two phases, then these water drops could become stabilised by the excess particles. This should be particularly true if the water drop does not contact the planar air-water surface until film growth is well under way. At this point the surface pressure of the particles on the planar interface will be high and the chance of the marble being stable are higher.

4.2.2 Effect of particle hydrophobicity

In a similar experiment to that discussed above 0.01 g of fumed silica, coated to differing extents with either DCDMS or PDMS, was added to 10 ml of water in a glass vessel 200 mm tall and 28 mm internal diameter. The system was then shaken for 20 s and the height of the particle film formed measured. In this way the effect of changing the particle hydrophobicity on the film growth could be observed.

Figure 4.5 shows the height of film growth as a function of % SiOH for 2 different types of surface coating, DCDMS (short chain) and PDMS (long chain). For both the DCDMS and PDMS coated silicas as the particles become more hydrophilic the amount of film growth seen is reduced. Interestingly, the biggest difference in behaviour between the DCDMS and PDMS coated silica is at high % SiOH i.e. low surface coverage. This is presumably because the larger PDMS groups are capable of obscuring large areas of silica surface relative to the same extent of coating of the smaller DCDMS chains. This renders a PDMS coated silica more hydrophobic for a given surface coverage than the DCDMS equivalent, a fact that is illustrated well here. Figure 4.6 shows a schematic illustration of the way that a PDMS coating can render a silica particle more hydrophobic for a given surface concentration than a DCDMS coating.

This effect is most noticeable at low surface coverage, comparison A, rather than high surface coverage, comparison B. This is because at low surface coverage

Figure 4.5. Variation of film height with particle hydrophobicity (expressed as % SiOH) for DCDMS and PDMS treated silica nanoparticles. For each experiment, 0.01 g particles was shaken for 20 s with 10 ml of water in a 28 mm (inner diameter) x 200 mm (height) measuring cylinder. Particles with % SiOH < 25% produced films which filled the available height, i.e. 200 mm.

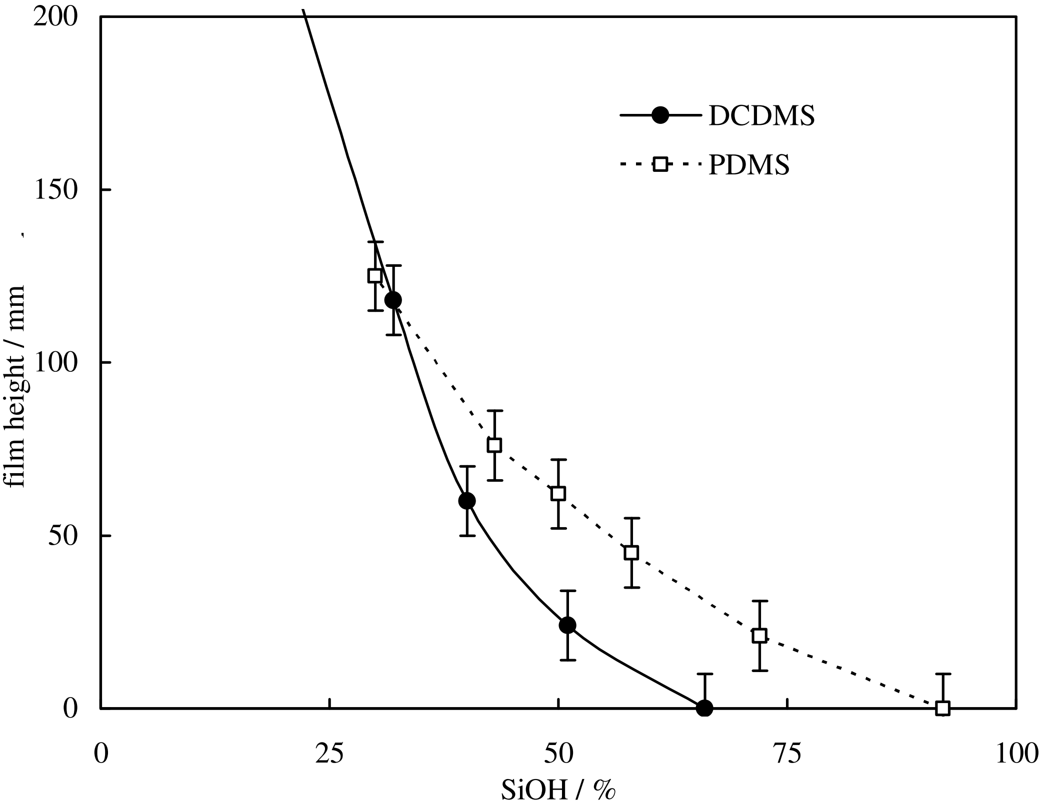

Figure 4.6. Schematic representation showing how the difference between the modification of a hydrophilic particle by either long or short chain hydrocarbons is most different at low surface coverage, comparison A, compared to high surface coverage, comparison B.

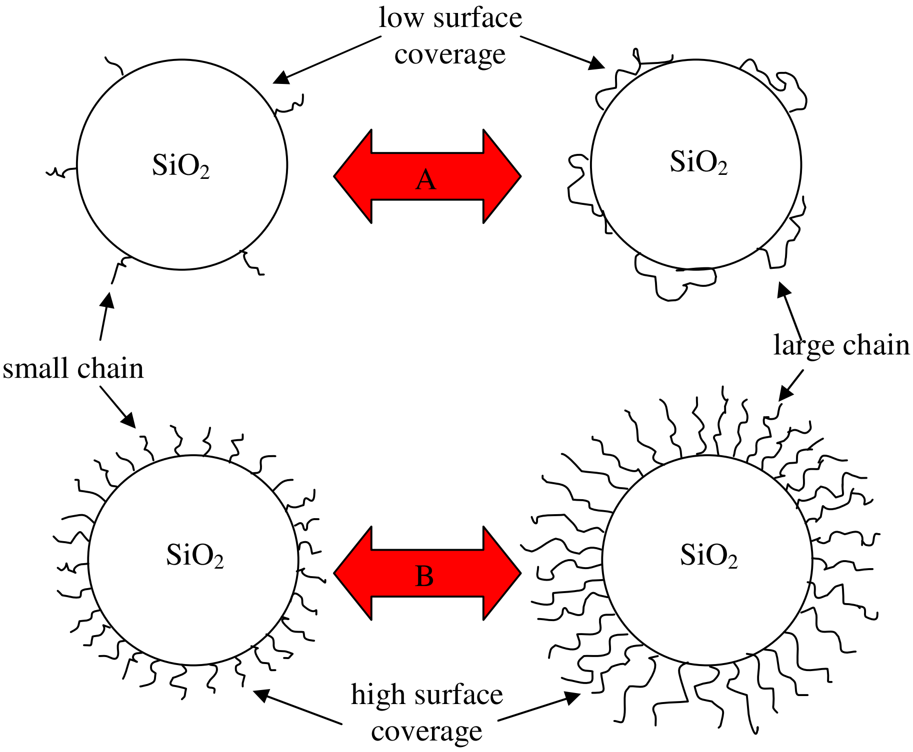

the larger chains are capable of obscuring a larger surface area on the particle than the smaller chain but at higher surface coverage the coating on the particle, in terms of what the solvent contacts, is the same i.e. it is only the depth of the coating which is different.

4.2.3 Effect of shaking

To investigate the role of shaking on the system 0.01 g of 20 % SiOH DCDMS coated particles was placed in a glass vessel, which was 200 mm tall and 28 mm internal diameter, with 10 ml of water. The vessel was then shaken once and the film allowed to grow to its full extent, the height was then recorded, the vessel shaken again and the process repeated until the film reached the top of the vessel. Figure 4.7 shows the results of this experiment plotting the height of the film after each shake versus the number of shakes of the system. The number of shakes here are sequential, i.e. it is the same system each time not a fresh system for each number of shakes. As can be seen, the film growth is reasonably linear with respect to the number of shakes. Each shake introduces fresh air-water surface which adsorbs more particles which in turn contribute to the height of the film. Presumably the film would keep growing until it either runs out of free particles to attach to the new interface, or the weight of the particles in the film becomes such that the surface pressure of the particles is unable to drive the film any higher. Neither of these conditions must have been met in the experiment performed here.

Figure 4.7. Variation of film height versus the number of shakes the system had experienced for 20% SiOH DCDMS silica nanoparticles. 0.01 g particles was shaken sequentially with 10 ml of water in a 28 mm (inner diameter) x 200 mm (height) measuring cylinder.

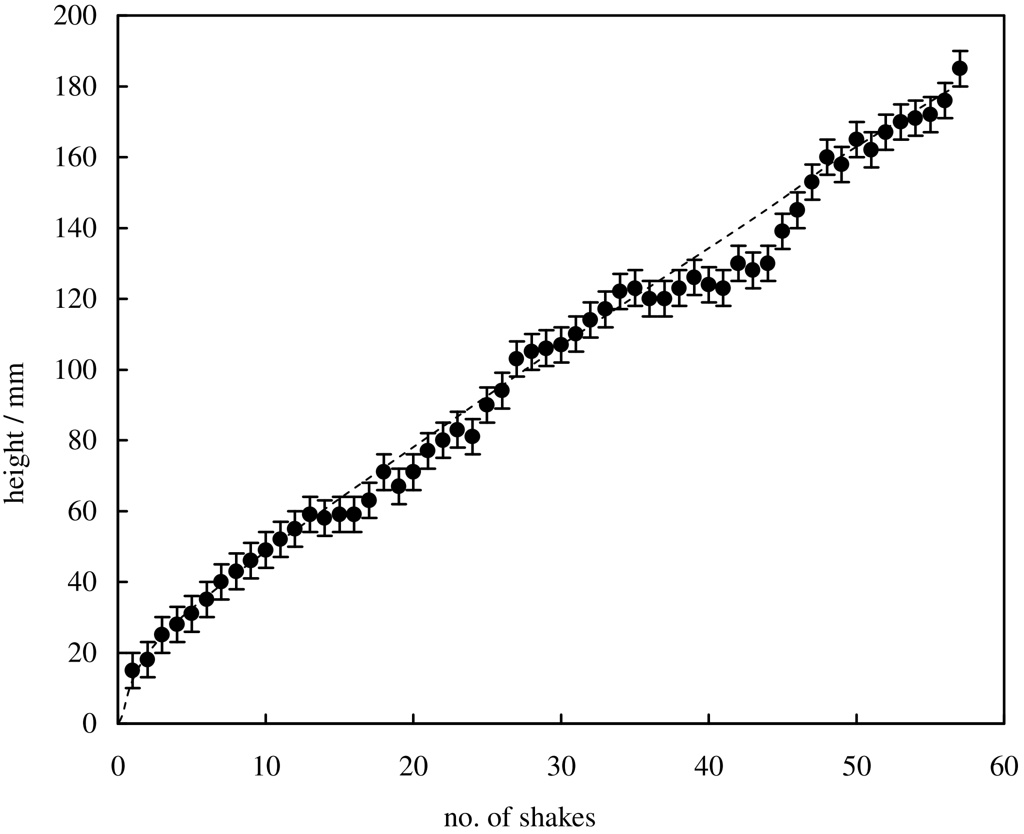

4.2.4 Effect of vessel diameter

Here we investigate the effect of the vessel diameter on the film growth phenomenon. If this phenomenon is due to the same mechanism set out in Chapter 3, i.e. conservation of particle laden interface formed under shaking, then the diameter of the vessel should play a role in the height of the film observed. The smaller the vessel diameter the smaller the planar air-water surface between the bulk air and water phases and hence, if the area of particle laden interface is conserved, the higher the film should grow. A fixed amount of hydrophobic particles were placed in vessels of various diameter and shaken for 20 s with water. If the diameter of the vessel is changed and the volume of the water is kept constant the depth of the water in the vessel will change. This can alter the way in which the system is shaken so to allow for this both systems with a constant depth of water and constant volume of water were studied.

4.2.4.1 Constant water volume

The effect of vessel diameter on the film height at constant water volume was explored. Figure 4.8 plots the height of the film versus the diameter of a vessel for a system that contains 0.01 g of 20 % DCDMS coated fumed silica and 10ml of water which has been shaken for 20 s. As can be seen as the diameter of the vessel is increased the height of the film decreased. This is to be expected if the film growth is driven by the conservation of air-water interface and the amount of

Figure 4.8. Plot of film height versus vessel diameter for systems with 0.01 g of 20% SiOH DCDMS silica particles and 10 ml of water shaken for 20 s in a 28 mm (inner diameter) x 200 mm (height) measuring cylinder.

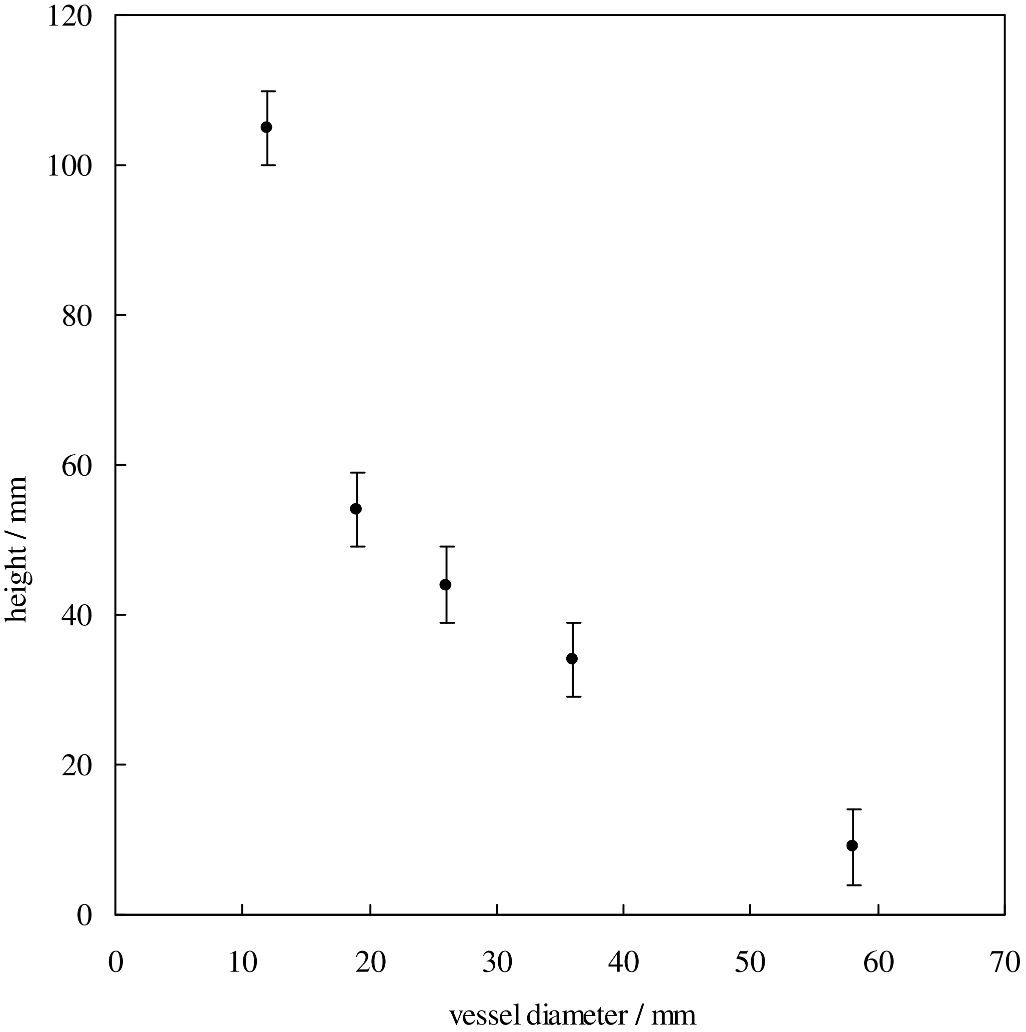

interface created under shaking is the same for each vessel. As the diameter of the vessel increases the amount of planar air-water surface increases. This means, assuming the area of particle laden air-water surface formed is the same in each vessel, that there is less particle laden interface remaining to drive up the walls of the vessel.

The total particle film area A is initially formed by bubble formation but, as the bubbles collapse, their surfaces transform into the climbing film. If it is hypothesised that the area A is constant under conditions of a constant particle mass and duration of shaking, then A is expected to be equal to the sum of the film area on the vessel walls (= πhD, where h is the film height and D is the vessel diameter) and the air-water surface area (=$\pi D2/4$). Re-arrangement gives equation 4.1

$$\left(h+\frac{D}{4}\right)=\frac{A}{\pi D} \tag{4.1}$$

which predicts that a plot of the left hand side versus $1/D$ should be linear. As seen in Figure 4.9, experimental data for systems with silica nanoparticles and a constant volume of water (10 ml) with 20 s duration of shaking are consistent with the model leading to equation 4.1. This indicates that under these conditions the amount of particle laden interface produced during shaking is independent of vessel diameter and the only effect of changing the diameter of the vessel is to reduce the area of planar air-water surface between the bulk air and water phases.

Figure 4.9. Derived plot showing the variation of film height h with vessel diameter D for systems with 0.01 g of 20% SiOH DCDMS silica particles and 10 ml of water shaken for 20 s.

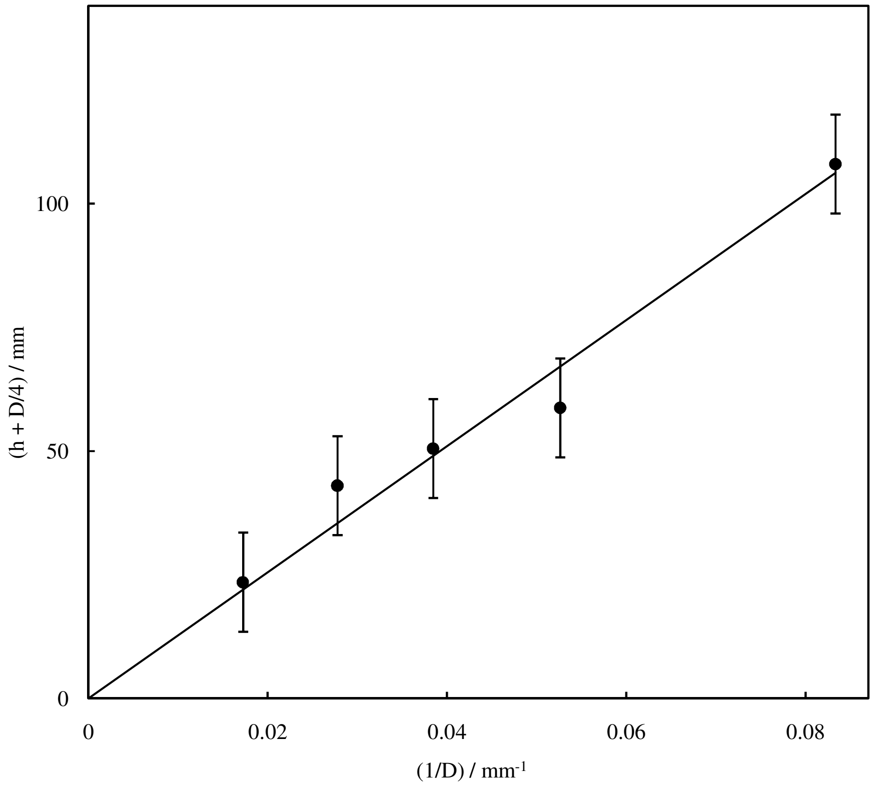

4.2.4.2 Constant water depth

The particle film climbing was studied by repeating the experiments discussed above but using a constant depth of water rather that a constant volume of water. Figure 4.10 plots the height of the film versus the diameter of a vessel for a system that contains 0.01 g of 20 % DCDMS coated fumed silica and 50 mm of water which has been shaken for 20 s. As can be seen here there appears to be no discernable trend in the height of the film versus the diameter of the vessel. Also, a plot similar to that shown in Figure 4.9, for a constant volume of water, is not linear indicating that under these conditions for a constant depth of water the amount of film formed during shaking is not constant. This is likely to be due to differences in shaking from one vessel to another.

4.2.5 Film climbing with other particles

The film growth phenomenon was not limited to systems containing hydrophobically modified fumed silica. The results described above refer to hydrophobised fumed silica nanoparticles. However, we have also observed similar patterns of film climbing behaviour for several different types of hydrophobic particles in water including PTFE particles and monodisperse spherical silica particles (0.6 μm diameter) coated with DCDMS. Overall, the phenomena seen here appear to be reasonably general and not dependent on particular particle size, type or polydispersity. A video showing a the growth of a PTFE particle film is included in

Figure 4.10. (a) Plot of film height (h) versus vessel diameter (d) for systems with 0.01 g of 20% SiOH DCDMS silica particles and 50 mm of water shaken for 20 s. (b) For the same system (h + D/4) versus 1/D.

(a)

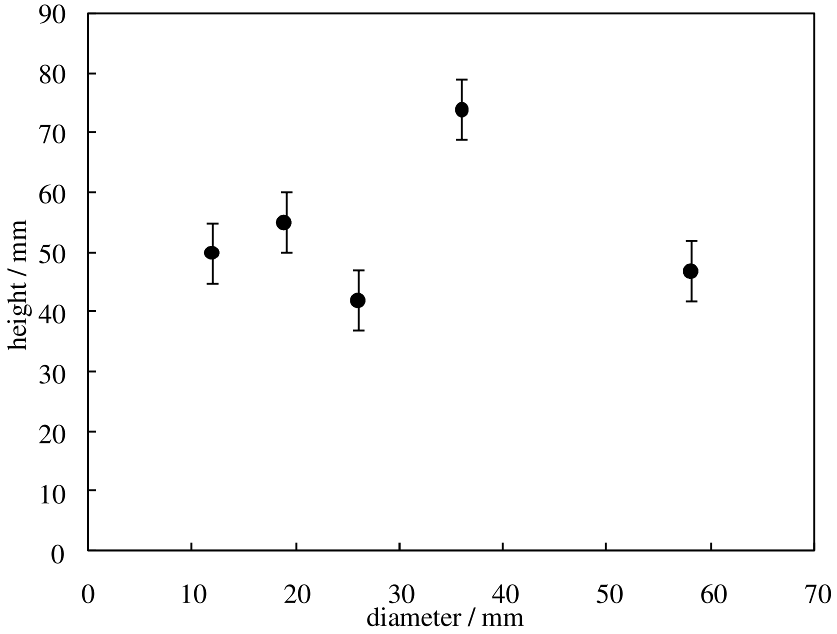

(b)

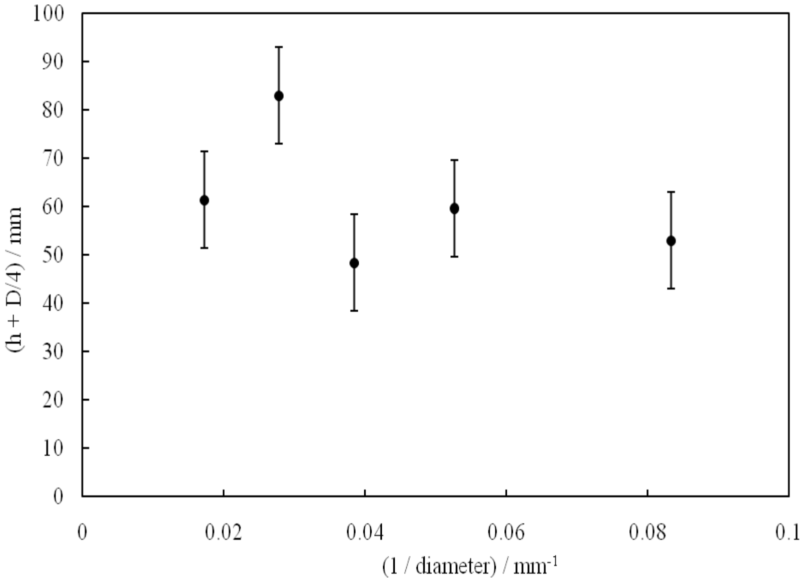

the supplementary electronic information (DVD attached to the inside cover of the thesis).

4.2.6 Foams stabilised by constricting film growth

Although not investigated fully here it is worth noting that it was possible to stabilise crude foams by restricting the growth of the particle film. When 0.001 g of 20 % DCDMS coated fumed silica particles were shaken with 1 ml of water in a home-built cell which had a well of dimensions 13 x 63 x 3 mm then stable foam bubbles could be observed. The crude foam was imaged using the camera on the DSA 10 and can be seen in Figure 4.11. Because the film is constricted in a small vessel the surface pressure of particles remains high and allows effective stabilisation of the foam bubbles. If the film is allowed to grow then no stable bubbles are observed. When the film growth was constricted the foam bubbles formed were stable for at least 2 hours.

4.2.7 Effect of vessel hydrophobicity

According to the mechanism set out in Chapter 3, film growth should be directed up the vessel walls when the contact angle of water with the vessel wall is less than 90^o but should go down the walls when the contact angle is greater than 90^o. To confirm this, DCDMS silica nanoparticles with 20% SiOH were shaken

Figure 4.11. Image of foam bubbles formed when 0.001 g of 20 % DCDMS coated fumed silica particles were shaken with 1 ml of water in a home-built cell which had a well of dimensions 13 x 63 x 3 mm. The width of the image is approximately 11 mm.

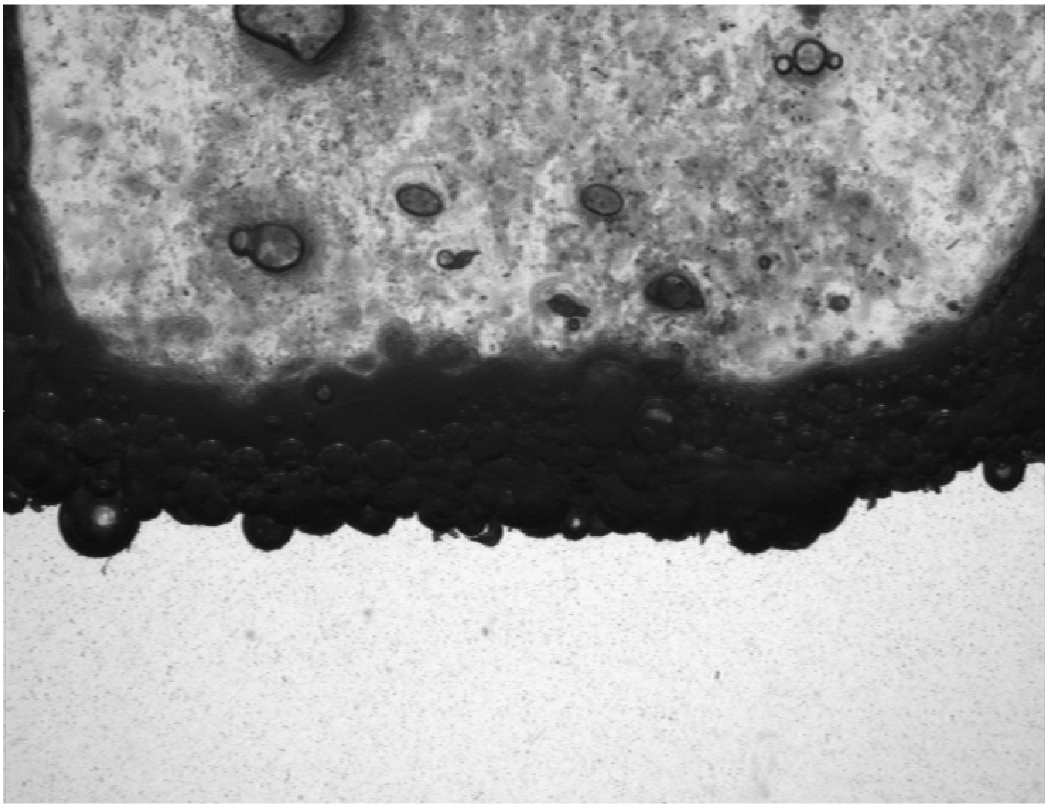

with 20 ml of water in a vessel with water contact angle of greater than 90^o (hydrophobised using 1 wt.% octadecyltrichlorosilane in toluene for 60 minutes at room temperature under nitrogen). Slight film movement downwards was observed but the resultant glass-air-water film was unstable. This is likely to be due to the large difference in density between air and water. The particles film is unable to extend down the side of the aqueous phase due to the weight of water which must be displaced.

4.3 Particle Films

The particle film growth phenomenon described is an excellent way of transferring hydrophobic particle films onto planar substrates. Films were produced in a home-built cell which had a well of dimensions 13 x 63 x 3 mm. Following addition of water and particles, a standard microscope slide was placed on top of the well to seal it. Shaking of the cell produced a particle film on the slide which could then be removed, dried and studied. Films of both fumed silica particles and Teflon particles were spread onto microscope slides and images using optical microscopy and SEM. Contact angle measurements were also made on the particle films.

4.3.1 Microscopy of particle films

Figure 4.12 shows optical and SEM images of 20% SiOH silica nanoparticle films deposited using the film cell. The mass ratio of silica to water (0.01:0.5) is high relative to the systems described in Figure 4.1 and so films with an excess of silica particles are expected. The micrographs show features in three distinct size regimes. The largest features are 5-10 μm and probably correspond to large agglomerates of silica. At an intermediate size range, there is a fairly random patchwork of connected silica aggregates on a length scale of about 0.2 μm. These features may correspond to silica which remains airborne during the shaking/film formation but which subsequently sediments onto the film. Finally, there are film regions comprising separated circular spots of 100 nm approximate diameter. These film regions appear to underlie the other regions and are thought to correspond to particles adsorbed in the grown film surfaces following water evaporation from the film. Consistent with the separation of these silica spots, it is known that hydrophobic particles (monodisperse silica of 3 μm diameter hydrophobised using DCDMS) adsorbed at the air-water surface show strong repulsion over very long ranges of the order of 10 μm.

4.3.2 Particle film wettability

Finally, it is well known that roughness can enhance the hydrophobicity of surfaces as probed by the contact angle of a water droplet placed on the surface.[6]

Figure 4.12. Optical (top) and S.E.M. (central and bottom) images of (a) 20% DCDMS coated fumed silica particle film and (b) a teflon particle film. The films were formed by shaking 0.01 g if particles and 0.5 ml of water for 30 seconds in the film growth cell. The scale bars are 50 µm, 5 µm and 1 µm from top to bottom. The optical micrographs are taken directly above the sample whereas the S.E.M. images are taken with a 40° tilt around the horizontal axis.

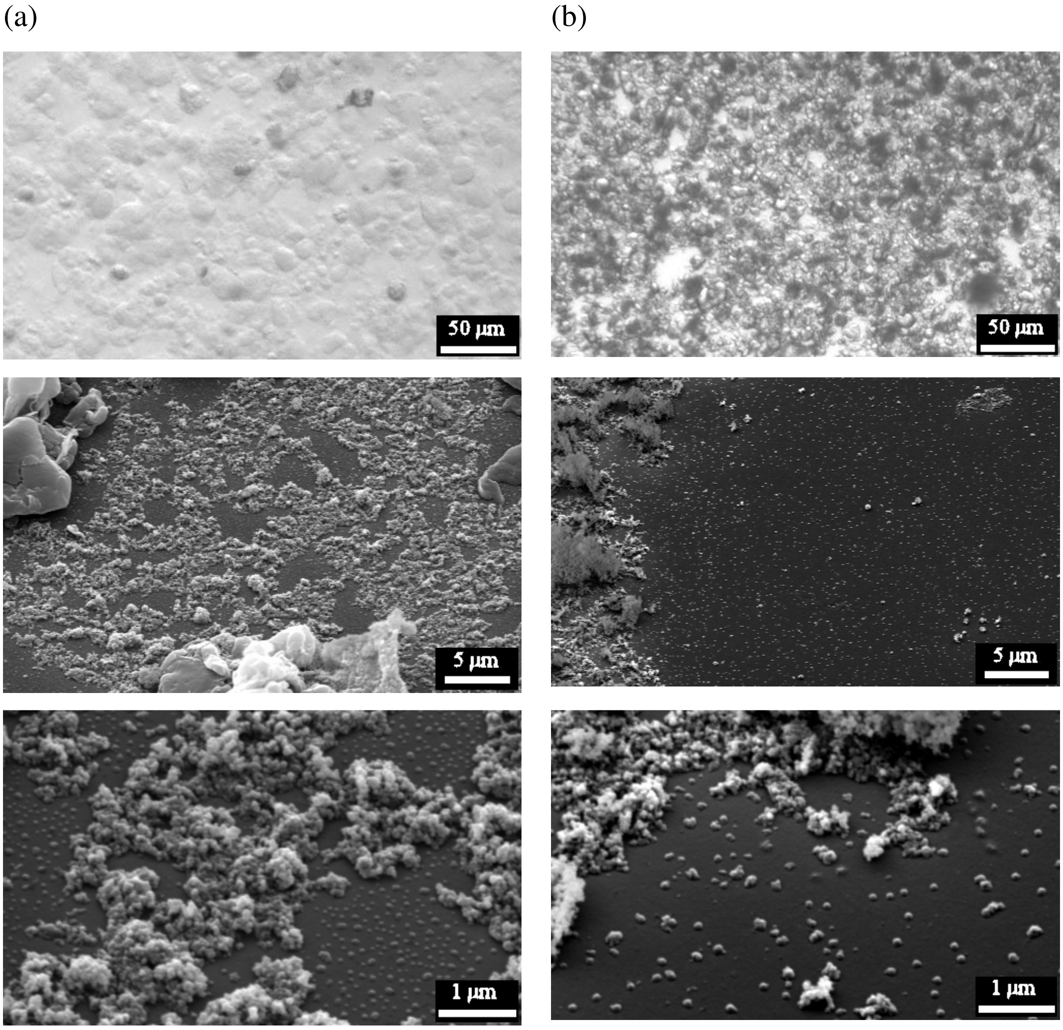

The effect is exemplified in nature by the Lotus and other plant leaf surfaces which have roughness covering multiple length scales, as noted for the films shown in Figure 4.12.[7] With this background in mind, the water droplet contact angles on the films under air shown in Table 4.1 where it can be seen that the roughness of the particle films produced enhances the surface hydrophobicity relative to the corresponding smooth surface. Figure 4.13 shows the appearance of a drop of water on both a hydrophobic silica particles film and Teflon particle film. As can be seen, the water barely wets the surface and contact angles measured are very high.

System	**Advancing contact angle / ^{o}**
Hydrophobised smooth glass	95
Film of 20% DCDMS SiOH silica particles	170
Smooth PTFE tape	144
Film of PTFE particles on glass	159

Table 4.1. Advancing three phase contact angle of a water drop under air on both hydrophobic silica and Teflon particle films. The contact angle of a water drop under air on the equivalent smooth surfaces is show.

4.4 Conclusions

The overall mechanism is similar to the particle-stabilised emulsion systems described in Chapter 3. Shaking the initial two-phase mixture forms foam bubbles.

Figure 4.13. Images of a drop of water on (a) a film of 20 % SiOH DCDMS coated silica, and (b) a Teflon particle film both under air. The scale bar is 2.5 mm.

(a)

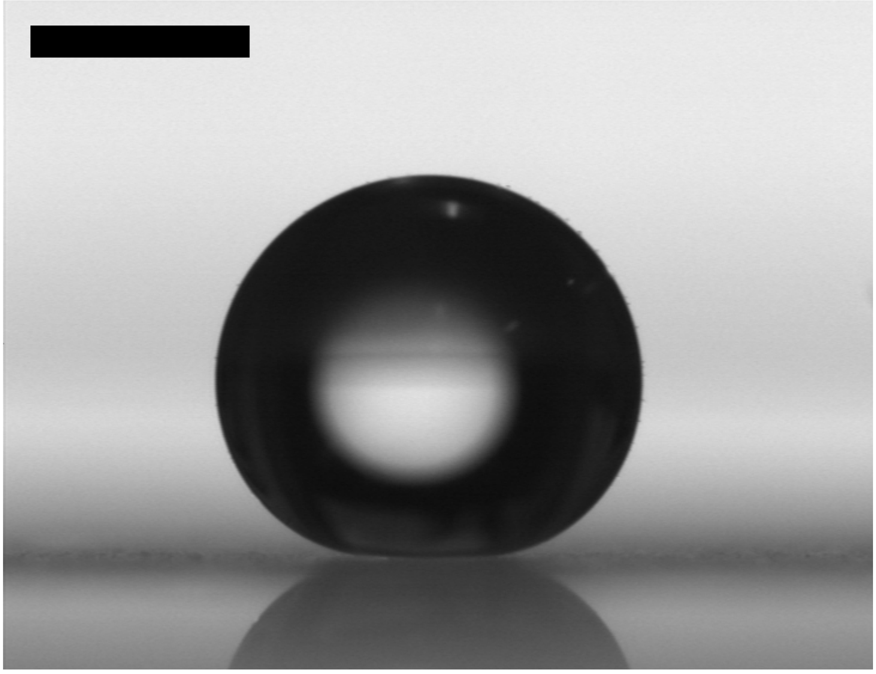

(b)

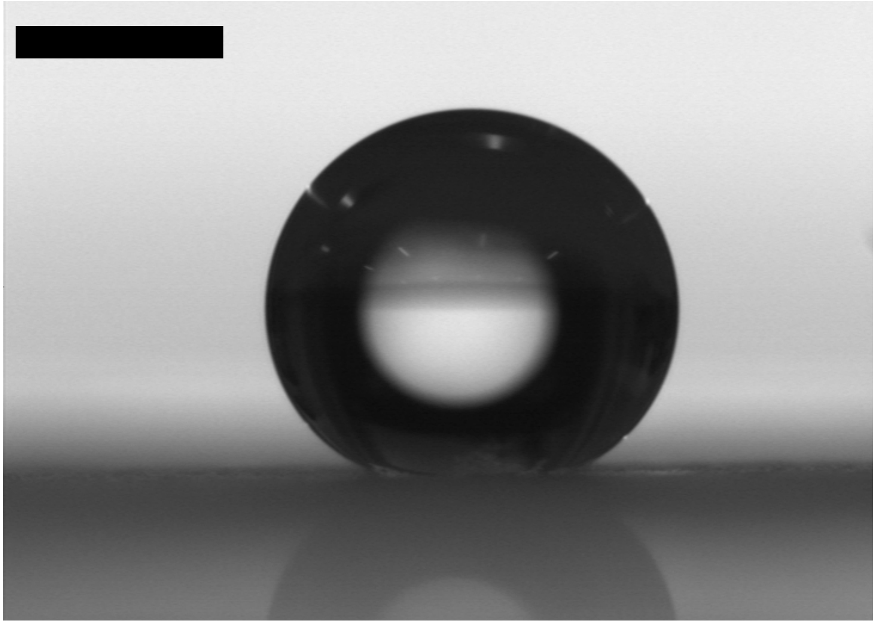

The foam bubbles are unstable with respect to coalescence with the planar air-water interface, presumably because the adsorption of silica particles at the curved and flat air-water surfaces is too low to prevent coalescence. However, the particles at low concentration in the surface are likely to be adsorbed irreversibly with an adsorption energy greatly in excess of thermal energy. In this situation, bubble coalescence reduces the total air-water surface area, increases the surface concentration of adsorbed particles and hence increases their surface pressure in the air-water interface separating the bulk phases. This increased surface pressure drives the film climbing up the vessel walls. Bubble coalescence will stop when the surface concentration of adsorbed particles is sufficient to stabilise the surfaces against coalescence, a feature which has many similarities with the phenomenon of limited coalescence observed in emulsions stabilised solely by particles. Film growth will stop when the surface pressure of the adsorbed particles has reduced below a critical level as a result of the area expansion. Within this mechanism, the process of bubble loss with film growth and the reverse process of bubble formation with film loss should be repeatedly reversible by shaking. This is observed experimentally. This is represented schematically in Figure 4.14. This phenomenon has since been observed and further explained by Nikolov and Wasan.[8]

The effect of changing the particle concentration, the hydrophobicity of particles, vessel diameter and shaking have been investigated and explained and all appear to be consistent with mechanism described above. Particle film growth

Figure 4.14. Schematic representation of the mechanism that brings about the rapid particle film growth witnessed when hydrophobic particles are shaken with water in a glass vessel.

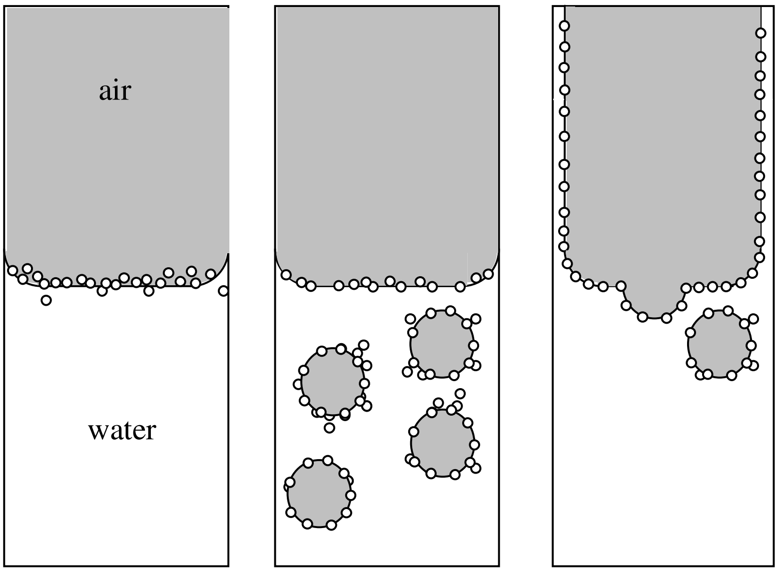

Hydrophobic particles at the surface of water (white) beneath air (grey) within a hydrophilic container

Shaking the mixture produces foam bubbles with a low surface concentration of particles adsorbed at the air-water interfaces

Coalescence of the foam bubbles with the flat air-water surface transfers particles to the interface between the bulk phases. The additional surface pressure of the adsorbed particles causes the particle-laden film to spread up the hydrophilic walls driven by foam bubble coalescence is a much more robust phenomenon occurring in a more simple system than the film growth driven by emulsion drop coalescence. Some of the properties of the films formed have been investigated by optical microscopy, TEM and contact angle measurements.

4.5 References

---

[1] K.S. Mayya and M. Sastry, *Langmuir*, **15**, 1902 (1999).

[2] B.P. Binks, J.H. Clint, P.D.I. Fletcher, T.J.G. Lees and P. Taylor, *Langmuir*, **22**, 4100 (2006).

[3] D-G. Li, S-H. Chen, S-Y. Zhao, X-M Hou, H-Y. Ma, X-G and Yang, *Appl. Surface Sci*, **200**, 62 (2002).

[4] A.D. Nikolov and D.T. Wasan, *Abst. Pap. Amer. Chem. Soc.*, U661 345-COLL Part 1, 225 (2003).

[5] B.P. Binks and R. Murakami, *Nature Mater.*, **5**, 865 (2006).

[6] P.J. Wagner, R. Furstner, W. Barthlott, and C. Neinhuis, J. *Exp.l Bot.*, **54**, 1 (2003).

[7] L. Gao and T.J. McCarthy, *Langmuir*, **22**, 2966 (2006).

[8] A.D. Nikolov and D.T. Wasan, *Langmuir*, **18**, 9933 (2008).

CHAPTER 5

EMULSIONS STABILISED BY HYDROPHILIC SILICA

5.1 Introduction

Adsorption of solid particles to the oil-water interface can stabilise an interface with respect to coalescence.[1,2,3] When studying particle-stabilised emulsions the particle wettability is an important property in determining what type of system is formed.[4] Not only does particle wettability govern which type of emulsion is recovered but it also has an important role in determining if the system is stable. Particles of intermediate wettability adsorb very strongly to the oil-water interface, forming very stable emulsions, whereas particles at the extremes of wettability, i.e. very hydrophilic or very hydrophobic, do not.[5] Normally changing the interaction of the particle with the surrounding solvent is achieved by modifying the surface of the particle with a species of a different wettability.[6] Hickey *et al.* have shown that charge-stabilised gold colloids in water can be directed to the oil-water interface by addition of ethanol to the aqueous phase.[7] It is shown that the surface charge density (σ) of the particles decreases with ethanol concentration resulting in an increase in the surface activity of the gold particles. Ethanol adsorption to the gold surface displaces charged species (citrate and gold chloride ions) and renders the particles more hydrophobic. Here, we investigate if increasing the surface activity of solid particles by the addition of a low dielectric co-solvent to the aqueous phase, making the aqueous phase a poorer solvent for the particles, is a common phenomenon or one specific to citrate-stabilised gold particles.

We have chosen to investigate the effect of co-solvent addition on the stability and type of dodecane-in-water emulsions stabilised by hydrophilic silica. Although the effect of the addition of organic co-solvent on the surface charge of species such as silica is still not fully understood, some efforts have been made in the literature to investigate the effect.[8] Binks and Whitby recently studied an oil, water and silica system where they investigated modifying all three phases to improve emulsion stability.[9] The stabiliser used in that study was hydrophilic, precipitated silica particles and a range of oils were studied including toluene, heptane, isopropyl myristate and methyl myristate. Simple emulsions of oil-in-water were not stable to coalescence or creaming when stabilised by silica particles alone. It was shown that the modification of the properties of the silica particles by the addition of low concentrations of salt, or surface-active species such as cationic quaternary surfactants, could increase the stability of the system to coalescence. Stable emulsions were also formed when hydrophilic silica was used to stabilise either polar oil-in-water drops or mixtures of both polar and non-polar oil-in-water drops at low aqueous phase pH. Some success was had when adding co-solvent (dimethyl sulphoxide and acetonitrile) to the aqueous phase to make the aqueous phase a poorer solvent for the hydrophilic silica and hence increase their surface activity.

5.2 Effect of co-solvent addition on the stability of emulsions

The effect of the addition of a range of alcohols (ethanol, propanol, butanol) and acetonitrile on dodecane-in-water emulsions stabilised by 100 % surface silanol (hydrophilic) silica is presented in the sections below. The emulsions were prepared by one of two protocols detailed in Section 2.2.3. Briefly, before homogenisation the hydrophilic silica particles were dispersed either into pure water then the co-solvent added (protocol 1) or the particles were dispersed into a premixed water / co-solvent solution (protocol 2). After the particle suspension was achieved the required amount of oil was added on top of the aqueous phase and the system homogenised.

5.2.1 Ethanol

Figure 5.1 shows how the volume fraction of water (ϕ_{WR}), oil (ϕ_{OR}) and cream (ϕ_{CR}) resolved with time vary as a function of the ethanol concentration in the aqueous phase for emulsions formed using protocol 1 and stabilised by 2 wt. % hydrophilic silica in water. The slight increase above unity in the value of ϕ_{OR} is more than likely due to the assumption that an equal amount of oil and water is lost during emulsification. All the systems produced were water continuous as determined by the drop test. ϕ_{ETH} is defined as the volume fraction of ethanol added to the aqueous phase where the aqueous phase volume is maintained at 5 ml. For example, 1 ml of ethanol added to the aqueous phase would give $\phi_{ETH} = 0.2$. The system containing no ethanol was unstable to coalescence and creaming. The less stable to coalescence a system is, the more

Figure 5.1. ϕ_{WR}, ϕ_{OR} and ϕ_{CR} as a function of ethanol content in the aqueous phase. The measurements were taken 15 minutes after emulsion formation for a system stabilised by 2 wt. % hydrophilic silica in water prepared by protocol 1.

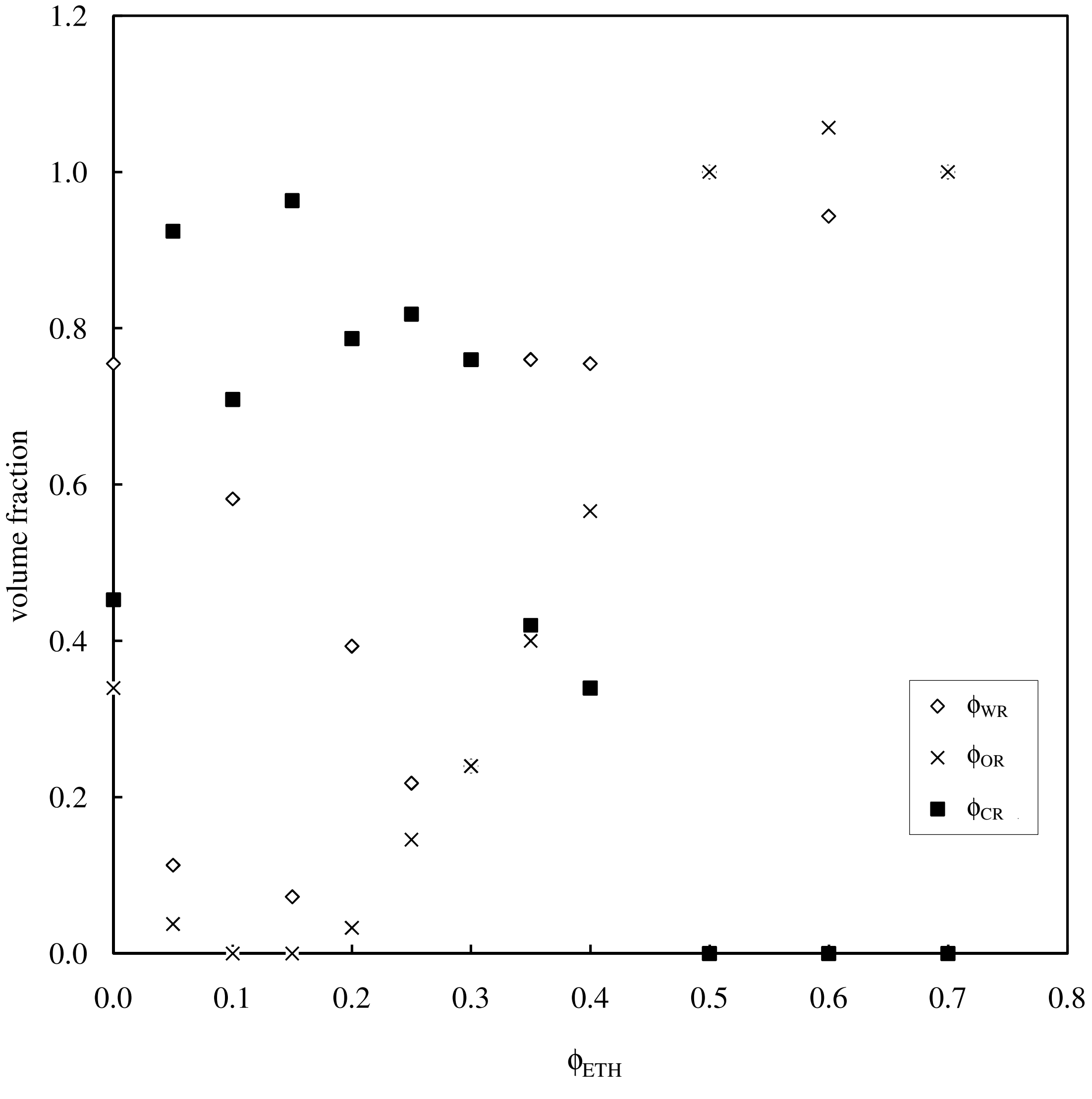

oil it will liberate and the higher ϕ_{OR} will be. Approximately 35 % of the original volume of oil was recovered after 15 minutes.

However, as can be clearly seen in Figure 5.1, ϕ_{OR} is strongly dependent on ϕ_{ETH}. ϕ_{OR} passes through a minimum at ϕ_{ETH} = 0.10 - 0.15 which corresponds to a maximum in the stability of the emulsion to coalescence. The systems that were most stable to coalescence also had the highest visual quality i.e. that appeared the whitest and most homogeneous. Figure 5.2 is a representation of the appearance of the vessels showing the volumes of oil, water and cream resolved after 15 minutes. The systems prepared using 0.10 and 0.15 volume fraction ethanol in the aqueous phase appeared white and homogeneous whereas the system produced with volume fractions either side of these values (i.e. 0 - 0.05 and 0.20 – 0.50) appeared grey and increasingly inhomogeneous at the extremes, i.e. ϕ_{ETH} = 0 and ϕ_{ETH} = 0.5.

The addition of small amounts of ethanol to silica-stabilised oil-in-water (o/w) emulsions can increase the stability of the system to coalescence. However, once this stabilisation is achieved, further addition of ethanol results in the lowering of the stability of the system to coalescence even beyond that of the system containing no ethanol. This effect was investigated over a longer time for systems formed using both protocol 1 and protocol 2. We aimed to establish if the method of preparing the systems had an effect on the increased stability towards coalescence and if the effect could be observed at extended times. Figure 5.3 shows ϕ_{WR}, ϕ_{OR} and ϕ_{CR} as a function of ϕ_{ETH} in the aqueous phase after 28 days. The systems are stabilised by 2 wt. % hydrophilic silica in the

Figure 5.2. Schematic representation of the appearance of the vessels 15 minutes after preparation. The emulsions contain 2 wt. % silica in water and were prepared using protocol 1.

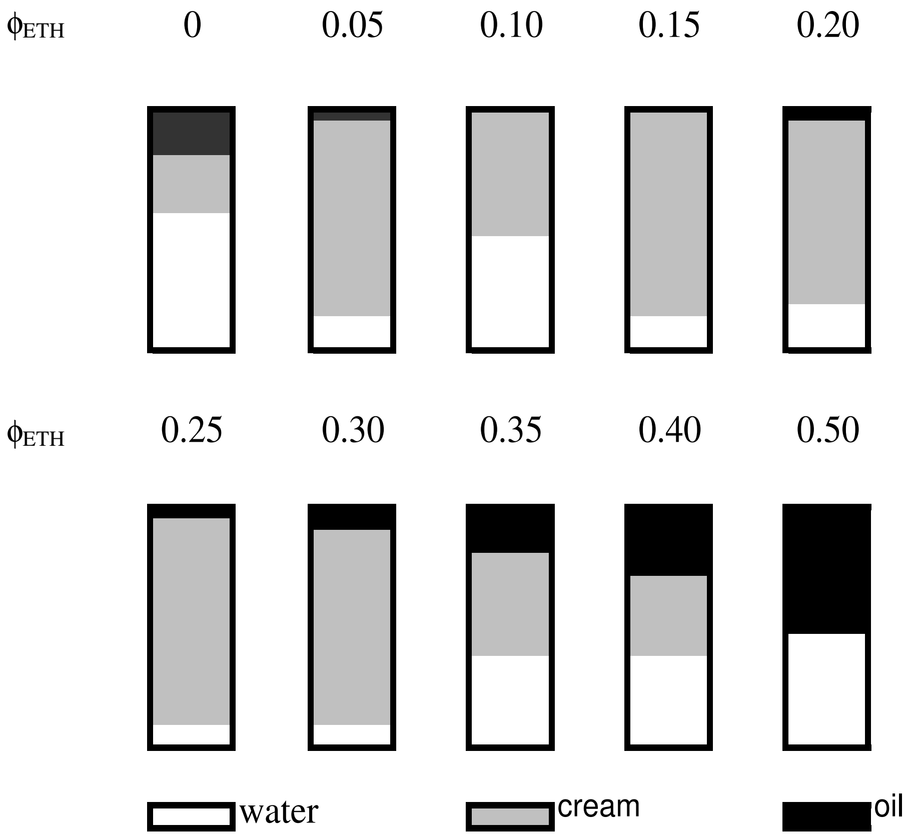

Figure 5.3. ϕ_{WR}, ϕ_{OR} and ϕ_{CR} as a function of ϕ_{ETH} in the aqueous phase. The measurements were taken 28 days after emulsion formation for a system stabilised by 2 wt. % silica prepared by (a) protocol 1 and (b) protocol 2.

(a)

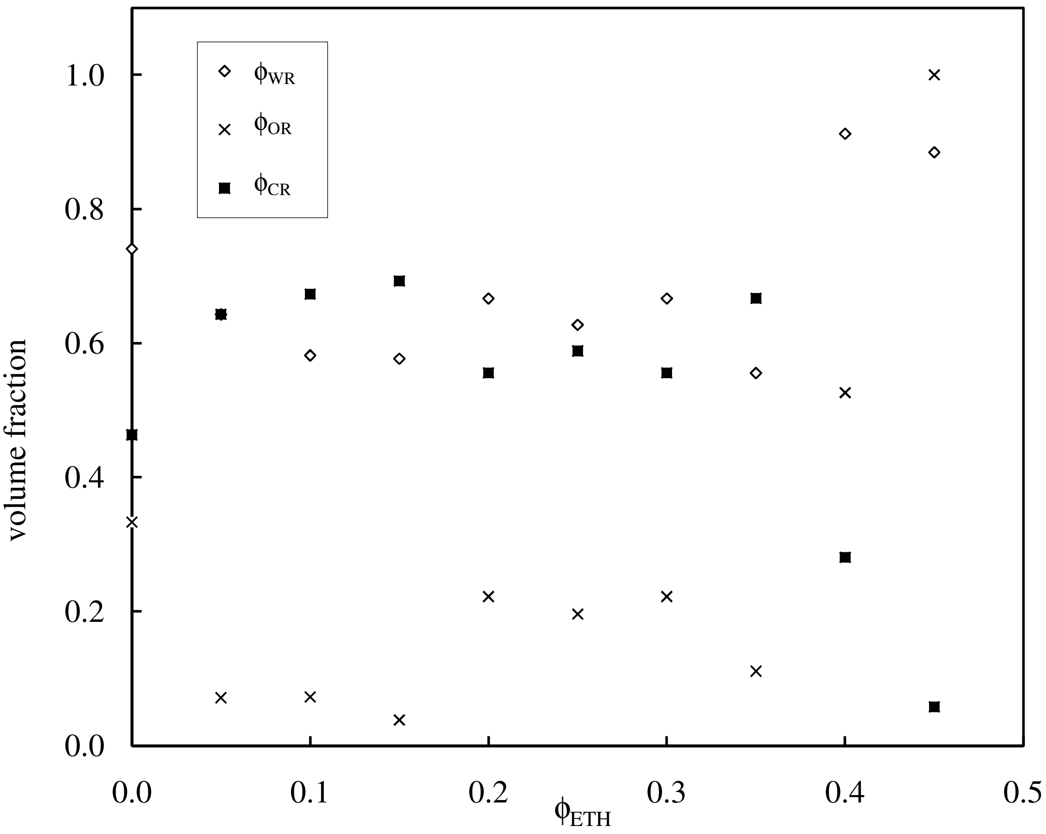

(b)

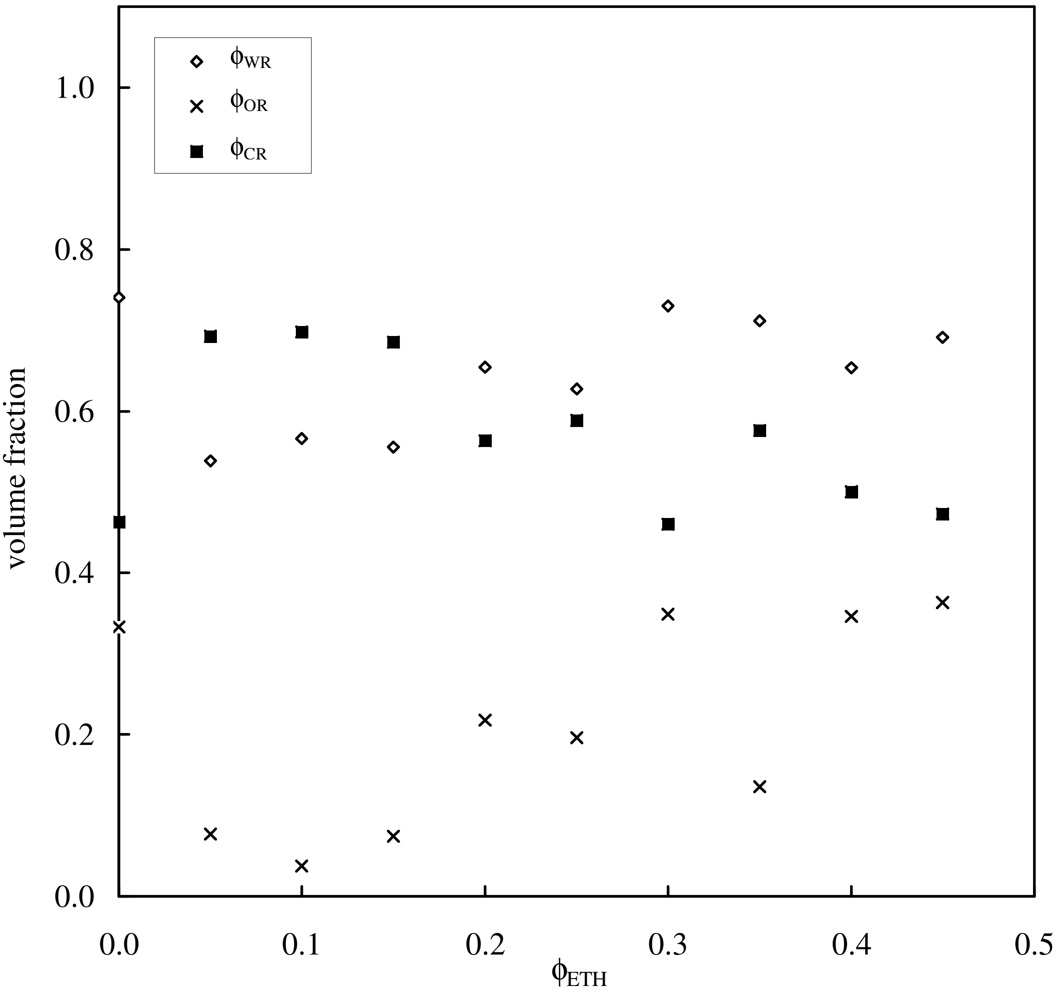

ϕ_{WR}
ϕ_{OR}
ϕ_{CR}
volume fraction
0.0
0.2
0.4
0.6
0.8
1.0
0.0
0.1
0.2
0.3
0.4
0.5
ϕ_{ETH}

aqueous phase and are formed using both protocol 1 and 2. In protocol 1 the silica is first dispersed into water and then the co-solvent is added, whereas in protocol 2 the silica is dispersed directly into the aqueous co-solvent solution. All systems formed are water continuous as determined by drop test. The maximum stability to coalescence can again be observed at low concentrations of ethanol with higher concentrations destabilising the system. Similar observations can be made as to the appearance of the systems after both 15 minutes and 28 days. In each case the systems that have the maximum stability to coalescence have the highest visual quality. To compare protocol 1 and protocol 2 more easily ϕ_{OR} is plotted against ϕ_{ETH} for both protocols in Figure 5.4. As can be seen there is little difference between the two protocols.

Optical microscopy was also used to study the emulsions. Samples were diluted with the corresponding aqueous phase and size distributions constructed. As can be seen in Figure 5.5 the average drop size increases from $\phi_{ETH} = 0$ to $\phi_{ETH} = 0.1$, remains relatively constant from $\phi_{ETH} = 0.1$ to $\phi_{ETH} = 0.3$ and increases dramatically again at $\phi_{ETH} = 0.4$. The two increases in drop size diameter corresponded to the initial increase in stability on addition of ethanol and the point where too much ethanol has been added and the system decreases in stability. Table 5.1 lists the average drop diameter and the uniformity of the emulsions (U) for increasing values of ϕ_{ETH} and Figure 5.6 plots this data.

Figure 5.4. ϕ_{OR} as a function of ϕ_{ETH} in the aqueous phase. The measurements were taken 28 days after emulsion formation for a preferred system stabilised by 2 wt. % hydrophilic silica prepared by protocol 1 (filled) and protocol 2 (open).

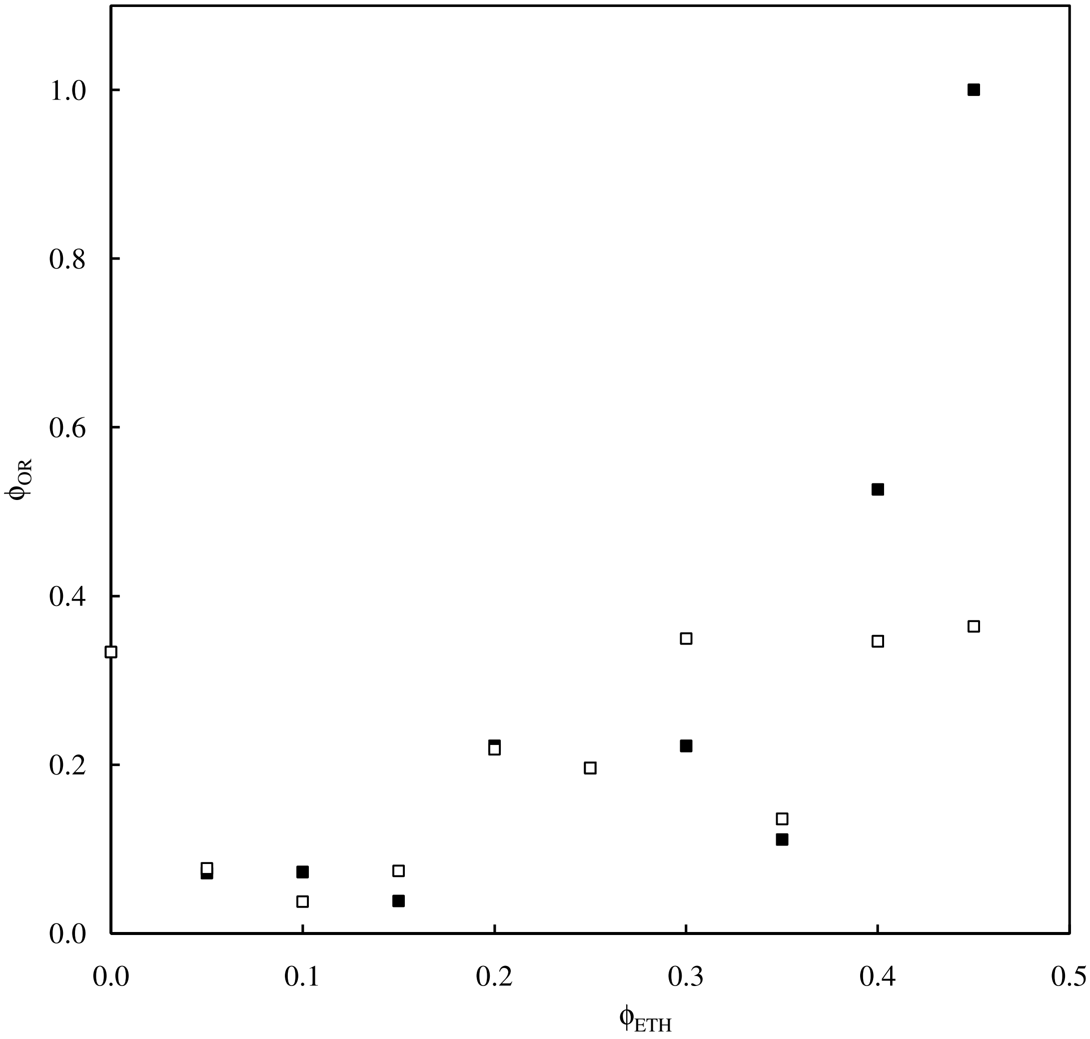

Figure 5.5. Optical microscopy images of a dodecane-in-water emulsion stabilised by 2 wt. % hydrophilic silica formed using protocol 2 with ϕ_{ETH} = (a) 0, (b) 0.1, (c) 0.2, (d) 0.3 and (e) 0.4. The scale bar represents 200 μm. The images were taken immediately after homogenisation

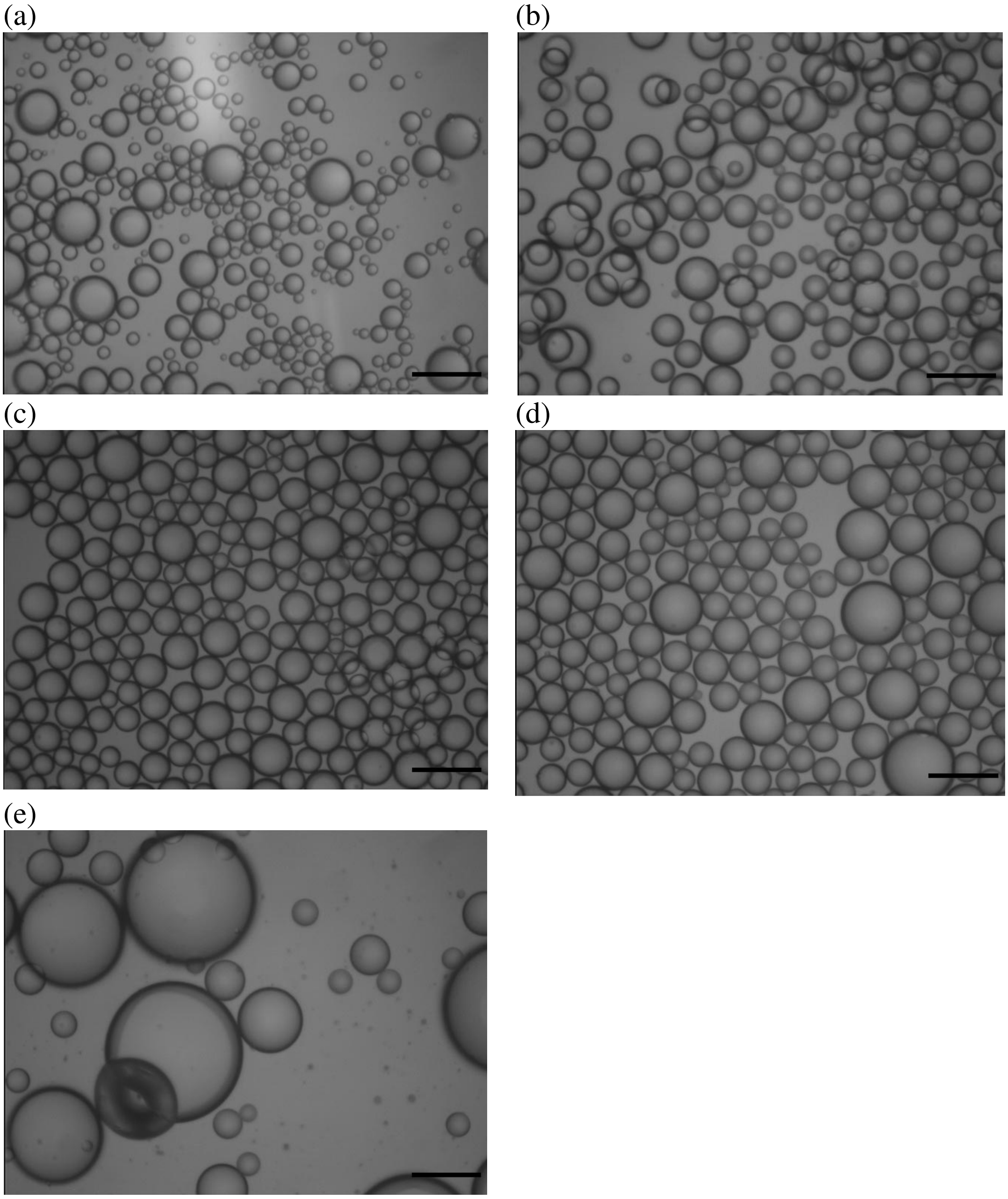

ϕ_{ETH}	**Mean drop diameter / µm**	**CV**
0.0	47	0.04
0.1	85	0.12
0.2	84	0.14
0.3	88	0.13
0.4	150	-

Table 5.1. Mean initial drop diameter and coefficient of variation (CV) of dodecane-in-water emulsions stabilised by 2 wt. % hydrophilic silica prepared using protocol.

A low value of the coefficient of variation (CV) indicates that the sample is more monodisperse. The emulsions become more monodisperse in the region where they are most stable. Since creaming is strongly dependent on drop size, and the mean drop diameter increases with ϕ_{ETH}, it would be expected that creaming would increase as ϕ_{ETH} increases. However, this is not observed. This may be due to the difference in stabilities to coalescence of the different systems. It is also interesting to note that the system which is the most stable does not have the smallest drop size. Possible mechanisms for the increased stabilisation of dodecane-in-water emulsions stabilised by hydrophilic silica when co-solvent is added will be discussed later.

Figure 5.6. Mean initial drop diameter of dodecane-in-water emulsions stabilised by 2 wt. % hydrophilic silica prepared using protocol against the volume fraction of ethanol.

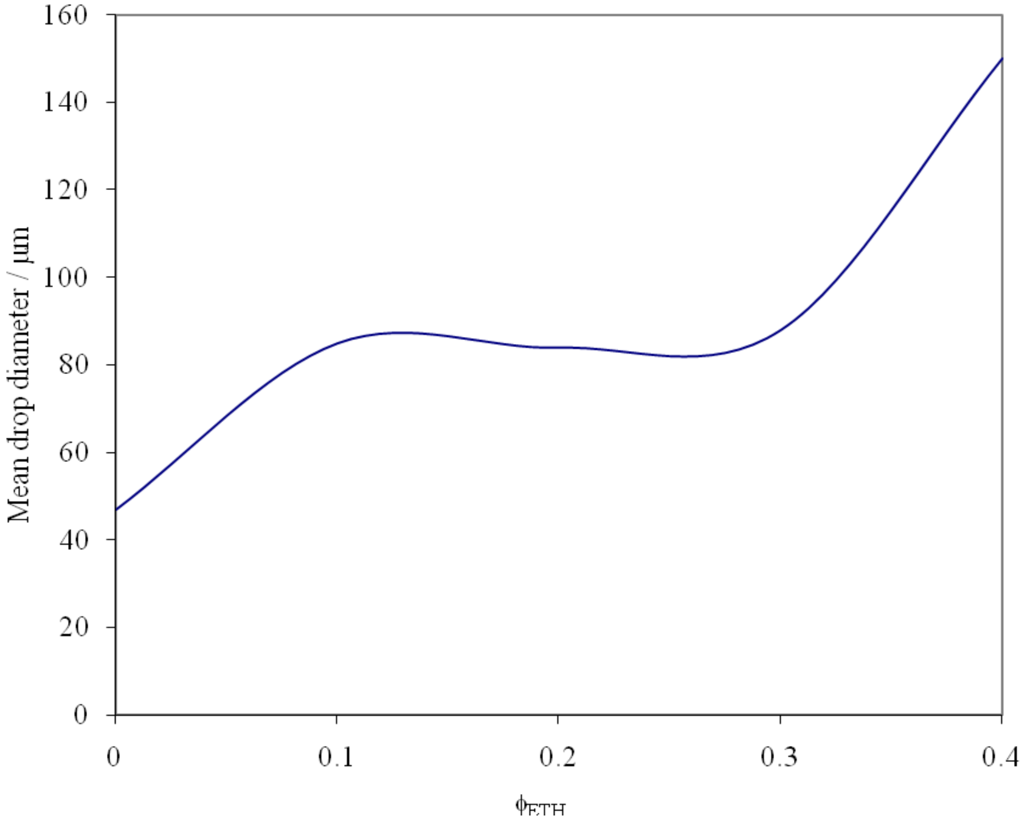

5.2.2 Other protic solvents

It has been shown that the addition of ethanol to the aqueous phase of a solid-stabilised emulsion can lead to enhanced stability to coalescence at low ethanol concentration and destabilisation at high ethanol concentration. To investigate this further, propanol and butanol were added in the same way. For each extra CH_2 group, the dielectric constant decreases. Table 5.2 lists the dielectric constants for these solvents and water.

Solvent	**Dielectric constant**
Water	80.4
Ethanol	24.3
Propanol	20.1
Butanol	17.8

Table 5.2. Dielectric constants at 25 °C.[10]

It was expected that as the dielectric constant decreased, the same effects seen for the addition of ethanol would be observed but at lower co-solvent concentrations. As can be seen in Figure 5.7 the onset of destabilisation is borne out sooner with increasing chain length. For ethanol, destabilisation is reached at the volume fraction of co-solvent (ϕ_{COS}) = 0.4, for propanol, $\phi_{COS} = 0.25$ and for butanol $\phi_{COS} = 0.2$.

Figure 5.7. ϕ_{OR} as a function of ϕ_{COS} in the aqueous phase. The measurements were taken 15 minutes after emulsion formation for a system stabilised by 2 wt. % hydrophilic silica.

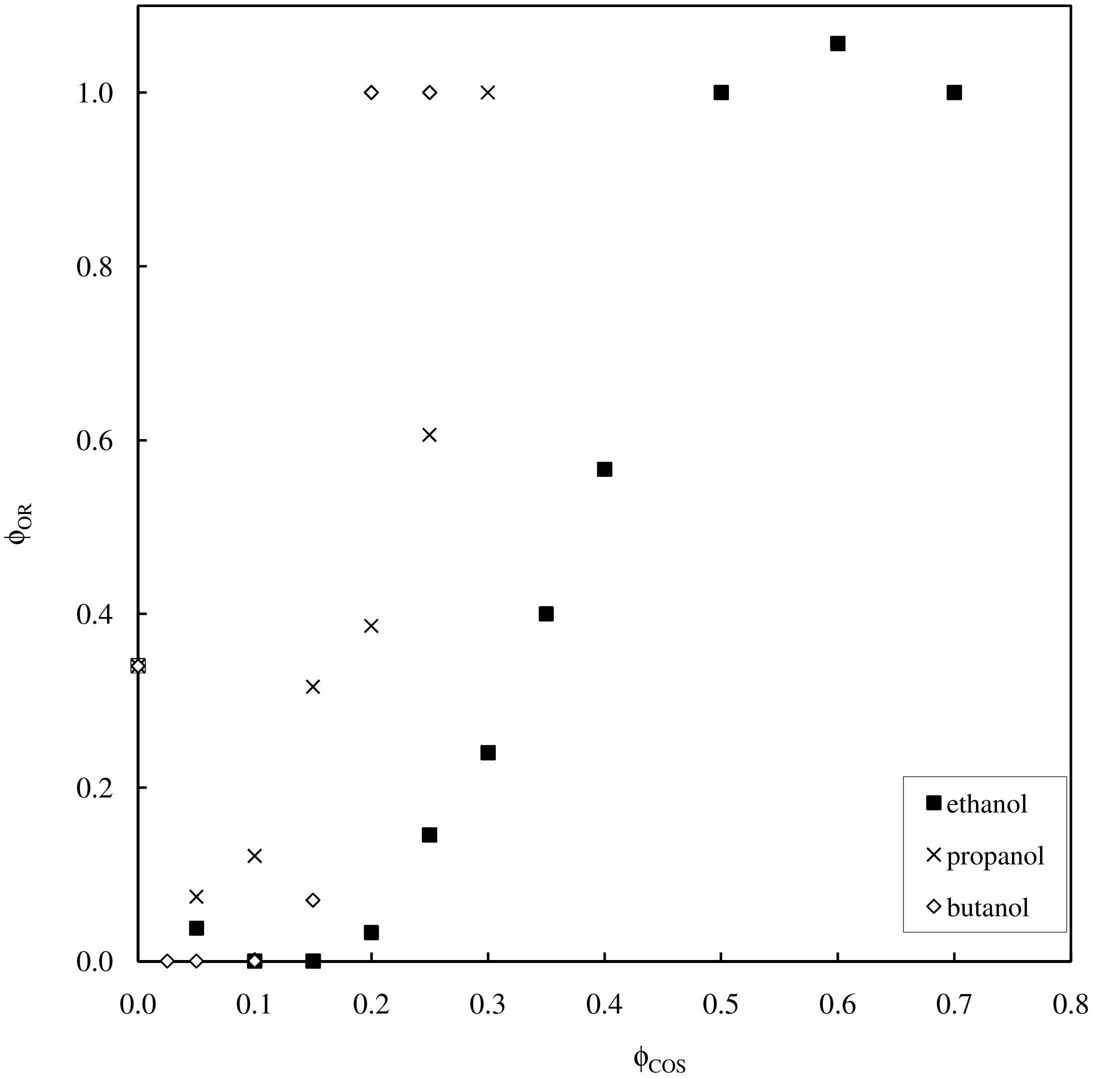

5.2.3 Aprotic solvents

The co-solvents used in the systems discussed so far have all been protic. In order to establish if the same trends would be observed with an aprotic solvent the stability of emulsions with respect to the addition of acetonitrile (ACE) was investigated. The experimental procedure was the same as for the previous co-solvents. The stability of this system can be seen in Figure 5.8. The trends are the same as those for the protic co-solvents. The stability to coalescence increases at low levels of co-solvent and decreases dramatically at higher concentrations. However, the decrease in stability towards coalescence after $\phi_{COS} = 0.05$ is more linear compared with that for the protic solvents.

5.3 Possible mechanisms

It has been shown that the addition of a small amount of a range of low dielectric co-solvents, both protic and aprotic, to the aqueous phase can enhance the stability of silica-stabilised o/w emulsions with respect to coalescence. It has also been observed that this is followed by destabilisation at higher co-solvent concentrations. Three related effects for stabilisation can be proposed.

5.3.1 Reduction in the surface charge density of silica

The lowering of the dielectric constant of a medium can reduce the surface charge density of a particle, such as silica, in that medium. Hickey *et al.* decreased the surface charge of gold particles from -0.010 C m^{-2} to -0.005 C m^{-2}

Figure 5.8. ϕ_{WR}, ϕ_{OR} and ϕ_{CR} as a function of ϕ_{ACE} in the aqueous phase. The measurements were taken 15 minutes after emulsion formation for a system stabilised by 2 wt. % hydrophilic silica prepared by protocol 1.

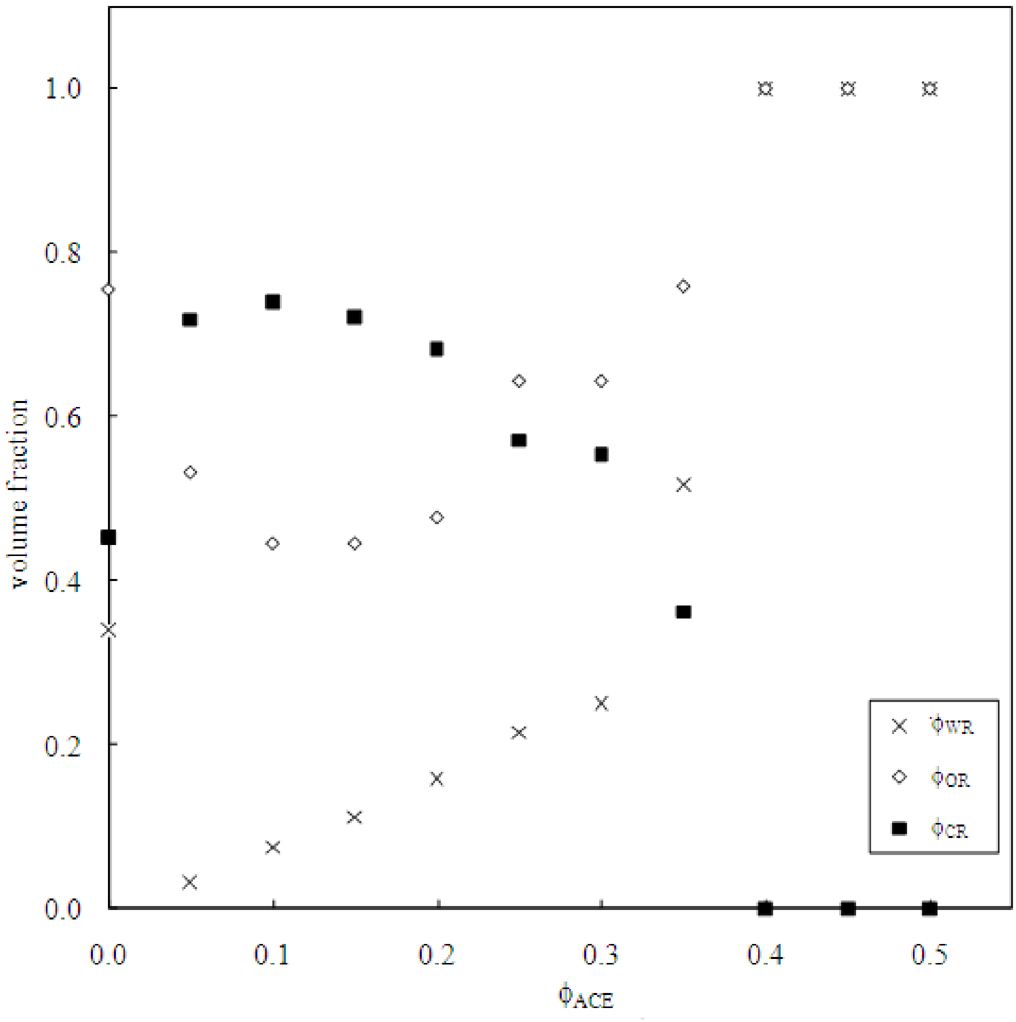

by increasing ϕ_{ETH} from 0 to 0.4.[7] The hydrophilicity of a silica particle originates from its surface charge. It can be imagined if the decrease in the dielectric constant reduces the surface charge on the silica, and hence increases the hydrophobicity, then the silica particles will be more effective at stabilising oil drops giving more stable emulsions. Fokkink and Ralston[11] have shown that a particle is most hydrophobic at its point of zero charge. Either side of this point, i.e. increasing positive or negative surface potential, the particle becomes more hydrophilic. The ability of a particle to stabilise an emulsion is dependent on its energy of attachment to that interface. This in turn is dependent on the three-phase contact angle the particle makes with the interface, i.e. the wettability of the particle.

5.3.2 Influence on adsorbed particle concentration

Hydrophilic particles, such as the ones used in this study, with similar surface charge repel each other both in bulk and at the oil-water interface. This repulsion limits the number of silica particles that can be located at the oil-water interface. If the charge on the silica surface is reduced, the repulsion between the silica particles would also be reduced and more silica particles could be accommodated at the oil-water interface. Since forming a physical barrier to coalescence is one of the major mechanisms of emulsion stabilisation by solid particles, it can be imagined that this would lead to an increase in emulsion stability. Figure 5.9 illustrates this schematically. Horozov *et al.* have studied, in detail, the behaviour of silica particles at the oil-water interface by optical microscopy.[12] They propose a mechanism for the stability of silica particle

Figure 5.9. Schematic representation of how reducing the charge of a solid particle at the oil-water interface can lead to an increase in the number of particles at the interface. In this example θ_{ow} is fixed.

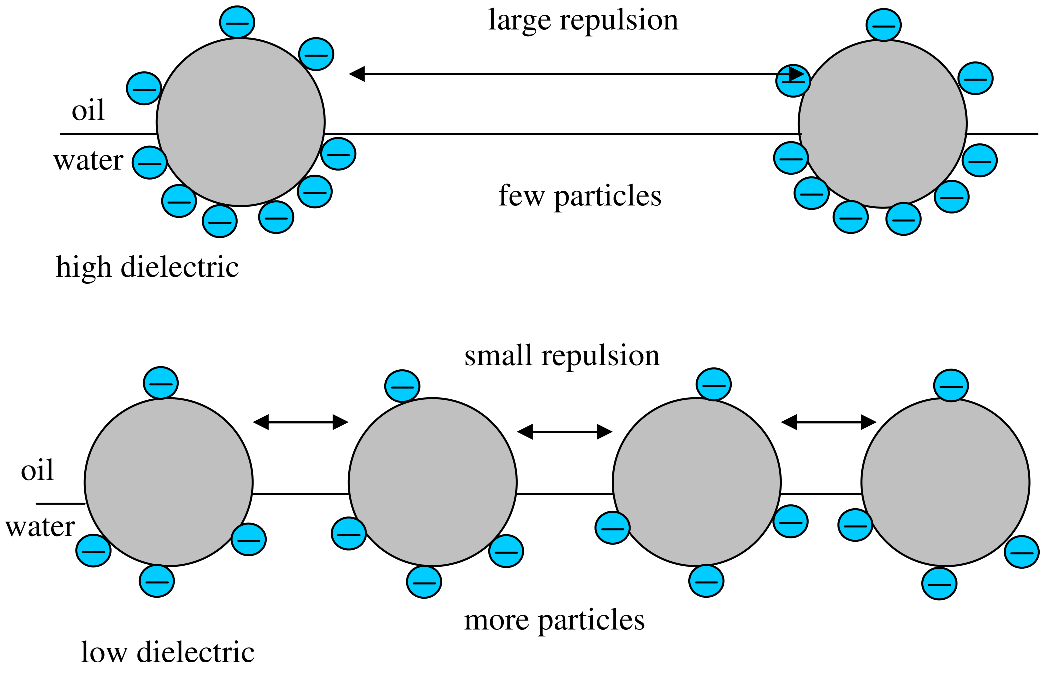

monolayers at the oil-water interface based on Coulombic repulsion through the oil phase.

Ashby *et al.* have shown theoretically that a reduction in the surface charge of a particle will lead to an increase in concentration of particles at both oil-water and air-water interfaces.[13] Therefore a decrease in surface charge should lead to an increase in the interfacial particle density and an increase in emulsion stability.

5.3.3 Aggregation of silica particles in bulk

The reduction of the surface charge on the silica particles due to the decrease in the dielectric constant of the medium could also have another effect. Silica particles are charge stabilised, i.e. it is the net repulsion due to like charges that prevents them from aggregating and sedimenting. A reduction in their overall charge could lead to flocculation particularly at higher co-solvent concentrations. It has been shown previously that the addition of electrolyte to a system stabilised by silica particles, which can also induce aggregation, can increase the stability with respect to coalescence[14]. The energy of attachment of a particle to an oil-water interface is dependent on the size of the particle as well as its wettability. Increasing the concentration of co-solvent may lead to an increase in the aggregate size. The aggregate size would increase and pass through an optimum size for emulsion stabilisation, eventually reaching a size where they are no longer stable in a dispersion but sediment. This is in agreement with observations made during the preparation of the emulsions. As the co-solvent concentration increased, the aqueous co-solvent/silica dispersions are more turbid to the eye.

Although it is likely that all of these mechanisms may play a role in the trends observed, the aggregation of the silica particles explains both the increase in stabilisation to coalescence and the subsequent destabilisation at higher co-solvent concentrations. This mechanism also helps to explain why in the systems which are most stable to coalescence the drop size is larger than in the system that contains no co-solvent and is unstable to coalescence. Normally if an oil-water interface is stable, and therefore easily formed, it would be expected that an increase in stability would coincide with a decrease in droplet size. However if the increase in stability is due to the aggregation of the silica particles then the following can occur. Without co-solvent, the silica particles are discrete but poor at stabilising the oil-water interface. This means that although the interface is not stable, the relatively large covering power of the discrete silica particles allows the formation of a large amount of interface i.e. small, unstable drops. When a small amount of co-solvent is added, and the particles become partially aggregated, the effective concentration of stabiliser is decreased, i.e. if each aggregate contains 10 silica particles the effective concentration of the particles would be 10 times smaller. However, these aggregated particles are more effective at stabilising the interface leading to stable drops, which because of the decrease in covering power, are larger than in the case with no co-solvent. Figure 5.10 is a schematic representation of the aggregation of silica particles leading to more stable emulsions and then the subsequent sedimentation as more co-solvent is added.

Figure 5.10. Schematic representation of particle aggregation leading to enhanced emulsion stability and then sedimentation. Top scheme shows effect of co-solvent on the particle dispersion and the bottom scheme shows how this affects the emulsion: (a) Discrete particles giving small unstable drops, (b) slightly aggregated particles giving larger more stable drops, and (c) large aggregates unstable to sedimentation leading to phase separation.

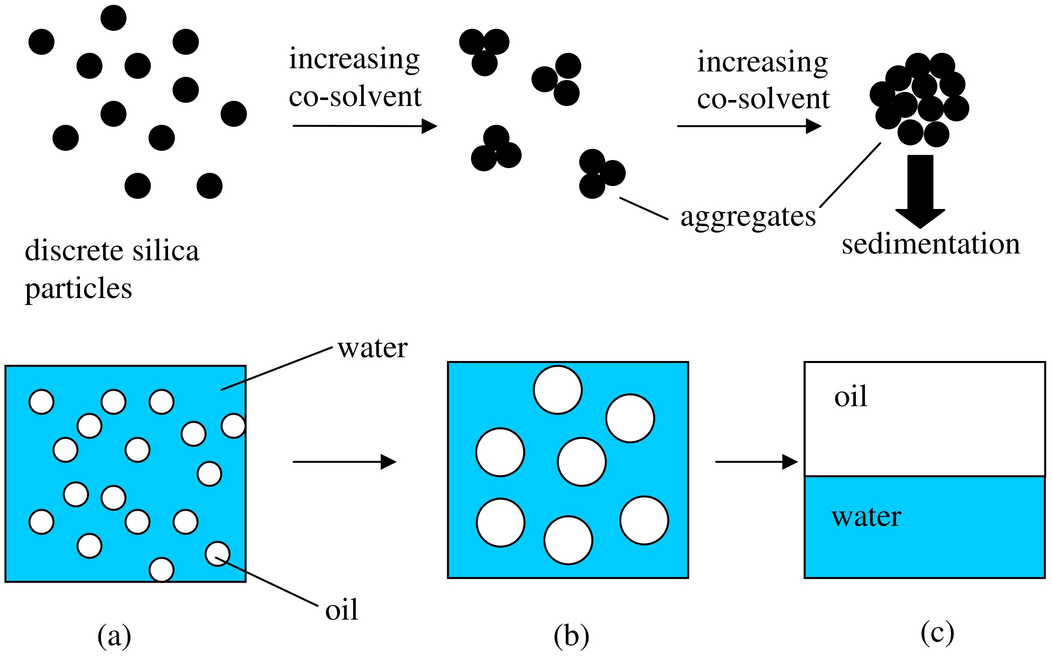

5.4 Investigation into possible mechanisms

5.4.1 Effect of co-solvent on three-phase contact angle

To begin the investigation into which of the mechanisms discussed above is responsible for the enhanced stability towards coalescence, a flat glass substrate was used to model the silica particle surface. The three phase contact angle θ_{OW} of an aqueous drop under oil was measured on this substrate as a function of ethanol concentration in the aqueous phase. Before measurement, the two phases were pre-equilibrated together for at least 6 hours. Table 5.3 lists the average values of θ_{OW} measured over three runs. Each run, measured on a new slide, consisted of averaging the values of θ_{OW} obtained from 3 or 4 drops. The average of the three runs is also shown. Figure 5.11 plots this data, along with the exact error in each value (calculated as the 95 % confidence factor), for each of the three runs and Figure 5.12 shows the average of these three runs. Although in Figure 5.11 (b) there appears to be a maximum, considering the data set as a whole it can be concluded that, within experimental reproducibility, there is little change in θ_{OW} with increasing ϕ_{ETH}. It is possible that θ_{OW} is constant because of compensation effects. Young's equation

$$\gamma_{so} = \gamma_{sw} + \gamma_{ow} \cos\theta_{ow} \tag{5.1}$$

can be re-arranged to express $\cos\theta_{OW}$, the cosine of the three-phase contact angle measured through the aqueous phase, in terms of γ_{SO}, γ_{SW} and γ_{OW} which are the surface energies of the solid-oil, solid-water and oil-water interfaces respectively

Table 5.3 Values of advancing θ_{ow} obtained as a function of ϕ_{ETH} for an aqueous ethanol drop on glass under dodecane. Occasionally during the experiment on a particular slide there would be almost complete spreading; this was thought to be an artifact of the cleaning process and the values are entered as -. Although separate error values were obtained for each of the values below, based on the spread of the contact angles, the error in each is approximately ± 5^{o}.

ϕ_{ETH}	Run 1 θ_{ow} / ^{o}	Run 2 θ_{ow} / ^{o}	Run 3 θ_{ow} / ^{o}	Average θ_{ow} / ^{o}
0.00	29	28	30	29
0.05	-	29	34	31
0.10	-	30	34	32
0.15	31	34	50	39
0.20	37	33	37	36
0.25	26	40	46	37
0.30	26	48	31	35
0.35	35	-	43	39
0.40	36	30	-	28
0.45	-	35	34	29
0.50	34	30	-	21

Figure 5.11. Average contact angles of water under dodecane for the pre-equilibrated systems as a function of ϕ_{ETH}. (a), (b) and (c) are runs 1, 2 and 3 respectively.

(a)

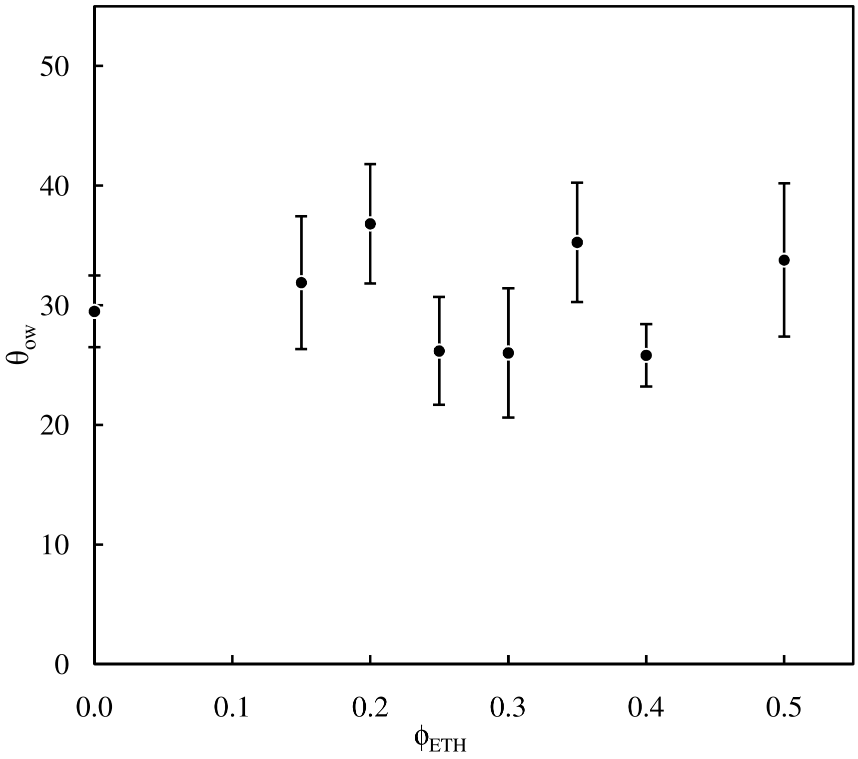

(b)

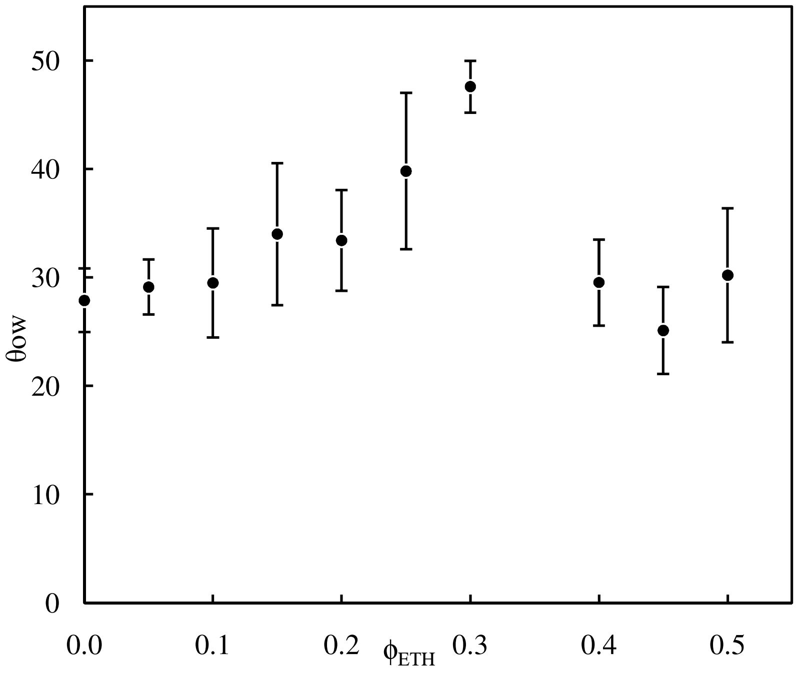
θOW
0
10
20
30
40
50
0.0
0.1
0.2
0.3
0.4
0.5
ϕ_{ETH}

(c)

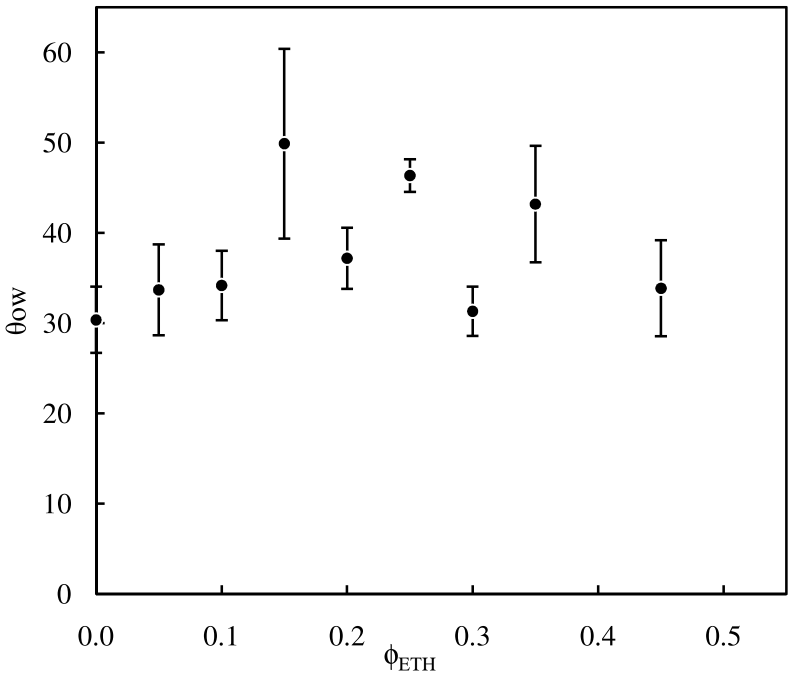
θOW
0
10
20
30
40
50
60
0.0
0.1
0.2
0.3
0.4
0.5
ϕ_{ETH}

Figure 5.12. Average contact angles over three runs for pre-equilibrated systems.

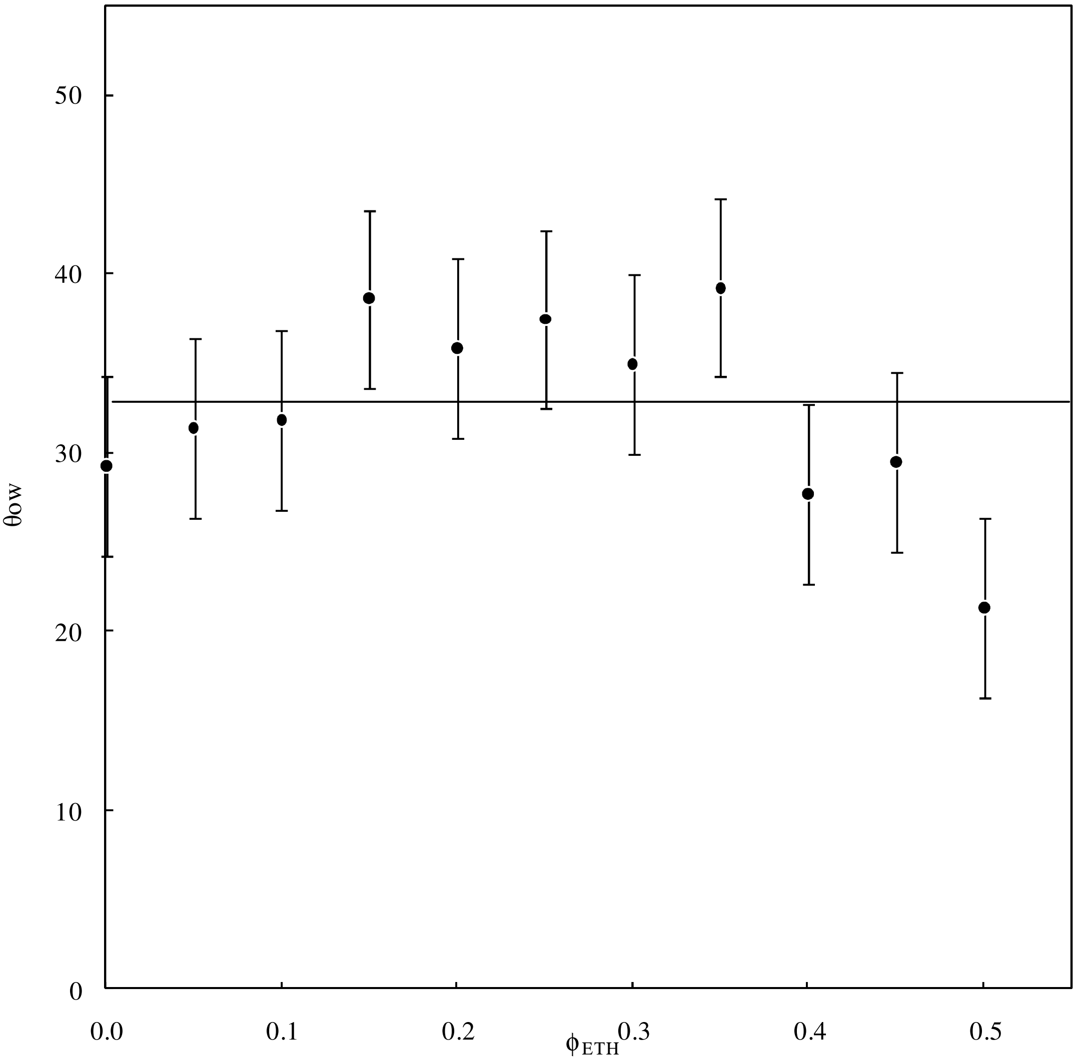

$$\cos\theta_{ow} = \frac{\gamma_{so} - \gamma_{sw}}{\gamma_{ow}}. \quad (5.2)$$

since $\cos\theta_{OW} > 0$ then $\gamma_{SO} > \gamma_{SW}$. It is reasonable to assume that γ_{OW} decreases with increasing ethanol concentration. If this is the case, and γ_{SO} remains constant, then γ_{SW} must increase by the same amount as $\Delta\gamma_{OW}$ for $\cos\theta_{OW}$ to remain constant.

In order to reduce the effect of surface roughness the experiment was repeated on a smooth silicon wafer with a ~ 3 nm coating of silica. Although this reduces the amount of contact angle hysteresis it also restricts the range of cleaning processes that can be used as anything more aggressive than sonication in ethanol removes the oxide layer exposing the wafer underneath. Figure 5.13 shows θ_{OW} as a function of ϕ_{ETH} with the estimated uncertainties. The plot is an average of 6 measurements taken independently on different silicon wafers. Within experimental error there is no change in θ_{OW} with increasing ϕ_{ETH}. This is consistent with the three-phase contact angle of an aqueous drop on glass under dodecane where the contact angle was also found not to change with increasing ϕ_{ETH}. Again, this is not conclusive evidence that the wettability of the silica particles is not modified by the presence of the ethanol molecules as it is possible that there is no change in contact angle due to a compensation effect of one of the interfacial tensions IFTs as discussed above. Although it is possible that a compensation effect could explain the apparent independence of θ_{OW} as a function of ϕ_{ETH}, if there was a wettability change significant enough to cause the

Figure 5.13. Average advancing and receding contact angles of an aqueous drop, containing various amounts of ethanol, on a flat silicon wafer under dodecane measured through the aqueous phase. The drop size was ~ 50 µl and the measurements were taken at 25 °C.

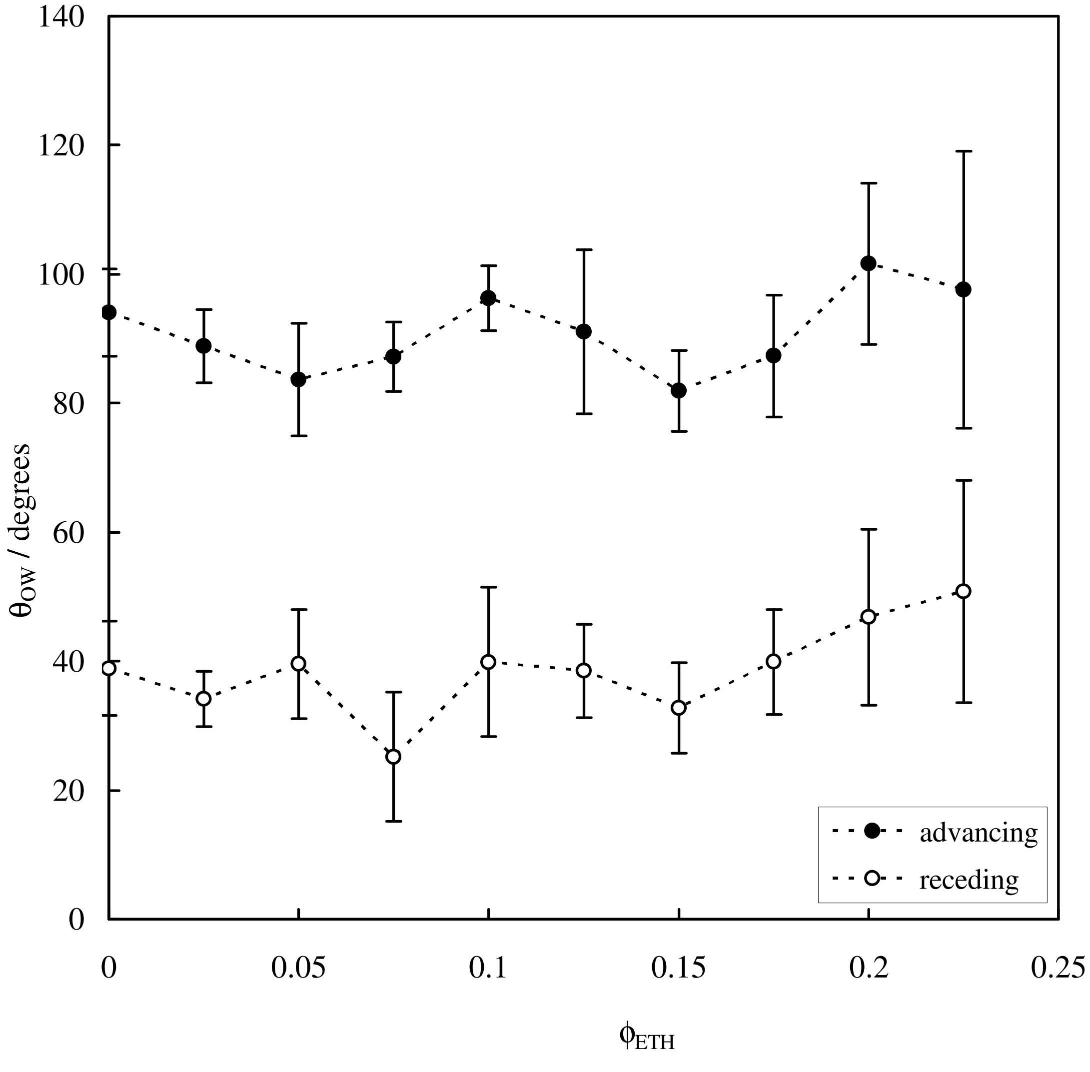

increase in stability observed then some change in θ_{OW} as a function of ϕ_{ETH} should be observed.

5.4.2 Study of oil-water interfacial tension

The aim of this study was to establish the effect of ethanol on the value of the oil-water IFT and to find where in the system the silica particles are located. A pendant drop of the aqueous system to be studied is formed in dodecane. The size of the drop is then altered by increasing or decreasing the amount of liquid using a micro-syringe controlled by a micrometer. Using this method it is possible to compare the bare IFT of dodecane and water with those systems containing ethanol, hydrophilic silica or both.

5.4.2.1 Water-dodecane

Figure 5.14 (a) shows the change in dodecane-water IFT as the aqueous drop is shrunk and then re-expanded and Figure 5.13(b) shows the appearance of the drop at various stages in the shrinking / expanding cycle. As is expected there is little change in the IFT (50 mN m^{-1}) of the bare dodecane-water interface as the volume, and hence surface area, of the drop is reduced. It is likely that the sharp increase in the IFT below 40 % of the original drop volume is an artefact of fitting the profile to the drop image and calculating the IFT. The mechanics of drop fitting is too complex to be covered here, however the shape parameter (B), defined in Song and Springer's papers, is particularly important and as the drop

Figure 5.14. (a) Water-dodecane IFT of a pure water drop in dodecane as a function of drop volume at 25 °C. The original drop volume was 78.8 μl.

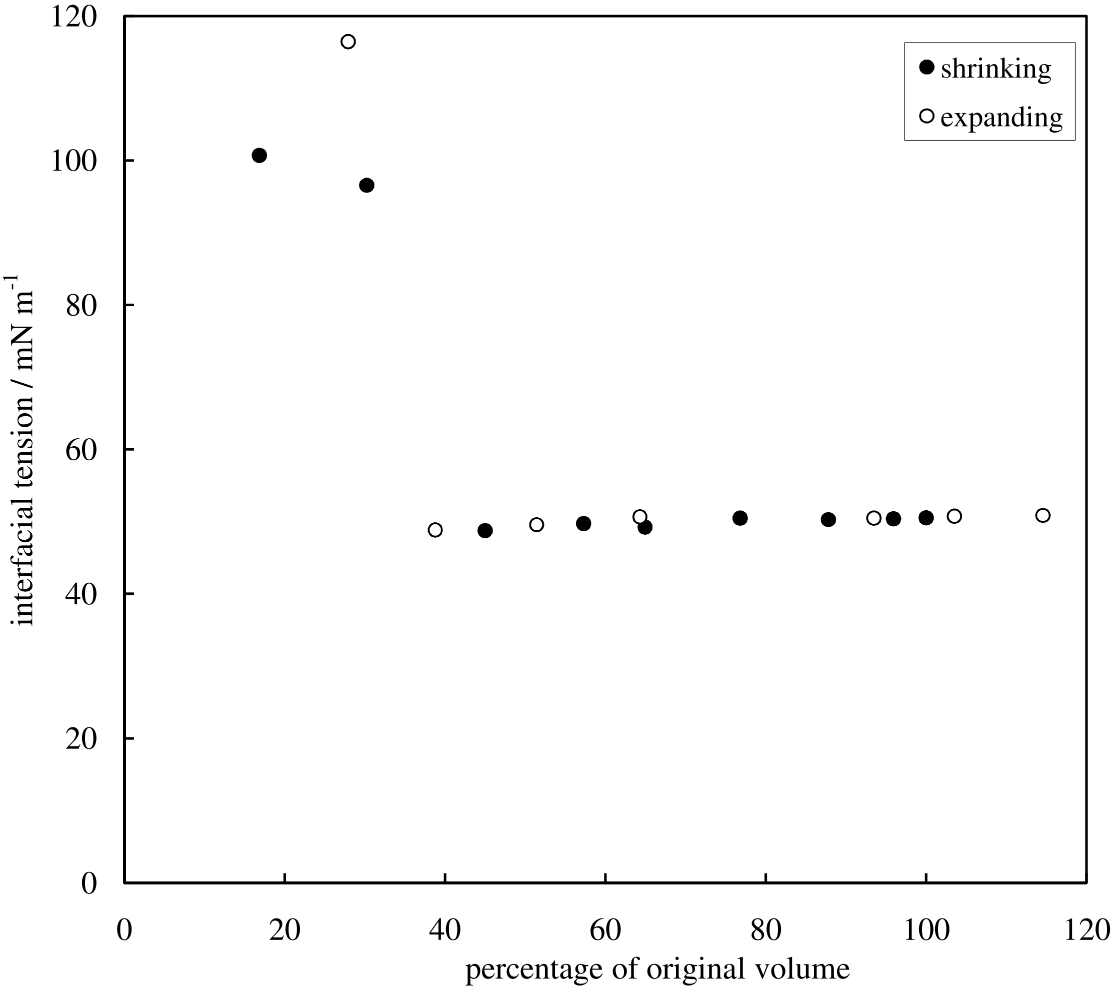

(b) Images of the pendant drop at (i) 100%, (ii) 57 %, (iii) 30 %, (iv) 51 %, and (v) 104 %. Images (ii) and (iii) are during shrinking and images (iv) and (v) are during expanding. The scale bas is 3 mm in length.

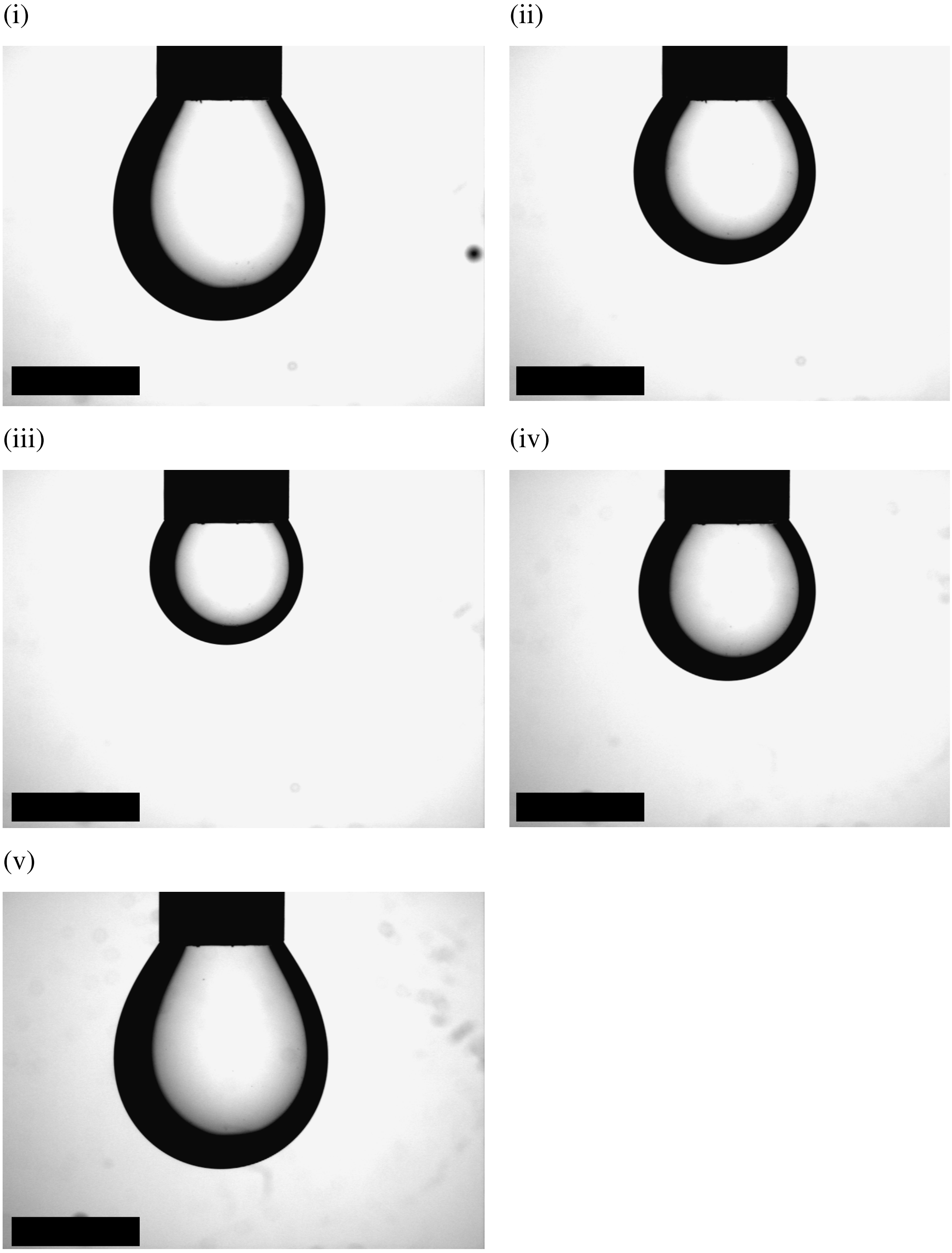

shrinks, therefore becoming more spherical, the uncertainty in the experiment increases.[15,16]

5.4.2.2 Water-dodecane with hydrophilic silica

An interesting system to study is the same as that discussed above but with hydrophilic silica particles present in the aqueous phase. There has been much discussion in the literature as to whether the presence of particles at an interface alters the IFT. The above experiment was repeated but with a concentration of 2 wt. % hydrophilic silica in the aqueous phase. Figure 5.15 (a) shows the change in IFT as a function of the initial drop size and Figure 5.15 (b) shows the appearance of the drop at various points in the shrinking / expanding cycle. Again there appears to be little or no change in the IFT as the drop is shrunk and the value of the IFT (48 mN m^{-1}) is only slightly lower than that of the pure water-dodecane system.

It is interesting to note that the IFT does not change as the drop is shrunk. This is an indication that as the surface area of the oil-water interface is decreased the particles are (a) not adsorbed or (b) expelled from the interface at a certain surface pressure. If the particles were strongly attached to the interface then it would be expected that at a certain coverage a monolayer would be formed and at particle concentrations above this, i.e. at smaller surface areas, the surface pressure would increase rapidly and the IFT would fall. It is worth noting that particles do not generate a surface pressure when they adsorb at concentrations less than a monolayer and hence do not decrease the IFT.[17]

Figure 5.15. (a) Water-dodecane IFT of a drop of 2 wt. % aqueous suspension of hydrophilic silica in dodecane as a function of drop volume at 25 °C. The original drop volume was 82.1 µl.

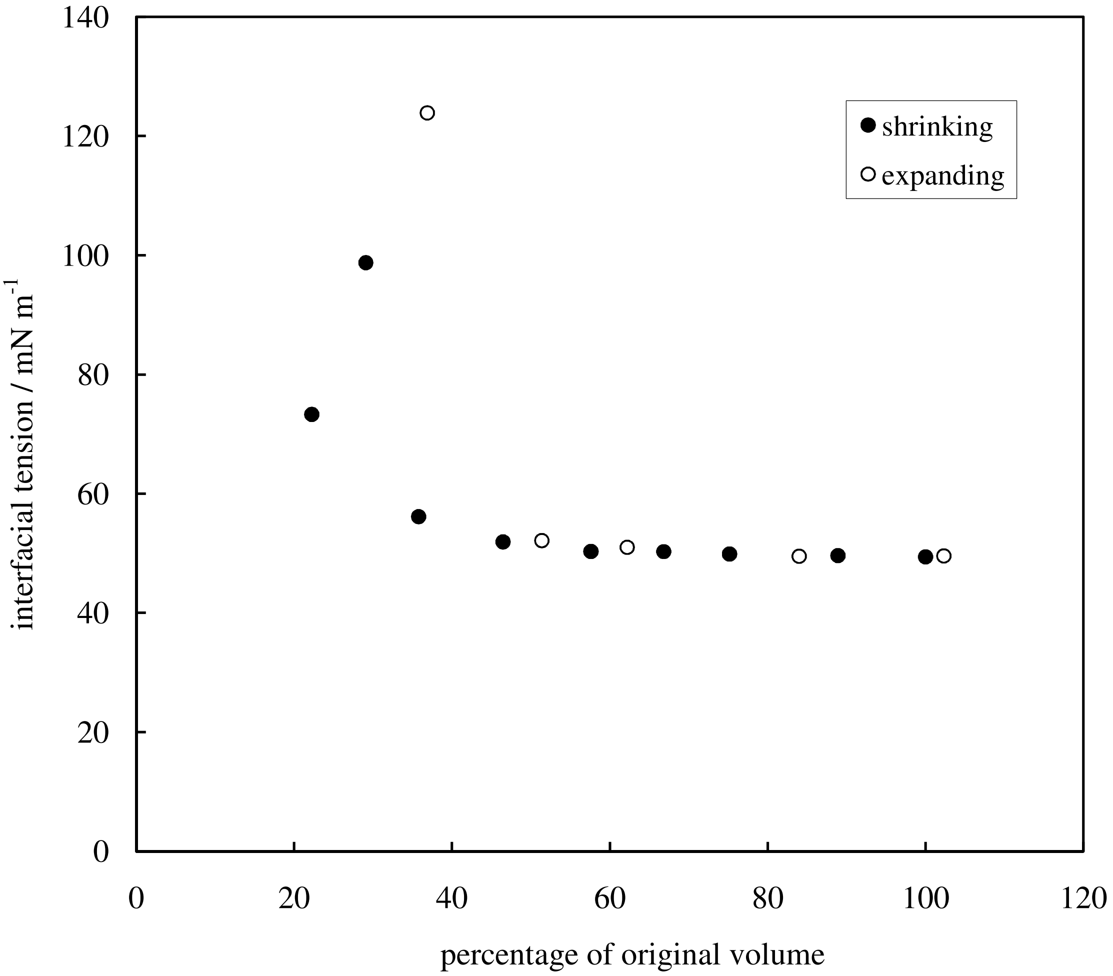

(b) Images of the pendant drop at (i) 100 %, (ii) 57 %, (iii) 35 %, (iv) 36 %, and (v) 103%. Images (ii) and (iii) are during shrinking and images (iv) and (v) are during expanding. The scale bar is 3 mm in length.

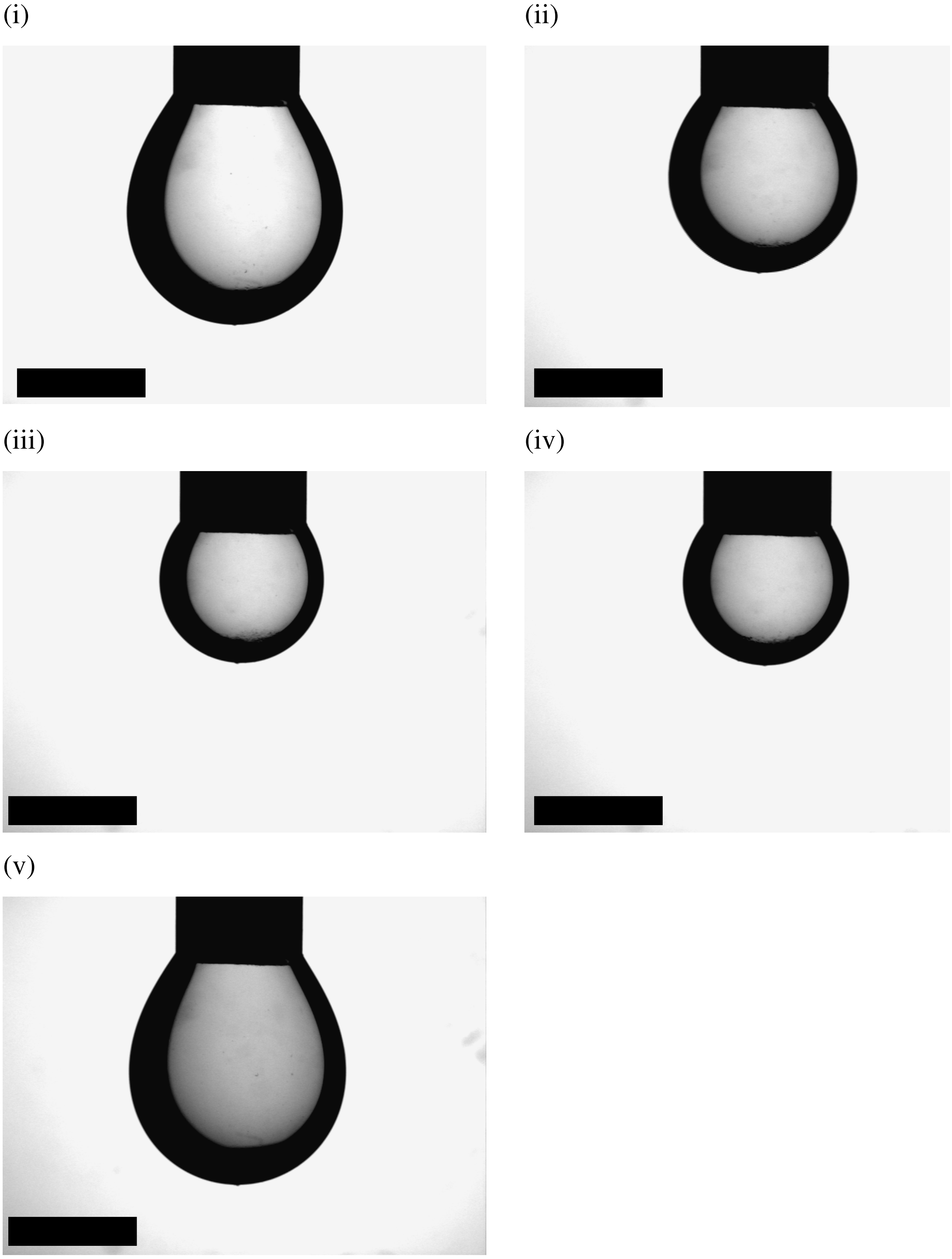

(i)

(ii)

(iii)

(iv)

(v)

5.4.2.3 *Water-dodecane with hydrophilic silica and ethanol*

The general aim of this section of work was to encourage the adsorption of hydrophilic silica particles to the oil-water interface by the addition of a low dielectric co-solvent to the aqueous phase in an analogous way to that of Hickey *et al.* (who used gold nanoparticles).[7] Here we investigate the effect of adding ethanol to the aqueous phase, both on the interfacial tension and on the location of the silica particles. Figure 5.16 (a) shows the change in IFT as a function of drop size for a system which contains 2 wt. % hydrophilic silica in the aqueous phase and has a $\phi_{ETH} = 0.5$. Figure 5.15=6 (b) shows the appearance of the drops at different points in the shrinking / expanding cycle.

The IFT is much lower when ethanol is present due to adsorption of the ethanol molecules at the oil-water interface. There is little conclusive difference in the shape of the IFT versus drop size plots, however there is a noticeable change in the appearance of the drop as the drop volume is decreased. It is apparent that there is a much higher concentration of particles at the oil-water interface when ϕ_{ETH} is high compared to the system which contains no ethanol. As the drop is shrunk beyond a certain volume, the oil-water interface distorts and is no longer spherical but ‘crinkles’. This is clear evidence that the addition of ethanol to the aqueous phase of this system encourages the silica particle to adsorb to the oil-water interface.

Figure 5.16. (a) Water-dodecane IFT of a drop of 2 wt. % suspension of hydrophilic silica in an aqueous ethanol solution (ϕ_{ETH} = 0.5) in dodecane as a function of drop volume at 25 ^{o}C. The original drop volume was 31.7 μl.

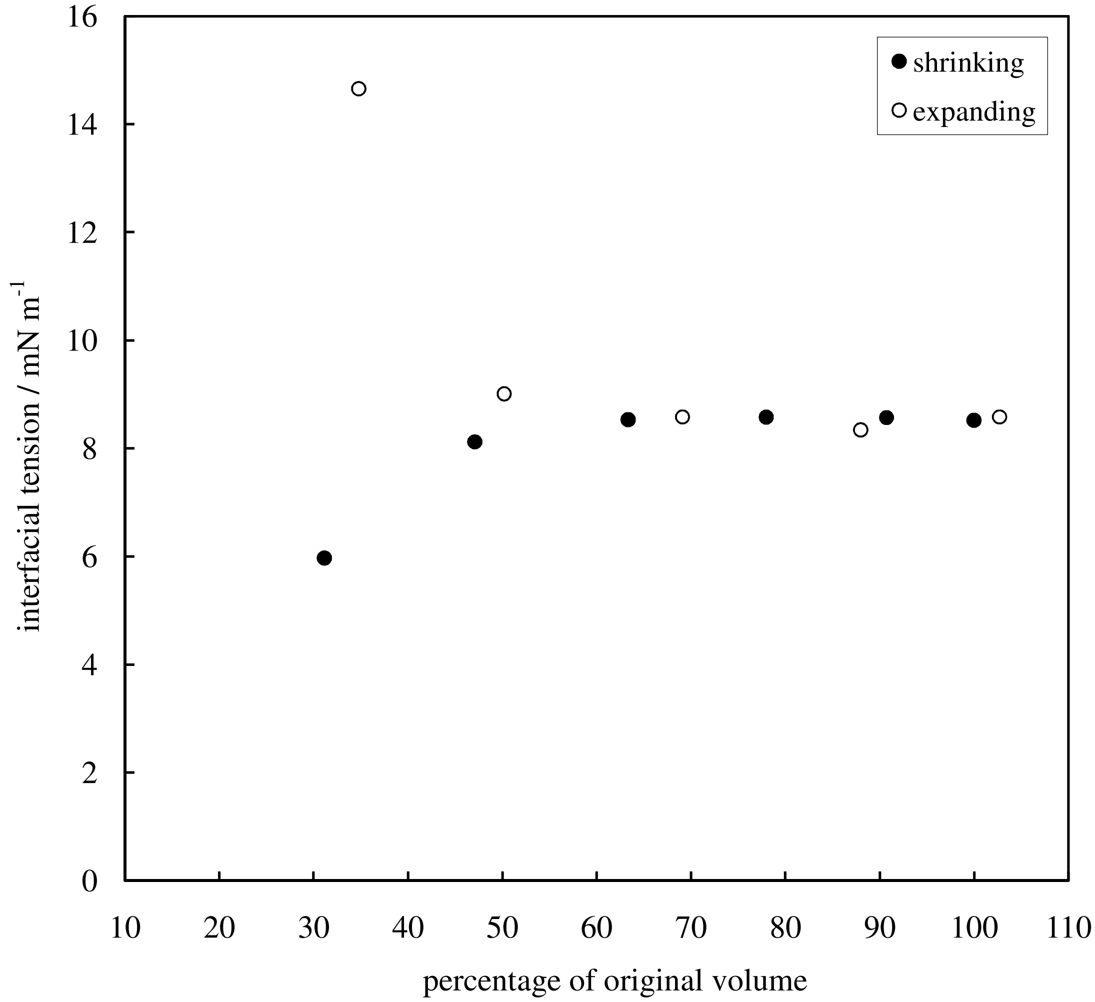

(b) Images of the pendant drop at (i) 100 %, (ii) 63 %, (iii) ~15 %, (iv) 50 %, and (v) 102 %. Images (ii) and (iii) are during shrinking and images (iv) and (v) are during expanding. (vi) skin formation at reduced volume. The scale bar is 3 mm in length.

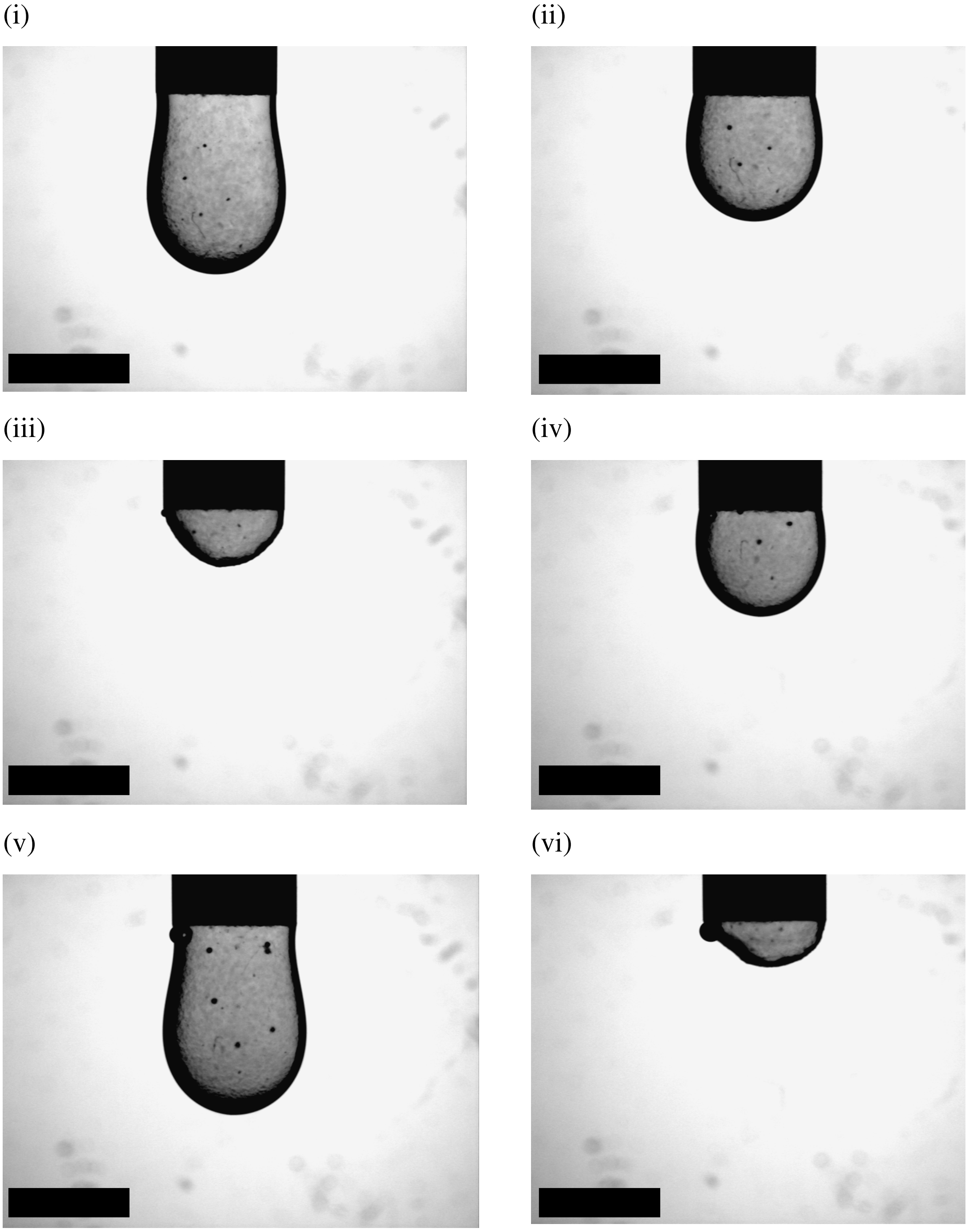

(i)
(ii)
(iii)
(iv)
(v)
(vi)

5.4.1.4 Water-dodecane with ethanol

For completeness, the same system as the one above was studied but in the absence of hydrophilic silica particles. The results, shown in Figure 5.17 (a) and (b), were as expected. The oil-water IFT was lowered by the presence of ethanol and the IFT values observed were very similar to those with particles present, which again shows that the adsorption of particles to the oil-water interface does not alter the tension significantly. The particles lowered the IFT by ~ 1.5 mN m^{-1}.

5.4.3 Sedimentation rates

As discussed, one of the possible explanations for the increase in emulsion stability towards coalescence, followed by subsequent de-stabilisation, is the aggregation of the hydrophilic silica particles. Particles adsorb at the oil-water interface by removing an area of high tension interface. Aggregated particles may be more effective at stabilising interfaces because they remove a larger area of high tension interface then when non-aggregated. However, the covering power of an aggregated system is less than that of non-aggregated and aggregated particles sediment more quickly than discrete particles.

DiStA 24 was used to study the sedimentation of hydrophilic silica particles as a function of ϕ_{ETH}. DiStA 24 sequentially images the samples and uses the saved images to follow the position of any boundary using the change in light scattering between the two regions.[18] This allows both the increase in light

Figure 5.17. (a) Water-dodecane IFT of a drop of aqueous ethanol solution (ϕ_{ETH} = 0.5) in dodecane as a function of drop volume at 25 ^{o}C. The original drop volume was 29.1 μl.

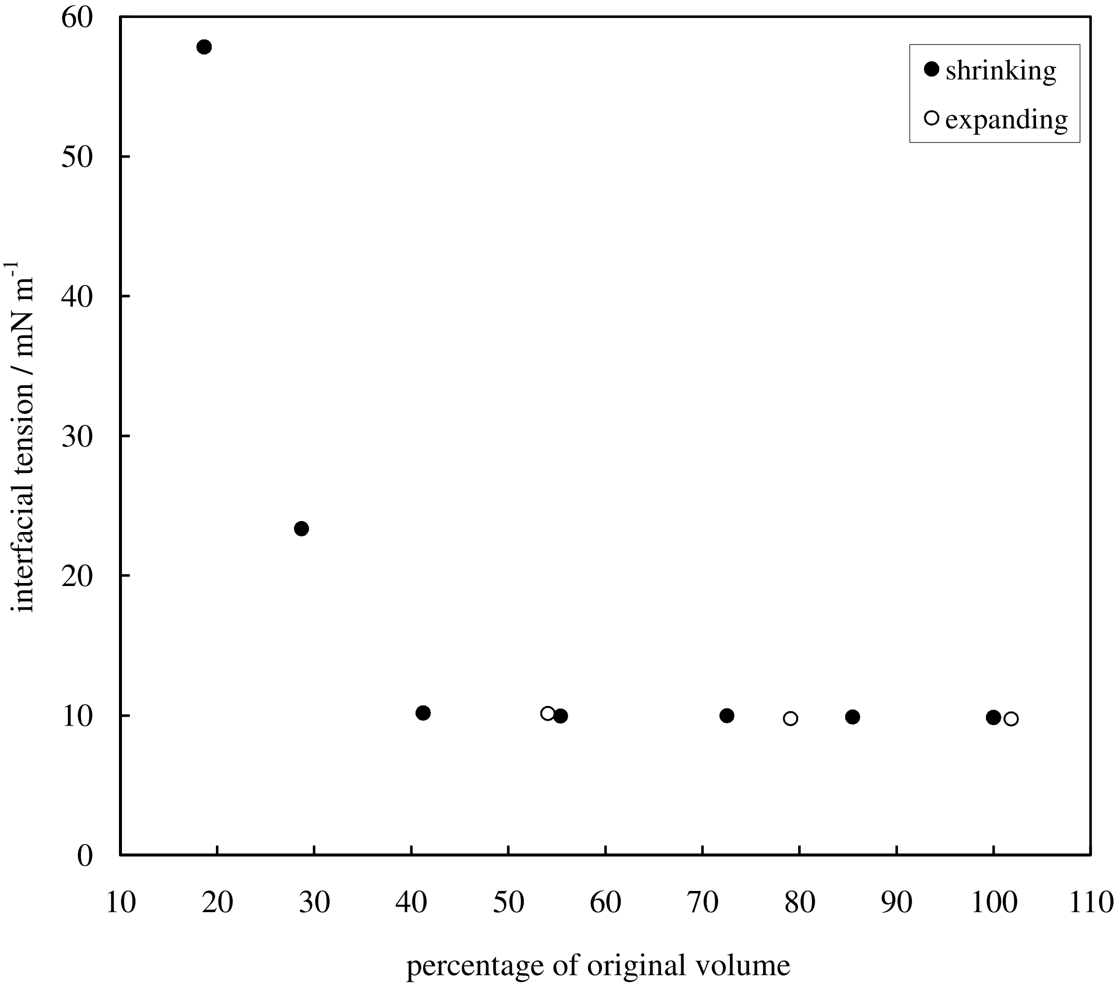

(b) Images of the pendant drop at (i) 100 %, (ii) 55 %, (iii) 18 %, (iv) 54 %, and (v) 101 %. Images (ii) and (iii) are shrinking and images (iv) and (v) are expanding. The scale bar is 3 mm in length.

(1)

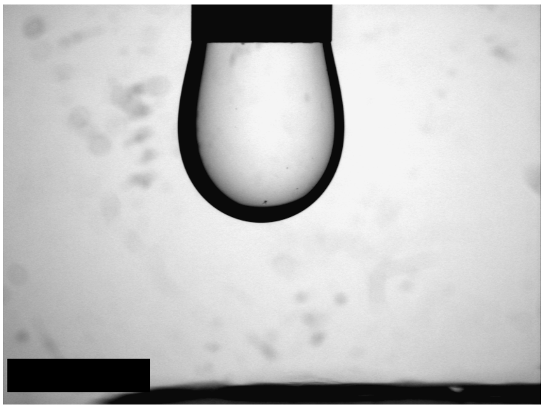

(2)

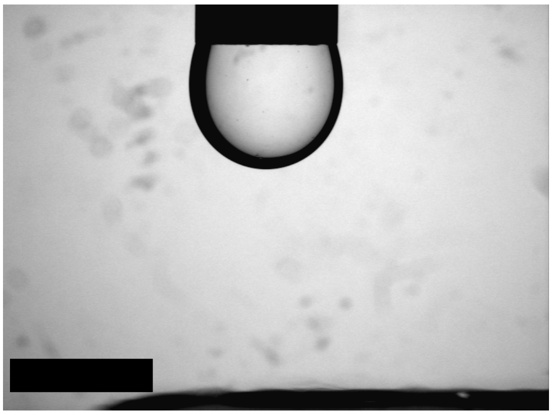

(3)

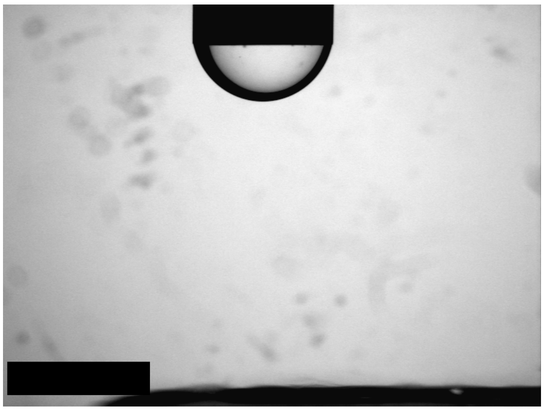

(4)

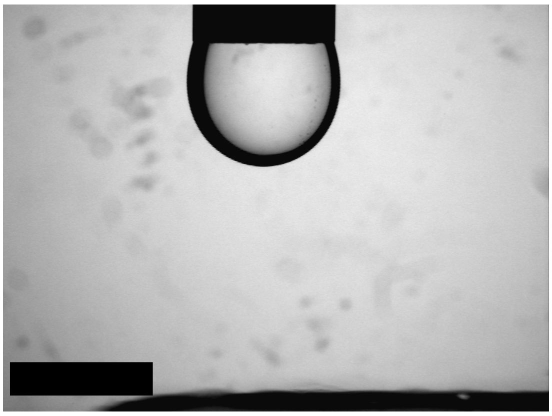

(5)

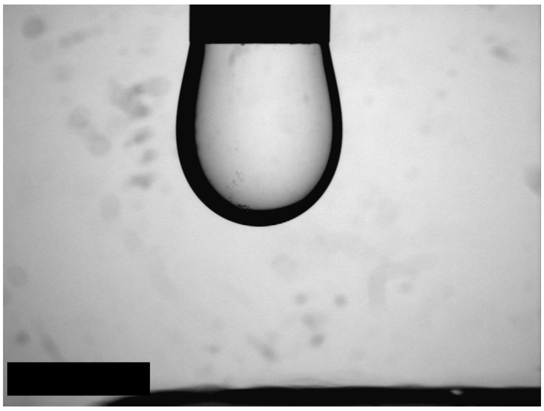

scattering due to the increase in particle concentration at the bottom of a sedimenting sample, along with the reduction in light scattering at the top of the vessel due to the depletion of the upper region of the sample, to be followed with time. Figure 5.17 shows the images of 11 samples containing 2 wt. % hydrophilic silica dispersed in aqueous ethanol solution of different concentrations. The samples were thermostatted at 25 ^{o}C throughout the experiment. It can be seen in Figure 5.18, along with the naked eye when the samples were removed from the equipment, that a larger volume of sediment was obtained as ϕ_{ETH} was increased. This is an indication that as the amount of ethanol in the aqueous phase is increased then the extent of aggregation also increases.

DiStA 24 also produces plots of the normalised light intensity, relative to time zero, as a function of height at different times throughout the experiment. An increase or decrease in this value with time indicates an increase or decrease respectively in particle concentration. It is possible to yield quantitative results using the information provided by DiStA 24, however the necessary analogous ideal systems have not been studied to allow this. Instead the data can be used qualitatively to indicate the effect of ϕ_{ETH} on the particle aggregation. Figure 5.19 shows the profile of the light intensity as a function of the height in the sample for a system in which hydrophilic silica is dispersed into (a) pure water and into (b) ϕ_{ETH} = 0.5 aqueous phase. Two plots are shown on each graph, one is the initial light intensity profile at the start of the experiment and the second is the light profile at the end of the experiment 57 hours later.

Figure 5.18. Vertical sections of hydrophilic silica dispersions in aqueous ethanol solutions, prepared by protocol 2, showing the build up of sediment with time at t = 0 and t = 57 hrs at 25 °C.

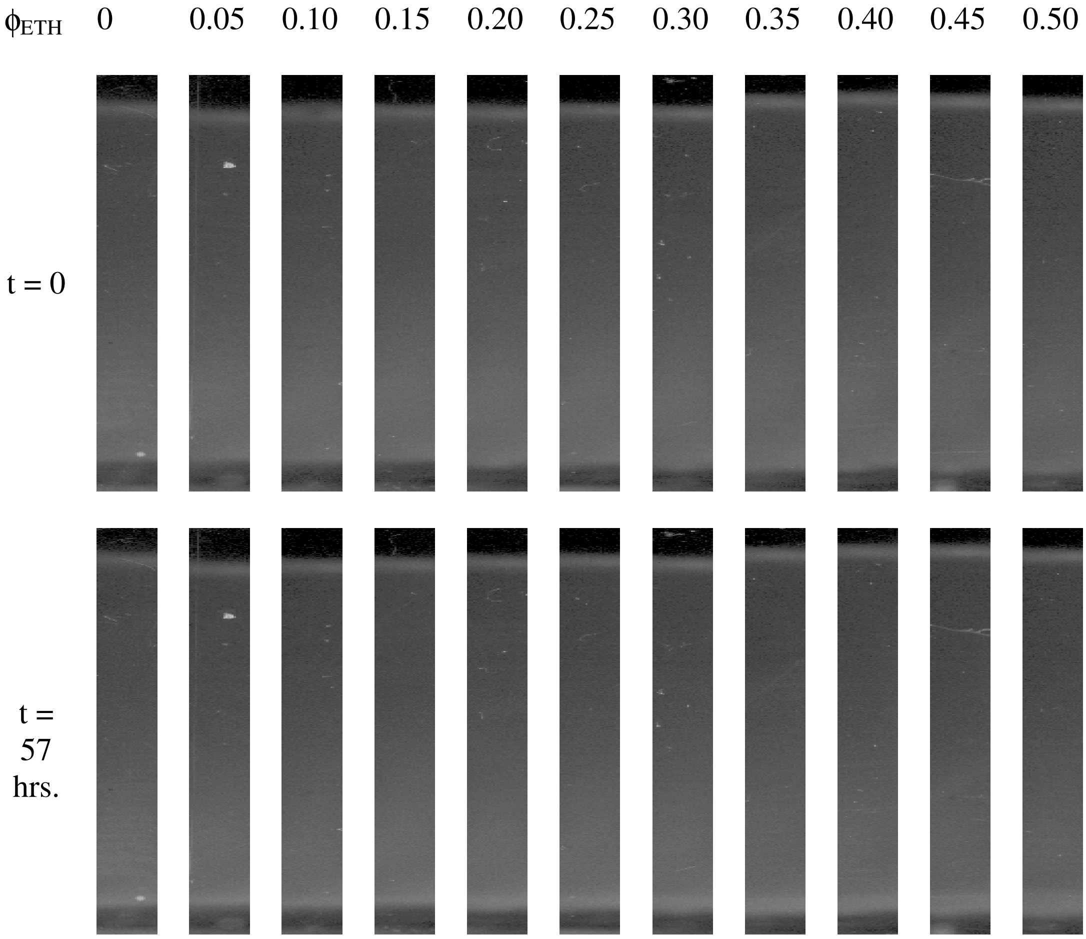

Figure 5.19. The light intensity profiles, at a given time, as a function of the height in the sample for (a) 2 wt. % dispersion of hydrophilic silica in water, and (b) 2 wt. % dispersion of hydrophilic silica in a ϕ_{ETH} = 0.5 aqueous ethanol solution. The experiment was thermostatted at 25 °C.

(a)

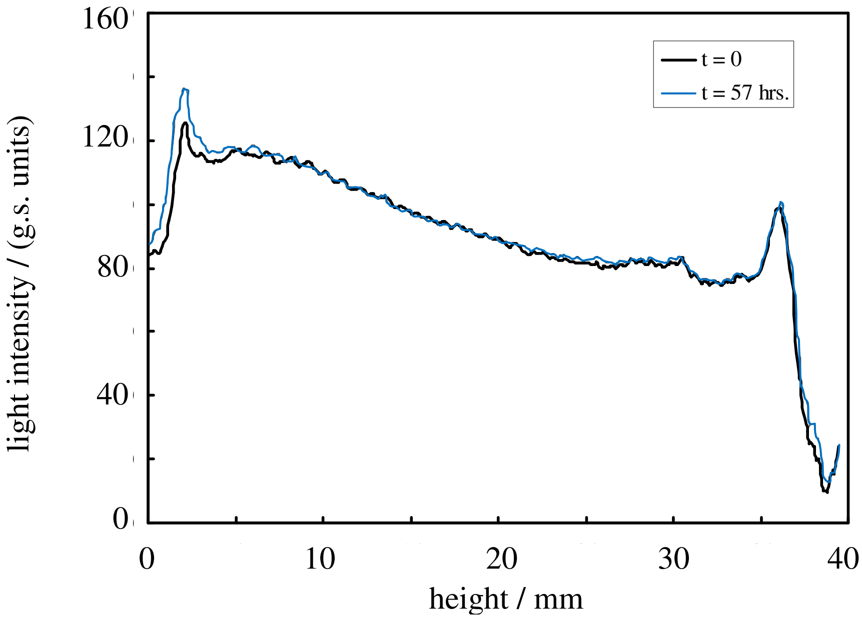

(b)

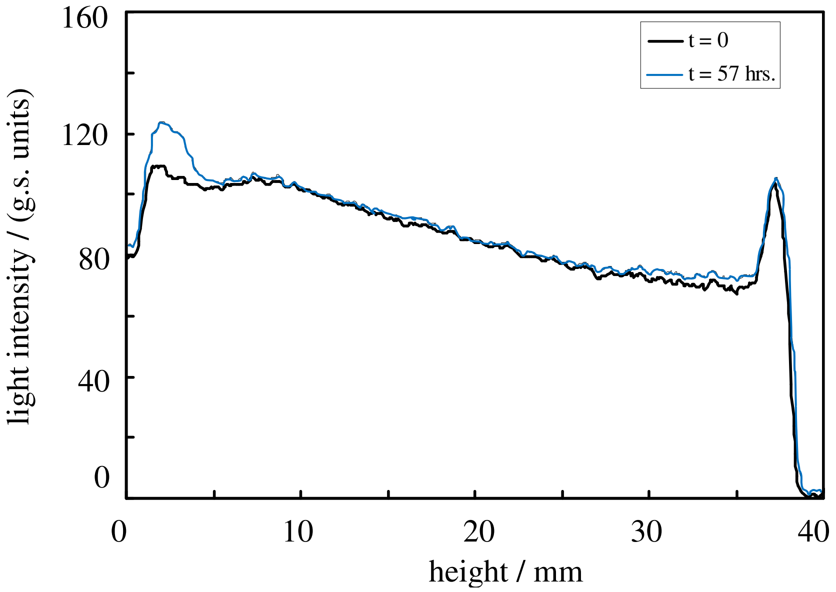

Figure 5.20 shows the difference in the two light intensity profiles, i.e. (light intensity)$_{t\,=\,57\text{ hrs.}}$ - (light intensity)$_{t\,=\,0}$, as a function of the height in the sample. Here a positive value indicates an increase in light scattering, therefore an increase in particle concentration, and a negative value represents a decrease in light scattering, and hence a decrease in particle concentration. The magnitude gives an indication as to the size of the change in the particle concentration. By comparing Figure 5.20 (a) and (b) there is a much larger increase in the light scattering at the bottom of the vessel containing the silica dispersed in the ethanol solution compared to the pure water system. This is an indication that the silica is in a more aggregated state when dispersed in an aqueous ethanol solution compared with a pure aqueous dispersion.

5.5 Conclusions

The addition of a small amount of low dielectric co-solvent to the aqueous phase of a dodecane-in-water emulsion stabilised by hydrophilic silica particles has been shown to increase the stability of the emulsion towards coalescence. Further addition of co-solvent leads to a subsequent destabilisation of the system beyond what would be observed with no co-solvent addition. Some possible mechanisms for the observed increase, and subsequent decrease have been suggested. These include the effect of particle aggregate size, particle-particle repulsion at the interface and surface charge density. Although all three mechanism could contribute to the observed behaviour only the effect of co-solvent on the silica particle aggregate size can explain both the increase and

Figure 5.20. The change in light intensity profiles, at 57 hours, as a function of the height of the sample for (a) 2 wt. % dispersion of hydrophilic silica in water, and (b) 2 wt. % dispersion of hydrophilic silica in a ϕ_{ETH} = 0.5 aqueous ethanol solution. The experiment was thermostatted at 25 ^{o}C.

(a)

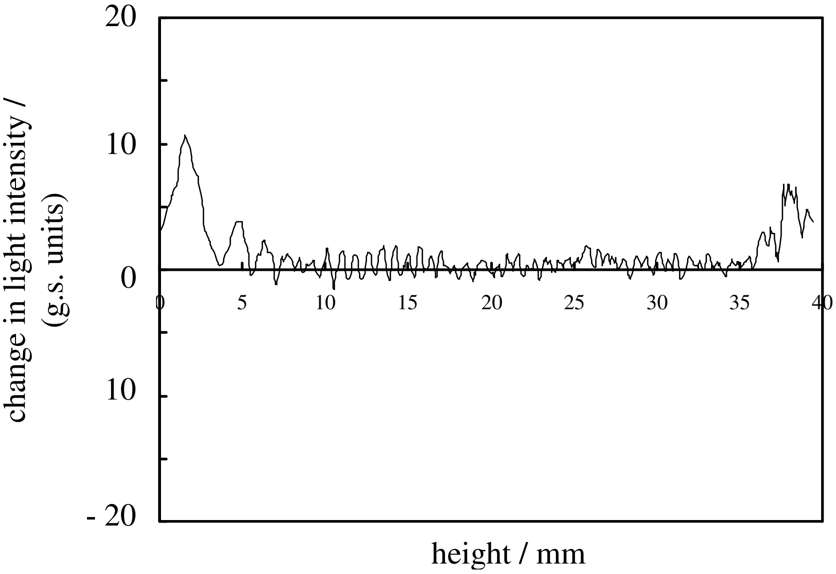

(b)

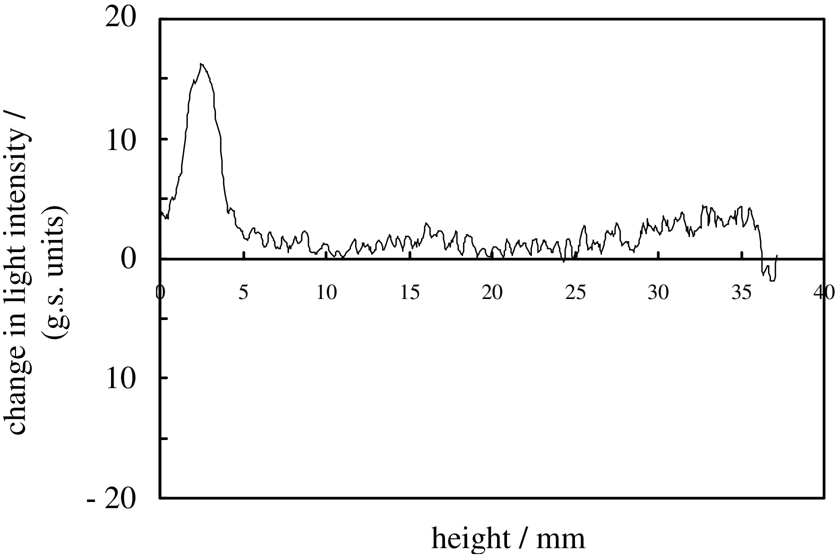

subsequent decrease in emulsion stability. The three-phase contact angle of an aqueous ethanol drop, measured through the aqueous phase, on a glass surface under dodecane did not change, within the experimental error, as a function of the ethanol volume fraction in the aqueous phase. Here it has been shown that the same experiment repeated on a smooth silicon wafer gives the same results, and although there is the possibility that this is due to a compensation effect in the interfacial tensions, it is evidence that the wettability of the silica particle remains unchanged.

The pendant drop experiments show that the presence of hydrophilic particles does not significantly lower the dodecane-water IFT but the addition of ethanol does. Even though the dodecane-water IFT is lowered by the adsorption of ethanol, silica particles were seen to adsorb to the interface. At high surface coverage or low dodecane-water interfacial areas, a skin of silica particles was seen to form at the interface which led to the distortion of the shape of the pendant drop.

Using DiStA 24 it was shown that at high ethanol volume fractions the sedimentation rate of hydrophilic silica particles was increased compared to that of silica particles dispersed in pure water. This is possibly due to an in increase in the aggregation of the silica particles because of a reduction in their surface charge. It is likely that the origin of the observed increase in stability towards coalescence of o/w solid-stabilised emulsions stabilised by hydrophilic silica is based not on a single effect but a combination of the effects investigated above.

5.6 References

---

[1] S. Abend, N. Bonnke, U. Gutschner and G. Lagaly, *Colloid Polym. Sci.*, **276**, 730 (1998).

[2] N. Garti, A. Aserin, I. Tiunova and H. Binyamin, *J. Am. Oil Chem. Soc.*, **76**, 383 (1999).

[3] J. Giermanska-Kahn, V. Schmitt, B.P. Binks and F. Leal-Caldron, *Langmuir*, **18**, 2515 (2002).

[4] B.P. Binks and S.O. Lumsdon, *Langmuir*, **16**, 3748 (2000).

[5] B.P. Binks and S.O. Lumsdon, *Langmuir*, **16**, 8622 (2000).

[6] S. Simovic and C.A. Prestidge, *Langmuir*, **20**, 8357 (2004).

[7] F. Reincke, S.G. Hickey, W.K. Kegel, and D. Vanmaekelbergh, *Angew. Chemie Int. Ed.*, **14**, 458 (2004).

[8] M. Kosmulski, *J. Colloid Interface Sci.*, **179**, 128 (1996).

[9] B.P. Binks and C.P. Whitby, *Colloids Surf. A*, **253**, 105 (2005).

[10] *CRC Handbook of Chemistry and Physics*, 75th edition, ed. by David R. Lide, CRC Press, Cleveland, OH (1994/5).

[11] L.G.J. Fokkink and J. Ralston, *Colloids and Surfaces*, **36**, 69 (1989).

[12] R. Aveyard, B.P. Binks, J.H. Clint and T.S. Horozov, *Langmuir*, **19**, 2822 (2003).

[13] N.P. Ashby, B.P. Binks and V.N. Paunov, *Langmuir*, **18**, 6946 (2002).

[14] B.P. Binks and S.O. Lumsdon, *Phys. Chem. Chem. Phys.*, **1**, 3007 (1999).

[15] B. Song and J. Springer, *J. Colloid Interface Sci.*, **184**, 64 (1996).

[16] B. Song and J. Springer, *J. Colloid Interface Sci.*, **184**, 77 (1996).

[17] E. Vignati, R. Piazza and T.P. Lockhart, *Langmuir***, 19**, 6650 (2003).

[18] B.P. Binks and T.S. Horozov, *Langmuir*, **21**, 9007 (2004).

CHAPTER 6

SPREADING OF SOLID-STABILISED OIL-IN-WATER EMULSIONS

6.1 Introduction

Emulsion technology is extensively applied in many industries such as cosmetics, pharmaceuticals, coating and paints, food manufacture and agrochemicals in both processing and formulation.[1,2,3] The emulsion may form part of the product, as in food manufacture, or may be used to deliver an active (oil soluble in the case of o/w emulsion) to the desired surface, as in cosmetics and agrochemicals.[4,5] The spreading of emulsion systems, in contrast to single phase systems, is not well described in the literature.[6] This section of work aims firstly to understand the spreading behaviour of a drop of o/w emulsion, stabilised by relatively hydrophilic silica particles, on a model, flat glass hydrophobic surface and secondly to investigate how the stability of the emulsion affects the observed spreading. Once this spreading has been defined the work then moves on to consider the real surface of plant leaves and seeds.

6.2 Spreading behaviour of dodecane-in-water emulsions

6.2.1 Solid-stabilised systems

A dodecane-in-water preferred emulsion (ϕ_o = 0.5) was stabilised by 2 wt. % of 88 % SiOH fumed silica (initially dispersed into the aqueous phase) and prepared by homogenisation for 2 min. at 11,000 rpm at natural pH. A drop (~ 50 μl) of this emulsion was placed onto the hydrophobic glass surface and the appearance followed with time. It is important to note that the drop was exposed to the ambient atmosphere, this will be discussed in more detail later. Figure 6.1 shows the appearance of this system with time. For a relatively long period (~ 2000 s) there is very little change in the appearance of the drop, only a reduction in size as the drop evaporates. The formation of a pre-spreading front, after the initial period in which no obvious change is occurred, can be seen at the edges of the drop which corresponds to an observed coarsening of the emulsion. Once formed, this front rapidly wets the hydrophobic surface and the emulsion phase separates to leave a slightly cloudy inner drop of an aqueous silica dispersion surrounded by clear oil which has completely wet the hydrophobic surface. The overall appearance of the system is very similar to that of a 'fried egg'.

Figure 6.2 shows a schematic representation of this process. During the evaporation process the emulsion system becomes unstable and liberates oil. This oil can be seen to form a pre-spreading front at the three phase contact line and lenses at the air-water surface (A). Finally the liberated oil forms a bulk oil

Figure 6.1. Appearance of a drop (~ 50 μl) of dodecane-in-water emulsion containing 0.5 volume fraction dodecane, stabilised by 2 wt. % fumed silica with 88 % SiOH groups, on a hydrophobic surface under air. The age of the drop is indicated below each image. The needle diameter is 0.3054 mm.

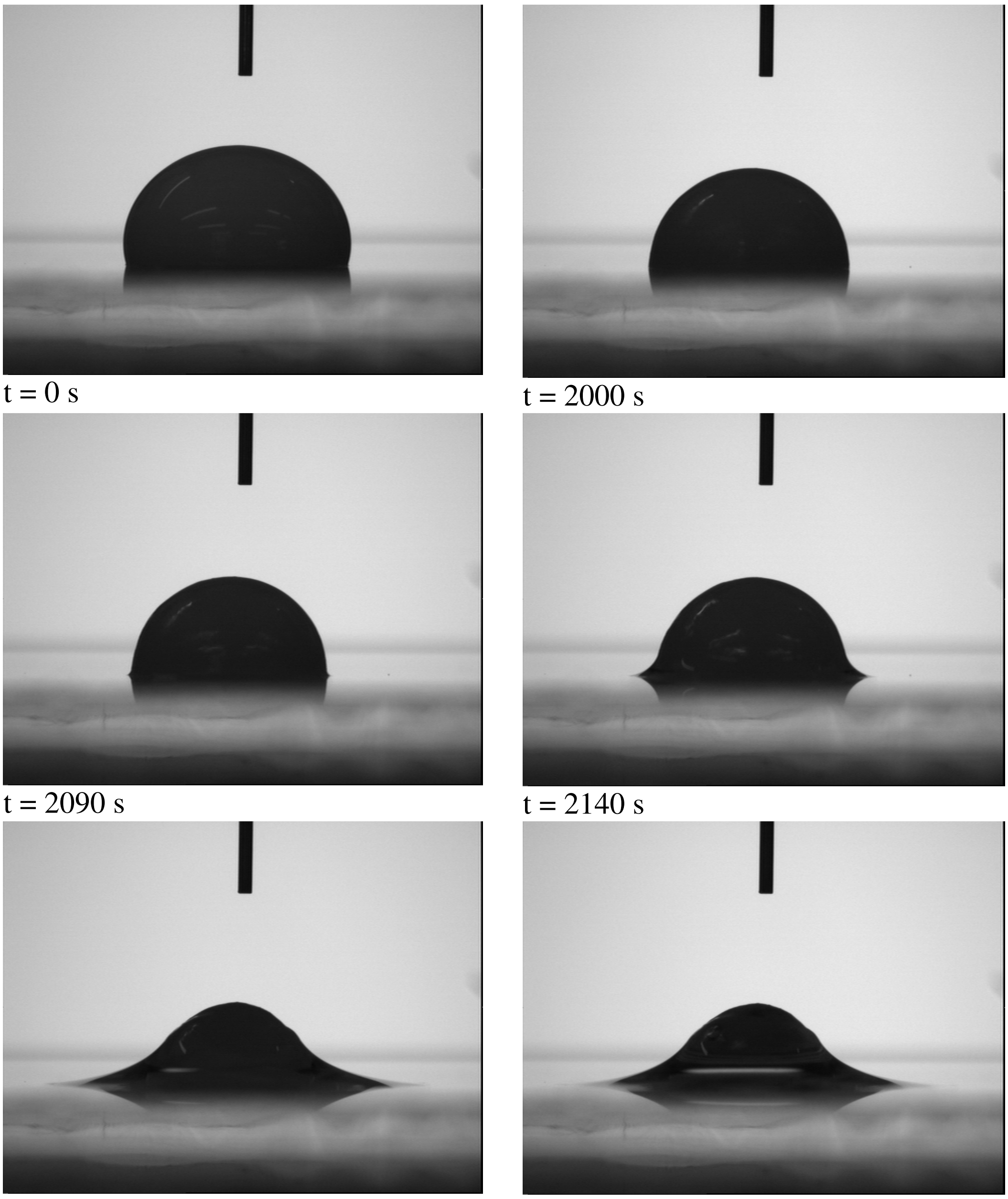

t = 0 s

t = 2000 s

t = 2090 s

t = 2140 s

t = 2550 s

t = 4400 s

phase which spreads on the hydrophobic surface causing the system to take on a ‘fried egg’ like appearance (B).

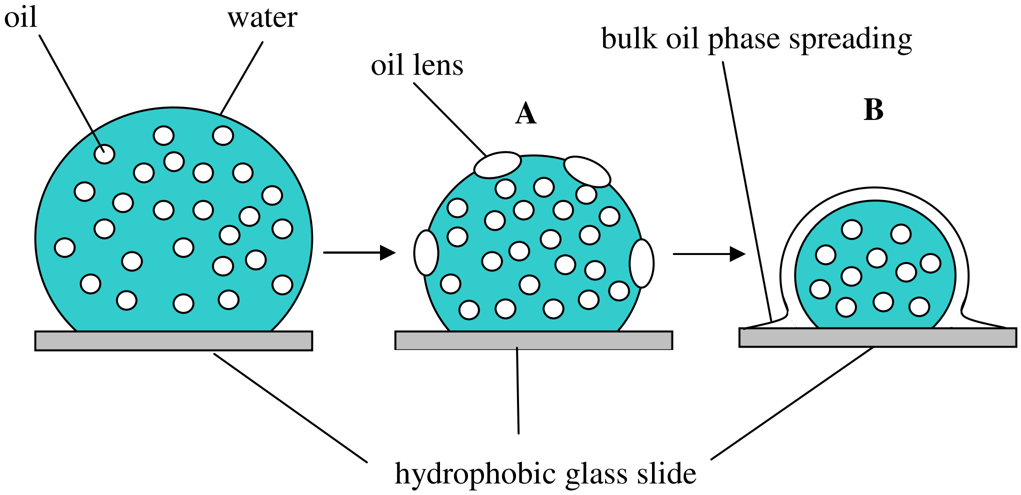

Figure 6.2. Schematic representation of the destabilisation and subsequent spreading of a drop of oil-in-water solid-stabilised emulsion on a hydrophobic surface as the system evaporates. No other emulsion breakdown mechanisms are represented, i.e. creaming.

It is important to note when considering the images in Figure 6.1 that the optics of the DSA 10 are set to provide a silhouette of a dark drop against a bright background. This helps the software detect the edge of the drop using contrast but it also obscures any visual detail of what is happening within the drop on the images captured. This experiment was repeated on several different hydrophobic surfaces (polystyrene, parafilm) under the same conditions and each time the same spreading phenomenon was observed.

Figure 6.1 shows that after a certain time, instability in the drop of emulsion is induced which leads to phase separation and the spreading of the released oil phase. In order to determine if this is related to the evaporation of the emulsion the experiment was repeated both under a high vapour pressure of water and under dodecane instead of air. When evaporation of the continuous phase is prevented, by either method, there is no unusual spreading behaviour. Figure 6.3 shows the appearance of the system studied under dodecane at the start of the experiment and at t = 4420 s (in all systems studied spreading had occurred at this time). This indicates that the evaporation of the emulsion plays a key role in the phase separation and subsequent unusual spreading behaviour.

The instability in the emulsion is induced because of the way that emulsion evaporates. Previous work has shown that the evaporation of the dispersed phase of an emulsion, in this case dodecane, is retarded relative to that of the pure liquid.[7,8] In addition to this, solid particles are more effective at retarding the evaporation of the dispersed phase than surfactant molecules. This was thought to be due to the fact that the dispersed phase (oil) has to evaporate through a thin film of continuous phase (water). The film of water covering the oil drop is much thicker in a solid-stabilised system compared with that of a surfactant system. The minimum thickness that a thin film surrounding an emulsions drop in a particle-stabilised system can be is one particle diameter compared with 2 molecule lengths in a surfactant-stabilised system. The increased thickness of the film in a solid-stabilised systems results in a greater retardation of the evaporation rate of the dispersed phase relative to the pure liquid. There are two possible explanations for the observed instability in the emulsion system which will be discussed with respect to a surfactant stabilised-system which is described below.

Figure 6.3. Appearance of a drop (~ 50 μl) of dodecane-in-water emulsion containing 0.5 volume fraction dodecane, stabilised by 2 wt. % fumed silica with 88 % SiOH groups, on a hydrophobic glass surface under dodecane. The age of the drop is indicated below each image. The needle diameter is 0.3054 mm.

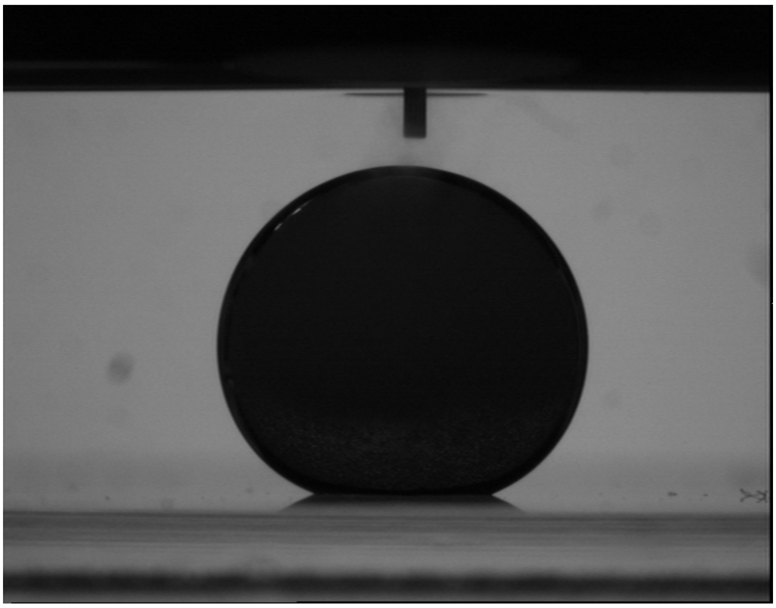

t = 0 s

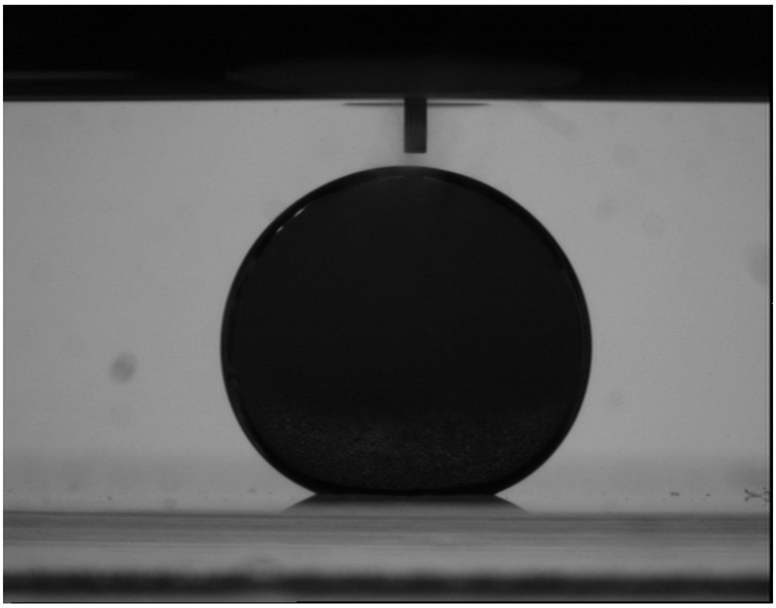

t = 4420 s

6.2.1 Surfactant-stabilised systems

A dodecane-in-water preferred emulsion was stabilised by 20 mM SDS, dispersed into the aqueous phase, prepared by homogenisation for 2 min. at 11,000 rpm. A drop (~ 50 μl) of this emulsion was placed onto the hydrophobic glass surface and the appearance followed with time. Again the emulsion was exposed to the atmosphere to allow evaporation. Figure 6.4 shows the appearance of the system with time.

The difference in drop shape, compared to the emulsion stabilised by solid particles, is due to the change in the IFT caused by the adsorption of SDS molecules at the three different interfaces, solid-oil, solid-aqueous and oil-aqueous. Unlike in the case of the solid-stabilised emulsion, no dramatic 'breaking' of the emulsion was observed. The emulsion coarsened, and therefore appeared greyer, but did not phase separate as it aged. It appeared to evaporate as an emulsion and the contact area of the drop with the hydrophobic surface did not change as the emulsion evaporated. Even at very extended times no unusual spreading was observed and the emulsion dried to a flat disc of SDS.

6.3 Spreading mechanism

There are two possible explanations for the induced coalescence of the solid-stabilised emulsion as it evaporates.

Figure 6.4. Appearance of a drop (~ 50 μl) of dodecane-in-water emulsion containing 0.5 volume fraction dodecane, stabilised by 20 mM SDS, on a hydrophobic glass surface. The age of the drop is indicated below each image. All of the images are the same magnification and the needle diameter is 0.3054 mm.

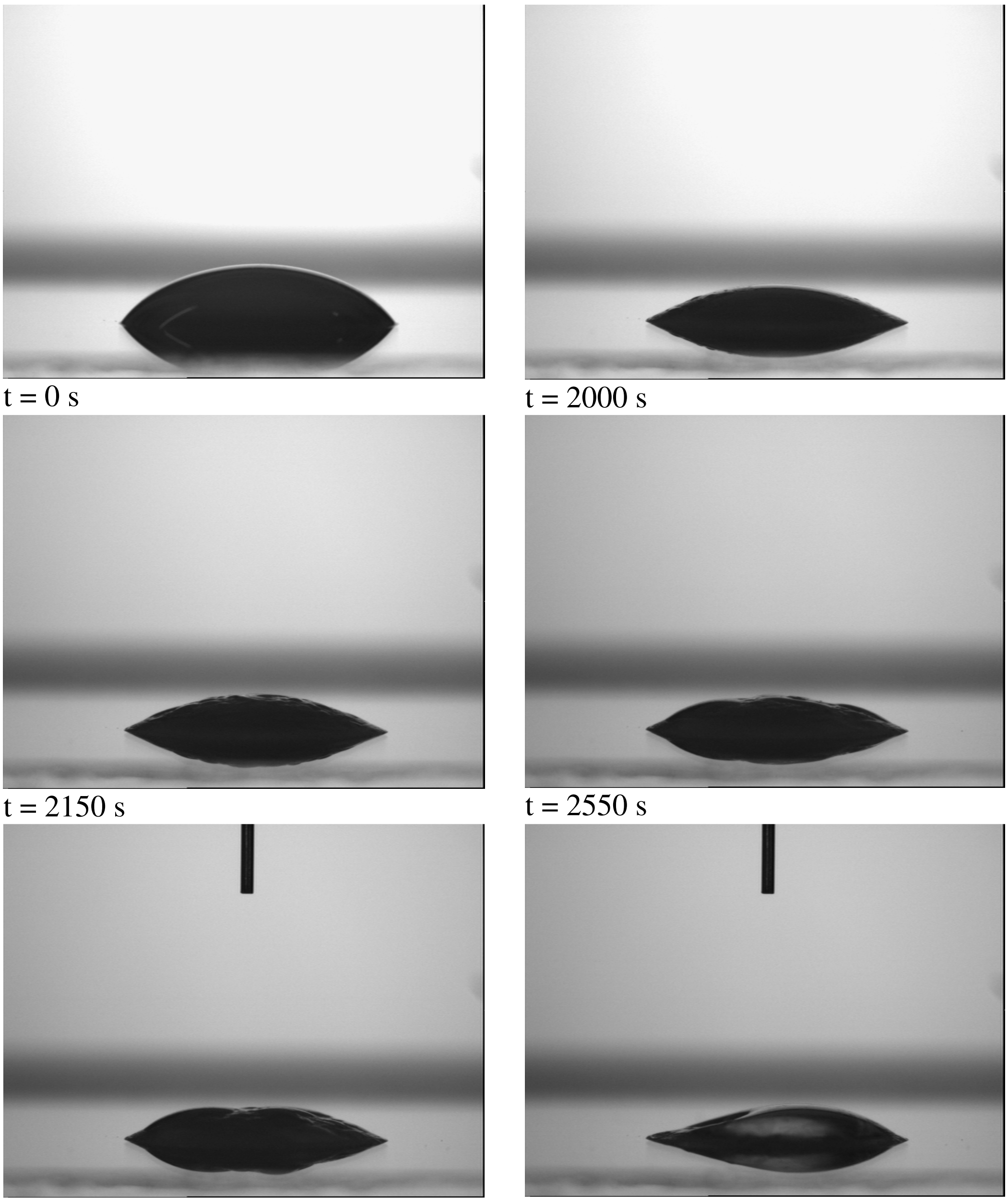

t = 0 s

t = 2000 s

t = 2150 s

t = 2550 s

t = 2780 s

t = 4500 s

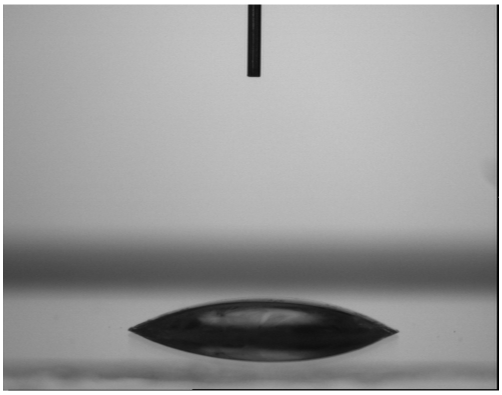

t = 5400 s

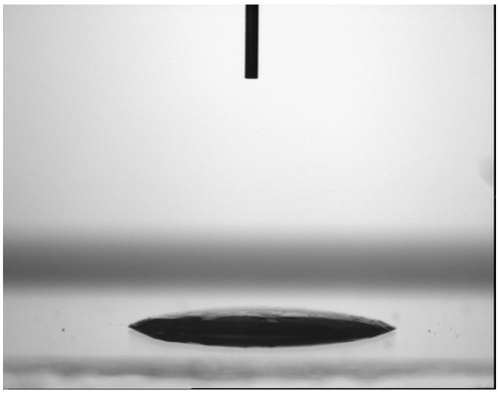

t = 16200 s

6.3.1 Catastrophic phase inversion

Unlike surfactant stabilised systems, solid-stabilised emulsions can exhibit phase inversion with respect to oil-water volume ratio called catastrophic phase inversion. Binks and Lumsdon investigated the effects of changing the oil-water volume ratio on the type of emulsion in a batch process, i.e. a fresh emulsion was formed at each volume fraction of oil.[9] It has already been shown that the evaporation rate of the continuous phase of an emulsion is faster then that of the dispersed phase, particularly in a system where the volatility of the oil used is less than that of water.[10,11] In this system it seems sensible to suggest that as the water evaporates (continuous phase) the effective volume fraction of oil (ϕ_o) increases. The system starts at $\phi_o = 0.5$ and would not have to increase greatly to where, if this was a batch emulsion experiment, phase inversion would be observed (around $\phi_o = 0.6$). It is possible that in the absence of shear the system simply phase separates rather than phase inverts.

6.3.2 Emulsion osmotic stress

In work by Bibette[12], a silicone oil-in-water emulsion stabilised by SDS was dialysed against an aqueous phase containing large polymer molecules. The osmotic pressure gradient created by the presence of the polymer molecules was sufficient to drive water from between the emulsion drops to form a high internal phase emulsion (HIPE). At some critical osmotic pressure the thin films of water between the oil droplets ruptured and coalescence occurred. It is possible that the evaporation of the aqueous phase from our emulsion drop is providing the same type of stress on the thin films separating the oil drops in the emulsion. Beyond a certain critical stress the films rupture and the emulsion phase separates. However it is worth noting that the osmotic film rupturing work was performed on HIPEs where the internal phase volume fraction was ~ 0.9. As will be shown, the dispersed phase volume fractions in these systems do not approach this figure so it can be concluded that the spreading mechanism is via catastrophic phase inversion.

6.4 Spreading of o/w solid-stabilised emulsions on hydrophobic slides

The catastrophic phase inversion of an emulsion of dodecane and water, stabilised by 1 wt. % per volume of the total emulsion of 78 % SiOH fumed silica, was determined as described in Section 2.2.9. Figure 6.5 (a) shows the plot of conductivity of the emulsion against the oil volume fraction and (b) the observations made during the drop test. This system phase inverts between $\phi_o = 0.6$ and 0.65.

Drops of the same emulsion were then placed on glass slides with different wettabilities ranging from unmodified (contact angle of a drop of water on the slide under air = 30 ^{o}) to hydrophobic (contact angle of a drop of water on the slide under air = 95 ^{o}). Across this range of wettabilities, for this system, no difference was noted in the spreading other than the shape of the drops due to the changing contact angle with the glass slide, i.e. no particle driven wetting.

Figure 6.5. (a) Conductivity of the continuous phase versus oil volume fraction for an emulsion of dodecane stabilised by 1 wt. % (of the emulsion) of 78 % SiOH fumed silica. (b) Observations made during the drop test.

(a)

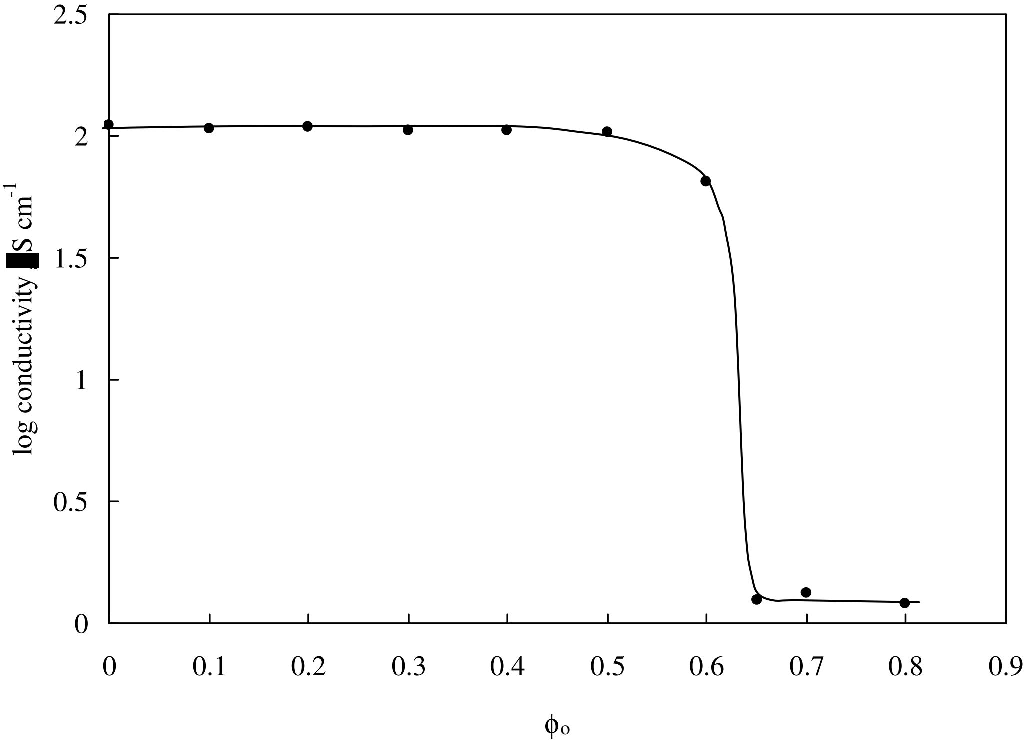

(b)

ϕ_o	**drop into aqueous phase**	**drop into oil phase**
0.10	drop dispersed	formed drop and sedimented
0.20	drop dispersed	formed drop and sedimented
0.30	drop dispersed	formed drop and sedimented
0.40	drop dispersed	formed drop and sedimented
0.50	drop dispersed	formed drop and sedimented
0.60	drop dispersed	formed drop and sedimented
0.65	formed drop and creamed	drop dispersed
0.70	formed drop and creamed	drop dispersed
0.80	formed drop and creamed	drop dispersed

Figures 6.6 - 6.10 show (a) the appearance of the drop of emulsion as it evaporated and (b) the volume fraction of oil in the emulsion drop with time for slides of different wettabilities. All of the images from Figure 6.10 evaporation experiment are presented for reference in Appendix II and a video (30 time normal speed) is contained in the electron supplementary information (DVD attached to inside cover of thesis).

In each case the point at which the first instability is observed (this was taken to be the point at which the first oil lens penetrated the air-water interface) corresponds to an oil volume fraction in the range 0.55 – 0.62. This is the same, or just very slightly below, that of the catastrophic phase inversion determined by the bulk method described above of 0.6 – 0.65. The agreement in the volume fraction of oil at which catastrophic phase inversion is observed in the bulk system, and instability is observed in the drops of emulsion, strengthens the conclusion that the system has reached the point at which if shear was applied the system would phase invert. In the absence of shear the system simply phase separates causing the unusual spreading behaviour.

The spreading behaviour of solid-stabilised o/w emulsions was studied on a range of glass slides each with a different hydrophobicity. This explored if the contact angle between the internal aqueous drop on the glass slide (under the spreading oil front) had any effect on the spreading of the oil phase and location of the particles after spreading had occurred. Figure 6.11 illustrates the angle which is being described and shows how if this angle is less then 90° then it could be possible to observe accelerated spreading due to the formation of

Figure 6.6. (a) Appearance of drop of dodecane-in-water emulsion stabilised by 2 wt. % fumed silica (78 % SiOH), volume fraction of oil = 0.5, as in evaporates on a slide (contact angle of a drop of water on the slide under dodecane advancing = 140^{o}, receding = 101^{o}). The needle diameter is 0.3054 mm. (b) The oil volume fraction in the emulsion drop with time closed points indicate no sign of instability, open points indicate instability observed. The needle diameter is 0.3054 mm.

(a)

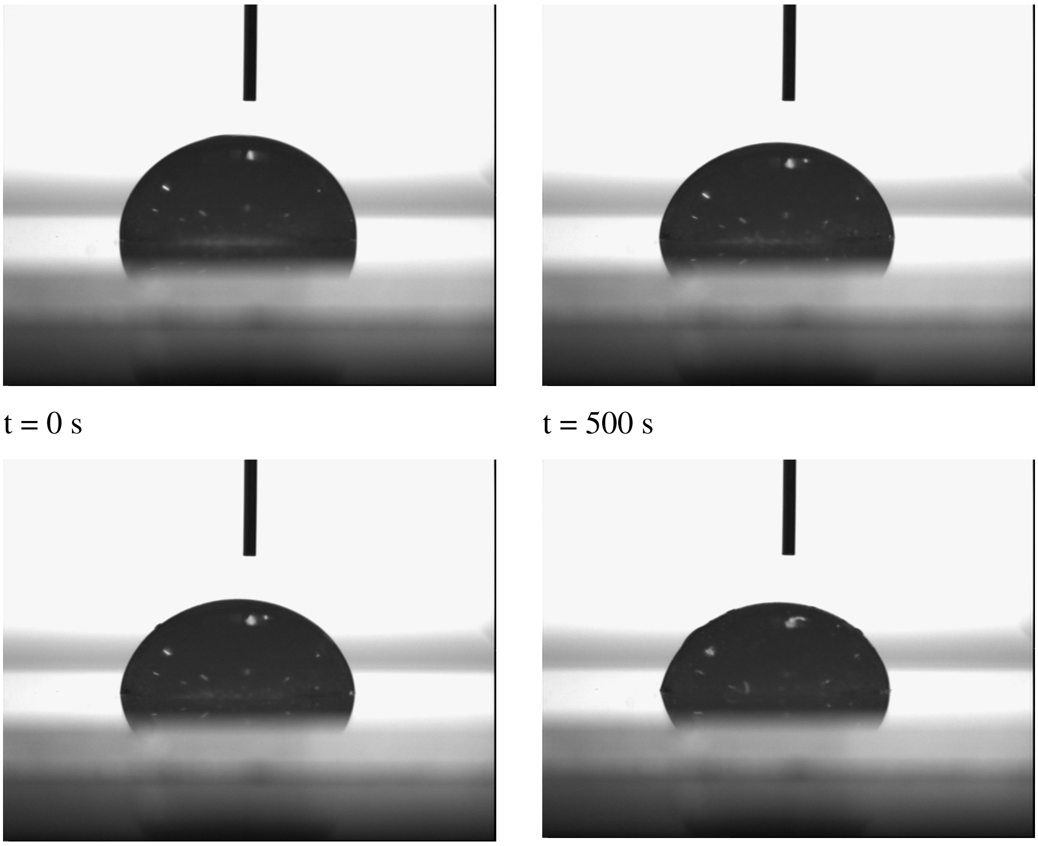

t = 0 s

t = 500 s

t = 600 s

t = 1000 s

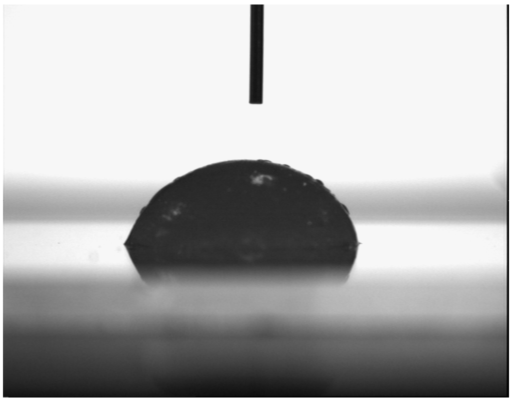

t = 1500 s

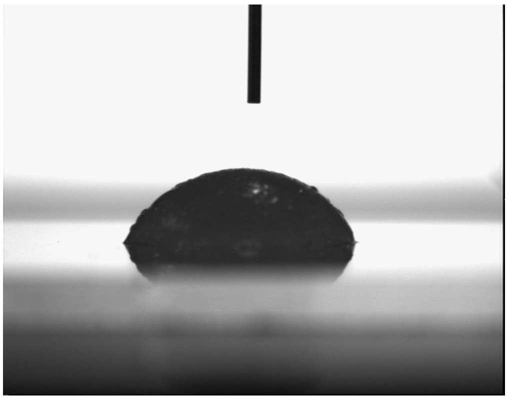

t = 2000 s

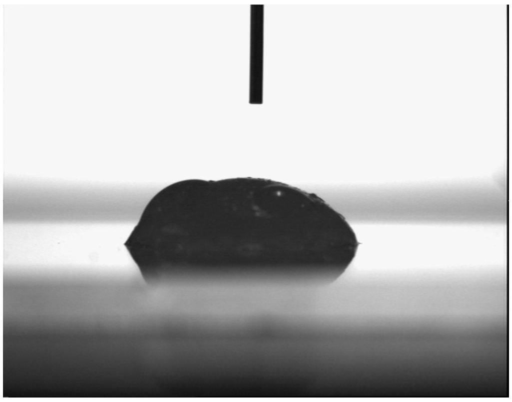

t = 2300 s

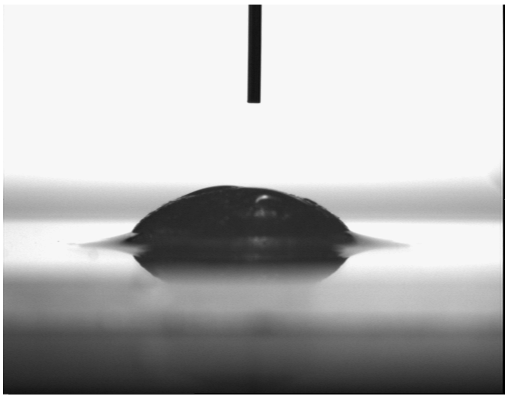

t = 2400 s

(b)

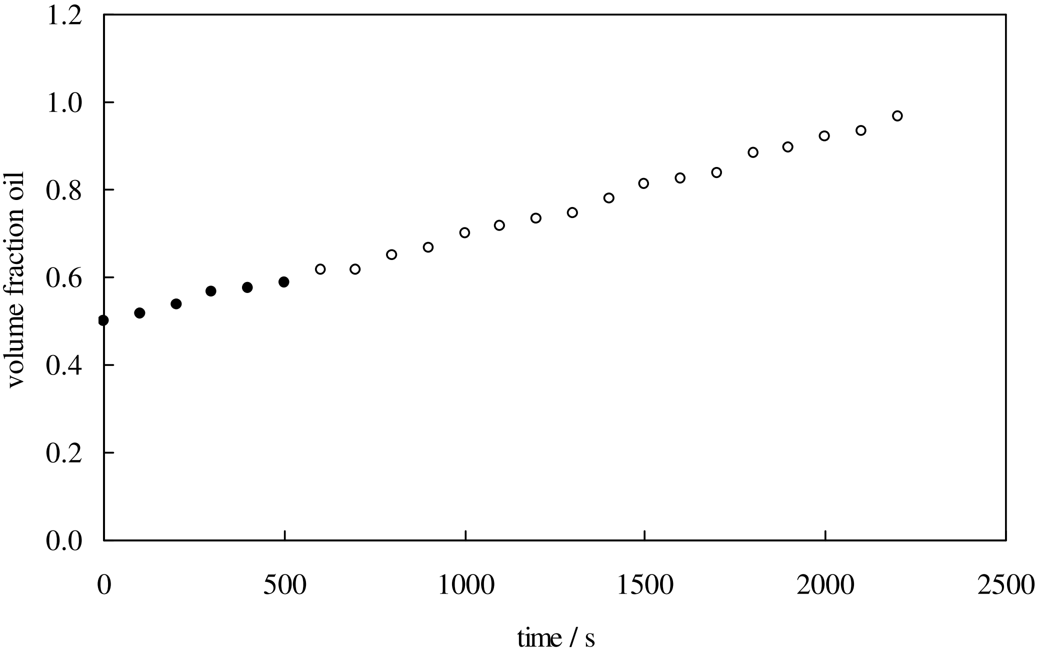

Figure 6.7. (a) Appearance of drop of dodecane-in-water emulsion stabilised by 2 wt. % fumed silica (78 % SiOH), volume fraction of oil = 0.5, as in evaporates on a slide (contact angle of a drop of water on the slide under dodecane advancing = 130^{o}, receding = 100^{o}). (b) The oil volume fraction in the emulsion drop with time closed points indicate no sign of instability, open points indicate instability observed. The needle diameter is 0.3054 mm.

(a)

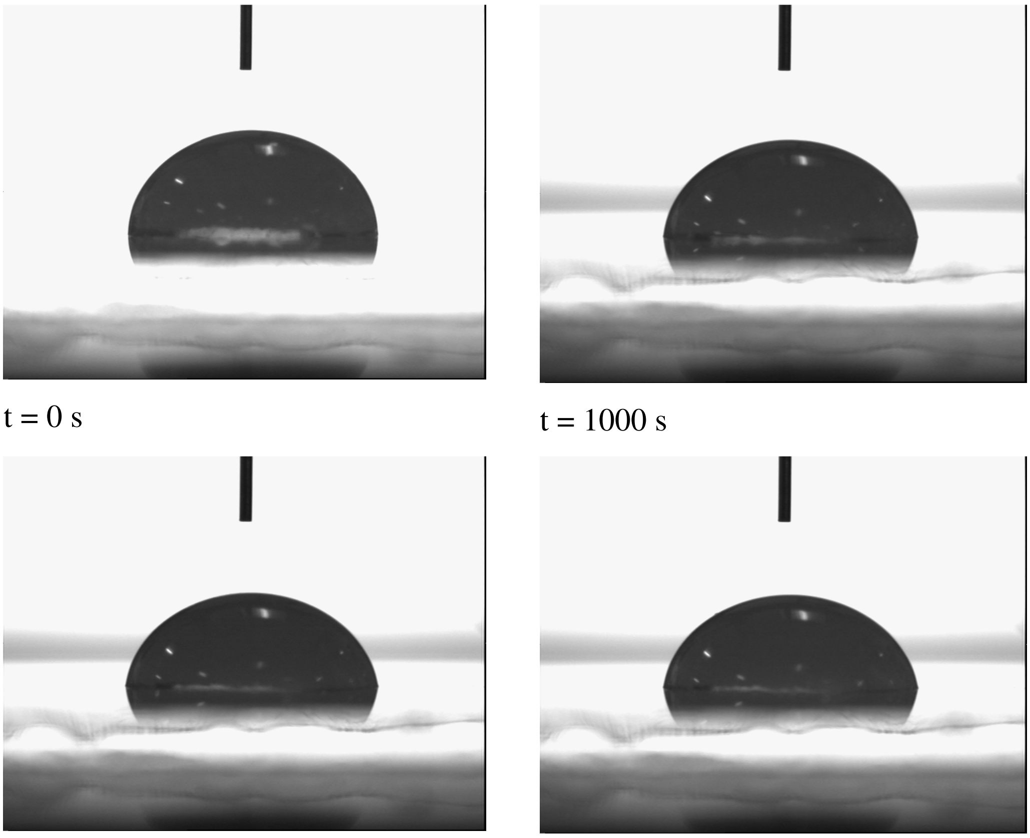

t = 0 s

t = 1000 s

t = 1500 s

t = 1700 s

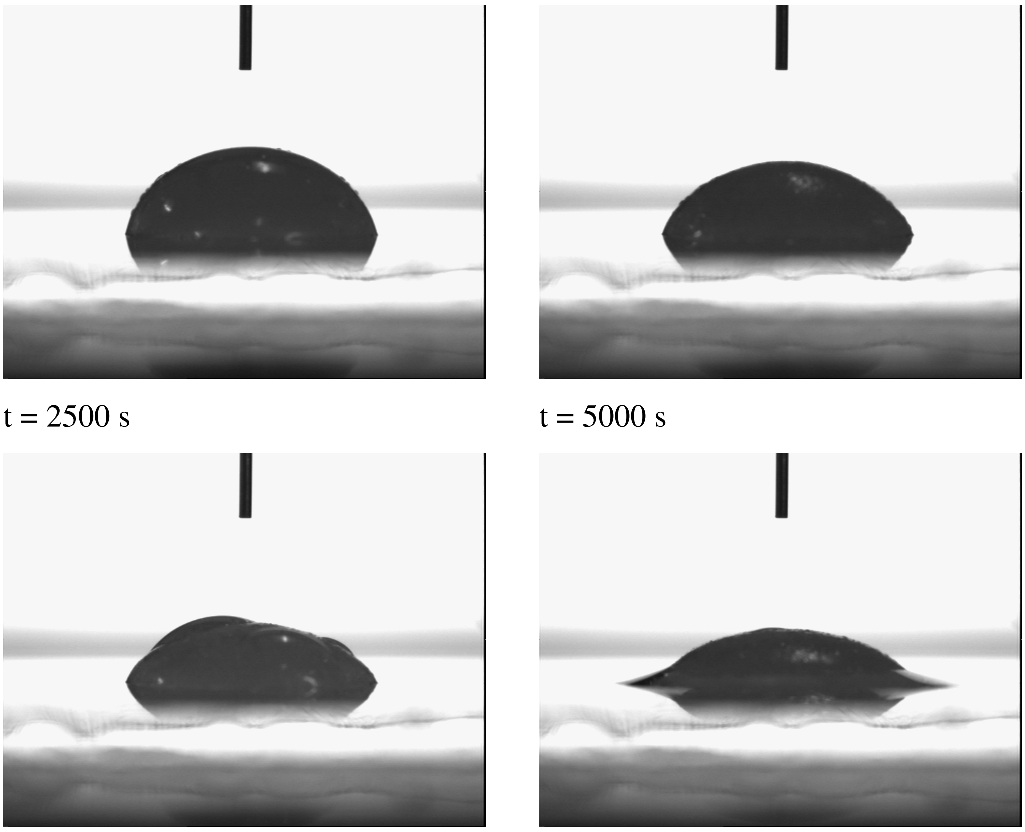

t = 2500 s

t = 5000 s

t = 6000 s

t = 6100 s

(b)

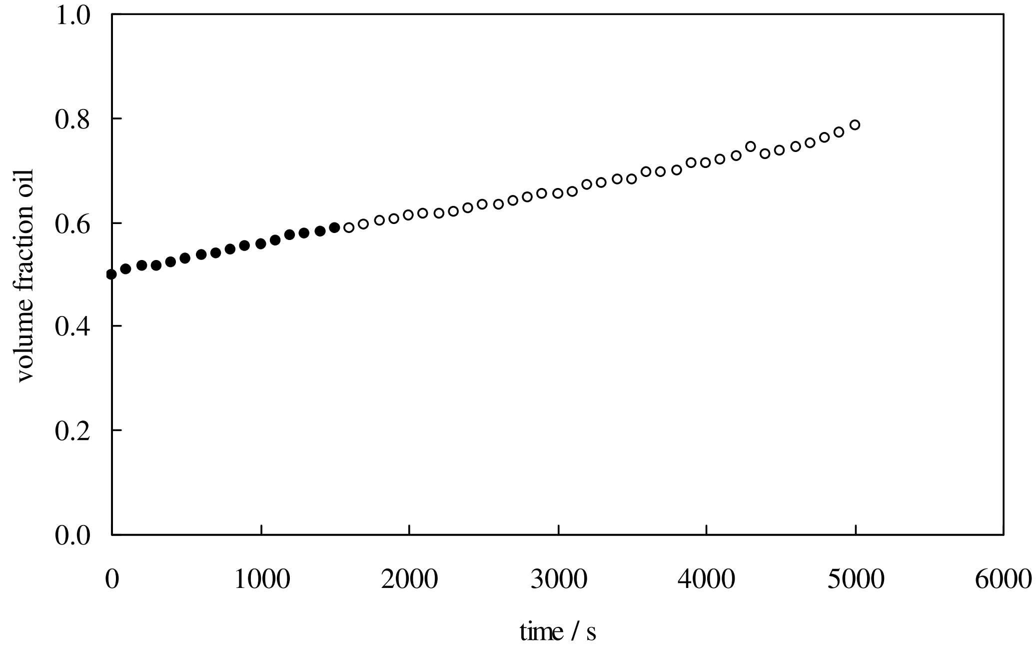

Figure 6.8. (a) Appearance of drop of dodecane-in-water emulsion stabilised by 2 wt. % fumed silica (78 % SiOH), volume fraction of oil = 0.5, as in evaporates on a slide (contact angle of a drop of water on the slide under dodecane advancing = 105°, receding = 87°). (b) The oil volume fraction in the emulsion drop with time closed points indicate no sign of instability, open points indicate instability observed. The needle diameter is 0.3054 mm.

(a)

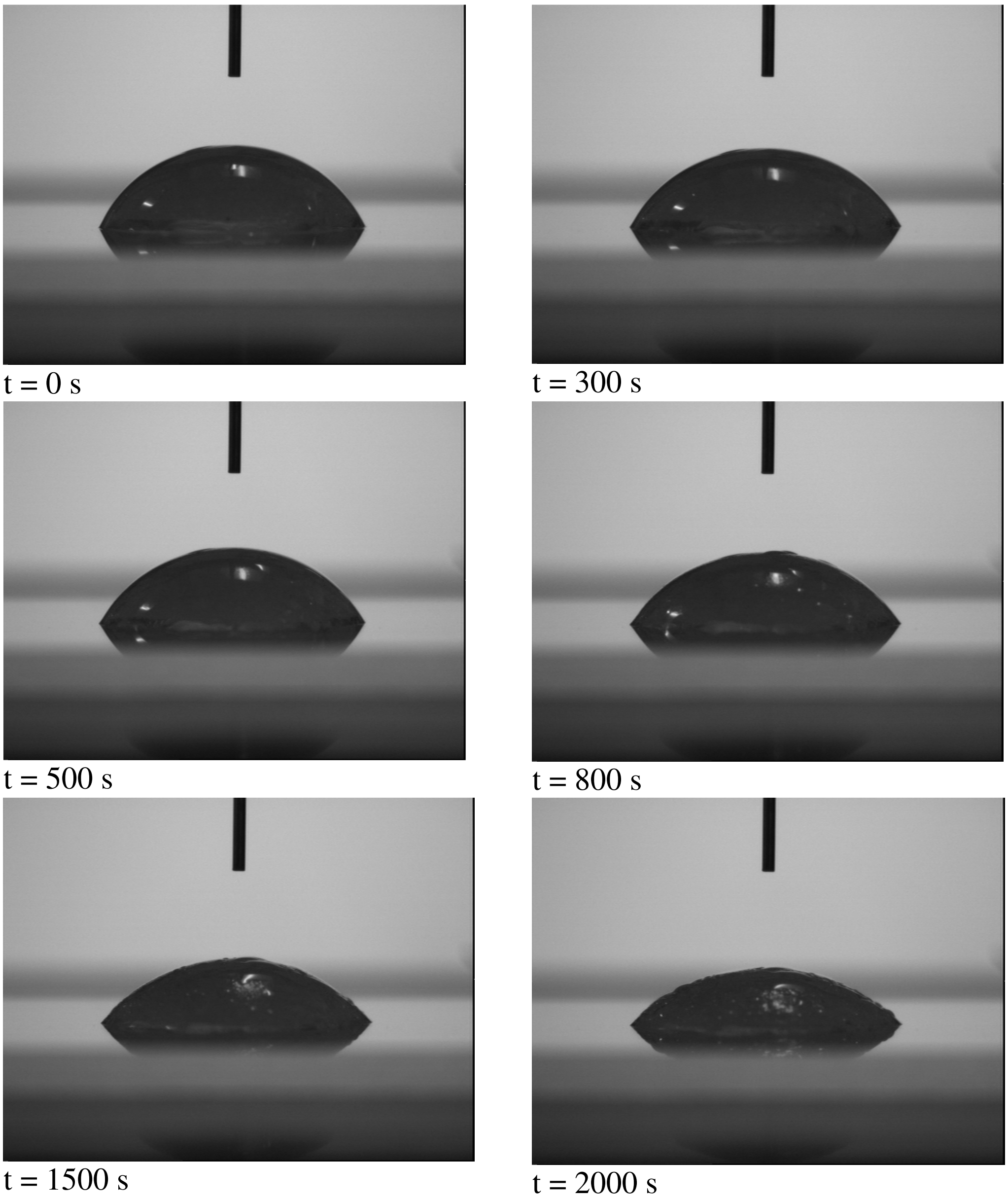

t = 0 s

t = 300 s

t = 500 s

t = 800 s

t = 1500 s

t = 2000 s

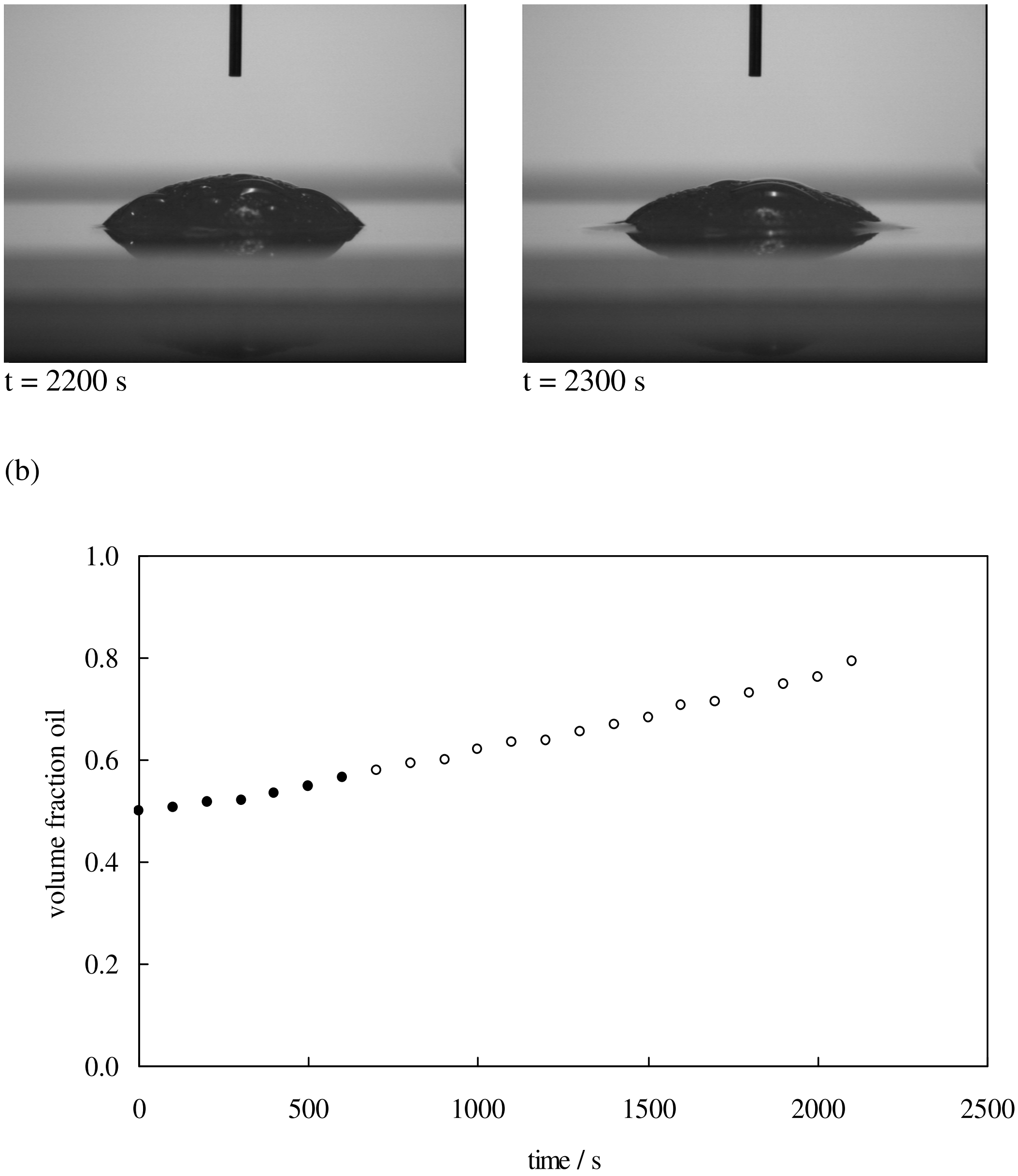

t = 2200 s

t = 2300 s

(b)

Figure 6.9. (a) Appearance of drop of dodecane-in-water emulsion stabilised by 2 wt. % fumed silica (78 % SiOH), volume fraction of oil = 0.5, as in evaporates on a slide (contact angle of a drop of water on the slide under dodecane advancing = 89^{o}, receding = 72^{o}). (b) The oil volume fraction in the emulsion drop with time closed points indicate no sign of instability, open points indicate instability observed. The needle diameter is 0.3054 mm.

(a)

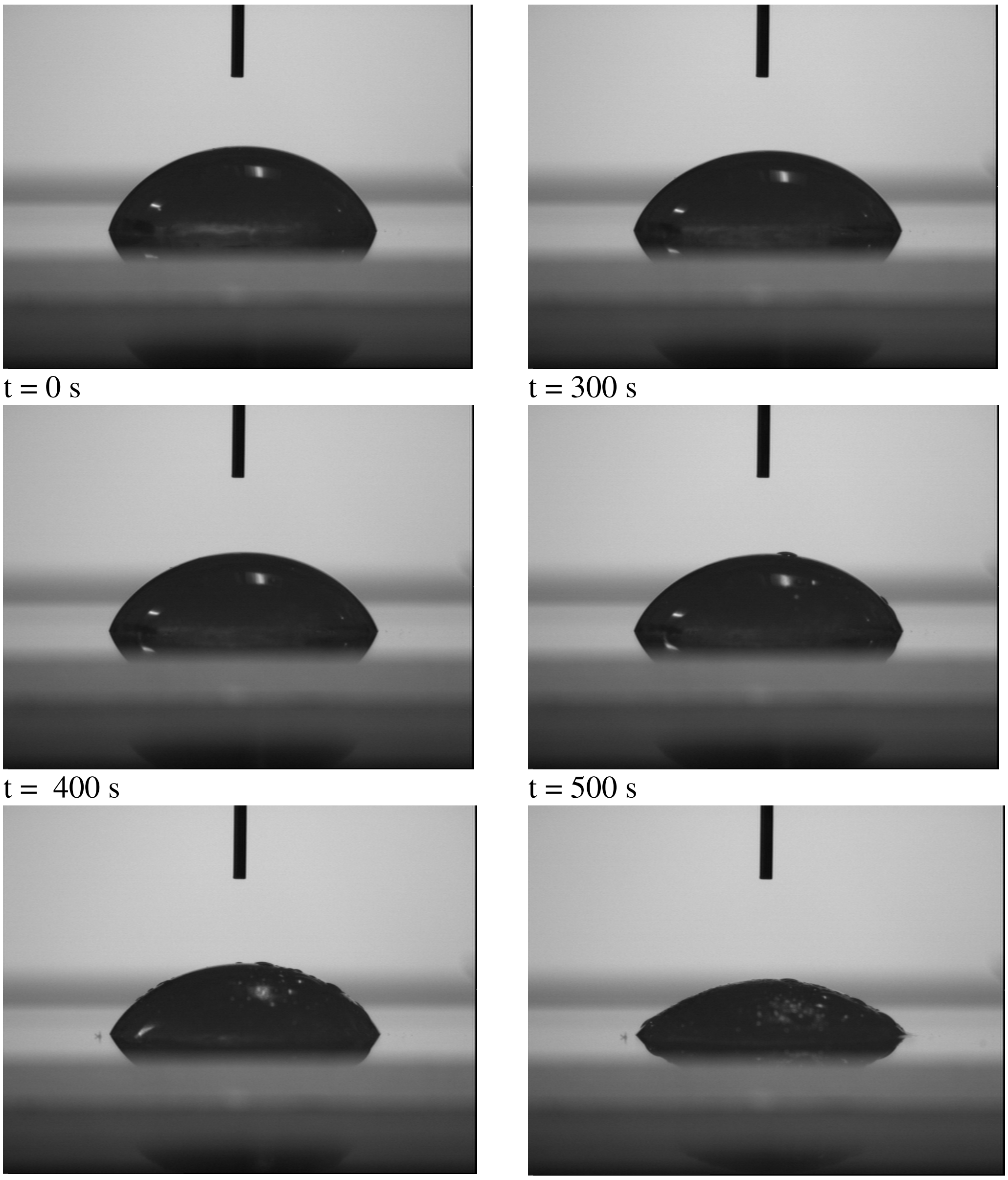

t = 0 s

t = 300 s

t = 400 s

t = 500 s

t = 1000 s

t = 1500 s

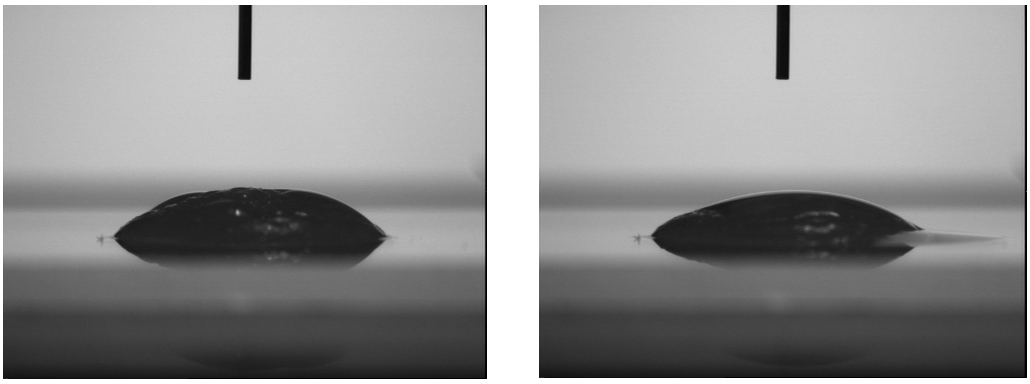

t = 2300 s

t = 2400 s

(b)

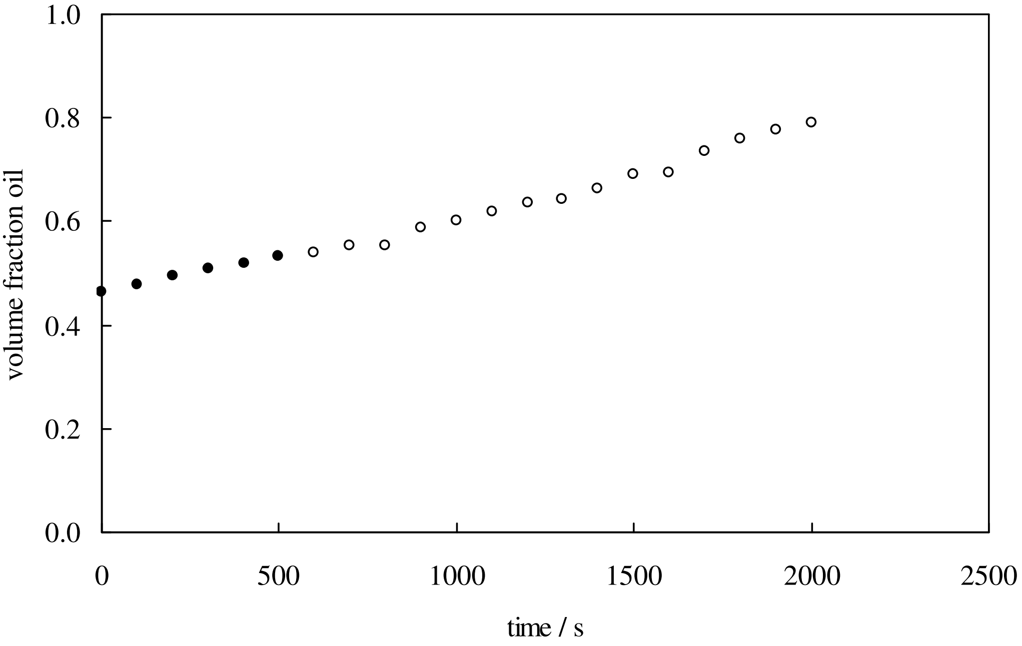

Figure 6.10. (a) Appearance of drop of dodecane-in-water emulsion stabilised by 2 wt. % fumed silica (78 % SiOH), volume fraction of oil = 0.5, as in evaporates on a slide (contact angle of a drop of water on the slide under dodecane advancing = 32°, receding = 23°). (b) The oil volume fraction in the emulsion drop with time closed points indicate no sign of instability, open points indicate instability observed. The needle diameter is 0.3054 mm.

(a)

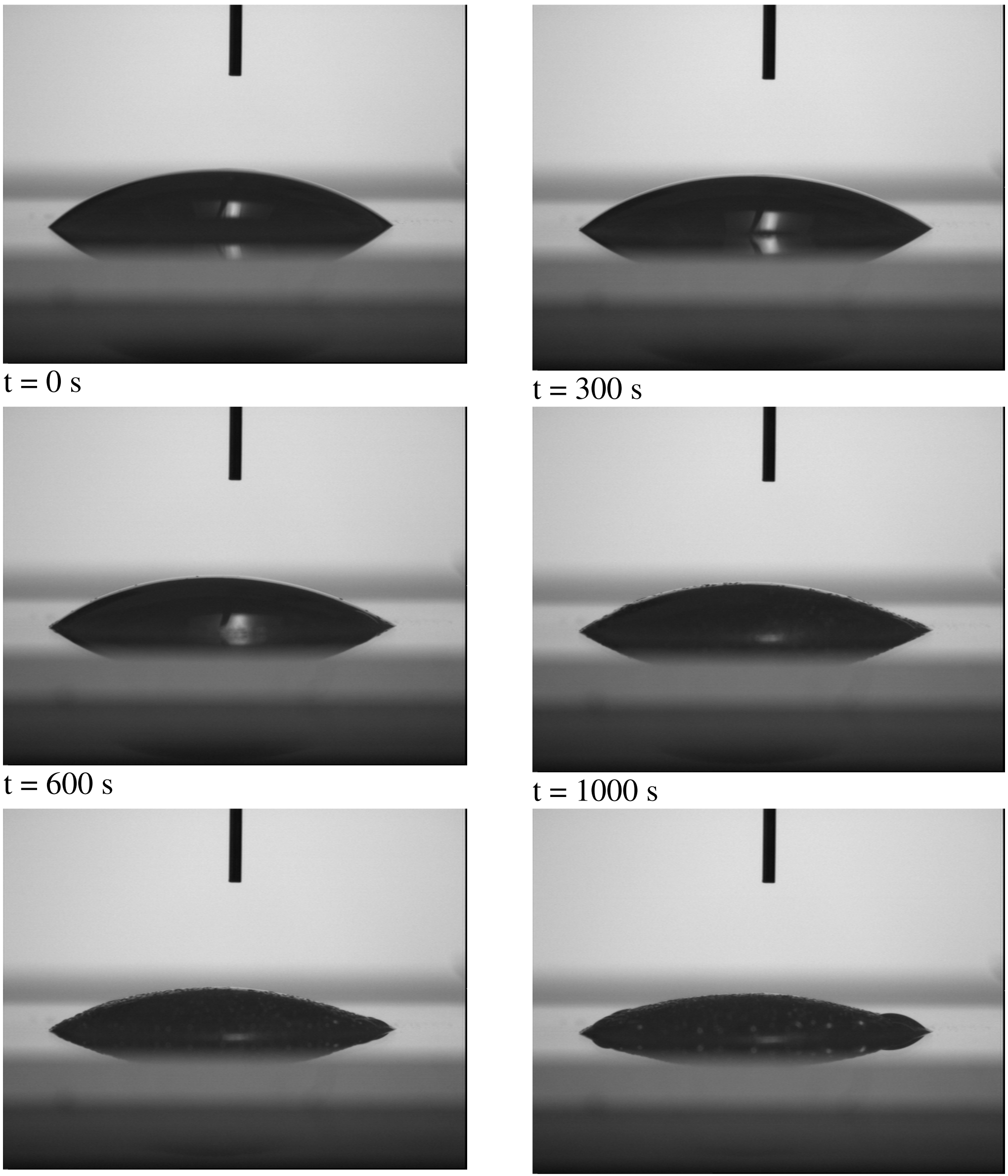

t = 0 s

t = 300 s

t = 600 s

t = 1000 s

t = 1500 s

t = 1800 s

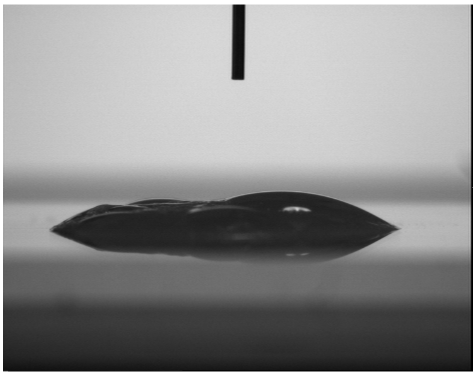
t = 2100 s

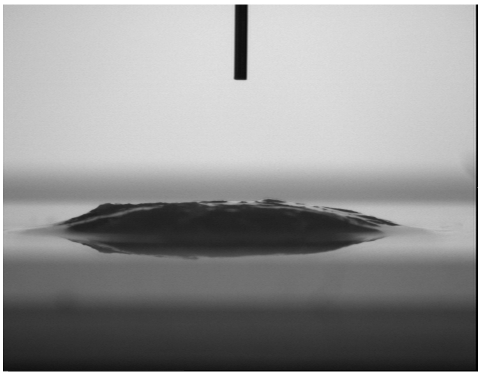
t = 2200

Figure 6.11. Schematic representation of the potential importance of the contact angle formed between the internal aqueous drop, under the spreading bulk oil phase, on the modified slide (circled in red) as the drop as the emulsion evaporates. The arrow underneath the drop represents the direction of potential particle spreading. The red arrow indicates the force which could be exerted by the surface pressure of the particles.

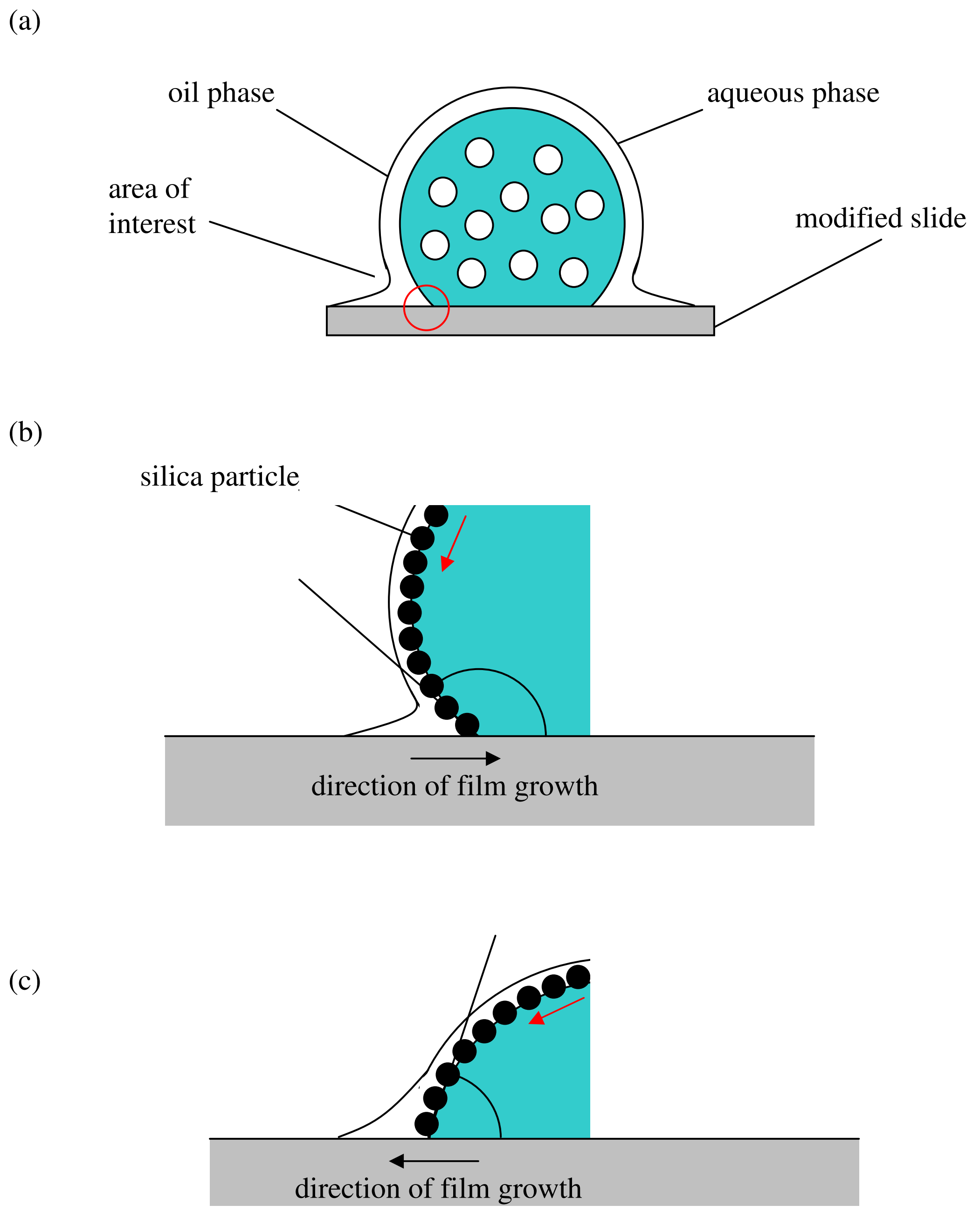

particle films similar to those responsible for the spreading observed in Chapters 3 and 4. However, examination of the glass slides by SEM, after the systems had completely evaporated, showed that the silica particles were only present in the area that supported the internal aqueous drop. No particles were found outside this footprint. The only effect observed by altering the hydrophobicity of the glass slide was an increase in the size of this footprint as the surface is made more hydrophilic i.e. the more hydrophilic the slide the larger the footprint.

It is worth noting that spreading occurs on all hydrophobic surfaces. The experiments described above were repeated on parafilm, latex and polystyrene in addition to the hydrophobically modified glass described above and leaf surfaces described in Section 6.6. In each case spreading was observed. As long as one of the oil lenses formed at the continuous phase-air surface can also contact the solid surface at the same time this spreading should be observed on any surface.

6.5 Silica macro-porous crusts from evaporated o/w solid-stabilised emulsion

When the emulsion systems described above are allowed to fully evaporate a silica crust is formed. One of the unusual properties of colloidal fumed silica is its ability to sinter at room temperature to form solids. The structure of the solids produced by evaporation of bulk emulsions was investigated in previous Ph.D. work.[13,14] The structures remaining after the evaporation of bulk samples of emulsion were studied, here the structure is a hollow crust of silica in the approximate shape of the internal aqueous after the emulsion has phase separated. Figure 6.12 shows some Scanning Electron Microscopy (SEM) images of the internal and external surfaces of the silica crust. It can be seen clearly that the silica particles have sintered to form a macro-porous solid with pore diameters in the range 5 – 15 μm. This matches the drop size of the emulsion evaporated to form the solid which also had drop diameters of ~ 10 μm.

The external surface of the crust, (a) and (b), is relatively smooth, even though it is porous, when compared with the internal surface, (c) and (d). It can be envisaged that as the oil droplets within the emulsion coalesce with the oil film coating the emulsion drop, the silica particles are transferred to the oil-water interface between the continuous phase of the emulsion and the free oil coating the emulsion drop. These are the silica particles which sinter to form the relatively smooth external surface of the silica crust. The rough internal surface of the crust is formed from residual creamed oil droplets remaining from the emulsion beneath the particles adsorbed to the air water surface.

6.6 Spreading of o/w solid-stabilised emulsions on leaf surfaces

Many agrochemical products are o/w emulsions.[15] The handling of the potentially toxic oil soluble actives is done in large quantities and by relatively untrained personnel on the farms where the products are used and because of this it is much safer and easier to handle in the form of water continuous emulsions.

Figure 6.12. Scanning electron microscopy of the silica structures left behind from the evaporation of a preferred dodecane-in-water solid-stabilised emulsion stabilised by 2 wt. % of fumed silica with 78 % SiOH groups. Images (a) and (b) are of the external surface of the crust. Images (c) and (d) are of the internal surface of the crust. The scale bar equals 20 μm in images (a) and (c) and 50 μm in images (b) and (d).

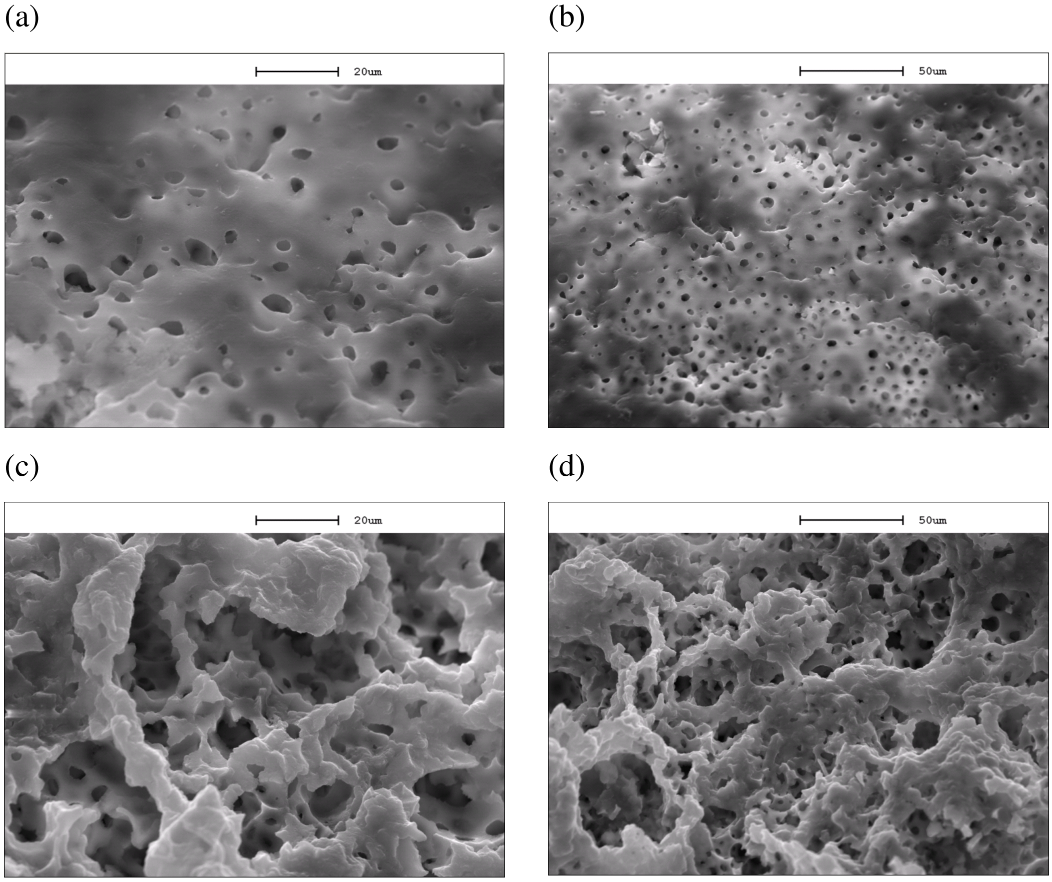

When delivering oil soluble actives in agrochemicals to plant surfaces through spraying emulsions it is beneficial to have large drops falling from the nozzle of the sprayer. Large drops fall quickly and reduce the possibility of 'drift'. Drift is when material which is sprayed above one field is blown onto surrounding areas.[16] Surfactant-stabilised systems naturally have low surface and interfacial tensions and because of the shear experienced during spraying they have a tendency to form very small drops increasing the chance of drift. Small drops take a relatively long time to fall to the ground. This is not a problem with solid-stabilised systems as the surface and interface tensions remain high and the drops produced during spraying large. The difficulty in spraying large drops, and therefore minimising drift, is that when the drop of emulsion lands on the surface of the leaf there is a relatively small contact area with the leaf, compared to that created when spraying many small drops. This phenomenon has the potential to defeat this limitation as a large drop can be sprayed which will fall quickly, therefore minimising drift, followed some time later by destabilisation of the system and liberation of the oil onto the plant surface maximising the contact area.

6.6.1 Leaf surfaces

Three different leaf surfaces, chosen to encompass the range of different wettabilites encountered in nature, were studied. The plants were grown in protective green houses in the absence of wind and watered from below. This reduces the risk of the wax crystal structure on the leaf surface being disturbed and increases the reproducibility of experiments. The plants studied were *Chenopodium Album* ('Fat Hen' – very hydrophobic), *Solanium Nigrun*

(‘Black Nightshade’ – moderately hydrophobic) and *Abuthilon Theopurasti* (‘Velvet Leaf’ – slightly hydrophobic).

Once a leaf is removed from the plant it will start to degrade as it wilts and dies. There was a noticeable degradation in the leaf surface over time as the experiment progressed because of this quantitative analysis of the data is difficult as the leaf surface is changing in shape and composure over the length of the experiment. However, it is still useful to consider the data in a qualitative sense as this is how this phenomenon could be harnessed for use in a product technology.

Figure 6.13 show the appearance of a drop of dodecane-in-water emulsion stabilised by 2 wt. % 78 % SiOH silica on each of the leaf surfaces. The spreading still occurs and the dodecane, once liberated from the emulsion, did cover 80 to 100 % of the available leaf surface.

6.6.2 Grain surfaces

Another potential application for this type of spread is in the treating of grains and seeds. Many grains are treated in bulk before sale and current processes rely on either painting or spraying actives. Again using this phenomenon the contact between active and grain could be maximised.

Figure 6.14 shows appearance of drop of dodecane-in-water emulsion stabilised by 2 wt. % fumed silica (78 % SiOH), volume fraction of oil = 0.5, as

Figure 6.13. Drops of dodecane-in-water emulsion stabilised by 2 wt. % fumed silica (78 % SiOH), the volume fraction of dodecane = 0.5, as it evaporates on (a) *Chenopodium Album* (‘Fat Hen’ – very hydrophobic), (b) *Solanium Nigrun* (‘Black Nightshade’ – moderately hydrophobic) and (c) *Abuthilon Theopurasti* (‘Velvet Leaf’ – slightly hydrophobic). Original drop volume was 50 μm.

(a)

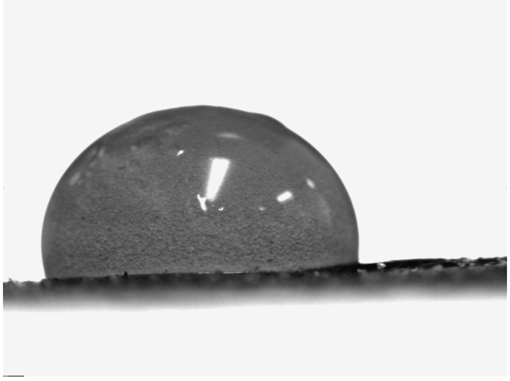

t = 0 s

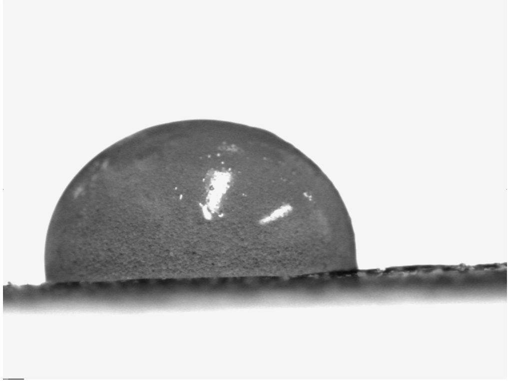

t = 900 s

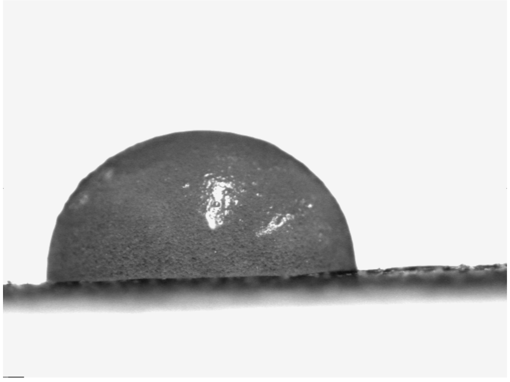

t = 1800 s

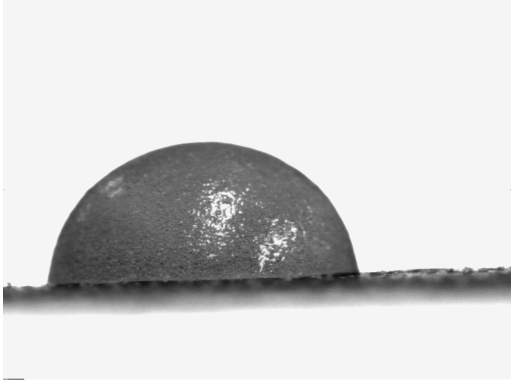

t = 2400 s

t = 2600 s

(b)

t = 0 s

t = 900 s

t = 1800 s

t = 2400 s

t = 2800 s

(c)

t = 0 s

t = 900 s

t = 1800 s

t = 2400 s

t = 2600 s

Figure 6.14. Appearance of drop of dodecane-in-water emulsion stabilised by 2 wt. % fumed silica (78 % SiOH), volume fraction of oil = 0.5, as in evaporates on a grain seed. The grain is ~ 3 mm in width.

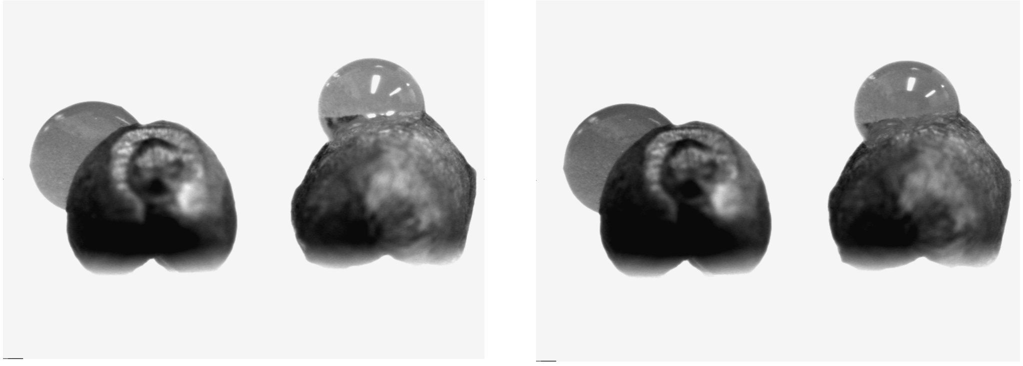

t = 0 s

t = 100 s

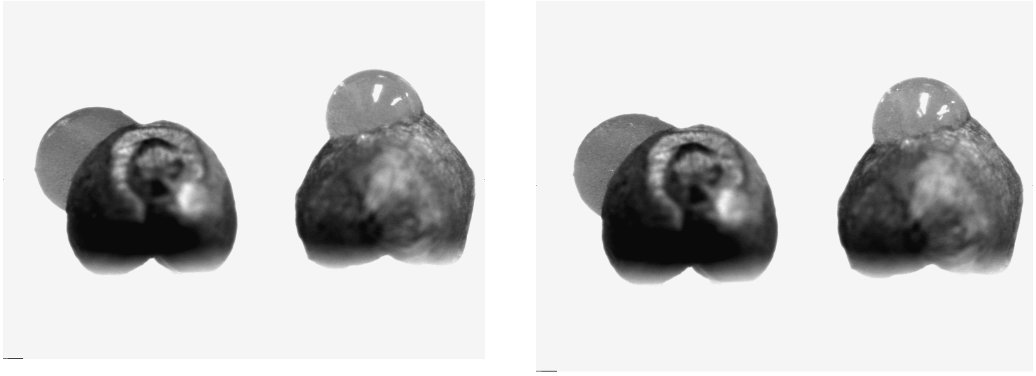

t = 300 s

t = 400 s

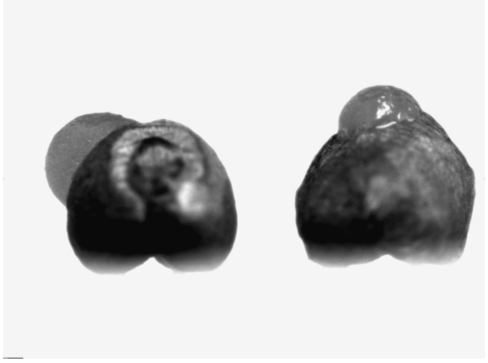

t = 500 s

in evaporates on a grain seed. Although more difficult to see, spreading still occurs on the grain surface between t = 400 and t = 500. The liberated oil coated the whole of the grain.

6.7 Conclusions

Solid-stabilised o/w emulsions have been seen to rapidly break and coalesce after a period of evaporation. This coalescence leads to unusual spreading behaviour where initially the drop of emulsion has a high contact angle on the hydrophobic surface (similar to that of water) but after coalescence the system forms spreading ‘wings’ from the aqueous drop. When spreading has ceased the contact area of the system with the hydrophobic surface is much larger than when the drop of emulsion is placed on the surface, i.e. before coalescence and spreading. Total evaporation of the drop of emulsion leads to the formation of a solid silica crust which has been investigated using SEM. In contrast to the solid-stabilised systems, SDS-stabilised systems exhibited no rapid coalescence and the system appeared to evaporate as an emulsion rather than phase separate and then evaporate. Because of this no free oil was liberated and no spreading was observed meaning that the contact area of the drop was the same throughout the evaporation process. The spreading occurs on a variety of surfaces including leaf and grain surfaces.

6.8 References

---

[1] A.R. Rahate and J.M. Nagarkar, *J. Dispersion Sci. Technol.*, **28**, 1077 (2007).

[2] D.J. McClements, E.A. Decker, Y. Park and J. Weiss, *Food Biophys.*, **3**, 210 (2008).

[3] S. Fatemi, M.K. Varkani, Z. Ranjbar and S. Bastani, *Prog. Org. Coat.*, **55**, 377 (2006).

[4] M.S. Miskandar, Y.B.C. Man, M.S.A. Yusoff and R.A. Rahman, *J. Am. Oil Chem. Soc.*, **79**, 1163 (1163).

[5] M.A. Faers and R. Pontzen, *Pest Manag.Sci.*, **64**, 820 (2008).

[6] X.D. Wang, D.J. Lee, X.F. Peng and J.Y. Lai, *Langmuir*, **23**, 8042 (2007).

[7] I. Aranberri, B.P. Binks, J.H. Clint and P.D.I. Fletcher, *Chem. Commun.* 2538 (2003).

[8] I. Aranberri, B.P. Binks, K.J. Beverley, J.H. Clint and P.D.I. Fletcher, *Langmuir*, **18**, 3471 (2002).

[9] B.P. Binks and S.O. Lumsdon, *Langmuir*, **16**, 8622 (2000).

[10] I. Aranberri, B.P. Binks, J.H. Clint and P.D.I. Fletcher, *Langmuir*, **20**, 2069 (2004).

[11] I. Aranberri, K.J. Beverley, B.P. Binks, J.H. Clint and P.D.I. Fletcher, *Langmuir*, **18**, 3471 (2002).

[12] J. Bibette, *Langmuir*, **8**, 3178 (1992).

[13] I.A. Askargorta, Ph.D. Thesis, University of Hull, (2003).

[14] B.P. Binks, *Adv. Mater.*, **14**, 1824 (2002).

[15] P. Mulqueen, *Adv.Colloid Int. Sci.*, **106**, 83 (2003).

[16] P. Spanoghe, M. De Schampheleire, P. Van der Meeren and Walter Steurbaut, *Pest Manag. Sci.*, **63**, 4 (2007).

CHAPTER 7

IN-SITU MODIFICATION OF HYDROPHOBIC SILICA

7.1 Introduction

The work presented in the previous chapters has concentrated on modifying the properties of particles by addition of material to either the particle surface, or to the bulk medium in which the particles are dispersed. Here we study the effects of removing the coating from a particle that is pre-modified. Hydrophobic silanised silica particles will be made more hydrophilic *in-situ*, both in the bulk phase and at the oil-water interface, by hydrolysis of the silane coating using base. Silica particles are soluble in high pH solution and exposure to base will remove the particle surface.[1] Removal of the hydrophobic silane coating of the silica should render it more hydrophilic and by changing the hydrophobicity of the particle this way it should be possible to alter the particles emulsion stabilisation characteristics and to cause phase inversion in an emulsion from w/o to o/w.[2,3] If such a phase inversion is observed then the particles have reached the correct hydrophobicity for phase inversion which is known to correspond to the maximum stabilising ability of the particles.[4]

7.2 Modification of hydrophobic particles in the bulk phase

Figure 7.1 shows the decrease in pH with time of a 2 wt. % dispersion of fully hydrophobic particles (H18) dispersed in a KOH solution (filled circles), a 2 wt. % dispersion of fully hydrophilic silica (N20) dispersed in a KOH solution (open circles) and of a solution of KOH containing no particles (crosses). The reaction was carried out at 40 ^{o}C with constant stirring and the initial pH = 11.5. Since there is no significant change in the pH of the solution which contains no particles at this temperature and for this time scale, CO_2 dissolving into the solution is not contributing to the decrease in pH of the systems containing particles. More interesting is the difference between the dispersion that contains purely hydrophilic particles and the dispersion that contains hydrophobic particles which suggests that the hydrophobic coating is being removed from the hydrophobic particles. If the KOH reacts to remove the hydrophobic coating of the silica particles (and perhaps dissolve some of the particles in the process) then the pH should drop accordingly. This is supported by experimental observations that as the reaction progresses the mm-sized “flocs” in the latter disappeared and the particle dispersion became uniform with a slight blue colour. This change in appearance of the system is consistent with the hydrophobic coating on the silica particles being removed and the particles having an increased hydrophilicity.

It is apparent that the initial reduction in pH is faster in the system that contained the hydrophilic particles than in the system that contained the hydrophobic ones. This can be explained because there are three processes

Figure 7.1. Decrease in pH with time of a 2 wt. % dispersion of fully hydrophobic particles (H18) dispersed in a KOH solution (filled circles), a 2 wt. % dispersion of fully hydrophilic silica (N20) dispersed in a KOH solution (open circles) and of a solution of KOH containing no particles (crosses). This reaction was carried out at 40 °C with constant stirring.

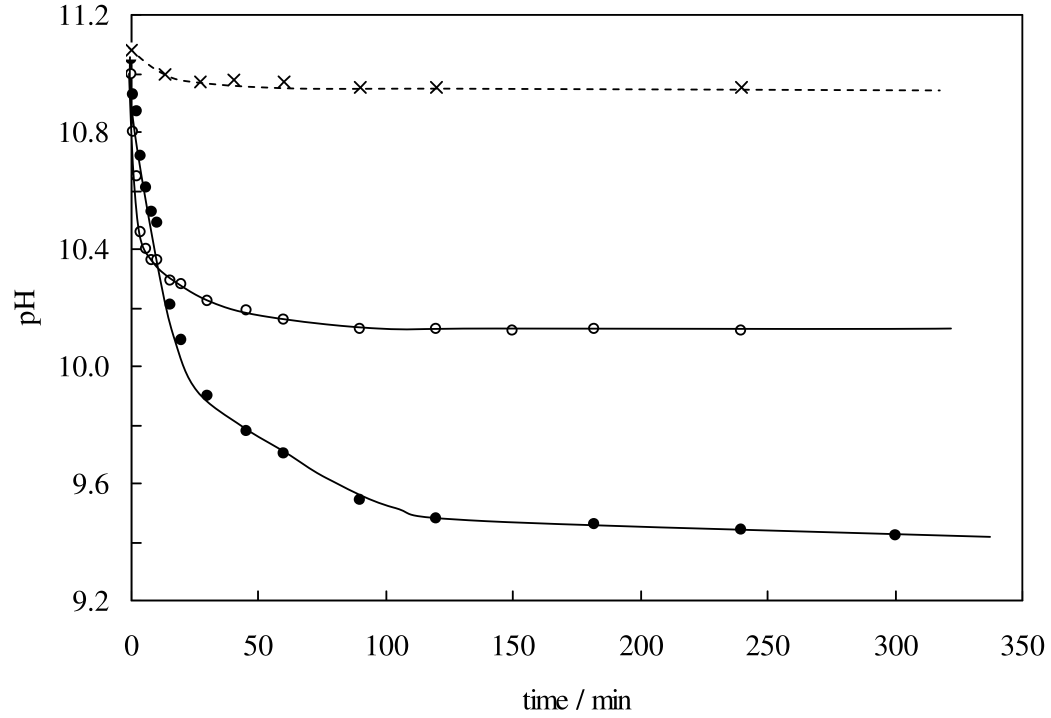

occurring in the system. The first is the titration of any surface Si-OH groups on the silica, the second is the hydrolysis of the bond between the silica particle and the hydrophobic coating and the third is the silica particle being dissolved. The relative shapes of the plots in Figure 7.1 are consistent with the following picture. In the case of the hydrophilic particles the surface Si-OH groups are initially titrated quickly leading to a rapid decrease in the pH of the system. The only remaining process then is that of the silica particles dissolving which must be slow otherwise the pH would not plateau. In the case of the hydrophobic particles their surface Si-OH groups are either coordinated to the hydrophobic coating or hindered by it. This results in a slower initial rate. However the plateau value for this system is a complete pH unit lower than that for the hydrophilic silica. Since the only difference between the two types of particles is the coating, it is reasonable to attribute the further reduction in the pH to the KOH used when hydrolysing the siloxane bond (Si-O-Si).

7.3 *In-situ* modification of hydrophobic silica particles – increase in emulsion stability

7.3.1 Elevated pH (11.5)

The experimental methods used in this section can be found in section 2.2.11 but briefly hydrophobic silica particles (H18, 20 % SiOH) were modified in the following way. 2 wt. % (per volume of the total emulsion) silica particles were initially dispersed into the aqueous phase (7.5 ml water) by wetting with ethanol. ~ 25 wt. % ethanol was added in order to sufficiently wet the particles and allow them to enter the aqueous phase (pH 7), the system was then sonicated for 2 minutes at 10 W using the ultrasonic probe. The ethanol was removed by 7 washing and centrifugation cycles. After the first sonication, when the concentration of the ethanol was high, the particles appeared well dispersed, i.e. homogeneous with no visible flocs. After each wash/centrifugation cycle, as the ethanol concentration decreased, the system became less homogeneous and mm sizes flocs were visible.

15 ml of emulsion was then prepared using the aqueous particle dispersion of hydrophobic particles. The emulsion was stabilised by 2 wt. % hydrophobic particles (H18, 20 % SiOH) initially dispersed into the aqueous phase. The oil used was squalane and the oil volume fraction was 0.5. In order for the coating on the particle to have sufficient opportunity to be hydrolysed the system was emulsified for 2 hours. The system was homogenised at 11,000 r.p.m. using the Ultra Turrax for 3 minutes followed by 30 seconds rest then another 3 minutes homogenisation etc. until the total homogenisation time was 2 hours. During homogenisation the system was thermostatted at 40 ^{o}C using a grant thermostat and the temperature of the system was checked at regular intervals to ensure that it did not deviate from this value. At 21 minute intervals the system was removed from the bath and the identity of the continuous phase identified by both conductivity measurements and by drop test. The appearance of the system was also noted. After homogenisation the system was stored in a water bath at 25 ^{o}C and the appearance of any phases with time noted.

The system was prepared as described above and, after washing, the pH of the aqueous phase was altered to 11 by the addition of a few drops of concentrated KOH. All measurements taken indicate that the emulsion was oil continuous throughout the 2 hours of homogenisation. Before homogenisation the aqueous phase was cloudy and the oil phase was clear. After the first spell of homogenisation the particles had transferred from the aqueous phase to the organic phase as indicated by a clear aqueous phase at the bottom of the vessel.

Figure 7.2 is a schematic representation of the system at different times during homogenisation. Initially a small amount of aqueous phase is not emulsified but after 21 minutes of homogenisation all the aqueous phase is located in the emulsion and there is no change in the appearance of the system after this time. This indicates that even though no phase inversion was observed the ability of the initially very hydrophobic particles to stabilise a w/o emulsion was increased. This is likely due to the removal of the hydrophobic coating rendering the particle more hydrophilic and more effective as an emulsifier.

Figure 7.3 plots the volume fraction of emulsion, oil and aqueous phase recovered after complete homogenisation as a function of time. The system was completely stable to coalescence over the time period studied but did sediment to give a clear supernatant oil phase and a white sedimented w/o emulsion phase.

Figure 7.2. Schematic representation of the appearance of a water-in-dodecane emulsion stabilised by 2 wt. % hydrophobic silica initially dispersed into the aqueous phase, $\phi_o = 0.5$, aqueous phase pH = 11 at various times during homogenisation at 11,000 r.p.m. Time is in minutes. At times longer than 21 minutes there was no change in the appearance of the system.

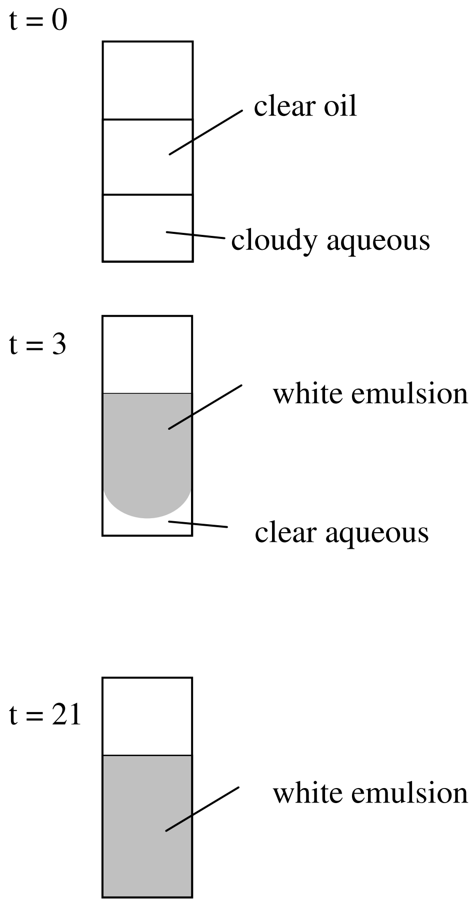

Figure 7.3. Volume fraction of emulsion, oil and aqueous phase recovered after homogenisation as a function of time for a water-in-dodecane emulsion stabilised by 2 wt. % hydrophobic silica initially dispersed into the aqueous phase, $\phi_o = 0.5$, aqueous phase pH = 11. The volume fractions of oil and aqueous phase are relative to their initial volumes.

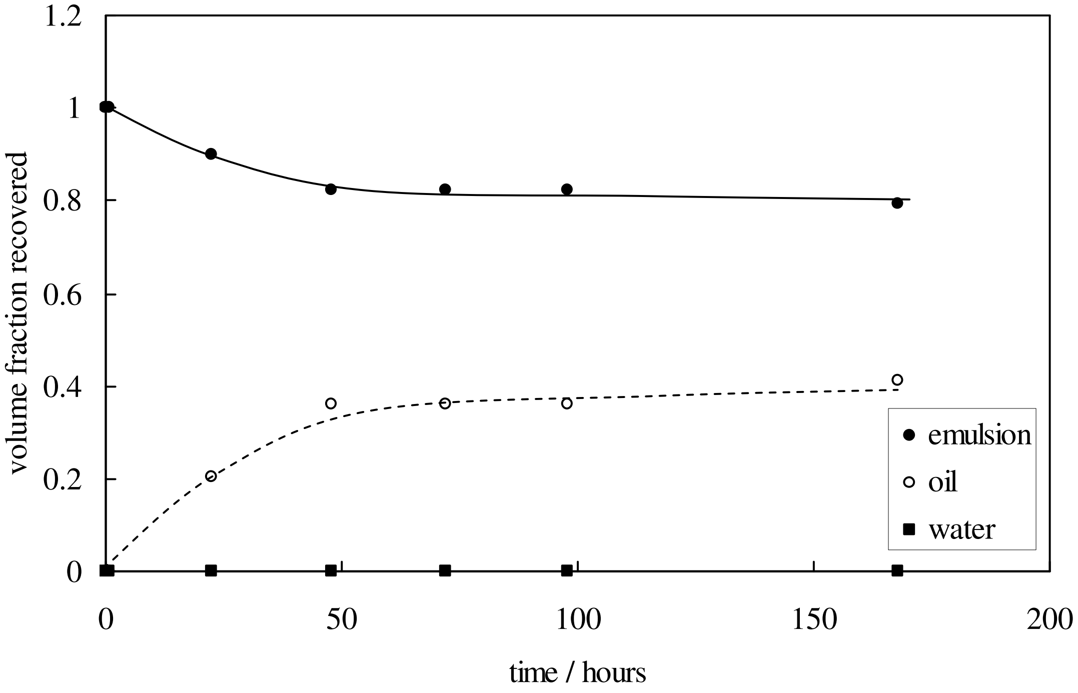

7.3.2 Natural pH (6.3)

The system was prepared as described above and the pH of the aqueous phase was not altered. All measurements taken indicate that the emulsion was oil continuous throughout the 2 hours of homogenisation. Before homogenisation the aqueous phase was cloudy and the oil phase was clear. After the first spell of homogenisation the particles had transferred from the aqueous phase to the organic phase as indicated by a clear aqueous phase at the bottom of the vessel. Figure 7.4 is a schematic representation of the system at different times during homogenisation. As can be seen, initially a small amount of aqueous phase is not emulsified. After 21 minutes of homogenisation the excess aqueous phase has still not been incorporated into the emulsion. Throughout the full 2 hours of homogenisation this excess aqueous phase remained.

Figure 7.5 plots the volume fraction of emulsion, oil and aqueous phase recovered after homogenisation as a function of time. The system was not stable to coalescence over the time period studied with some aqueous phase being liberated. This system sedimented to give a clear supernatant oil phase and a white sedimented emulsion phase.

Phase inversion was not observed in either the high or natural pH systems. Not enough hydrophobic coating was removed from the particles in the

Figure 7.4. Schematic representation of the appearance of a water-in-dodecane emulsion stabilised by 2 wt. % hydrophobic silica initially dispersed into the aqueous phase, ϕ_o = 0.5, natural aqueous phase pH (6.3) at various times during homogenisation at 11,000 r.p.m. Time is in minutes. At times longer than 21 minutes there was no change in the appearance of the system.

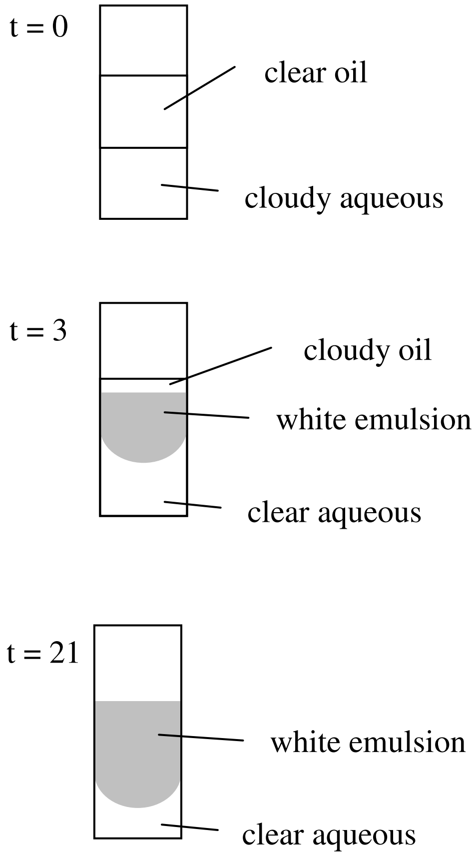

Figure 7.5. Volume fraction of emulsion, oil and aqueous phase recovered after homogenisation as a function of time for a water-in-dodecane emulsion stabilised by 2 wt. % hydrophobic silica initially dispersed into the aqueous phase, ϕ_o = 0.5, natural aqueous phase pH (6.3). The volume fractions of oil and aqueous phase are relative to their initial volumes.

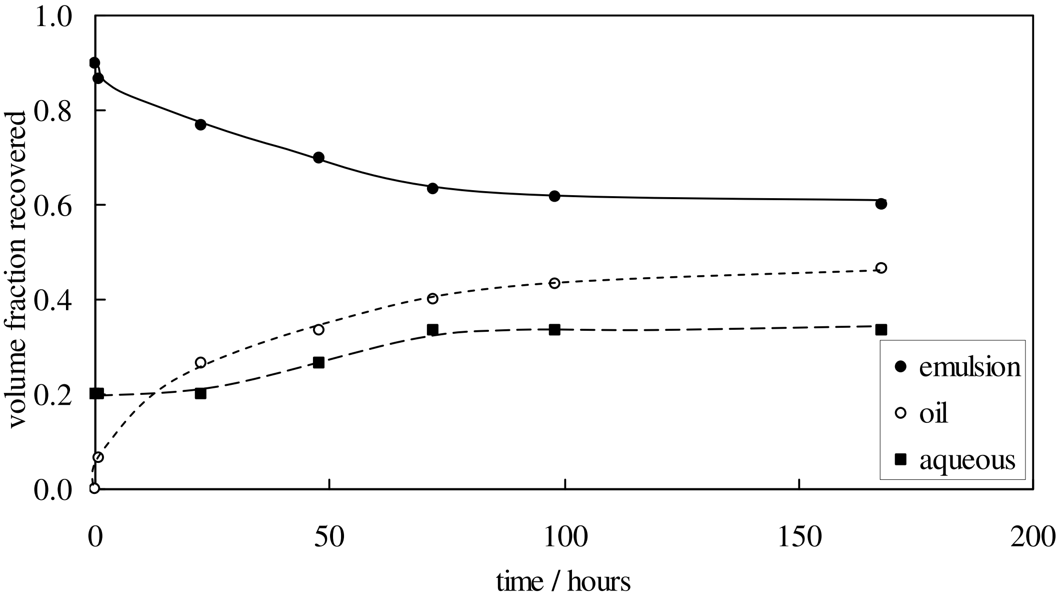

high pH system to render them sufficiently hydrophilic to invert the emulsion from w/o to o/w. However, the high pH system emulsified more aqueous phase and was more stable to coalescence than the natural pH system indicating that the particles modified *in-situ* stabilised the emulsion more effectively. This suggests that the particles had a contact angle closer to 90^{o} in the high pH system compared to the natural pH system. If the change in emulsion stability was due to an increase in hydrophilicity of the hydrophobic silica particles then it is reasonable to assume that given the correct experimental conditions phase inversion can be induced.

7.4 *In-situ* modification of hydrophobic silica particles – phase inversion

In order to establish if phase inversion was possible the above experiment was repeated using silica particles with a higher free surface silanol content i.e. more hydrophilic. The silica particles had an initial free silanol content of 42 % meaning that they were already much closer to the hydrophobicity at which an emulsion would become water continuous and should be easier to phase invert. The same experimental conditions as the experiments above were used and separate systems were studied with initial aqueous solution pH ranging from 8 through to 10. The continuous phase type was established by conductivity and drop test every 3 minutes and the experiment stopped after 60 minutes. Notes were also made on the appearance of the system each time the continuous phase type was established. In the experiments above when the hydrophobic particles were initially dispersed into the aqueous phase they transferred into the oil phase after the first period of homogenisation. For simplicity in this series of experiments the particles were dispersed directly into the oil.

Figure 7.6 shows, for an initial water-in-squalane preferred emulsion stabilised by 2 wt. % fumed silica with 42 % free surface SiOH groups for different initial aqueous pH values, what the continuous phase of the emulsion is with time. For each pH value it is the same emulsion being measured i.e. the system is homogenised for 3 minutes, the continuous phase type established, homogenised again for a further 3 minutes, the continuous phase type determined again etc. As can be seen it was possible to induce phase inversion in all of the systems by exposing the hydrophobic silica particles to aqueous base. It is interesting to note that given that the particles were dispersed into the oil phase and the base the aqueous phase the modification must occur at the oil-water interface. The time at which the inversion occurred is dependent on the pH of the system with phase inversion occurring sooner for the higher pH systems.

For every system, more water was incorporated into the emulsion as the base was given time to remove the coating on the silica particles and make them more hydrophilic. As phase inversion approached there was a noticeable chance in the rheology of the system with the emulsion becoming viscous and appearing under homogenisation to shear-thin. Once phase inversion had occurred the subsequent o/w emulsion was very viscous and completely stable to creaming and coalescence for at least 4 weeks.

Figure 7.6. Continuous phase type, established by conductivity and drop test measurements, of an initial water-in-squalane emulsion stabilised by 2 wt. % of silica particles (42 % free surface SiOH) . Particles were dispersed into the oil phase using ultrasound for 2 min. @ 10 W. Aqueous phase was altered using concentrated KOH and contains 10 mM NaCl. Emulsion was homogenised continuously at 20 ^{o}C.

	Time / min.																
Initial pH	3	6	9	12	18	21	24	27	30	33	36	39	42	45	48	51	54
8.00	O	O	O	O	O	O	O	O	O	O	W	W	W	W	W	W	W
9.03	O	O	O	O	O	O	O	O	O	O	W	W	W	W	W	W	W
9.50	O	O	O	O	O	O	O	O	O	O	W	W	W	W	W	W	W
9.70	O	O	O	O	O	O	O	O	O	W	W	W	W	W	W	W	W
9.87	O	O	O	O	O	O	O	O	W	W	W	W	W	W	W	W	W
10.00	O	O	O	O	O	O	O	W	W	W	W	W	W	W	W	W	W
10.10	O	O	O	O	O	O	W	W	W	W	W	W	W	W	W	W	W
10.15	W	W	W	W	W	W	W	W	W	W	W	W	W	W	W	W	W

7.5 Conclusions

It is possible to increase the effectiveness of hydrophobic silica particles to stabilise w/o emulsions by removing the hydrophobic coating using base. This can be done *in-situ* at the oil-water interface and leads to very stable emulsions. It is also possible, under the correct experimental conditions, to render the silica particles sufficiently hydrophilic to induce phase inversion of the system from w/o to o/w and the time at which this occurs was shown to be dependent on the concentration of base present in the aqueous phase. The o/w emulsions produced by modifying the hydrophobic particles *in*-situ were very stable.

7.6 References

---

[1] Y. Niibori, M. Kunita, O. Tochiyama and T. Chida, *J. Nucl. Sci. Technol*, **37**, 349 (2000).

[2] B.P. Binks and S.O. Lumsdon, *Langmuir*, **16**, 3748 (2000).

[3] R. Aveyard, B.P. Binks and J.H. Clint, *Adv. Colloid. Interfac.*, **100**, 503 (2003).

[4] B.P. Binks, *Curr. Opin. Colloid Interface Sci.*, **18**, 1270 (2002).

CHAPTER 8

SUMMARY OF MAIN CONCLUSIONS AND FUTURE WORK

8.1 Conclusions

A range of different systems containing solid particles have been investigated. Rapid film growth caused by both coalescence of particle laden emulsion droplets and particle laden foam bubbles has been demonstrated. A mechanism which explains the phenomenon of the formation of these rapid climbing films has been presented. We propose that as the emulsion droplet/foam bubble coalesces with the planar interfaces particle are transfer from the droplet/bubble onto the planar interface. When the interfacial concentration of particles reaches a monolayer the next coalescence event drives film formation. This mechanism is shown to be consistent with the study of a single drop of the oil phase rising through a bulk aqueous phase and coalescing with a planar oil-water interface. In addition, the receding contact angle of a pre-equilibrated system changes from below 90^o to above 90^o for hydrophobicity is in agreement with the observations of the direction of film growth in a series of hydrophobically modified vessels. In the films driven by foam bubble coalescence the effect of changing the particle concentration, the hydrophobicity of particles, vessel diameter and shaking have been investigated and explained and all appear to be consistent with mechanism described above. Particle film growth driven by foam bubble coalescence is a much more robust phenomenon occurring in a more simple system than the film growth driven by emulsion drop coalescence.

The addition of a small amount of low dielectric co-solvent to the aqueous phase of a dodecane-in-water emulsion stabilised by hydrophilic silica has been shown to increase the stability of the emulsion towards coalescence. Further addition of co-solvent leads to a subsequent destabilisation of the system beyond that which would be observed with no co-solvent addition. Some possible mechanisms for the observed increase, and subsequent decrease have been suggested. The likely explanation is that is a combination of factors one of which is the increase in flocculation of the silica particles induced by the co-solvent.

Unlike a surfactant stabilised system, solid-stabilised o/w emulsions have been seen to rapidly break and coalesce after a period of evaporation due to the *in-situ* catastrophic phase inversion. This coalescence leads to unusual spreading behaviour where initially the drop of emulsion has a high contact angle on the hydrophobic surface (similar to that of water) but after coalescence the system forms spreading ‘wings’ from the aqueous drop. The spreading occurs on a variety of surfaces including leaf and grain surfaces.

It is possible to increase the effectiveness of hydrophobic silica particles to stabilise w/o emulsions by removing the hydrophobic coating using base. This can be done *in-situ* at the oil-water interface and leads to very stable emulsions. It is also possible, under the correct experimental conditions, to render the silica particles sufficiently hydrophilic to induce transitional phase inversion in the system from w/o to o/w and the time at which this occurs was shown to be dependent on the concentration of base present in the aqueous phase. The o/w emulsions produced by modifying the hydrophobic particles *in-situ* to induce phase inversion were very stable.

8.2 Future work

The work describing the *in-situ* catastrophic phase inversion of o/w solid-stabilised emulsions could be further developed by investigating the potential for the liberated oil to carry an oil soluble active ingredient onto a hydrophobic surface. The oil phase could be coloured with a phosphorescent dye which could be used to track the spreading of the liberated oil on hydrophobic surfaces such as leaves. In addition to this, a systematic study of the effect of the system properties such as oil:water volume ratio, oil polarity particle type and particle wettability would be interesting. It should also be possible to develop an experimental rig which uses a pendant drop approach to study this behaviour. This would remove any effects that the surface has on the phenomenon. The drop volume could be tracked using the DSA 10 in pendant drop mode or through a gravimetric approach.

The short section of work report in Chapter 7 was completed at the end of the Ph.D. project and although interesting it is far from complete. Our understanding of the phenomenon of *in-situ* removal of a hydrophobic coating on a hydrophilic particle could be greatly increased by considering the following possible investigations.

- Investigation of the point at which phase inversion occurs for a range of silica particles possessing different % SiOH. If the hypothesis that the base removes the hydrophobic coating rendering the particle more hydrophilic and increasing emulsion stability and causing phase inversion is correct then the more hydrophobic coating the longer it should take to phase invert.

- Investigation of the effect of different coatings types on the silica particles i.e. DCDMS (short chain) versus PDMS (long chain).

- At the extreme it should be possible to take the hydrophobic particle and remove all of the hydrophobic coating. If this was done in an emulsion system then the following should be observed. As the coating from the hydrophobic particle is removed, and the contact angle of the particle approached that needed for phase inversion, then the w/o emulsion becomes more stable. At some point the particles will be sufficiently hydrophilic to induce phase inversion from w/o to o/w. Then if there is sufficient base to continue removing the hydrophobic coating a decrease in emulsion stability will be observed as the contact angle moves away from that needed to invert the system until eventually the particle becomes so hydrophilic it is no longer an effective stabiliser for emulsions.

- If it is possible to observe the phenomenon described above then it would be interesting to investigate the effect that the interface plays on the modification of the particle. Given that the base is confined to the aqueous phase and the particle is trapped at the interface there is the possibility that particles would be asymmetrically modified, i.e. so called Janus particles.[1] Janus particles are attracting an increasing amount of interest in the literature but most formation techniques only yield small quantities of particles.[2,3] However, recent techniques have been reported which may generate yields sufficient to allow the surface properties of these amphiphilic particles to be studied.[4]

- If a particle which is modified in the bulk phase is so hydrophilic that it is no longer effective as an emulsifier and for an equivalent amount of base the same particle modified *in-situ* is an effective emulsion stabiliser then this is evidence that the interface is playing a role in determining the extent of the particle modification preferring the particles to have the contact angle which equates to maximum stability of the interface.

- It may also be interesting to investigate the contact angle of planar silica surfaces, modified in the same way as the particles used in this study, as they are exposed to base to see if there is any correlation between macroscopic contact angle and the behaviour of the particles in the emulsion system.

8.3 References

---

[1] A. Walther, M. Hoffmann and A.H.E. Müller, *Angew. Chem. Int. Ed.*, **47**, 711 (2008).

[2] B.B. Wang, B. Li, B. Zhoa and C.Y. Li, *J. Am Chem. Soc.*, **130**, 11594 (2008).

[3] A. Walther and A.H.E. Muller, *Soft Mater*, **4**, 663 (2008).

[4] L. Cheng, G.L. Hou, J.J. Miao, D.Y. Chen, M. Jiang and L. Zhu, *Macromolecules*, **41**, 8159 (2008).

Appendix I

Visual basic code

This section contains the visual basic code used to calculate the volume of the evaporating drops of emulsion as described in Section 2.2.10.

```
Function Volume()
  Pi = 4 * Atn(1)
  Dim Y As Integer
  Dim X As Integer
  Dim Z As Integer
  Range("Sheet2!b11:b30").ClearContents
  For Z = 1 To 18
  Volume = 0
  Threshold = Range("Sheet2!a" & (10 + Z)).Value
  For X = 1 To 500
  Intensity = Worksheets("data").Cells(1, X).Value
  If Intensity = 0 Then GoTo 100
  Next X
100 W = X - 1
  For Y = 1 To 500
  For X = 1 To W
  Intensity = Worksheets("data").Cells(Y, X).Value
```

```
    If Intensity < Threshold Then GoTo 200

    Next X

200 R = W - X + 1

dV = Pi * R ^ 2

    Volume = Volume + dV

    If Intensity = 0 Then GoTo 300

    Next Y

300 Range("Sheet2!b" & (10 + Z)).Value = Volume

    Next Z

End Function
```

Appendix II

Evaporation of solid-stabilised emulsions

This section contains images of the drop of solid-stabilised emulsion as it evaporates as described briefly in Figure 6.10. The appearance of the drop is shown for each minute of the experiment. The system is a drop of dodecane-in-water emulsion stabilised by 2 wt. % fumed silica (78 % SiOH), volume fraction of oil = 0.5, as in evaporates on a hydrophobically modified slide. Every image stored is presented in the electronic supplementary information (DVD attached to the inside cover of the thesis). The time that each image was taken is given beneath the image.

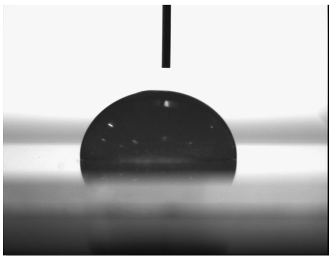
0 s

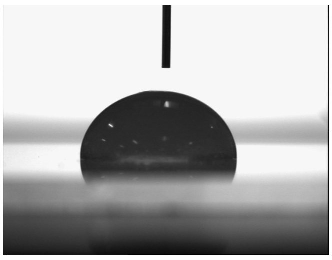
60 s

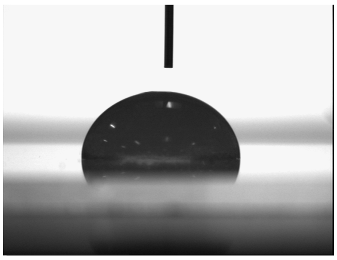
120 s

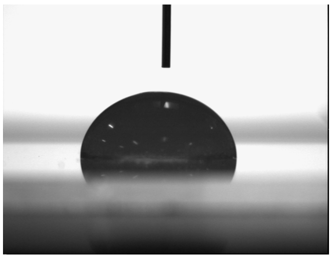
180 s

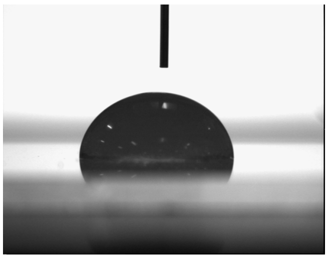
240 s

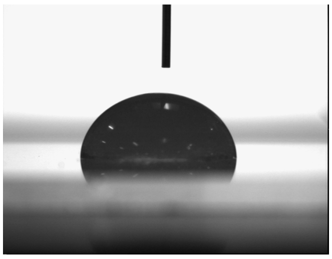
300 s

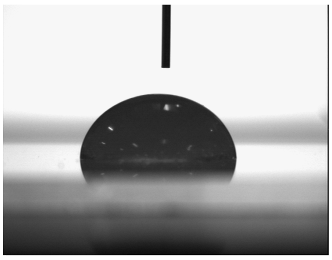

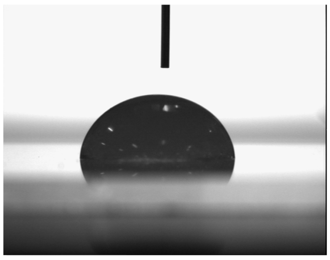

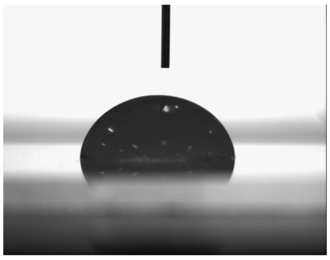

360 s

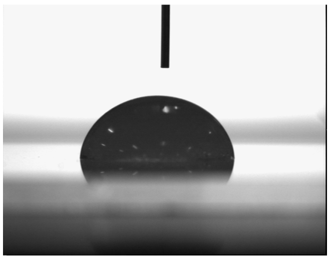

420 s

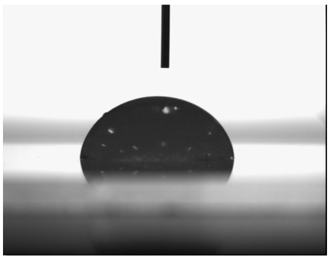

480 s

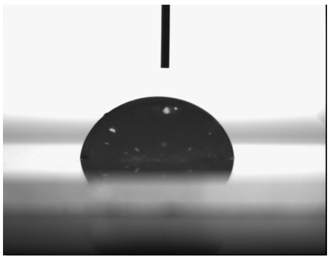

540 s

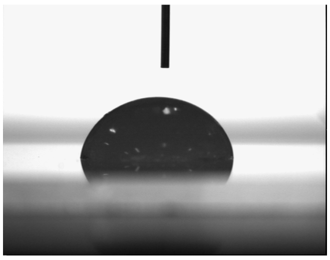

600 s

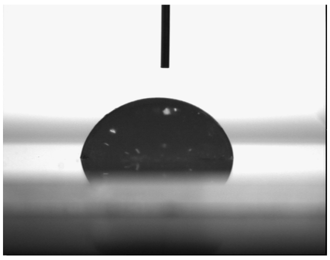

660 s

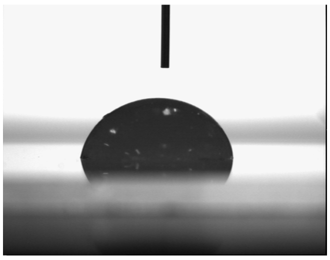

720 s

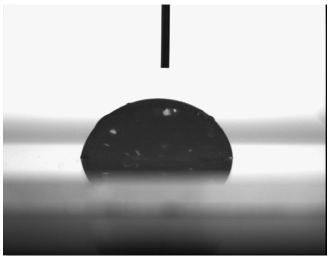

780 s

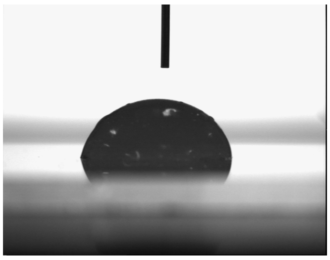

840 s

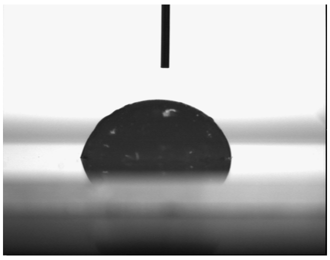

900 s

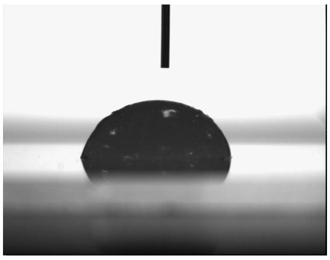

960 s

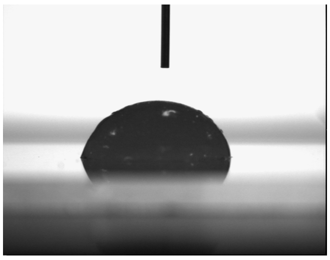

1040 s

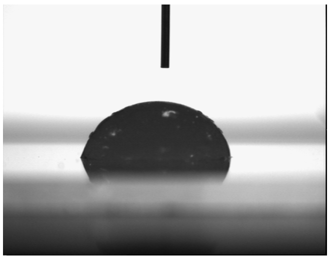

1100 s

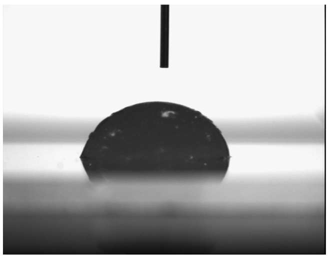

1160 s

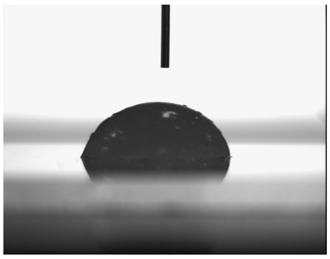

1220 s

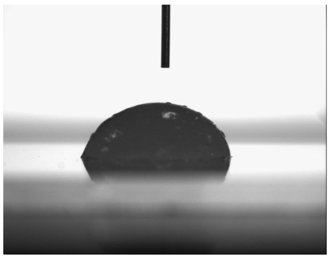

1280 s

1340 s

1400 s

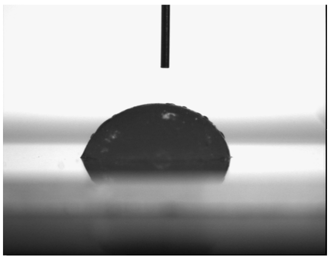
1460 s

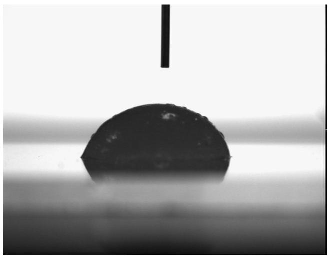
1520 s

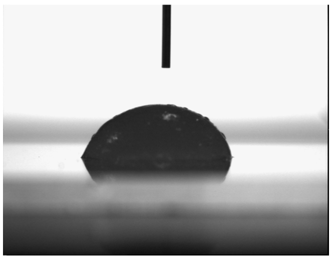
1580 s

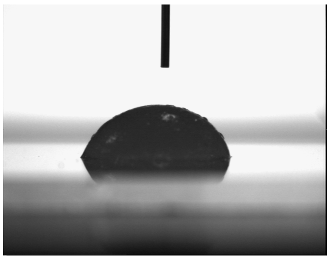
1620 s

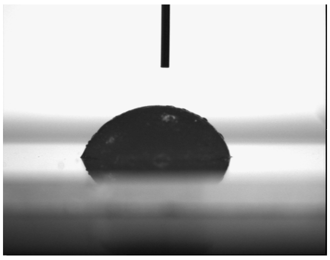
1680 s

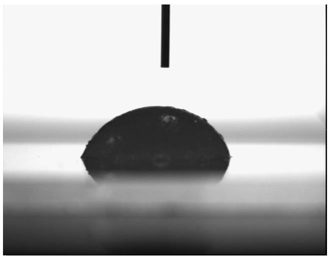
1740 s

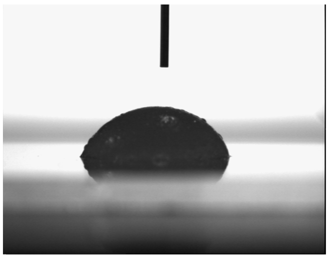
1800 s

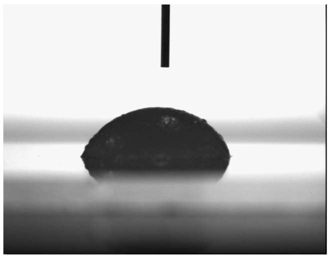
1860 s

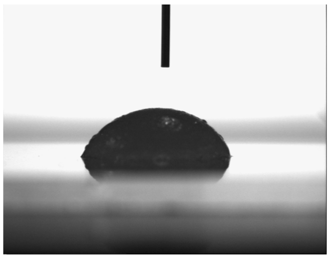
1920 s

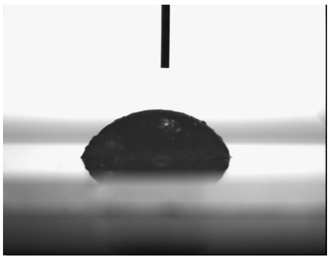
1980 s

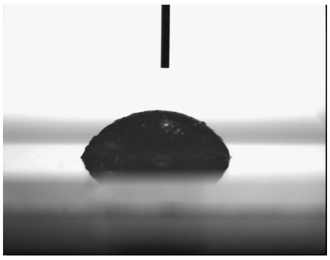
2040 s

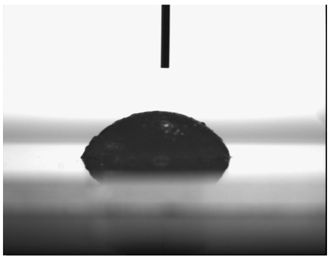
2100 s

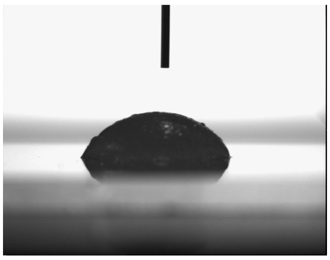
2160 s

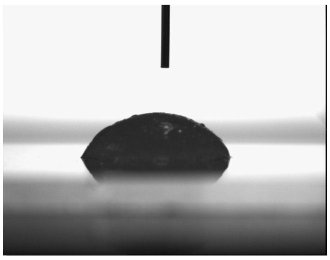
2220 s

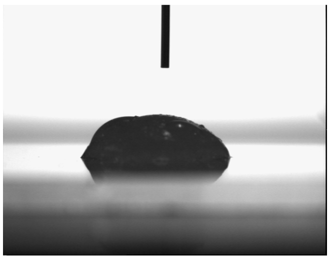
2280 s

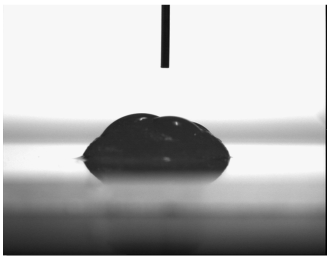
2340 s

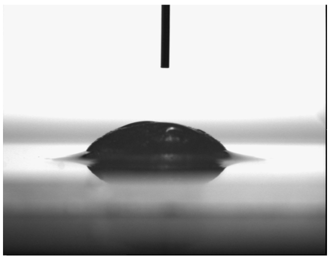
2400 s

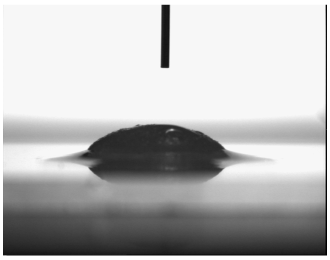
2460 s

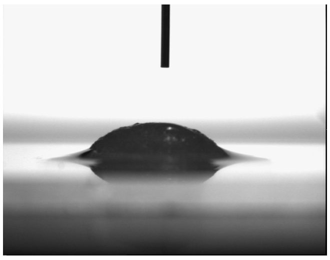
2520 s

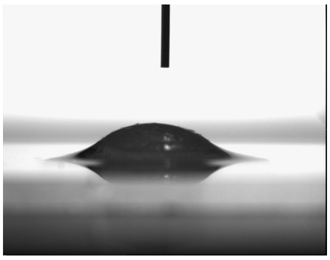
2580 s

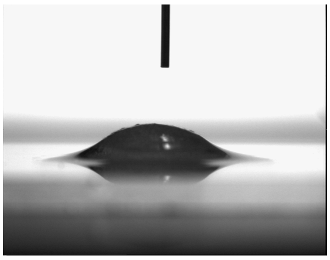
2640 s

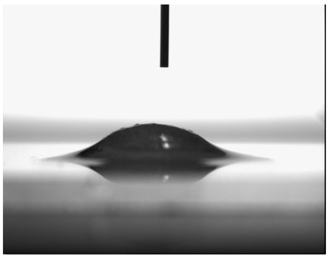
2700 s

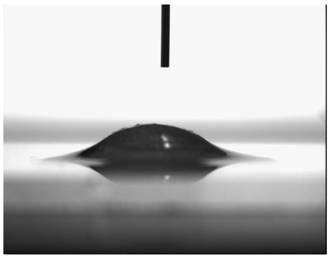
2760 s

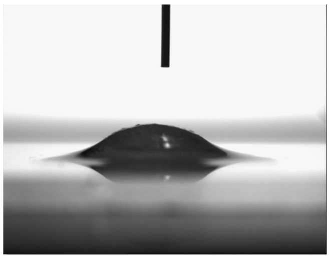
2820 s

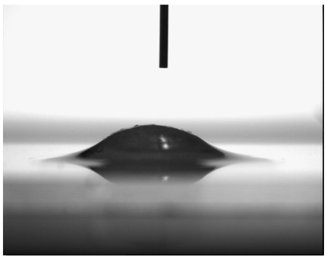
2880 s

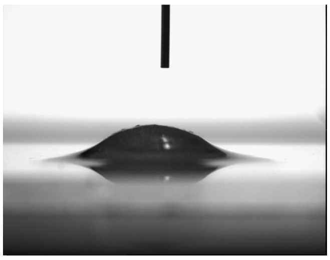
2940 s

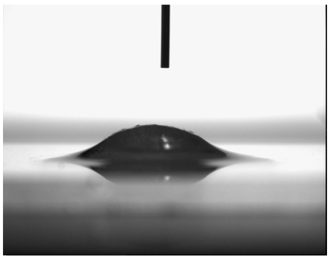
3000 s

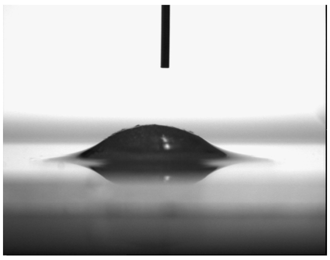
3060 s

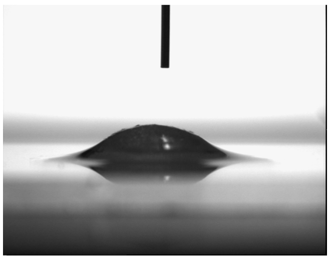
3120 s

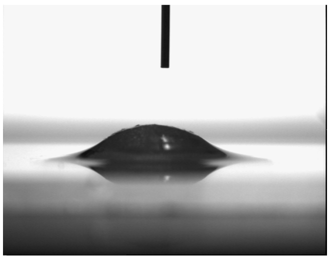
3180 s

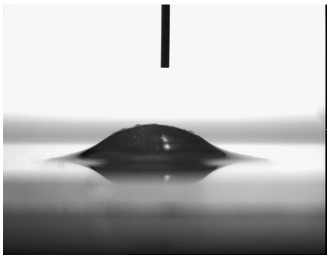
3240 s

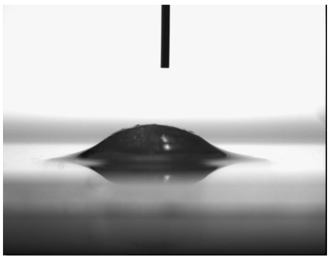
3300 s

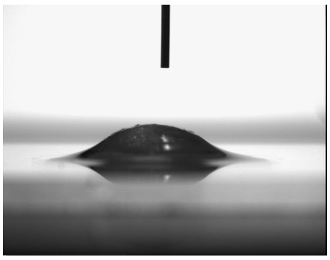
3360 s

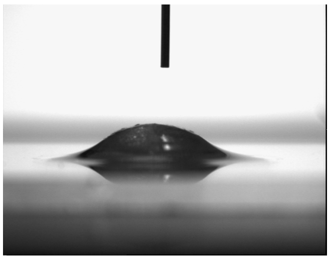
3420 s

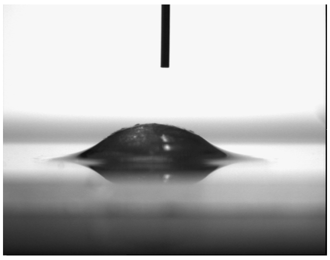
3480 s

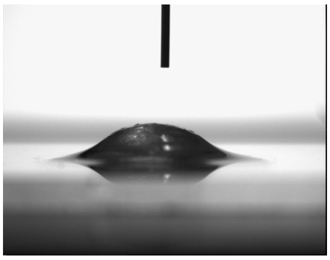
3540 s